



TECHNICAL UNIVERSITY OF MOLDOVA

JOURNAL OF ENGINEERING SCIENCE

Technical and applied scientific publication founded on 9 February 1995
Alternative title: Meridian ingineresc

2021
Vol. XXVIII (3)

ISSN 2587-3474
eISSN 2587-3482

TECHNICAL UNIVERSITY OF MOLDOVA (PUBLISHING HOUSE)
„TEHNICA UTM” (PRINTING HOUSE)

According to the Decision of the NAQAER No. 19 from 06.12.2019, JES is classified as B+ journal

Main subjects areas of the Journal of Engineering Science:

A. Industrial Engineering

- Mechanical Engineering and Technologies
- Applied Engineering Sciences and Management
- Materials Science and New Technologies
- Electrical Engineering and Power Electronics
- Energy systems
- Light Industry, New Technologies and Design
- Industrial and Applied Mathematics
- Vehicle and Transport Engineering

B. Electronics and Computer Science

- Electronics and Communication
- Microelectronics and Nanotechnologies
- Biomedical Engineering
- Computers and Information Technology
- Automation

C. Architecture, Civil and Environmental Engineering

- Architecture, Urbanism and Cadaster
- Civil Engineering and Management
- Energy Efficiency and New Building Materials
- Environmental Engineering

D. Food Engineering

- Food Technologies and Food Processes
- Food Industry and Management
- Biotechnologies, Food Chemistry and Food Safety
- Equipment for Food Industries

The structure of the journal corresponds to the classification of scientific publications:
Engineering, Multidisciplinary.

How to publish a paper:

1. Send the manuscript and information about the author to the **Editorial Board address:**
jes@meridian.utm.md
2. Manuscripts are accepted only in English, by e-mail, in template file (www.jes.utm.md)
3. After a review, you will be notified of the editorial board's decision.
4. After the Journal has been published, we will send it to you immediately by mail.

Editor-in-Chief

Dr. hab. prof. univ. Viorel BOSTAN

Technical University of Moldova

viorel.bostan@adm.utm.md

Editorial Board

Abdelkrim Azzouz, Dr. Eng., Professor, Quebec University of Montreal, Canada
Adrian Gheorghe, PhD, Professor, Old Dominion University, Norfolk, Virginia, 23529, USA
Adrian Gaur, PhD, Professor, University "Ștefan cel Mare", Suceava, Romania
Alexander Pogrebnyak, PhD, Professor, Sumy State University, Ukraine
Aurel-Mihail Țițu, PhD, Professor, "Lucian Blaga" University of Sibiu, Romania
Boris Gaina, Dr.hab., Professor, Acad. of the Academy of Sciences of Moldova
Camelia Vizireanu, Dr. Eng., Professor, "Dunarea de Jos" University of Galati, Romania
Cornel Ciupan, PhD, Professor, Technical University of Cluj Napoca, Romania
Cristoph Ruland, PhD, Professor, University of SIEGEN, Germany
Dimitr P. Karaivanov, PhD, Professor, University of Chemical Technology and Metallurgy, Sofia, Bulgaria.
Dumitru Mnerie, PhD, Professor, "Politehnica" University of Timișoara, Romania
Dumitru Olaru, PhD, Professor, Technical University "Gh. Asachi", Iași, Romania
Dumitru Țiuleanu, Dr. hab., Corr. Mem. of the Academy of Sciences of Moldova
Florin Ionescu, PhD, Professor, University Steinbeis, Berlin, Germania
Gabriel Neagu, PhD, Profesor, National Institute for Research and Development in Informatics, Bucharest, Romania
George S. Dulikravich, PhD, Florida International University, U.S.A.
Gheorghe Badea, PhD in Engineering, Professor, Technical University of Civil Engineering Bucharest, Romania
Gheorghe Manolea, PhD, Professor, University of Craiova, Romania
Grigore Marian, PhD, Professor, Agrarian State University of Moldova, Chisinau, Republic of Moldova
Hai Jiang, PhD, Professor, Department of Computer Science, Arkansas State University, U.S.A.
Heinz Frank, PhD, Professor, Reinhold Würth University, Germany
Hidenori Mimura, Professor, Research Institute of Electronics, Shizuoka University, Japan
Ion Bostan, Dr. hab., Professor, Acad. of the Academy of Sciences of Moldova
Ion Paraschivoiu, PhD, Professor, Universite Technologique de Montreal, Canada
Ion Rusu, Dr. hab., Professor, Technical University of Moldova
Ion Tighineanu, Dr. hab., Professor, Acad. of the Academy of Sciences of Moldova
Ion Vișa, PhD, Professor, University Transilvania of Brașov, Romania.
Laurențiu Slătineanu, PhD, Professor, Technical University „Gh. Asachi”, Iași, Romania.
Lee Chow, PhD, Professor, University of Central Florida, USA
Leonid Culiuc, Dr. hab., Acad. of the Academy of Sciences of Moldova
Livia Nistor-Lopatenco, PhD, Associate Professor, Technical University of Moldova
Mardar Maryna, Doctor of Technical Science, Professor, Odessa National Academy of Food Technologies, Odessa, Ukraine
Natalia Tislinschi, PhD, Associate Professor, Technical University of Moldova
Nicolae Opopol, Dr. hab., Professor, Corr. Member of the Academy of Sciences of Moldova
Oleg Lupan, Dr. hab., Professor, Technical University of Moldova
Pavel Tatarov, Dr. hab., Professor, Technical University of Moldova
Pavel Topală, Dr. hab., Professor, State University „Aleco Russo” from Bălți, Republic of Moldova
Peter Lorenz, PhD, Professor University of Applied Science Saar, Saarbrücken, Germania
Petru Cașcaval, PhD, Professor, "Gheorghe Asachi" Technical University of Iasi, Romania

Petru Stoicev, Dr. hab., Professor, Technical University of Moldova, Chisinau, Republic of Moldova
 Polidor Bratu, PhD, Professor, president ICECON S.A., București, Romania
 Radu Munteanu, PhD, Professor, Technical University of Cluj Napoca, Romania
 Radu Sorin Văcăreanu, PhD, Professor, Technical University of Civil Engineering Bucharest, Romania
 Rafał Gołębski, Dr., Associate Professor, Czestochowa University of Technology, Poland
 Sergiu Zaporozan PhD, Professor, Technical University of Moldova
 Spiridon Crețu, PhD, Professor, Technical University „Gh. Asachi”, Iași, Romania.
 Stanislav Legutko, PhD, Professor, Poznan University of Technology, Poland
 Stefan Tvetanov, PhD, Professor, University of Food Technologies, Bulgaria
 Ștefan-Gheorghe Pentiuc, PhD, Professor, University “Stefan cel Mare” of Suceava, Romania
 Svetlana Albu, Dr. hab., Professor, Technical University of Moldova
 Thierry Pauporté, PhD, Professor, Ecole Nationale Supérieure de Chimie de Paris, France
 Thomas Luhmann, Dr. Eng., Professor, Jade University of Applied Sciences, Germany
 Titu-Marius Bajenescu, Dr. Eng., Professor, Swiss Technology Association, Electronics Group Switzerland
 Valentin Arion, PhD, Professor, Technical University of Moldova, Chișinău, Republic of Moldova
 Valentina Bulgaru, PhD, Associate Professor, Technical University of Moldova, Chișinău, Republic of Moldova
 Valeriu Dulgheru, Dr. hab., Professor, Technical University of Moldova, Chișinău, Republic of Moldova
 Vasile Tronciu, Dr. hab., Professor, Technical University of Moldova, Chișinău, Republic of Moldova
 Victor Ababii, PhD, Professor, Technical University of Moldova, Chișinău, Republic of Moldova
 Victor Șontea, PhD, Professor, Technical University of Moldova, Chișinău, Republic of Moldova
 Wilhelm Kappel, PhD, Institute of Research INCDIE ICPE-CA, Bucharest, Romania
 Vladimir Zavialov, Dr. hab., Professor, National University of Food Technology, Ukraine
 Vladislav Resitca, PhD, Associate Professor, Technical University of Moldova, Chișinău, Republic of Moldova
 Yogendra Kumar Mishra, Dr. hab., Kiel University, Germany
 Yuri Dekhtyar, Dr.hab., Professor, Acad. of Latvian Academy of Sciences, Riga Technical University, Riga, Latvia

Responsible Editor:

Dr. hab. Rodica STURZA
 Technical University of Moldova
rodica.sturza@chim.utm.md

Editorial Production:

Dr. Nicolae Trifan
 Dr. Svetlana Caterenciuc
 Rodica Cujba

CONTENT

Abstracts	8
A. Industrial Engineering		
Tuan-Linh Nguyen	Industrials simulation modeling technology application to improve the efficiency in automatic production line equipment	28
Alexandru Buga	Setting of the angle of incidence for generating Lamb waves by non-contact method.....	41
Alexei Botez, Elena Rusu	Design aspects of installation devices of the support rings	51
Grigore Ambrosi	Ignition and combustion of single solid particles as non-isothermal methods of chemical kinetics.....	64
Lev Kalinin, Dmitrii Zaitsev, Mihai Tirsu, Irina Golub, Danila Kaloshin	Energy characteristics of phase regulating device based on "Star" circuit.....	71
Adinife Patrick Azodo, Olasunkanmi Salami Isamaila, Sampson Chisa Owbor	Fitness and comfort assessment of footwear: an anthropometric appraisal	80
B. Electronics and Computer Science		
Veaceslav Perju	Multiple classification algorithms unimodal and multimodal target recognition systems.....	87
Badri Narayan Mohapatra, Bhagwat Nagargoje, Prajwal Zurunge, Suraj More	Artificial intelligence in stock market investment.....	96
C. Architecture, Civil and Environmental Engineering		
Corina Chelmenciuc, Constantin Borosan	Regression analysis of the energy produced in cogeneration and supplied to district heating systems.....	101
Ameer Baiee	Development ultra-high strength cementitious characteristics using supplementary cementitious materials	111
Ramesh Babu Aremanda, Nahom Yohannes, Yosief Ghezae	Performance studies on water flow control using P, PI and PID controllers.....	126
D. Food Engineering		
Alexei Baerle	Microencapsulation of functional components in the food technology: partially optimistic view.....	139

Tatiana Cușmenco, Elisaveta Sandulachi, Viorica Bulgaru Artur Macari	The role of berries in quality and safety ensuring of goat's and cow's milk yoghurt.....	158
Aurica Chirsanova, Tatiana Capcanari, Alina Boistean Rodica Sturza, Valentin Mitin, Irina Mitina, Dan Zgardan, Antoanela Patras, Emilia Behta	Palynological, physico-chemical and biologically active substances profile in some types of honey in the Republic of Moldova	175
	Development of the real-time pcr methodology for testing mycotoxigenic microorganisms in grape marc	187

CONȚINUT

Abstracte	8
A. Industrial Engineering		
Tuan-Linh Nguyen	Aplicații tehnologice de modelare a simulării industriale pentru îmbunătățirea eficienței în echipamentele de linie de producție automata.....	28
Alexandru Buga	Setarea unghiului de incidență pentru generarea undelor Lamb prin metoda non-contact	41
Alexei Botez, Elena Rusu	Aspecte de proiectare a dispozitivelor de instalare a inelelor de support	51
Grigore Ambrosi	Aprindere și ardere a particulelor solide unice ca metode neizotermale de cinetică chimică.....	64
Lev Kalinin, Dmitrii Zaitsev, Mihai Tirsu, Irina Golub, Danila Kaloshin	Caracteristicile energetice ale dispozitivului de reglementare a fazelor pe baza circuitului „Stea”	71
Adinife Patrick Azodo, Olasunkanmi Salami Isamaila, Sampson Chisa Owbor	Evaluarea confortului încălțământeii: o evaluare antropometrică	80
B. Electronics and Computer Science		
Veaceslav Perju	Algoritmi de clasificare multiplă unimodali și sisteme multimodale de recunoaștere a țintelor.....	87
Badri Narayan Mohapatra, Bhagwat Nagargoje, Prajwal Zurunge, Suraj More	Inteligență artificială în investiții pe piața de active.....	96

C. Architecture, Civil and Environmental Engineering

Corina Chelmenciuc, Constantin Borosan	Analiza de regresie a energiei produse în cogenerare și livrată în sistemul centralizat de alimentare cu căldură.....	101
Ameer Baiee	Dezvoltarea caracteristicilor de puteri ultra-înalte a cimenturilor utilizand materiale de cimentare suplimentare.....	111
Ramesh Babu Aremanda, Nahom Yohannes, Yosief Ghezae	Studii de performanță privind controlul debitului de apă P, PI și PID	126

D. Food Engineering

Alexei Baerle	Microincapsularea componentelor funcționale în tehnologia alimentară: viziune parțial optimistă.....	139
Tatiana Cușmenco, Elisaveta Sandulachi, Viorica Bulgaru Artur Macari	Rolul pomusoarelor în asigurarea calității și siguranței iaurtului de lapte de capră și de vacă	158
Aurica Chirsanova, Tatiana Capcanari, Alina Boistean	Profilul palinologic, fizico-chimic și a substanțelor biologice active din unele tipuri de miere din Republica Moldova	175
Rodica Sturza, Valentin Mitin, Irina Mitina, Dan Zgardan, Antoanela Patras, Emilia Behta	Dezvoltarea metodologiei real-time pcr pentru testarea microorganismelor micotoxigenice în tescovina de struguri	187

[https://doi.org/10.52326/jes.utm.2021.28\(3\).01](https://doi.org/10.52326/jes.utm.2021.28(3).01)
CZU 004.94

INDUSTRIALS SIMULATION MODELING TECHNOLOGY APPLICATION TO IMPROVE THE EFFICIENCY IN AUTOMATIC PRODUCTION LINE EQUIPMENT

Tuan-Linh Nguyen*, ORCID ID: 0000-0002-1960-9794

Department of Mechanical Engineering, Hanoi University of Industry, Hanoi City, Vietnam

**Corresponding author: Tuan-Linh Nguyen, nguyentuanlinh@hau.edu.vn*

Received: 06. 12. 2021

Accepted: 08. 06. 2021

Abstract. Currently, the application of technical advances to production plays an important role in improving productivity and saving production costs. The techniques applying information technology bring high efficiency, accuracy, reliability, pre-assessment of the results. Modeling and simulation are method that are widely used from research, design, manufacturing to operate the systems. With the help of computers, with high computational speed and large memory, the modeling method was strongly developed, bringing great efficiency in research and production practice. The assessment of effective use of equipment in the production line has a decisive role in increasing the productivity and decreasing cost. Therefore, the analysis and evaluation of the production line by the simulation model method is highly practical, bringing many effects in the management and use of equipment. In this study, a simulation of a specific problem was performed to estimate the simulated workshop. Then, building a new plan and comparing the proposed plane with the original plan to provide the reasonable solutions for the production process to effectively use the equipment in the production line.

Keywords: *modeling and simulation, effective use, equipment, automatic production line.*

Rezumat. În prezent, aplicarea progreselor tehnice la producție joacă un rol important în îmbunătățirea productivității și economisirea costurilor de producție. Tehnicile care aplică tehnologia informației aduc eficiență ridicată, acuratețe, fiabilitate, preevaluare a rezultatelor. Modelarea și simularea sunt metode utilizate pe scară largă în cercetare, proiectare, fabricare pentru a opera sistemele. Cu ajutorul computerelor cu viteză de calcul mare și memorie mare, metoda de modelare a fost puternic dezvoltată, aducând o mare eficiență în practica de cercetare și producție. Evaluarea utilizării eficiente a echipamentelor în linia de producție are un rol decisiv în creșterea productivității și scăderea costurilor. Prin urmare, analiza și evaluarea liniei de producție prin metoda modelului de simulare este extrem de practică, aducând multe efecte în gestionarea și utilizarea echipamentelor. În acest studiu, a fost efectuată o simulare a unei probleme specifice pentru a estima atelierul simulat. Apoi, construirea unui nou plan și compararea planului propus cu planul original pentru a oferi soluții rezonabile pentru procesul de producție pentru a utiliza în mod eficient echipamentele din linia de producție.

Cuvinte cheie: *modelare și simulare, utilizare eficientă, echipament, linie de producție automată.*

[https://doi.org/10.52326/jes.utm.2021.28\(3\).02](https://doi.org/10.52326/jes.utm.2021.28(3).02)
CZU 621.3.092.53:534.2

SETTING OF THE ANGLE OF INCIDENCE FOR GENERATING LAMB WAVES BY NON-CONTACT METHOD

Alexandru Buga*, ORCID ID: 0000-0002-4342-0502

Technical University of Moldova, 168 Ștefan cel Mare Blvd., MD-2004, Chișinău, Republic of Moldova

*Corresponding author: Alexandru Buga, alexandru.buga@precesia.utm.md

Received: 06. 17. 2021

Accepted: 08. 10. 2021

Abstract. The article examined the problem of the experimental setting of incidence angles for the generation of Lamb waves in plate-type parts by the non-contact ultrasonic control method. This type of control is mainly done by the use of two types of waves: Rayleigh, which detects invisible defects on the surface of parts, and Lamb waves mode A_0 and S_0 . Mostly used is the mode A_0 due to the propagation over distances of interest in the tested materials. One of the primary aim during the testing process is to position the ultrasonic transducers (transmitter and receiver) at oblique angles of incidence on a surface. The transducers should be positioned on an access face of the plate, as is common in industrial practice, at a fixed distance from the measured plate, and leaving an air gap between transducers and the tested plate. The ultrasonic transducers are moved simultaneously linearly or in zigzag on the surface of the plate-type part to measure the hidden defects (cracks, pores, inclusions) that appear in the composite materials during the manufacturing process or during the operation. The presented work brings new insights into the setting of the angle of incidence for generating lamb waves by non-contact method.

Keywords: *non-contact ultrasonic control, invisible defects measurement, Lamb waves, ultrasonic transducers, angle of incidence.*

Rezumat. În articol este examinată problema setării experimentale a unghiurilor de incidență pentru generarea undelor Lamb în piese de tip placă prin metoda de control non-contact cu ultrasunete. Acest tip de control se face în principal prin utilizarea a două tipuri de unde: Rayleigh, care detectează defecte invizibile pe suprafața pieselor, și modul de undă Lamb A_0 și S_0 . Cel mai utilizat este modul A_0 datorită propagării pe distanțe de interes în materialele testate. Unul dintre obiectivele principale în timpul procesului de testare este poziționarea traductoarelor cu ultrasunete (emițător și receptor) la unghiuri de incidență oblică pe o suprafață. Traductoarele ar trebui să fie poziționate pe o față de acces a plăcii, așa cum este obișnuit în practica industrială, la o distanță fixă de placa măsurată și lăsând un spațiu de aer între traductoare și placa testată. Traductoarele cu ultrasunete sunt deplasate simultan liniar sau în zig-zag pe suprafața piesei de tip placă pentru a detecta defectele ascunse (fisuri, pori, incluziuni) care apar în materialele compozite în timpul procesului de fabricație sau în timpul exploatării. Lucrarea prezentată aduce noi perspective asupra setării unghiului de incidență pentru generarea undelor Lamb prin metoda non-contact.

Cuvinte cheie: *control cu ultrasunete fără contact, detectarea defectelor invizibile, unde Lamb, traductoare cu ultrasunete, unghi de incidență.*

[https://doi.org/10.52326/jes.utm.2021.28\(3\).03](https://doi.org/10.52326/jes.utm.2021.28(3).03)
CZU 621.887.002.5

DESIGN ASPECTS OF INSTALLATION DEVICES OF THE SUPPORT RINGS

Alexei Botez*, ORCID ID: 0000-0001-8357-076X
Elena Rusu, ORCID ID: 0000-0002-2473-0353

Technical University of Moldova, 168 Stefan cel Mare Blvd., MD-2004, Chisinau, Republic of Moldova

**Corresponding author: Alexei Botez, alexei.botez@gddti.utm.md*

Received: 06. 23. 2021

Accepted: 08. 11. 2021

Abstract. The processes of manufacturing machines and appliances show a continuous tendency to increase the degree of automation. An important role in the automation of manufacturing processes is played by the constructive technologicality of the product. It is important to use a minimum number of components, which have a construction as technological as possible in terms of automation. In this context, the use of supporting rings as fasteners is welcome. The design of the installation devices of these rings requires the knowledge of their deformation forces, information that is missing in the profile literature. The authors set their goal to develop the method for calculating the forces required to deform the supporting rings with a rectangular transverse profile and their maximum allowable deformations. The calculation relationships were obtained by formalizing the supporting ring through a bar with a fixed end and studying its deformation using Mohr's integral. The article lists some types of the supporting rings used in the construction of machines and appliances, their advantages and disadvantages, aspects of their automatic installation: deformation and installation methods, precision of joint orientation, optimal design, calculation of forces required for deformation and the maximum permissible deformation value. As a result of the research carried out, recommendations were developed regarding the calculation of some constructive parameters of the devices for installing the supporting rings.

Keywords: *supporting ring, mounting process, deformation forces, accuracy of orientation.*

[https://doi.org/10.52326/jes.utm.2021.28\(3\).03](https://doi.org/10.52326/jes.utm.2021.28(3).03)
CZU 621.887.002.5

DESIGN ASPECTS OF INSTALLATION DEVICES OF THE SUPPORT RINGS

Alexei Botez*, ORCID ID: 0000-0001-8357-076X,
Elena Rusu, ORCID ID: 0000-0002-2473-0353

Technical University of Moldova, 168 Stefan cel Mare Blvd., MD-2004, Chisinau, Republic of Moldova

**Corresponding author: Alexei Botez, alexei.botez@gddti.utm.md*

Received: 06. 23. 2021

Accepted: 08. 11. 2021

Rezumat. Procesele de fabricație a mașinilor și aparatelor arată o tendință continuă de creștere a gradului de automatizare. Un rol important în automatizarea proceselor de fabricație îl are tehnicitatea constructivă a produsului. Este important de utilizat un număr minim de componente, care au o construcție cât mai tehnologică în ceea ce privește automatizarea. În acest context, este binevenită utilizarea inelelor de susținere ca elemente de fixare. Proiectarea dispozitivelor de instalare a acestor inele necesită cunoașterea forțelor lor de deformare, informații care lipsesc în literatura de profil. Autorii și-au stabilit obiectivul de a dezvolta metoda de calcul a forțelor necesare deformării inelelor de susținere cu un profil transversal dreptunghiular și a deformărilor maxime admise. Relațiile de calcul au fost obținute prin formalizarea inelului de susținere printr-o bară cu un capăt fix și studierea deformării acestuia utilizând integralul lui Mohr. Articolul enumeră câteva tipuri de inele de susținere utilizate în construcția de mașini și aparate, avantajele și dezavantajele acestora, aspectele instalării lor automate: metode de deformare și instalare, precizia orientării articulației, proiectarea optimă, calculul forțelor necesare pentru deformare și valoarea maximă admisă a deformării. În urma cercetărilor efectuate, au fost elaborate recomandări cu privire la calcularea unor parametri constructivi ai dispozitivelor pentru instalarea inelelor de susținere.

Cuvinte cheie: *inel de susținere, proces de montare, forțe de deformare, precizie de orientare.*

[https://doi.org/10.52326/jes.utm.2021.28\(3\).04](https://doi.org/10.52326/jes.utm.2021.28(3).04)
CZU 544.45:546.27

IGNITION AND COMBUSTION OF SINGLE SOLID PARTICLES AS NON-ISOTHERMAL METHODS OF CHEMICAL KINETICS

Grigore Ambrosi*, ORCID ID: 0000-0001-7232-2998

Technical University of Moldova, 168 Ștefan cel Mare și Sfânt Blvd., Chisinau, Republic of Moldova

**Corresponding author: Grigore Ambrosi, grigore.ambrosi@tran.utm.md*

Received: 06. 17. 2021

Accepted: 08. 12. 2021

Abstract. The ignition and combustion of single particles of crystalline boron continue to produce major scientific interest due to the particularities of the process and diversity of potential applications of boron compounds. The full valorization of boron energetic potential is a very current scientific challenge. The objective of the paper is to systematize the methodology for evaluating the kinetic parameters of boron ignition and combustion reactions in various oxidizing gaseous environments. Experimental dependencies between the ignition temperature and the particle size, as well as the combustion time as a function of oxidizing temperature are used for the calculation of the kinetic constants. As a main result, the kinetic parameters of the ignition and combustion reactions of boron in oxygen and water vapor are calculated.

Keywords: boron, thermodynamics, reaction, oxidation, heterogeneous, calculation, parameter, experiment.

Rezumat. Aprinderea și arderea particulelor unice de bor cristalin continuă să producă un interes științific major datorită particularităților procesului și diversității aplicațiilor potențiale ale compușilor de bor. Valorificarea completă a potențialului energetic al borului este o provocare științifică foarte actuală. Obiectivul lucrării este de a sistematiza metodologia de evaluare a parametrilor cinetici ai reacțiilor de aprindere și ardere a borului în diferite medii gazoase oxidante. Pentru calcularea constantelor cinetice sunt utilizate dependențe experimentale între temperatura de aprindere și dimensiunea particulelor, precum și timpul de ardere în funcție de temperatura de oxidare. Ca rezultat principal, se calculează parametrii cinetici ai reacțiilor de aprindere și combustie ale borului în oxigen și vapori de apă.

Cuvinte cheie: bor, termodinamică, reacție, oxidare, eterogenă, calcul, parametru, experiment.

[https://doi.org/10.52326/jes.utm.2021.28\(3\).05](https://doi.org/10.52326/jes.utm.2021.28(3).05)
CZU 621.314.25

ENERGY CHARACTERISTICS OF PHASE REGULATING DEVICE BASED ON "STAR" CIRCUIT

Lev Kalinin, ORCID: 0000-0003-1894-5734,
Dmitrii Zaitsev, ORCID: 0000-0001-7207-1754,
Mihai Tirsu*, ORCID: 0000-0002-1193-6774,
Irina Golub, ORCID: 0000-0001-8053-9329,
Danila Kaloshin, ORCID: 0000-0001-7194-2175

Institute of Power Engineering, 5 Academiei str., Chisinau, Republic of Moldova

**Corresponding author: Mihai Tirsu, tirsu.mihai@gmail.com*

Received: 05. 12. 2021

Accepted: 06. 28. 2021

Abstract. The electric power industry development mean increases the electric grids flexibility through the use of various devices type (FACTS) controlled by means of power electronics and being an element of the Smart Grid. This type of device includes a phase-shifting transformer (PST), which redistributes power flows in the branches of electrical networks. In connection with the relevance of this topic, new technical solutions appear that implement similar functions, which entails the need for a comparative analysis of such developments in order to optimize the energy characteristics of this kind of equipment. The aim of the work is to develop schematic version of the PST made according to the "star" scheme and analyze its operation in typical modes. During the study, the energy characteristics of the device were determined. The possibility of reducing the typical power of the phase-shifting device due to the use of capacitive compensation is analyzed.

Keywords: *phase-shifting transformer, angle of phase shift, electronic power switches, control strategy, rated capacity.*

Rezumat. Dezvoltarea industriei energiei electrice înseamnă creșterea flexibilității rețelelor electrice prin utilizarea diferitelor tipuri de dispozitive (FACT), controlate prin intermediul electronicii de putere și fiind un element al rețelei inteligente. Acest tip de dispozitiv include un transformator cu schimbare de fază (PST), care redistribuie fluxurile de energie în ramurile rețelelor electrice. În legătură cu relevanța acestui subiect, apar noi soluții tehnice care implementează funcții similare, ceea ce implică necesitatea unei analize comparative a acestor evoluții pentru a optimiza caracteristicile energetice ale acestui tip de echipamente. Scopul lucrării este de a dezvolta versiunea schematică a PST realizată conform schemei „stea” și de a analiza funcționarea acesteia în moduri tipice. În timpul studiului, au fost determinate caracteristicile energetice ale dispozitivului. Este analizată posibilitatea reducerii puterii tipice a dispozitivului de schimbare de fază datorită utilizării compensării capacitive.

Cuvinte cheie: *transformator cu schimbare de fază, unghi de schimbare de fază, întrerupătoare electronice de putere, strategie de control, capacitate nominală.*

[https://doi.org/10.52326/jes.utm.2021.28\(3\).06](https://doi.org/10.52326/jes.utm.2021.28(3).06)

CZU 685.34.017.8

FITNESS AND COMFORT ASSESSMENT OF FOOTWEAR: AN ANTHROPOMETRIC APPRAISAL

Adinife Patrick Azodo^{1*}, ORCID ID: 0000-0002-2373-1477,
Olasunkanmi Salami Isamaila^{1,2}, ORCID ID: 0000-0002-9875-8594,
Sampson Chisa Owzor², ORCID ID: 0000-0003-2126-7903

¹Department of Mechanical Engineering, Federal University of Agriculture Abeokuta, Nigeria

²Department of Mechanical Engineering, Federal University Wukari, Taraba state, Nigeria

*Corresponding author: Adinife Patrick Azodo, azodopat@gmail.com

Received: 06. 04. 2021

Accepted: 07. 12. 2021

Abstract. Suitability determination of any product designed for specific types of consumers is possible through the effective use of anthropometric information. This study assessed anthropometric data utilization in footwear designs and patterns as an indicator of fitness and comfort in footwear production. The data collected for analysis were the length and the breadth dimensions of footwear design pattern from eighteen footwear cottage shops and the foot anthropometric parameter from a total of four hundred and thirty-three (433) (males (226) and females (207)) subjects. The instrumentation design for the data collection was a digital vernier caliper (model Mitutoyo 500-506-10). The analysis of the foot anthropometry dimension and the design footwear pattern data obtained showed a lack of bilateral symmetry for the male and female gender. The fitness and comfortable foot support function of the footwear analyzed using a paired samples t-test between the footwear design pattern dimensions, and the foot anthropometric parameters disclosed $p > 0.05$ in all cases – not significant. This study concluded that tailoring a product design to the users' population reduces the mismatch challenges, grants fitness, and comfort to the users.

Keywords: *foot anthropometry, footwear, fitness, production, cottage firm.*

Rezumat. Determinarea adecvării oricărui produs conceput pentru anumite tipuri de consumatori este posibilă prin utilizarea eficientă a informațiilor antropometrice. Acest studiu a evaluat utilizarea datelor antropometrice în modele de încălțăminte ca indicator al fitnessului și confortului în producția de încălțăminte. Datele colectate pentru analiză au fost lungimea și lățimea dimensiunilor modelului de proiectare a încălțăminte de la optsprezece magazine de încălțăminte și parametrul antropometric al piciorului dintr-un total de patru sute treizeci și trei (433) bărbați (226) și femei (207). Proiectarea instrumentelor pentru colectarea datelor a fost un etrier digital vernier (model Mitutoyo 500-506-10). Analiza dimensiunii antropometriei piciorului și a datelor obținute din modelul de încălțăminte de proiectare a arătat o lipsă de simetrie bilaterală pentru sexul masculin și feminin. Funcția de fitness și suport confortabil pentru picioare a încălțăminte analizate folosind un test pereche între dimensiunile modelului de proiectare a încălțăminte și parametrii antropometrici ai picioarelor dezvăluite ($p > 0,05$ în toate cazurile) nu este semnificativ. Acest studiu a concluzionat că adaptarea unui design de produs la populația utilizatorilor reduce provocările de nepotrivire, acordă posibilitate de fitness și confort utilizatorilor.

Cuvinte cheie: *antropometrie a piciorului, încălțăminte, fitness, producție, firmă cottage.*

[https://doi.org/10.52326/jes.utm.2021.28\(3\).07](https://doi.org/10.52326/jes.utm.2021.28(3).07)
CZU 623.4.021+004.42

MULTIPLE CLASSIFICATION ALGORITHMS UNIMODAL AND MULTIMODAL TARGET RECOGNITION SYSTEMS

Veaceslav Perju*, ORCID ID: 0000-0002-7755-4277

Agency for Military Science and Memory, 47 Tighina Str., Chisinau, Republic of Moldova

**Corresponding author: Veaceslav Perju, vlperju@yahoo.com*

Received: 06. 11. 2021

Accepted: 08. 12. 2021

Abstract. Target recognition is of great importance in military and civil applications – object detection, security and surveillance, access and border control, etc. In the article the general structure and main components of a target recognition system are presented. The characteristics such as availability, distinctiveness, robustness, and accessibility are described, which influence the reliability of a TRS. The graph presentations and mathematical descriptions of a unimodal and multimodal TRS are given. The mathematical models for a probability of correct target recognition in these systems are presented. To increase the reliability of TRS, a new approach was proposed – to use a set of classification algorithms in the systems. This approach permits the development of new kinds of systems - Multiple Classification Algorithms Unimodal and Multimodal Systems (MAUMS and MAMMS). The graph presentations, mathematical descriptions of the MAUMS and MAMMS are described. The evaluation of the correct target recognition was made for different systems. The conditions of systems' effectiveness were established. The modality of the algorithm's recognition probability maximal value determination for an established threshold level of the system's recognition probability was proposed, which will describe the requirements for the quality and, respectively, the costs of the recognition algorithms. The proposed theory permits the system's design depending on a predetermined recognition probability.

Keywords: *target, recognition, system, unimodal, multimodal, algorithm, probability.*

[https://doi.org/10.52326/jes.utm.2021.28\(3\).07](https://doi.org/10.52326/jes.utm.2021.28(3).07)
CZU 623.4.021+004.42

MULTIPLE CLASSIFICATION ALGORITHMS UNIMODAL AND MULTIMODAL TARGET RECOGNITION SYSTEMS

Veaceslav Perju*, ORCID ID: 0000-0002-7755-4277

Agency for Military Science and Memory, 47 Tighina Str., Chisinau, Republic of Moldova

**Corresponding author: Veaceslav Perju, vlperju@yahoo.com*

Received: 06. 11. 2021

Accepted: 08. 12. 2021

Rezumat. Recunoașterea țintelor are o mare importanță în aplicațiile militare și civile - detectarea obiectelor, securitatea și supravegherea, accesul și controlul frontierelor etc. În articol sunt prezentate structura generală și principalele componente ale unui sistem de recunoaștere a țintelor (SRȚ). Sunt descrise caracteristicile precum disponibilitatea, caracterul distinctiv, robustețea și accesibilitatea, care influențează fiabilitatea unui SRȚ. Sunt date prezentările grafice și descrierile matematice ale unui SRȚ unimodal și multimodal. Sunt prezentate modele matematice pentru o probabilitate de recunoaștere corectă a țintei în aceste sisteme. Pentru a crește fiabilitatea SRȚ, a fost propusă o nouă abordare - utilizarea unui set de algoritmi de clasificare în sisteme. Această abordare permite dezvoltarea de noi tipuri de sisteme - Sisteme cu algoritmi de clasificare multiple unimodale și multimodale (SACMUM și SACMMM). Sunt date prezentările grafice, descrierile matematice ale SACMUM și SACMMM. Evaluarea recunoașterii țintei corecte a fost dată pentru diferite sisteme. Au fost stabilite condițiile de eficacitate a sistemelor. A fost propusă modalitatea de determinare a valorii maxime a probabilității de recunoaștere a algoritmului pentru un nivel de prag stabilit al probabilității de recunoaștere a sistemului, care va determina cerințele pentru calitate și, respectiv, costurile algoritmilor de recunoaștere. Teoria propusă permite proiectarea sistemului în funcție de o probabilitate de recunoaștere predeterminată.

Cuvinte cheie: țintă, recunoaștere, sistem, unimodal, multimodal, algoritm, probabilitate.

[https://doi.org/10.52326/jes.utm.2021.28\(3\).08](https://doi.org/10.52326/jes.utm.2021.28(3).08)
CZU 336.76:004.8

ARTIFICIAL INTELLIGENCE IN STOCK MARKET INVESTMENT

Badri Narayan Mohapatra*, ORCID ID: 0000-0003-1906-9932,
Bhagwat Nagargoje, Prajwal Zurunge, Suraj More

Savitribai Phule Pune University, AISSMS IOIT, Pune, INDIA

*Corresponding author: Badri Narayan Mohapatra, badri1.mohapatra@gmail.com

Received: 06. 28. 2021

Accepted: 08. 11. 2021

Abstract. This study investigates the selection of stock from huge stock markets and by using good selection tools so that it will give a good return value. It helps investor to find an easy decision regarding their investment in stock market individually with effective collection of trading activities. Many artificial intelligence (AI) techniques are untested in the financial crisis scenario. This research really helpful to the investor in the stock selection and stock purchase decision. AI is also a one of the hottest topic for most industries, researchers and investors. The financial market is easy to analyze with multiple charts, due to the application of artificial intelligence.

Keywords: *stock market, artificial intelligence, trading, investment, financial.*

Rezumat. Acest studiu investighează selecția acțiunilor de pe piețe imense de acțiuni și prin utilizarea unor instrumente de selecție bune, astfel încât să ofere o valoare rentabilă bună. Ajută investitorul să găsească o decizie ușoară în ceea ce privește investiția lor pe piața de valori individual, cu o colectare eficientă a activităților de tranzacționare. Multe tehnici de inteligență artificială (AI) nu sunt testate în scenariul de criză financiară. Această cercetare este foarte utilă pentru investitor în selectarea acțiunilor și decizia de cumpărare a acțiunilor. AI este, de asemenea, unul dintre cele mai fierbinte subiecte pentru majoritatea industriilor, cercetătorilor și investitorilor. Piața financiară este ușor de analizat cu mai multe diagrame, datorită aplicării inteligenței artificiale.

Cuvinte cheie: *bursă, inteligență artificială, tranzacționare, investiții, financiar.*

[https://doi.org/10.52326/jes.utm.2021.28\(3\).09](https://doi.org/10.52326/jes.utm.2021.28(3).09)
CZU 697.34:621.311.2

REGRESSION ANALYSIS OF THE ENERGY PRODUCED IN COGENERATION AND SUPPLIED TO DISTRICT HEATING SYSTEMS

Corina Chelmenciu*, ORCID ID: 0000-0002-5126-8539,
Constantin Borosan, ORCID ID: 0000-0003-1975-4577

Technical University of Moldova, 168 Stefan cel Mare blvd., Chisinau, MD-2004 Republic of Moldova

**Corresponding author: Corina Chelmenciu, corina.chelmenciu@tme.utm.md*

Received: 07. 15. 2021

Accepted: 08. 14. 2021

Abstract. Currently, the district heating systems (DHSs) are intensively promoted both nationally and globally. The advantages of using these systems in urban areas compared to individual heating systems are practically indisputable. Still, it is essential that the calculation underlying the assessment of the economic profitability of the projects to connect the new heat consumers to DHS be made correctly by taking into account all the necessary investments and the benefits obtained from the additional amount of energy sale. The article presents the methodology for the optimal regression model selection that can be applied to predict the additional electricity produced in cogeneration mode in case of the new heat consumer connection to the DHS, based on the actual data of the thermal and electrical energy supplied to network from a CHP in the Republic of Moldova. At the same time, it is demonstrated that between the thermal energy supplied to a new consumer connected to DHS and the additional electricity produced in the cogeneration mode, there is a direct and linear correlation.

Keywords: *cogeneration, equation of a straight line, heating season, new consumer's connection to the DHS, regression analysis.*

Rezumat. La momentul actual, sistemele centralizate de alimentare cu energie termică (SACET) sunt intens promovate atât la nivel național cât și la nivel mondial. Avantajele utilizării acestor sisteme în localități urbane în comparație cu sisteme individuale de încălzire, sunt practic incontestabile, dar este important ca calculul care stă la baza evaluării rentabilității economice a proiectelor de racordare a noilor consumatori la SACET, să fie realizat corect prin luarea în considerație a tuturor investițiilor necesare, cât și a beneficiilor obținute în rezultatul vânzării unei cantități suplimentare de energie. În lucrare este prezentată metodologia selectării modelului optim de regresie care poate fi aplicat în scopul predicției volumului de energie electrică suplimentară produsă în cogenerare în cazul racordării unui consumator nou de energie termică la SACET, în baza unor date reale ale valorilor energiilor termice și electrice livrate în rețea de la un CET din Republica Moldova. Totodată, este demonstrat faptul că între energia termică livrată unui consumator nou racordat la SACET și energia electrică suplimentară produsă în regim de cogenerare, există o corelație directă și liniară.

Cuvinte cheie: *cogenerare, ecuația liniei drepte, model de regresie, sezon de încălzire, racordarea unui nou consumator la SACET.*

[https://doi.org/10.52326/jes.utm.2021.28\(3\).10](https://doi.org/10.52326/jes.utm.2021.28(3).10)
CZU 693.54:666.972

DEVELOPMENT ULTRA-HIGH STRENGTH CEMENTITIOUS CHARACTERISTICS USING SUPPLEMENTARY CEMENTITIOUS MATERIALS*

Ameer Baiee*, ORCID ID: 0000-0001-5393-7022

Babylon University, Babylon, Iraq

*Corresponding author: Ameer Baiee, eng.ameer.tuama@uobabylon.edu.iq

Received: 06. 22. 2021

Accepted: 08. 12. 2021

Abstract. For sustainability purposes, supplementary cementitious materials (SCMs) are considered essential components for gaining ultra-high strength properties of concrete and mortar. This study experimentally investigates the influence of single, binary, and ternary partial cement replacements of the SCMs on the performance of ultra-high-strength mortar. The investigated SCMs were included ground granulated blast furnace slag (GGBS), densified silica fume (DSF), un-densified silica fume (UDSF), and Fly ash (FA). Three replacements ratios were implemented; 10%, 20%, and 30% in addition to mortar without SCMs to work as a control mix for comparison reasons. 27 mixes were designed to quantify the replacement ratio that explains the best performance, through examining the workability, compressive and tensile strength of each mix. In addition, XRD test was carried out to identify the various decomposition phases of the hardened mortar. The results indicated that binary replacement of 15% GGBS and 15% UDSF exhibited the best performance among all other replacements ratios.

Keywords: *binary replacement, supplementary cementitious materials, single replacement, ternary replacement, ultra-high strength, XRD patterns.*

Rezumat. În scopuri de durabilitate, materialele cimentare suplimentare (SCM) sunt considerate componente esențiale pentru obținerea proprietăților de rezistență ultra-înaltă a betonului și mortarului. Acest studiu investighează experimental influența înlocuirilor parțiale simple, binare și ternare de ciment ale SCM-urilor asupra performanței mortarului de înaltă rezistență. SCM-urile investigate au inclus zgură de furnal granulat la sol (GGBS), fum de silice densificat (DSF), fum de silice nedensificat (UDSF) și cenușă zburătoare (FA). Au fost implementate trei rapoarte de înlocuire, cu respectiv 10%, 20% și 30% în plus față de mortarul fără SCM, un amestec de control pentru comparație. 27 de amestecuri au fost proiectate pentru a cuantifica raportul de înlocuire care explică cele mai bune performanțe, examinând lucrabilitatea, rezistența la compresiune și la tracțiune a fiecărui amestec. În plus, s-a efectuat testul XRD pentru a identifica diferitele faze de descompunere a mortarului întărit. Rezultatele au indicat faptul că înlocuirea binară a 15% GGBS și 15% UDSF a prezentat cea mai bună performanță dintre toate celelalte rapoarte de înlocuire.

Cuvinte cheie: *înlocuire binară, materiale cimentare suplimentare, înlocuire unică, înlocuire ternară, rezistență ultra-mare, modele XRD.*

[https://doi.org/10.52326/jes.utm.2021.28\(3\).11](https://doi.org/10.52326/jes.utm.2021.28(3).11)
CZU 628.17:681.515

PERFORMANCE STUDIES ON WATER FLOW CONTROL USING P, PI AND PID CONTROLLERS

Ramesh Babu Aremanda*, ORCID ID: 0000-0002-6609-8640,
Nahom Yohannes, ORCID ID: 0000-0001-8926-5141,
Yosief Ghezae, ORCID ID: 0000-0001-9602-3546

*Department of Chemical Engineering, Mai Nefhi College of Engineering & Technology (MCOETEC), P.O. Box 344,
Asmara, Eritrea.*

*Corresponding author: Ramesh Babu Aremanda, ramesh.nitrkl@gmail.com

Received: 05. 28. 2021

Accepted: 08. 11. 2021

Abstract. The main purpose of this study is to revitalize the concept of wise and controlled supply of water for domestic, industrial and agricultural applications which facilitate sustainable usage of fresh water resources. As Eritrea is striving to manage its water resources, attention paid primarily to enable water flow control mechanisms in municipal water distribution systems. A table top process control trainer (PCT) was tested through proportional(P), integral (I) and derivative (D) control mechanisms using Ziegler-Nichols second method to evaluate the tuning variables. Applying exclusively P control action, critical period of oscillation (P_{cr}) was estimated as 1.4 sec at proportional band value of 9. P, PI and PID controller performance studies were conducted with tuned variables on the water flow control system at different step disturbances between 20 – 50 % and their corresponding responses were characterized. P controller exhibited faster responses with consistent increments in offset, PI controller recorded highest overshoot values with negligible offset and prolonged settling times. PID controller showed less overshoot values and faster response times than PI but it increased chatter on the control output signal. The study revealed that the system can be safely controlled between 0-80 LPH. If the offset is not a major concern, P controller would be reflected suitable with simple design and minimum expenditure, else PI controller makes offset to zero though it possesses higher settling times. In other words, PID controller is complex using more tuning parameters, need expensive maintenance, and has resulted an intermittent noise in the output signal.

Keywords: *Control System, Flow controllers, Step Disturbances, Sustainable Supply of Water, Tuning of PID Controllers, Water Flow control, Ziegler and Nichols Method.*

[https://doi.org/10.52326/jes.utm.2021.28\(3\).11](https://doi.org/10.52326/jes.utm.2021.28(3).11)
CZU 628.17:681.515

PERFORMANCE STUDIES ON WATER FLOW CONTROL USING P, PI AND PID CONTROLLERS

Ramesh Babu Aremanda*, ORCID ID: 0000-0002-6609-8640,
Nahom Yohannes, ORCID ID: 0000-0001-8926-5141,
Yosief Ghezae, ORCID ID: 0000-0001-9602-3546

*Department of Chemical Engineering, Mai Nefhi College of Engineering & Technology (MCOETEC), P.O. Box 344,
Asmara, Eritrea.*

*Corresponding author: Ramesh Babu Aremanda, ramesh.nitrkl@gmail.com

Received: 05. 28. 2021

Accepted: 08. 11. 2021

Rezumat. Scopul principal al acestui studiu este de a revitaliza conceptul de furnizare înțeleaptă și controlată de apă pentru aplicații menajere, industriale și agricole care facilitează utilizarea durabilă a resurselor de apă dulce. Întrucât Eritreea se străduiește să își gestioneze resursele de apă, atenția este acordată în primul rând pentru a permite mecanismelor de control al fluxului de apă în sistemele municipale de distribuție a apei. Un antrenor de control de proces de masă (PCT) a fost testat prin mecanisme de control proporțional (P), integral (I) și derivat (D) folosind a doua metodă Ziegler-Nichols pentru a evalua variabilele de reglare. Aplicând exclusiv acțiunea de control P, perioada critică de oscilație (P_c) a fost estimată la 1,4 sec cu o valoare proporțională a benzii de 9. Studiile de performanță ale controlerelor P, PI și PID au fost efectuate cu variabile reglate pe sistemul de control al debitului de apă la diferite perturbări de pas între 20 - 50% și răspunsurile lor corespunzătoare au fost caracterizate. Controlerul P a prezentat răspunsuri mai rapide cu creșteri consistente în offset, controlerul PI a înregistrat cele mai mari valori de depășire cu offset neglijabil și timpi de decontare prelungite. Controlerul PID a prezentat valori mai mici de depășire și timpi de răspuns mai rapide decât PI, dar a crescut conversația pe semnalul de ieșire al controlului. Studiul a relevat că sistemul poate fi controlat în siguranță între 0-80 LPH. Dacă decalajul nu prezintă o preocupare majoră, controlerul P ar fi reflectat adecvat cu un design simplu și cheltuieli minime. Altfel controlerul PI face decalajul la zero, deși are timpi de decontare mai mari. Cu alte cuvinte, controlerul PID este complex, folosind mai mulți parametri de reglare, necesită o întreținere costisitoare și a rezultat un zgomet intermitent în semnalul de ieșire.

Cuvinte cheie: *sistem de control, regulatoare de debit, perturbări în trepte, alimentare durabilă cu apă, reglarea controlerelor PID, control al debitului de apă, metoda Ziegler și Nichols.*

[https://doi.org/10.52326/jes.utm.2021.28\(3\).12](https://doi.org/10.52326/jes.utm.2021.28(3).12)
CZU 663.1:[637.146+663.81]

MICROENCAPSULATION OF FUNCTIONAL COMPONENTS IN THE FOOD TECHNOLOGY: PARTIALLY OPTIMISTIC VIEW

Alexei Baerle*, ORCID ID: 0000-0001-6392-9579

*Technical University of Moldova, 168 Stefan cel Mare Blvd., MD-2004,
Chişinău, Republic of Moldova*

*Corresponding author: Alexei Baerle, alexei.baerle@chim.utm.md

Received: 07. 03. 2021

Accepted: 08. 16. 2021

Abstract. This work deals with the use of microencapsulation of biologically active compounds (BAC) as an alternative method of protection and prolongation of their functional properties in the food products. The main methods for the formation of microcapsules (MC) are considered. Biopolymer materials, suitable for MCs production, are outlined. Some technological solutions, suitable for microencapsulation and successfully used in other industries, present interest only for laboratory researches in the food science, but are not suitable for industrial scale food production. It is discussed why the methods of simple and complex coacervation, liposomal entrapment are thermodynamically advantageous for obtaining microcapsules in comparison with others. To achieve further progresses of microencapsulation in food technologies, the direct integration of the microencapsulation into the food production technological cycle is necessary. Products should initially have a texture and consistency that allow microcapsules to be resistant to premature aggregation. MCs should not exfoliate or break down, while execute their functions of protection and targeted delivery of biologically active compounds. Only high viscous colloidal systems, as traditional fermented dairy products (kefir, yoghurts, ice cream, curd and cheese) and fruit juices with pulp, are mostly suitable for supplementation of them by BACs using microencapsulation.

Keywords: *biopolymers, biologically active compounds (BAC), coacervation, complex coacervation, fermented dairy products, microencapsulation's thermodynamic.*

[https://doi.org/10.52326/jes.utm.2021.28\(3\).12](https://doi.org/10.52326/jes.utm.2021.28(3).12)
CZU 663.1:[637.146+663.81]

MICROENCAPSULATION OF FUNCTIONAL COMPONENTS IN THE FOOD TECHNOLOGY: PARTIALLY OPTIMISTIC VIEW

Alexei Baerle*, ORCID ID: 0000-0001-6392-9579

*Technical University of Moldova, 168 Stefan cel Mare Blvd., MD-2004,
Chişinău, Republic of Moldova*

*Corresponding author: Alexei Baerle, alexei.baerle@chim.utm.md

Received: 07. 03. 2021

Accepted: 08. 16. 2021

Rezumat. Această lucrare se referă la utilizarea microîncapsulării compușilor biologic activi ca metodă alternativă de protecție și prelungire a proprietăților lor funcționale în produsele alimentare. Sunt luate în considerare principalele metode de formare a microcapsulelor și prezentate materiale biopolimerice, utilizate pentru producția MC comestibile. Unele soluții tehnologice, potrivite pentru microîncapsulare și folosite cu succes în alte industrii, prezintă interes numai pentru cercetările de laborator în cadrul științei alimentelor, dar nu sunt potrivite pentru producția de alimente pe scară industrială. Se discută avantajele termodinamice ale metodelor de coacervare simplă și complexă, „prinderii lipozomale” pentru obținerea microcapsulelor în comparație cu alte metode. Pentru realizarea progreselor ulterioare ale microîncapsulării în tehnologiile alimentare este necesară integrarea directă a microîncapsulării în ciclul tehnologic al producției de alimente. Produsele ar trebui să aibă inițial o textură și o consistență, care ar permite microcapsulelor să fie rezistente la agregarea prematură. Microcapsulele nu trebuie să se exfolieze sau să se descompună în timp ce își îndeplinesc funcțiile de protecție și livrare țintită a compușilor biologic activi. Doar sistemele coloidale cu vâscozitate ridicată, ca exemplu, produse lactate fermentate tradiționale (chefir, iaurturi, înghețată, caș și brânză) și sucurile de fructe cu pulpă sunt potrivite pentru suplimentarea acestora cu compuși bioactivi incluși prin procedee de microîncapsulare.

Cuvinte cheie: *biopolimeri, compuși biologic activi, coacervare, coacervare complexă, produse lactate fermentate, termodinamica microîncapsulării.*

[https://doi.org/10.52326/jes.utm.2021.28\(3\).13](https://doi.org/10.52326/jes.utm.2021.28(3).13)
CZU 637.146.34:634.7

THE ROLE OF BERRIES IN QUALITY AND SAFETY ENSURING OF GOAT'S AND COW'S MILK YOGHURT

Tatiana Cușmenco*, ORCID ID: 0000-0001-6628-0752,
Elisaveta Sandulachi, ORCID ID: 0000-0003-3017-9008,
Viorica Bulgaru, ORCID ID: 0000-0002-1921-2009,
Artur Macari, ORCID ID: 0000-0003-4163-3771

Technical University of Moldova, 168 Stefan cel Mare blvd., Chisinau, Republic of Moldova

*Corresponding author: Tatiana Cușmenco, tatiana.cusmenco@sa.utm.md

Received: 06. 27. 2021

Accepted: 08. 25. 2021

Abstract. The yogurt was obtained from a combination of 50% goat's milk and 50% cow's milk with the inclusion of scald fruits of aronia (*Aronia melanocarpa*), raspberries (*Rubus idaeus*), strawberry (*Fragaria xanassa*). Physico-chemical and microbiological indices were determined, according to standard methods, after manufacture and storage, after 1, 5, 10, 15 days. Compared to other samples, yogurt with aronia showed the best values of the dynamics specific to the development of microorganisms: $2.93 \cdot 10^7$ cfu/ml; the growth rate of lactic acid bacteria at fermentation 0.95μ ; physico-chemical indices: titratable acidity $85 \pm 0.078^\circ\text{T}$, pH 4.28 ± 0.002 , water activity 0.875 ± 0.025 ; total dry matter $18.45 \pm 0.31\%$, viscosity 2500 ± 0.023 mPa s, ash content $0.89 \pm 0.10\%$ and the optical density 2.531 ± 0.054 nm. Yeasts and molds were not detected in any of the samples. From a physico-chemical point of view, in storage, in all fruit yogurt samples the titratable acidity showed increasing values, pH remaining in the range of permissible values. In storage fruits formed an association to control the microbiological risk and stability of yogurt. Fruit yogurt shows a synergism with *Streptococcus thermophilus*, *Lactobacillus delbrueckii subsp. bulgaricus*, *Lactococcus lactis subsp lactis biovar diacetylactis*. The overall Pearson coefficient ($P_c = f(\text{pH and MC})$ for all fruit yogurt samples is -0.95066 .

Keywords: fermentation, growth curve, lactic acid, lactic acid bacteria, metabolic process, microbial counts (MC), starter culture, synergism.

[https://doi.org/10.52326/jes.utm.2021.28\(3\).13](https://doi.org/10.52326/jes.utm.2021.28(3).13)
CZU 637.146.34:634.7

THE ROLE OF BERRIES IN QUALITY AND SAFETY ENSURING OF GOAT'S AND COW'S MILK YOGHURT

Tatiana Cușmenco*, ORCID ID: 0000-0001-6628-0752,
Elisaveta Sandulachi, ORCID ID: 0000-0003-3017-9008,
Viorica Bulgaru, ORCID ID: 0000-0002-1921-2009,
Artur Macari, ORCID ID: 0000-0003-4163-3771

Technical University of Moldova, 168 Ștefan cel Mare blvd., Chisinau, Republic of Moldova

*Corresponding author: Tatiana Cușmenco, tatiana.cusmenco@sa.utm.md

Received: 06. 27. 2021

Accepted: 08. 25. 2021

Rezumat. Iaurtul a fost obținut dintr-o combinație de 50% lapte de capră și 50% lapte de vacă cu includerea fructelor opărite de aronia (*Aronia melanocarpa*), zmeură (*Rubus idaeus*) și căpșuni (*Fragaria xanassa*). Indicii fizico-chimici și microbiologici au fost determinați conform metodelor standard, după fabricare și depozitare timp de 1, 5, 10, și 15 zile. Comparativ cu alte probe, iaurtul cu aronia a arătat cele mai bune valori ale dinamicii specifice dezvoltării microorganismelor: $2.93 \cdot 10^7$ cfu / ml; rata de creștere a bacteriilor lactice la fermentare $0,95 \mu$; indici fizico-chimici: aciditate titrabilă $85 \pm 0,078^\circ\text{T}$, pH $4,28 \pm 0,002$, activitate a apei $0,875 \pm 0,025$, substanță uscată totală $18,45 \pm 0,31\%$, vâscozitate $2500 \pm 0,023$ mPa s, conținut de cenușă $0,89 \pm 0,10\%$ și densitatea optică $2,531 \pm 0,054$ nm. Drojdiile și mușgaiurile nu au fost detectate în niciuna dintre probe. Din punct de vedere fizico-chimic, în depozitare, în toate probele de iaurt de fructe, aciditatea titrabilă a prezentat valori crescătoare, pH rămânând în intervalul valorilor admise. Din punct de vedere microbiologic, în depozitare fructele au format o asocierie pentru a controla riscul microbiologic și stabilitatea iaurtului. Iaurtul de fructe prezintă un sinergism cu *Streptococcus thermophilus*, *Lactobacillus delbrueckii* subsp. *bulgaricus*, *Lactococcus lactis* subsp. *lactis* biovar *diacetylactis*. Coeficientul general Pearson ($P_c = f(\text{pH și MC})$) pentru toate probele de iaurt de fructe este $-0,95066$.

Keywords: acid lactic, bacterii lactice, cultură starter, curba de creștere, fermentare, număr de microorganisme, proces metabolic, sinergism.

[https://doi.org/10.52326/jes.utm.2021.28\(3\).14](https://doi.org/10.52326/jes.utm.2021.28(3).14)
CZU 638.165.8:581.331.2(478)

PALYNOLOGICAL, PHYSICO-CHEMICAL AND BIOLOGICALLY ACTIVE SUBSTANCES PROFILE IN SOME TYPES OF HONEY IN THE REPUBLIC OF MOLDOVA

Aurica Chirsanova*, ORCID ID: 0000-0002-1172-9900,
Tatiana Capcanari, ORCID ID: 0000-0002-0056-5939,
Alina Boistean, ORCID ID: 0000-0002-5374-5853

Department of Food and Nutrition, Technical University of Moldova, 168 Stefan cel Mare Blvd., MD-2004, Chişinău, Republic of Moldova

*Corresponding author: Aurica Chirsanova, aurica.chirsanova@toap.utm.md

Received: 07. 10. 2021

Accepted: 08. 28. 2021

Abstract. Three types of monofloral honey (rapeseed honey, buckwheat and lavender) from the Republic of Moldova were analyzed. The results of the palynological analysis showed that the samples had a dominant type of pollen (at least 45%). In the case of lavender honey, the pollen of the plant *Lavandula angustifolia* is present in an average value of 74.83 ± 0.3 ; in rapeseed honey - *Brassica napus* and for buckwheat honey - *Fagopyrum esculentum* in average values as follows: 56.07 ± 0.3 and $68.08 \pm 0.2\%$ respectively. The study of the content of biologically active substances showed that buckwheat honey is the richest in polyphenols (9.00 ± 0.11 mg gallic acid / kg) and carotenoids (4.24 ± 0.57 mg β carotE / kg), and maximum content of flavonoids is in rapeseed honey (4.52 ± 0.28 mg catechin / kg). Thus, the obtained results confirm that the honey from the Republic of Moldova falls within the limits recommended by the international regulation assuming adequate working conditions, handling, collection and storage of honey by beekeepers from the Republic of Moldova.

Keywords: honey, palynological analysis, physico-chemical properties, biologically active substances.

Rezumat. Au fost analizate trei tipuri de miere monoflorală (miere de rapiță, hrișcă și lavandă) din Republica Moldova. Rezultatele analizei palinologice au arătat că probele au avut un tip de polen dominant (cel puțin 45%). În cazul mierii de lavandă este prezent polenul plantei *Lavandula angustifolia* în valoare medie de $74,83 \pm 0,3$; în mierea de rapiță - *Brassica napus* și pentru mierea de hrișcă - *Fagopyrum esculentum* în valori medii după cum urmează: $56,07 \pm 0,3$ și $68,08 \pm 0,2\%$ respectiv. Studiul conținutului substanțelor biologice active a arătat că mierea de hrișcă este cea mai bogată în polifenoli ($9,00 \pm 0,11$ mg gallic acid/kg) și caratenoide ($4,24 \pm 0,57$ mg β carotE/kg), iar conținut maximal de flavanoide este în mierea de rapiță ($4,52 \pm 0,28$ mg catechin/kg). Astfel, rezultatele obținute confirmă că mierea din Republica Moldova se încadrează în limitele recomandate de reglementarea internațională presupunând condiții adecvate de lucru, de manipulare, colectare și depozitare a mierii de către apicultorii din Republica Moldova.

Cuvinte cheie: miere, analiză palinologică, proprietăți fizico-chimice, substanțe biologice active.

[https://doi.org/10.52326/jes.utm.2021.28\(3\).15](https://doi.org/10.52326/jes.utm.2021.28(3).15)
CZU 663.252.61:579

DEVELOPMENT OF THE REAL-TIME PCR METHODOLOGY FOR TESTING MYCOTOXIGENIC MICROORGANISMS IN GRAPE MARC

Rodica Sturza¹, ORCID ID: 0000-0002-2412-5874,
Valentin Mitin², ORCID ID: 0000-0001-9328-9672,
Irina Mitina², ORCID ID: 0000-0002-1550-6739,
Dan Zgardan^{1*}, ORCID: 0000-0002-1296-0864,
Antoanela Patras³, ORCID ID: 0000-0002-4054-4884,
Emilia Behta^{1,4}, ORCID ID: 0000-0001-8519-9714

¹Technical University of Moldova, 168 Stefan cel Mare Blvd., Chisinau, RM

²Institute of Genetics, Physiology and Plant Protection, 20 Pădurilor st., Chisinau, RM

³"Ion Ionescu de la Brad" Iasi University of Life Sciences, 3 Mihail Sadoveanu Alea, Iași, Romania

⁴"Nicolae Testemitanu" State University of Medicine and Pharmacy, 165 Stefan cel Mare Bd., Chisinau, RM

*Corresponding author: Dan Zgardan, dan.zgardan@enl.utm.md

Received: 07. 23. 2021

Accepted: 08. 28. 2021

Abstract. Agro-industrial waste management is an important problem of modern society as agriculture and food industry are important sources of waste. Wine production generates a considerable amount of winemaking waste (grape marc). Grape marc can be a source of natural dyes, antioxidants and could have various applications, if it is confirmed that it does not contain technogenic contaminants or unwanted microorganisms, for example, producers of mycotoxins. The paper developed the Real -Time Polymerase Chain Reaction (Real-Time PCR) methodology for testing the presence of potentially mycotoxigenic fungal species capable of producing ochratoxin A (OTA), which could be applied before grape marc processing. Based on the non-ribosomal peptide sequence of OTA, involved in ochratoxin biosynthesis, the primers have been developed for the detection of microorganisms potentially capable of producing ochratoxin A.

Keywords: *Mycotoxin, OTA, Real-Time PCR, grape marc, Aspergillus, Penicillium.*

Rezumat. Gestionarea deșeurilor agroindustriale prezintă o problemă importantă a societății moderne, deoarece agricultura și industria alimentară sunt surse importante de deșeuri. Producția de vin generează o cantitate considerabilă de deșeuri de vinificație (tescovină de struguri). Tescovina de struguri poate fi o sursă de coloranți naturali, antioxidanți și ar putea avea diverse aplicații, dacă se confirmă că nu conține contaminanți tehnogeni sau microorganisme nedorite, de exemplu, producători de micotoxine. Lucrarea a dezvoltat metodologia de reacție în lanț a polimerazei în timp real (PCR în timp real) pentru testarea prezenței speciilor fungice potențial micotoxigene capabile să producă ochratoxină A (OTA), care ar putea fi aplicată înainte de prelucrarea tescovinei de struguri. Pe baza secvenței peptidice non-ribozomale a OTA, implicată în biosinteza ochratoxinei, au fost dezvoltate primerii necesari pentru detectarea microorganismelor potențial capabile să producă ochratoxina A.

Cuvinte cheie: *Micotoxină, OTA, PCR în timp real, tescovină de struguri, Aspergillus, Penicillium.*

[https://doi.org/10.52326/jes.utm.2021.28\(3\).01](https://doi.org/10.52326/jes.utm.2021.28(3).01)

CZU 004.94



INDUSTRIALS SIMULATION MODELING TECHNOLOGY APPLICATION TO IMPROVE THE EFFICIENCY IN AUTOMATIC PRODUCTION LINE EQUIPMENT

Tuan-Linh Nguyen*, ORCID ID: 0000-0002-1960-9794

Department of Mechanical Engineering, Hanoi University of Industry, Hanoi City, Vietnam

*Corresponding author: Tuan-Linh Nguyen, nguyentuanlinh@hau.edu.vn

Received: 06. 12. 2021

Accepted: 08. 06. 2021

Abstract. Currently, the application of technical advances to production plays an important role in improving productivity and saving production costs. The techniques applying information technology bring high efficiency, accuracy, reliability, pre-assessment of the results. Modeling and simulation are method that are widely used from research, design, manufacturing to operate the systems. With the help of computers, with high computational speed and large memory, the modeling method was strongly developed, bringing great efficiency in research and production practice. The assessment of effective use of equipment in the production line has a decisive role in increasing the productivity and decreasing cost. Therefore, the analysis and evaluation of the production line by the simulation model method is highly practical, bringing many effects in the management and use of equipment. In this study, a simulation of a specific problem was performed to estimate the simulated workshop. Then, building a new plan and comparing the proposed plane with the original plan to provide the reasonable solutions for the production process to effectively use the equipment in the production line.

Keywords: *modeling and simulation, effective use, equipment, automatic production line.*

Introduction

Today it is possible to see that all areas of human activity use the method of modeling and simulation at different levels. This is especially important in the realm of controlling technical and social systems because control is the process of acquiring information from the system, identifying the system according to a certain pattern and delivering decide appropriate to control the system [1]. This process is continued continuously to bring the movement system to a predetermined goal. Through modeling and simulation, we can analyze, study complex systems, determine the operating characteristics and behaviors of the systems. The simulation results are used to design, manufacture as well as determine the operating mode of the system. From there, thanks to the method of modeling and simulation, it is possible to give many scenarios to choose the optimal plan. The simulation model can be used in the following 4 categories:

- Device explanation to identify the system or problem.
- Analysis to identify elements, components and events related to the system.

- Inspect the general design and evaluate proposed solutions.
- Predict and assist in future development planning.

Nowadays, besides the aforementioned method, the simulation method is strongly developed and widely applied. Models that are built on a simulation method are called simulation models or numerical models. Simulation method allows to bring into the model many factors close to reality. Simultaneously, the model is solved on computers with fast calculation speed and large capacity, so the results obtained are highly accurate [2]. Therefore, the simulation method has created conditions to solve complex problems such as modeling problems with large, random, and nonlinear systems with time-varying parameters [3]. The simulation method is especially effective when it is necessary to model large systems whose basic feature is a hierarchical structure, a subsystem structure, between subsystems and the control center exchange information with each other. Simulation method is also effective when modeling systems with random elements, inadequate information, information will be added during simulation, during the information exchange between people controls with objects [4, 5]. Simulation method is applied to model in many fields such as engineering, economics, society, biology, especially large, complex systems, etc. with many random affecting factors [6]. In addition, the application of artificial intelligence and neural networks is a development direction for technology solutions [7].

In the system design stage, modeling helps the designer to select the structure and parameters of the system to synthesize the system. At the fabrication stage, modeling helps to choose materials and fabrication technology. At the system operation stage, modeling helps the operator solve the optimization problems, predict system states.

Especially in the case of combining the expert system with modeling method, it can solve many control problems, save time as well as material and financial costs.

Material and Methods

The production system includes many functional subsystems such as supplying materials, energy, processing, and processing; assembling and completing products; consumption distribution. The production process control is the control center. The input of the system is the customer's order, the output of the system is the final product.

From the figure 1, we see that in a control system, there are many elements commonly called entities, each with its properties. A process that causes a change in the system is called an activity. An action that changes the system's state is called an event. The set of variables that reflect the state of the system at a time is called state variables.

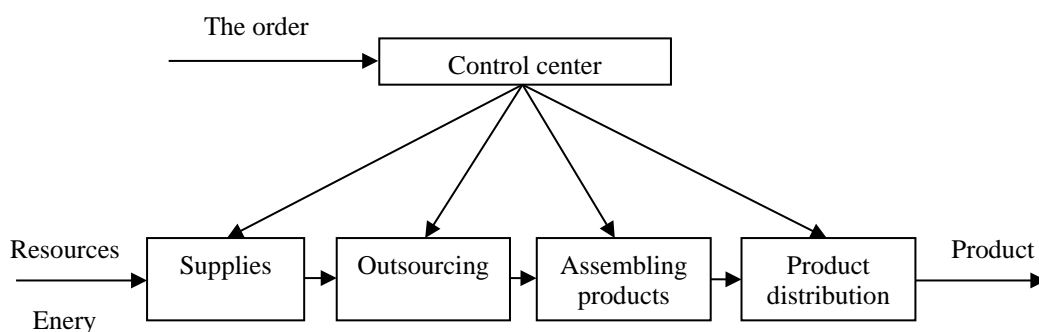


Figure 1. Production process control system.

There are two methods of studying the system: research on the real system and research on its substitution model. It is clear that research on the real systems gives honest and objective results. However, in many cases conducting research on real systems faces many difficulties, so the best and most convenient method is to study on its model. That is why the modeling method is focused on research and development and this method plays an important role in the development of science and technology [8].

The modeling process is carried out as follows. Call the simulated system S . The first step is to model the system S with its internal relationships. For convenience in modeling, we often divide the S system into several subsystems according to certain criteria $S = S_1, S_2, \dots, S_i, \dots, S_n$. Next, mathematically describe the subsystems and their relationships. Usually there is a relationship of energy exchange and information exchange between subsystems. The second step is to model the surrounding environment E , where the system S works, with the interactive relationships between S and E . Once the model of S and E is available, conducting the above experiments model, i.e., for S and E to work in a certain condition. The result is a set of system parameters, often referred to as the determination of a system work point. These experiments were repeated many times and the simulation results were evaluated by statistical probability. The simulation results are more accurate if the number of experiments, also known as simulation steps, is larger. In theory the simulation step are finite but must be large enough and depends on the requirement of accuracy.

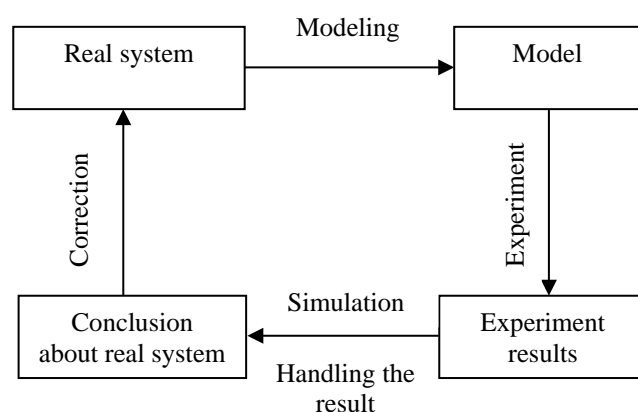


Figure 2. The process of research by simulation method.

When conducting simulation studies, it is often performed the following steps:

Step 1: Develop simulation goals and research plans

The first is to clearly define the simulation research objective. That goal is represented by evaluation criteria, by a system of questions that need to be answered.

Step 2: Collect data and define the principal model M

Depending on the simulation goal, we collect the information and corresponding data of S system and E environment. On that basis, we build the principal model M . The principal model that is the anti-mathematical model reflect the nature of the S -system.

Step 3: Validate the principal model

Validation of the model principal is to check the model's validity. A principal model must reflect the true nature of system S and E environment but at the same time must not be too complicated and cumbersome. If the principal model M fails to meet the requirements, it is necessary to collect more information and data to rebuild the model.

Step 4: Build an M simulation on the computer

Mmp simulation models are programs that run on computers also known as numerical modeling or simulation models. These programs are written in common languages such as FORTRAN, PASCAL, C ++ or specialized languages for simulation such as GPSS, SIMSCRIPT, SLAM II, SIMPLE ++, and so on.

Step 5: Test run.

After installing the program, run the test to see if the simulation model correctly reflects the system S and E environment characteristics. At this stage also fixes programming errors.

Step 6: Verify the simulation model.

After the test run, it is possible to verify and evaluate whether the simulation model is satisfactory or not, if not, go back from step 2.

Model validation and validation are two important procedures for verifying that the built model should be usable or not. Verification is to check whether the programming is correct, the computer program can run, the input and output data is convenient and accurate or not. Validation of the model is to evaluate whether the model reflects the nature of the real system or not, whether the simulation results meet the research requirements.

Step 7: Planning the simulation experiment

In this step some simulation conditions must be defined. The first is to determine the first condition, the final condition, or the simulation length. Next to determine the number of tests, also known as the number of independent simulation runs. For the simulation data to be completely independent of each other, each run the simulation uses a different random seed. Finally determine the simulation time of each part or whole model. Based on the simulation results (in step 9) calibrate the experimental plan to get results with the precision required.

Step 8: Simulation experiment

Run the test program according to the built plan in step 7. This is the step to perform the simulation. The results from this step are simulation output.

Step 9: Processing simulation results

Simulation experiments often give lots of data with statistical probability. Therefore, to get the final result with high accuracy, it is required to use statistical probability method to process the output data. These results should be presented in an explicit format conducive to storage and use.

Step 10: Use and store results

Use the simulation results for the intended purpose and archive them as documents that can be used over and over again.

Application of modeling and simulation for automatic production line***Requirements of the problem***

When building an automatic production line, the problem is from the requirement of productivity, labor, and equipment to be used effectively to avoid expensive investment or not using up the equipment, machinery and labor. The following is a simulation model that simulates an automatic painting workshop, for example a simulation model of a mobile phone cover coating workshop.

The steps in the model are as follows:

1. Embryos of the foundry of the foundry have been treated with burr and check for errors and defects and are sent to the paint shop for painting and plating as required.
2. The product will be put into the coating machine under the hanging conveyor. After going through the paint machine, it will be transferred to the drier to dry the product and continue to the aluminum plating machine. Finally, the product will be checked by the worker to remove the defects, if the product has any error, it will be transferred to the drier position for re-implementation. Products are made in the workshop through the steps below.

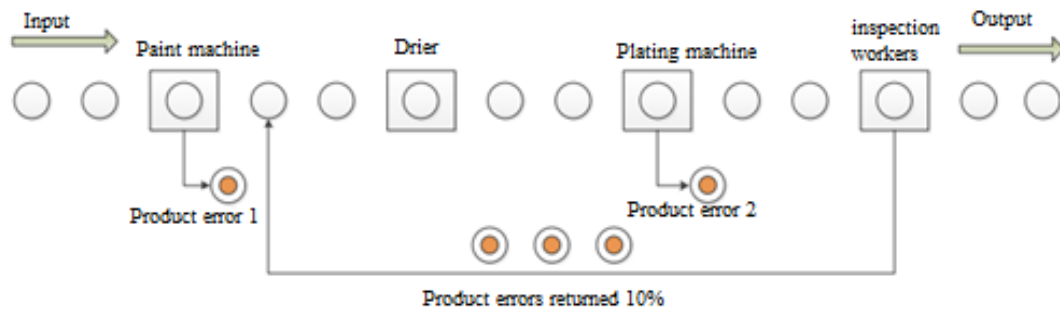


Figure 3. Painting and plating workshop diagrams.

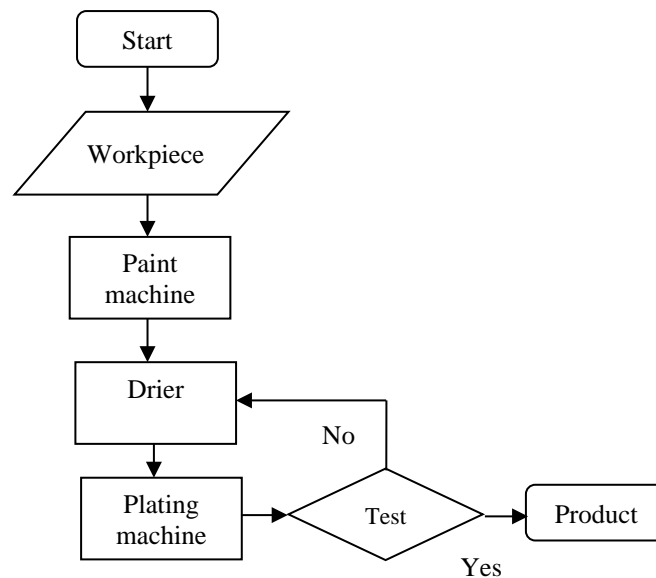


Figure 4. Painting and plating workshop block diagrams.

Computer animation is used for the purpose of judging true or false or to depict the system developed and shown below.

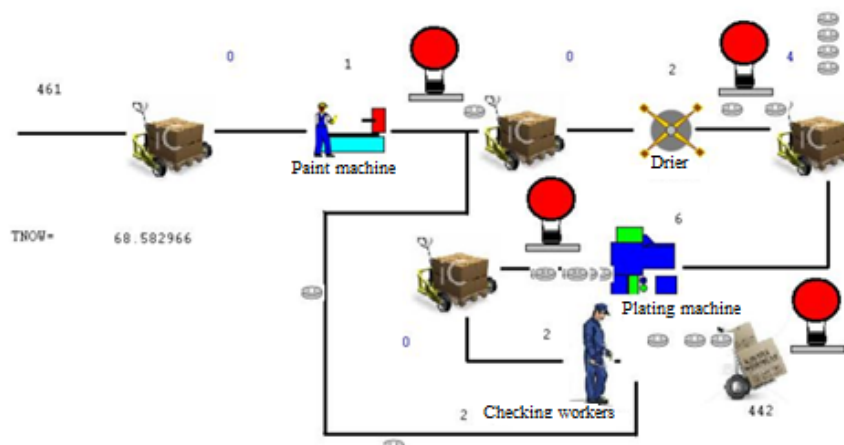


Figure 5. Model of painting and plating workshop scene.

The operation mode of the workshop is as follows:

1. The plastic billet is taken to the paint machine area to paint the product.
2. They are then transported to the drier for drying.
3. They are then shipped to the chrome plating machine.
4. Finally, they go to the site of the inspector to check the quality of the product surface. If guaranteed, they would be shipped to the next factory. Otherwise, they will be transported back to the drier site for drying or to an aluminum plating machine for rework.

The operation of the system will be simulated under the following assumptions:

1. The arrival times between the two products for the paint machine is exponentially functional with a value of 0.14 minutes.
2. The paint machines operate side by side and the delivery time is a uniform probability between 0.15 and 0.25 minutes.
3. The driers also operate side by side and the delivery time is a uniform probability between 0.25 and 0.35 minutes.
4. The plating machines also operate side by side with uniform distribution time between 0.4 and 1 minute.
5. The inspection workers also work side by side at the test stations. The distribution time as uniform probability is between 0.2 and 0.3 minutes. On average about 90% meet the requirements and move on to the next workshop. The remaining 10% of defective products will be sent back to the drier for rework and returned every 10 minutes.
6. Defective products after painting and plating operations are automatically classified. The classification time is 1 minute.

Production line modeling

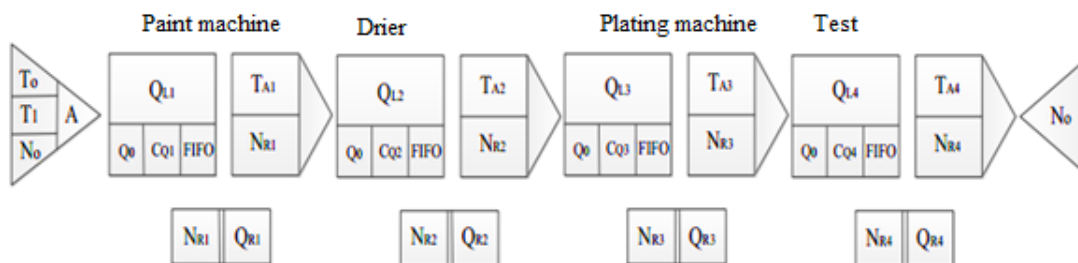


Figure 6. Modeling of the steps of the painting and plating process.

In which:

1. Input (ENTRANCE):

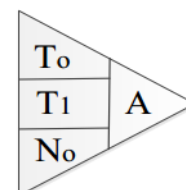
Functions: Simulates incoming objects.

Properties:

T_0 : Time between next visits; T_1 : Time of the first arrival of the object.

N_0 : Maximum number of objects possible through the node.

A : Properties of the object.



2. Queue (QUERY):

Function: Simulate the queue.

Properties:

QL: The current length of the queue; Q0: Recommended queue length.

CQ: The capacity of the queue.

OQ: Service principle: FIFO (first in first out), LIFO (first in, first out), priority.

3. Activities (ACTIVITY):

Function: Simulate serving.

Properties:

TA: Time during the service; NR: Number of sources performing service.

4. Source (RESOURCES):

Functions: Simulating a source is available.

Properties:

NR: Number of sources; QR: The ability of the source.

5. Ending (EXIT):

Functions: Simulates leaving objects.

Properties:

No: Number of objects leaving the system.

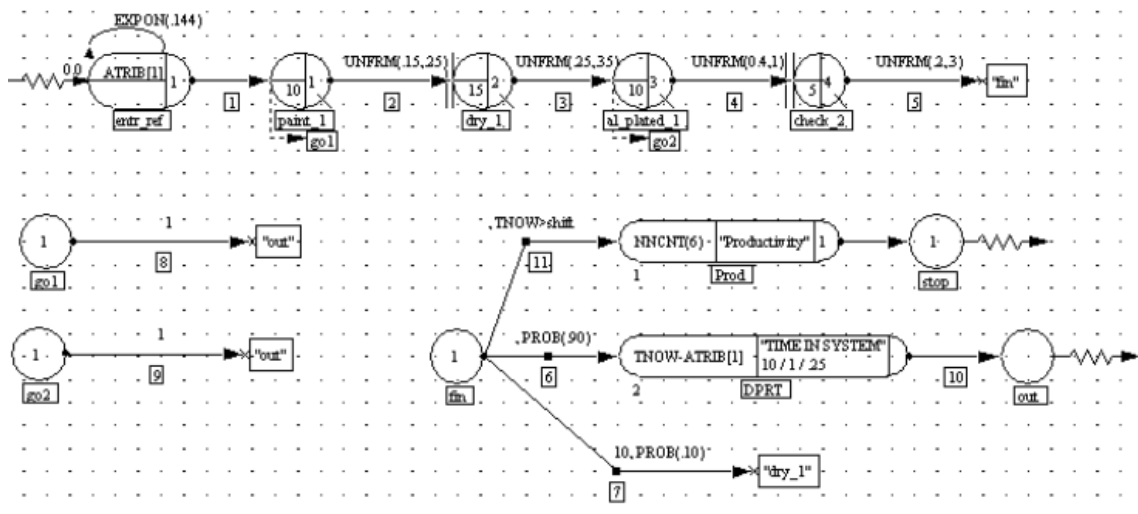
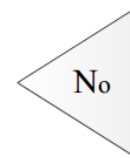
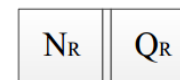
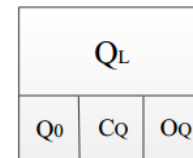
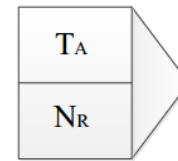


Figure 7. Network model of painting and plating workshop.

Data collection:

The data collected at the present time is as below:

$T_0 = \text{EXPON}(0.144)$; $T_1 = 0$;

$TA_1 = \text{UNFRM}(0.15, 0.25)$; $TA_2 = \text{UNFORM}(0.25, 0.35)$; $TA_3 = \text{UNFORM}(0.4, 1)$;

$TA_4 = \text{UNFORM}(0.2, 0.3)$;

$CQ_1 = 10, CQ_2 = 15, CQ_3 = 10, CQ_4 = 5$

OQ-FIFO

NR1 is a coating machine; NR2 is the drier; NR3 is an aluminum plating machine; NR4 is the inspection worker.

QR1 is the paint machine number; QR2 is the number of dryers; QR3 is the aluminum number; QR4 is the number of workers checked.

The value of QR1; QR2; QR3; QR4 will depend on the scenarios.

Calculate the number of runs required

In the production workshop, there are the following conditions:

- Working time for one shift: $60 \times 8 = 480$ minutes.
- The output per shift: 3000 details
- With confidence level: 99%.

The required parameters will be calculated by running the sample a finite number of times then based on those parameters to calculate the number of runs needed.

With 99% confidence we follow the Student standard distribution.

We use the formula:

$$\bar{x} - t_{v-1, 1-\alpha} \cdot \frac{s}{\sqrt{5}} \leq \mu \leq \bar{x} + t_{v-1, 1-\alpha} \cdot \frac{s}{\sqrt{5}} \quad (1)$$

x: Average value

S: Standard deviation

μ : Average density

$t_{v-1, 1-\alpha}$: Coefficient of the Student standard distribution

Number of runs: 5; Degree of freedom: 4

The value variation: 30 products are equivalent to 1% of output per shift. We use the following formula to calculate the number of runs needed

$$\mu \leq \bar{x} + t_{v-1, 1-\alpha} \cdot \frac{s}{\sqrt{n}} \quad (2)$$

So

$$n \leq \left(t_{v-1, 1-\alpha} \cdot \frac{s}{\mu - \bar{x}} \right)^2 \quad (3)$$

$$\bar{x} = 3274.4$$

$$S = 54.848$$

$$t_{v-1, 1-\alpha} = 3.365$$

$$\text{So } N = 152 \text{ times.}$$

Results and discussion

The results obtained after using the above parameters.

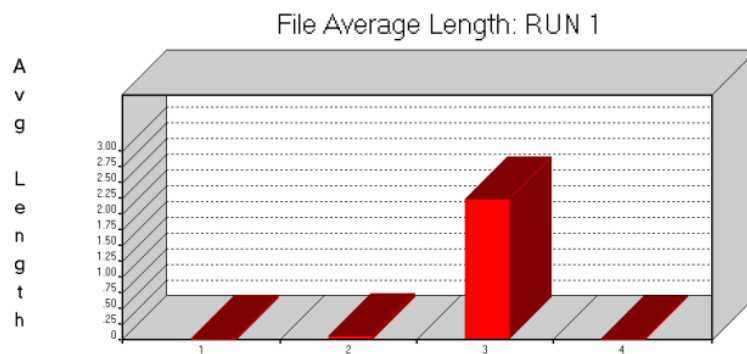


Figure 8. Average queue length.

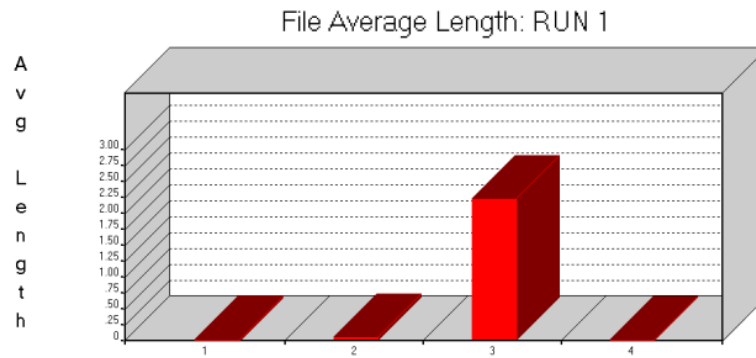


Figure 9. Average waiting time in line.

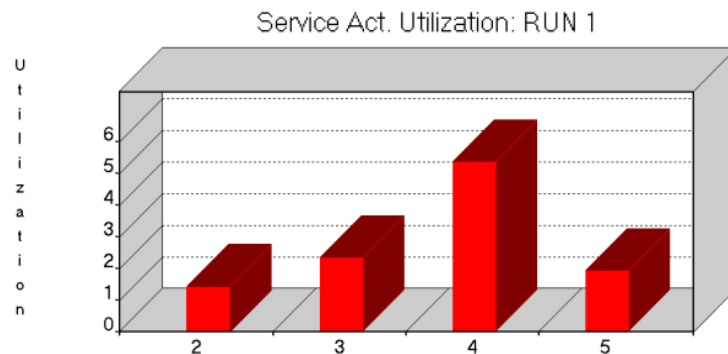


Figure 10. Average resource usage.

Analyze the results obtained about the system with the information in Table 1:

Table 1

Paint shop system status	
System information	Status
Bottlenecks	The maximum mean queue length was recorded in action 3, in the plating machine area
Waiting time in line	Small average waiting time in a queue
Power usage level	<ul style="list-style-type: none"> - Maximum power usage is recorded in action 4 at the galvanizing machine site. - In the 2nd largest source usage check area recorded in the 3rd column of activity in the dryer area. - In the test area for the third largest level of resource usage, which is recorded in the column 5 activity in the area of the inspected worker. - Finally, the power usage level is recorded in activity 2 in the paint machine area. - In the paint machine area the average value is 1.402 with the standard distribution value of 1.17. - In the drying area, the mean value was 2.327 with a standard distribution value of 1.421 - In the plating machine area, the average value is 5.344 with a standard distribution value of 1.222 - At the position of the inspecting worker, the mean is 1.911 with the standard distribution value of 1.781

A scenario designs for the production process:

From the analysis of the current state of the workshop, the scenario is studied on the use of the source as follows:

- At the coating machine, there are 6 machines, but the actual number of machines used is

$$n_{cut} = \bar{x} + 3s = 1.402 + 3 * 1.17 = 4.912 \quad (4)$$

In 99% of the cases given as the normal distribution, only 5 out of 6 machines were used to make the product. From the above results it is concluded that reducing the number of paint machines in the paint area does not decrease productivity. Scenarios for the cases are shown in Table 2.

Table 2

Scenario with different number of paint machines

Scenario	Number of paint machines
WS2_Paint1	1
WS2_Paint2	2
WS2_Paint3	3
WS2_Paint4	4
WS2_Paint5	5

The system will simulate more than 152 runs to achieve p1% of the time interval of the yield prediction with an average 99% confidence level.

- In the inspection area, there are 8 workers, but in reality the number of workers needed is

$$n_{cut} = \bar{x} + 3s = 1.911 + 3 * 1.781 = 7.254 \quad (5)$$

In 99% of the cases given the normal distribution, only 7 out of 8 workers used it to make the product. From the above results it is concluded that reducing the number of workers in the test area does not decrease productivity.

Table 3

Scenario with different number of workers

Scenario	Number of workers
WS2_CHK1	1
WS2_CHK2	2
WS2_CHK3	3
WS2_CHK4	4
WS2_CHK5	5
WS2_CHK6	6
WS2_CHK7	7

Improved resource use is the plating machines. All six plating machines are used as follows:

$$n_{All-plate} = \bar{x} + z.s \quad (6)$$

$$z = \frac{n_{All-plate} - \bar{x}}{s} = \frac{6 - 5.344}{1.22} = 0.54 \quad (7)$$

Given $z = 0.54$ regions below the mean curve of 0.2257 leads to the conclusion that most 23% of cases are using the same 99% confidence interval. So, in the case productivity can be improved in two ways:

+ Reduce processing time: this problem cannot be done because machines and technology are limited. For these reasons this approach was not considered.

+ Replace plating machines with more productive ones: this option would require a short-term investment to purchase new machines but in the long run will contribute to the company's profits by increasing productivity.

Product processing time here is limited in productivity of test workers with product speed $[0.2 \div 0.3]$ minutes per product. Therefore, this yield has practical value as the number of machines required to keep the yield with the time of [UNIFORM, (0.15,0.35)].

Table 4

Scenario with number of new plating machines	
Scenario	Number of plating machines
WS2_AI1	1
WS2_AI2	2
WS2_AI3	3
WS2_AI4	4
WS2_AI5	5

The source usage in the scenarios given in the diagram is as follows:

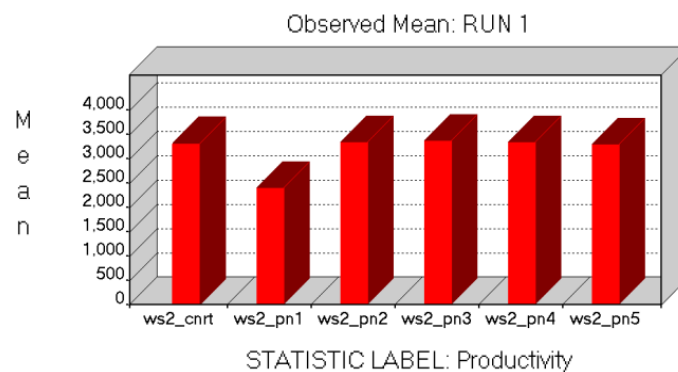


Figure 11. Productivity chart with scenarios with different number of painting machines.

From the above chart, it can be seen that: A steady state of productivity is used with 3 machines. The increase in the number of machines does not increase the productivity, the small change in productivity is obtained due to the mean to shift from the random nature of the mean yield. Therefore, the production line does not reduce productivity if only 3 out of 6 machines are used in the paint machine area.

The productivity charted with different scenarios of the number of workers tested his as.

Through the above chart, it can be seen that: The steady state of productivity is received when the line has 3 inspection workers and the increase in the number of inspection workers does not increase productivity. Small variation in yield is obtained by the mean to shift from the randomness of the mean yield. Thus, the line does not reduce productivity if only 3 out of 8 workers are employed in the test area.

The chart comparing the current scenario and the new scenario has reduced the number of machines and the number of test workers.

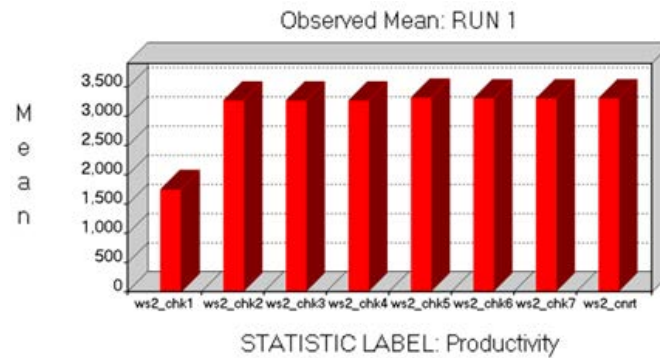


Figure 12. Productivity chart with different scenarios of the number of workers tested.

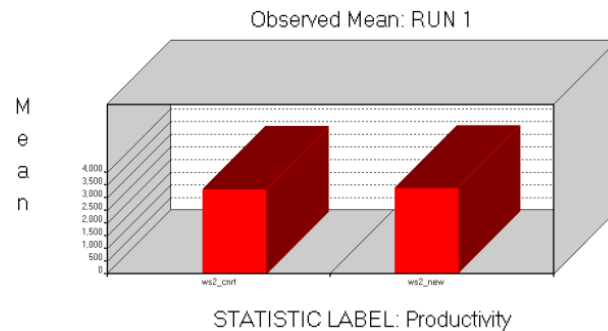


Figure 13. The chart comparing the current scenario and the new scenario has reduced the number of machines and the number of test workers.

Productivity chart with new number of plating machines for improved equipment management.

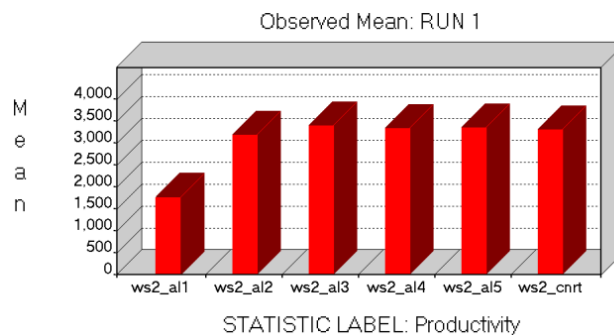


Figure 14. Productivity chart with new number of plating machines for improved equipment management.

The above chart shows that: The steady state of productivity is obtained when the line has 3 plating machines. Increasing the number of machines does not increase productivity, productivity is limited by the number of input part ratios of the workshop. Small variation in yield is obtained by the mean to shift from the randomness of the mean yield.

From the above results it can be seen that the productivity will be suitable when using 3 machines with product speed within the UNIFORM limit [0.15,0.35]. If you want to increase productivity, the percentage of input details of the workshop must also increase.

Conclusion

Through this research, the process of modeling simulation and production analysis was carried out in a manufacturing workshop. On that basis, we have analyzed the requirements and designed an experimental model to simulate the operation of the automatic coating and plating line. The model addresses a number of requirements:

- Visual and general description of the distribution of equipment in the workshop.
- Simulate the activities of the equipment in the chain.
- Simulation helps the manager to come up with the plan to use the equipment effectively, contributing to improving productivity and reducing product costs.

Through this research will be the basis to help production lines to build new or adjust equipment and labor to bring productivity and reduce costs for production.

References

1. A. Alan B. Pritsker, *Introduction to Simulation and SLAM II*. 3rd ed., Systems Publishing Corporation, West Lafayette, Indiana, 1986.
2. A. Alan B. Pritsker, O'Reilly, Jean J, *Simulation with Visual SLAM II and Awesim*, John Willey & Sons Inc, US, 1997.
3. A. Alan B. Pritsker, O'Reilly, Jean J, *Introduction Simulation SLAM II*, John Willey & Sons Inc, US, 1986.
4. Pritsker corporation, *Awesim total simulation project support. User's Guide*. Symix systems, Inc, 1999.
5. A. Alan B. Pritsker, Jean J. O'Reilly, *Simulation with Visual SLAM and AweSim*. John Wiley & Sons, US, 1999.
6. Carrie, A., *Simulation of Manufacturing Systems*, John Willey & Sons, Inc, US, 1988.
7. Vantrong Thai, Junsheng Cheng, *Optimizing SVM's parameters based on backtracking search optimization algorithm for gear fault diagnosis*. Journal of Vibroengineering, 2019. DOI:10.21595/jve.2018.19859.
8. Nguyen Thanh Nhan, *Production process improvement in transportation industry in north Vietnam through research and application of advanced discrete event simulation modeling techniques*. Ph.D thesis, 2008.

[https://doi.org/10.52326/jes.utm.2021.28\(3\).02](https://doi.org/10.52326/jes.utm.2021.28(3).02)
CZU 621.3.092.53:534.2



SETTING OF THE ANGLE OF INCIDENCE FOR GENERATING LAMB WAVES BY NON-CONTACT METHOD

Alexandru Buga*, ORCID ID: 0000-0002-4342-0502

Technical University of Moldova, 168 Ștefan cel Mare Blvd., MD-2004, Chișinău, Republic of Moldova

*Corresponding author: Alexandru Buga, alexandru.buga@precesia.utm.md

Received: 06. 17. 2021

Accepted: 08. 10. 2021

Abstract. The article examined the problem of the experimental setting of incidence angles for the generation of Lamb waves in plate-type parts by the non-contact ultrasonic control method. This type of control is mainly done by the use of two types of waves: Rayleigh, which detects invisible defects on the surface of parts, and Lamb waves mode A_0 and S_0 . Mostly used is the mode A_0 due to the propagation over distances of interest in the tested materials. One of the primary aim during the testing process is to position the ultrasonic transducers (transmitter and receiver) at oblique angles of incidence on a surface. The transducers should be positioned on an access face of the plate, as is common in industrial practice, at a fixed distance from the measured plate, and leaving an air gap between transducers and the tested plate. The ultrasonic transducers are moved simultaneously linearly or in zigzag on the surface of the plate-type part to measure the hidden defects (cracks, pores, inclusions) that appear in the composite materials during the manufacturing process or during the operation. The presented work brings new insights into the setting of the angle of incidence for generating lamb waves by non-contact method.

Keywords: *non-contact ultrasonic control, invisible defects measurement, Lamb waves, ultrasonic transducers, angle of incidence.*

Introduction

First applications of composite materials in the automotive industry were those in the field of car bodies manufacturing: in 1953 the body of the Corvette Chevrolet (USA) was entirely made of glass-epoxy; in 1968 the rims of the Citroen SM were made of epoxy glass; in 1970 - the bumper of the Renault R5 was made of epoxy glass; in 1980 John Barnard, an engineer in the McLaren Formula 1 team, built the first carbon Kevlar chassis and from other composite materials; in 2002 the body of the McLaren Mercedes SLR series car was made entirely of carbon fiber. As regarding to the use of composite materials in the aircraft manufacturing industry, it is worth mentioning the Boeing 787 Dreamliner passenger plane, which was made of the following materials: 50% - composite materials based on carbon fiber, 20% - aluminum, 15% - titanium, 10% - steel, and 5% other materials [1]. Composite materials are also widely used in the aerospace industry, such as the thermal shield of the HERMES spacecraft (*Heliophysics Environmental and Radiation Measurement Experiment Suite*) which

"tiles" are composed of composites, based on reinforcements of carbon fibers and matrices of silicon carbide (called C/SiC or C/C-SiC composites). This heat shield resists to at least thirty landings [2].

Main advantages of composite materials are economic and qualitative aspects because the use of these materials allow saving significant amounts of expensive and traditional materials, the latter once becoming deficient. Herein, composite materials demonstrate continuously improving quality and increased duration of operation in conditions of high performance [3]. Therefore, for industrialized countries composite materials represent a priority area, occupying the forefront of the continuous process of technological innovation in the construction of cars, planes, ships due to mechanical strength and rigidity (increased tensile strength R_m , Kevlar composite has R_m twice larger than glass), resistance to corrosion, chemical agents and high temperatures (ex. Kevlar, Teflon up to 500°C, and ceramic fibers such as SiC, Si₃N₄, and Al₂O₃ between 1400°C and 2000°C). Low density (composites with epoxy resins reinforced with Si, B, C fibers, have a density less than 2 g/cm³), dimensional stability (low coefficient of thermal expansion), resistance to variable stress and wear and high durability in operation (under the same operating conditions 1 kg of Kevlar replaces 5 kg of steel, at an equal service life) represent other important advantages of composite materials [4].

Previously published researches showed different methods to test composite and non-composite materials. For instances, there has been widely described non-contact ultrasonic control but without mentioning about angle of incidence for generating Lamb waves [5, 6]. The study conducted by Gheorghe I. Gheorghe et al (2011) showed the practical application of the Intelligent Mechatronic Equipment for dimensional control of non-composite materials [7, 8]. Others published the results of another type of mechatronic equipment use for the tightness checking of non-composite materials [9]. However, these methods are not reliable due to easy damage of the tested material because the process of control applies the immersion when the contact with water may cause the damage of the material, or compressed air.

Gholizadeh S. reviewed non-destructive testing (NDT) methods of composite materials which use contact and non-contact control technologies [10]. These methods have been successfully used for a long period of time due to the fact that composite materials are mostly used in critical-safety applications for example in aircraft primary constructions. Assuming that factors such as efficiency and safety should be used in analyzing the best method to be used, the method chosen should minimize the costs incurred in the operation. Therefore, it is important to bring to the light inexpensive but highly efficient method to test composite and non-composite materials by the non-contact ultrasound method [11]. This engineering innovation is based on an equipment that doesn't need special qualification of the operator, as compared to other non-destructive testing methods. In particularly, an advantage of this method is the possibility to determine the damage of the material structure that may occur under the load, the effect of the damage on the load-bearing capacity of structures, as well as the analysis of the behavior of composites in difficult working conditions (temperature and humidity variations, vibrations, the effect of chemical agents, mechanical impact, etc.).

Nowadays are described various techniques of the non-contact ultrasound control method. For example, Petroni P. et al. (2006) proposes to place the transmitter transducer in transmission configuration, but the receiver to be placed obliquely on the same side of the emitter, in order to let it acquire the scattered waves generated by the defect [12]. Authors

investigated Delta configuration using non-contact probes in an attempt to evaluate potentials and performance of the studied techniques, and defect identification capabilities. The research team concluded that an important issue for defect detection capability is the determination of the optimal probes position.

Experimental part

Lamb waves represent elastic waves which were first described in 1917 by the English mathematician Horace Lamb. They propagate in solid plates in two wave modes, and their velocities depend on the relationship between wave length and plate thickness. The symmetrical mode S_0 of the Lamb waves is easier to be transmitted and received as compared to asymmetric mode A_0 through the non-contact technique [13]. The mechanism of detecting the defect in solid plates consists of "scattering" the Lamb waves in the defect area. This process forms an increased attenuation of the ultrasound with respect to a defect-free plate, similarly, the phase speed reaches a lower level in the defect plate than in the defect-free one [14].

The defect index represents the change of amplitude on the axis of movement of the transducers. However, for the excitation of Lamb waves in a plate, it is necessary to know the oblique angle of the incidence [15]. The relationship between the excitation angle and the phase velocity of Lamb waves can be written according to Snell's law by the Eq.(1) [16]:

$$\phi_1 = \left(\frac{c_{air}}{c_f} \sin \phi_2 \right) = \arcsin \left(\frac{c_{air}}{c_f} \right); \quad (1)$$

Where: $\phi_1 = \phi_2$ - is the excitation angle of the n Lamb waves; C_f - is the phase velocity of the n Lamb wave; C_{air} - is the propagation speed of ultrasound in the air.

According to Snell's law, if excitation angle ϕ_1 is known, the phase velocity of Lamb waves mode A_0 can be found out. For this reason, was designed and manufactured a device to help find experimentally the excitation angle of Lamb mod A_0 waves in the plates (Figure 1):

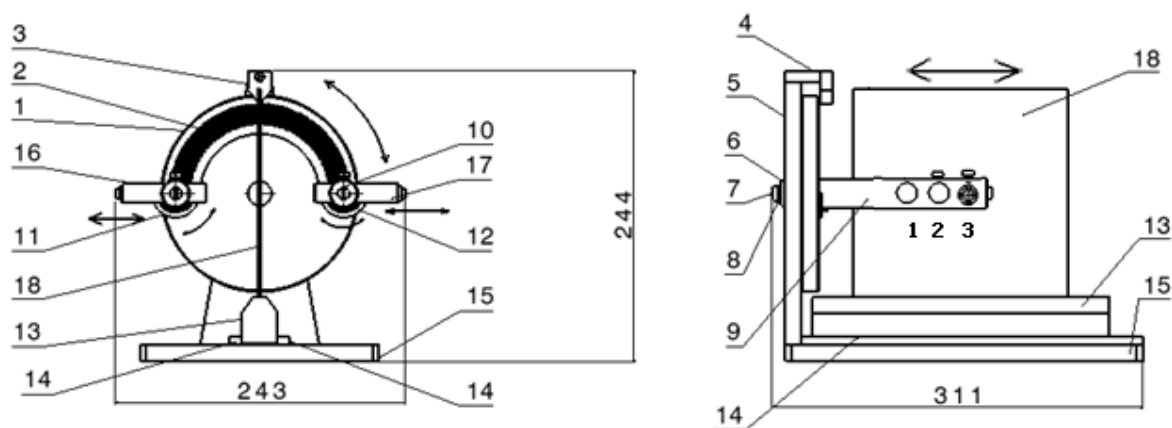


Figure 1. Schematic presentation of the device for finding the optimal excitation angle of Lamb waves asymmetrically mode A_0 in plates.

1 - wheel; 2- the main rapporteur; 3 - needle; 4 - needle support; 5 - wheel support; 6 - bush; 7 - axle; 8 - axle snap ring; 9 - support for emission transducers; 10 - support for reception transducers; 11 - secondary rapporteur 1; 12- secondary rapporteur 2; 13 - plate holder; 14 - guides; 15 - base plate; 16 - non-contact ultrasonic emission transducer; 17 - non-contact ultrasonic reception transducer; 18 - plate to testing.

To find the optimal excitation angle of the Lamb waves mode A_0 in the plate, proceed as follows:

- insert a sample (Figure 1, p. 18) with maximum dimensions of 180 mm x 200 mm (plates with relatively small thicknesses compatible with non-contact control such as aluminum, reinforced composite plates, or sandwich plates in the plate holder (Figure 1, p. 13).
- Non-contact ultrasonic transducers (Figure 1, p. 16 - 17) are fixed in transducer supports (Figure 1, p. 9-10) at the beginning at a maximum distance from the plate, and it's connected by wires (Figure 2, p. 19) to the ultrasonic equipment SITAU 32:128:2 LF (Figure 2, p. 20) which in turn is connected to the computer (Figure 2, p. 22) by wires (Figure 2, p. 21) for viewing, recording and processing signals with the maximum amplitudes obtained (Figure 2).
- By rotating the wheel (Figure 2, p.1) together with the non-contact transducers (Figure 2, p. 16 - 17) with minimum possible rotation step $0,5^\circ$ stops when the maximum amplitude is observed on the monitor. Record the angle obtained (the value on the main rapporteur (Figure 1, p.2) opposite the indicator (Figure 1, p. 3) is φ_i .

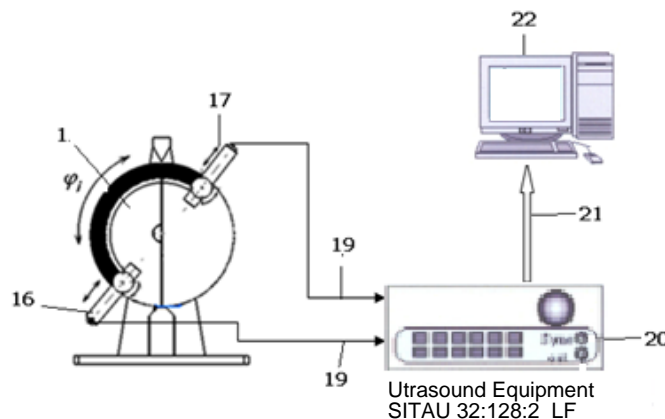


Figure 2. Ultra-acoustic system for finding the optimal excitation angle of Lamb A_0 mode waves in the plate.

- The next step consists of rotating the transducer supports (Figure 3, p. 9 - 10) around their axis to find the φ_1 and φ_2 angles, also the transducers approach or their removal from the plate to obtain the maximum amplitude, the values A and B (Figure 3).
- The obtained values (A , B , C , φ_i , φ_1 , and φ_2) will be used later for the positioning and fixing of the non-contact ultrasonic transducers (Figure 3, p. 16 - 17) in the manual non-contact investigation device with ultrasound of the plates (Figure 10) with larger dimensions but with the same structure and thickness, with and without defects.

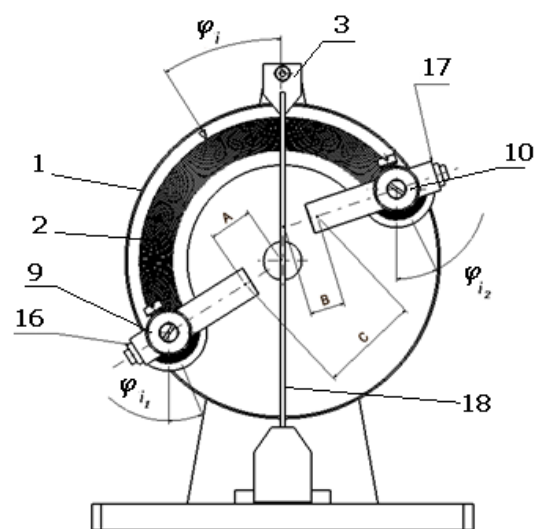


Figure 3. Device for experimental determination of the values A , B , C , φ_i , φ_1 and φ_2 .

In the first experiment, was used an aluminum plate with dimensions of 180 x 200 x 2.5 (mm) and a pair of non-contact ultrasonic transducers with the optimal frequency of 450 kHz positioned in the transmission respectively reception mode (Figure 2). The transmitter was energized with rectangular pulses and a current voltage of 750 V using the ultrasonic system SITAU 32: 128: 2 LF. The received signal was amplified to 34 dB using the built-in noise reduction amplifier in the SITAU 32: 128: 2 LF ultrasonic system. To obtain a better signal/noise ratio (SNR), 54 signals were emitted at each measurement step. The experimentally obtained signals were stored in the PC for further processing in MATLAB and the formation of ultrasound images.

An aluminum plate (Figure 1, p. 18) was inserted into the plate holder (Figure 1, p. 13) between the transducers (Figure 2, p. 16 - 17), the wheel (Figure 1, p. 1) was rotated in an angular field from $+30^\circ$ till -30° , step by step with 0.5° .

Experimentally, a type B image was obtained, which shows a dependence between the received signal and the rotation angle φ_i of the non-contact transducers for 450 kHz (Figure 4).

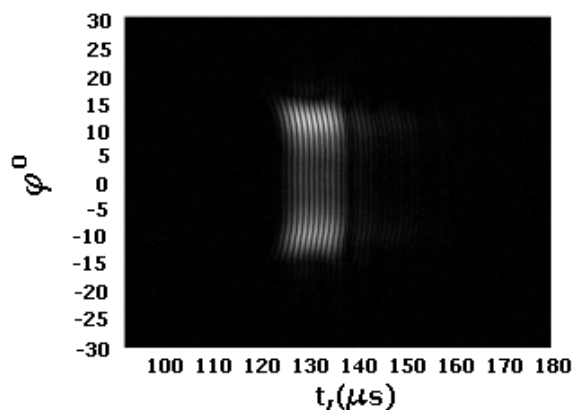


Figure 4. Type B image of A_0 asymmetric mode Lamb waves obtained by rotating the wheel from -30° till $+30^\circ$ using non-contact transducers at $f=450$ kHz (aluminum plate 2.5 mm thickness).

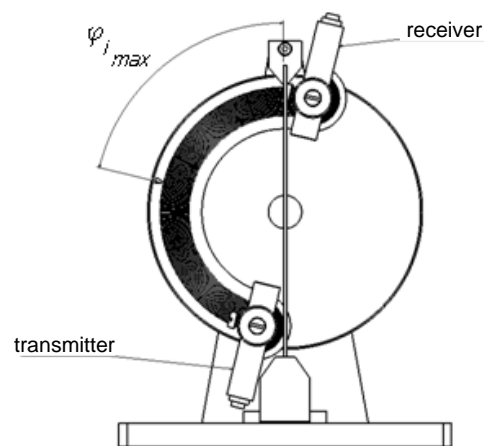


Figure 5. Obtaining the shortest time of wave propagation in the plate by rotating the wheel at the $\varphi_{i \max}$ angle.

It was observed that the shortest time of the propagation of the ultrasonic waves corresponds to the maximum angle $\varphi_{i \max}$ (Figure 5):

This is explained by the fact that the speed of ultrasound propagation in the aluminum plate is much higher than the speed of ultrasound in the air [17].

The optimal angle of excitation of the Lamb waves mode A_0 in the aluminum plate with 2.5 mm thickness obtained experimentally at the frequency of 450 kHz corresponds to the maximum amplitudes (Figure 6).

A type B image was also obtained to shows a dependence between the received signal and the rotation angle φ_i of the non-contact transducers for 250 kHz (Figure 7).

The phase velocity of the Lamb waves asymmetric mode A_0 can be measured with an uncertainty of 2.5% in the case of non-contact investigation techniques.

From the diagram, figure 8, it can be seen that in the aluminum plate there are only Lamb waves asymmetric mode A_0 , the optimal excitation angle respectively reception is $\pm 10,7^\circ$.

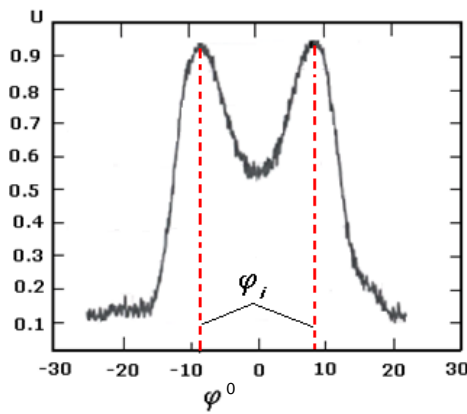


Figure 6. The maximum amplitudes obtained by rotating the main wheel from $+30^\circ$ till -30° at the frequency of 450 kHz, $\varphi_i = \pm 9^\circ$ are the optimal angles for excitation and reception.

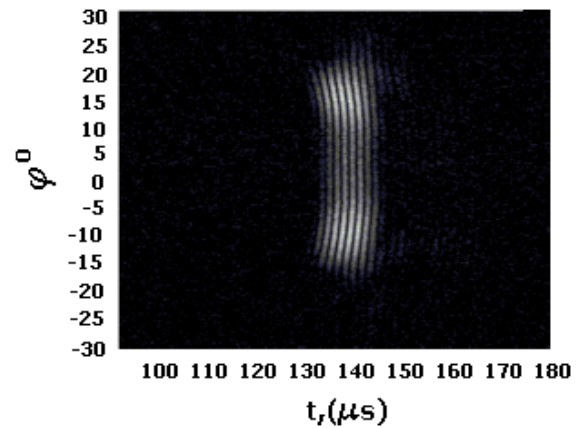


Figure 7. Type B image of the signals received by rotating the main wheel from -30° till $+30^\circ$ by using non-contact transmission and reception transducers with $f = 250$ kHz.

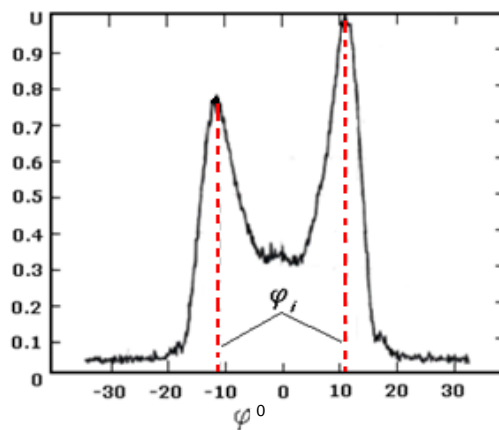


Figure 8. Maximum amplitudes of Lamb waves mode A_0 obtained at $f = 250$ kHz. $\varphi_{1,2} = \pm 10.7^\circ$ are the optimal oblique angles of incidence for excitation and reception.

Given the optimal angle, according to Snell's law showed in Eq.(1), can be calculated the phase velocity of propagation Lamb waves mod A_0 through the aluminum plate at the frequency of 250 kHz, the result is 1850 m/s. The speed of propagation of ultrasound in the air during the measurements was 345.4 m/s at 22.3° C and relative air humidity of 35%. In the Table 1 is shown the data of the experimental measurements and the calculated data:

Table 1

f, kHz	Incidence angle (ϕ_i) Degree	Experimental measurement		Calculated	
		c mode S_0 , m/s	c, mode A_0 , m/s	c, mode S_0 , m/s	c, mode A_0 , m/s
250 kHz	10.7°	5470	1850	5481	1893
450 kHz	9°	5190	2250	5222	2253

Dispersion curves of the phase velocities and of the group velocities of the Lamb waves in the 2.5 mm aluminum plate thickness are presented in the Figure 9. They were calculated according to the analytical solution, considering that the propagation speed of the longitudinal ultrasonic waves in aluminum is 6320 m/s and of the transverse ones 3130 m/s [18].

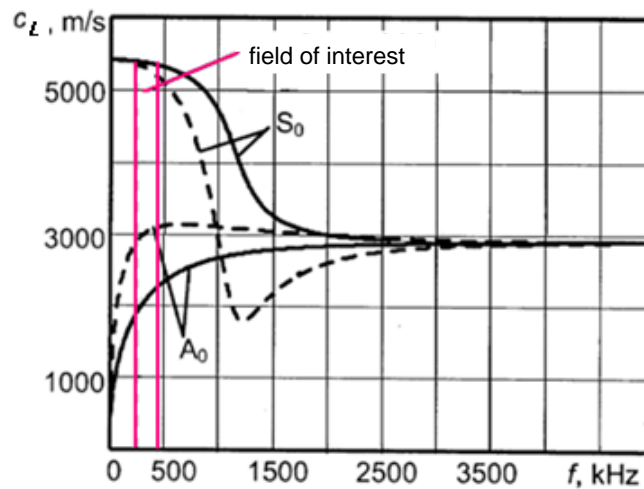


Figure 9. Dispersion curves of the measured velocities phase (continuous lines) and of the group (dashed lines) propagation velocities of Lamb mode A_0 and S_0 waves.

It was observed that the asymmetric group speeds increase and the symmetric ones decrease with the frequency. The influence of frequency can also be mentioned on the angle of generation of Lamb waves in plates. After recording the obtained constants (A , B , C , ϕ_i , ϕ_1 , and ϕ_2) the transducers can be removed and fixed in the manual device (Figure 10) with the same values for the investigation of 2.5 mm thick aluminum plates.

The same procedure will be done for each material, for example: must to find the optimal excitation angle of the Lamb A_0 waves for the carbon fiber reinforced plate, record the values A , B , C , ϕ_i , ϕ_1 , and ϕ_2 , remove the transducers and fix them manually with the same values for the investigation of carbon fiber reinforced plates with or without defects, with the same structural composition and thickness.

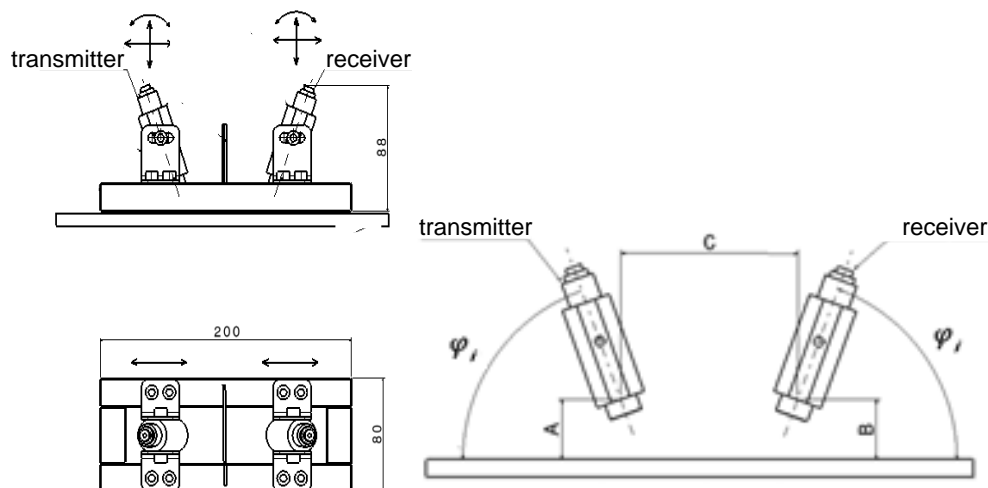


Figure 10. Manual device of investigation (left), fixing non-contact acoustic transducers (right).

In the next experiment, the transmitting transducer was inserted into the hole no.2 and the receiving one into the hole no.3, so the distance between the axes of the non-contact transducers reached 25 mm. The one-way carbon fiber reinforced plate 1.1 mm thick was inserted into the composite plate support (Figure 11):

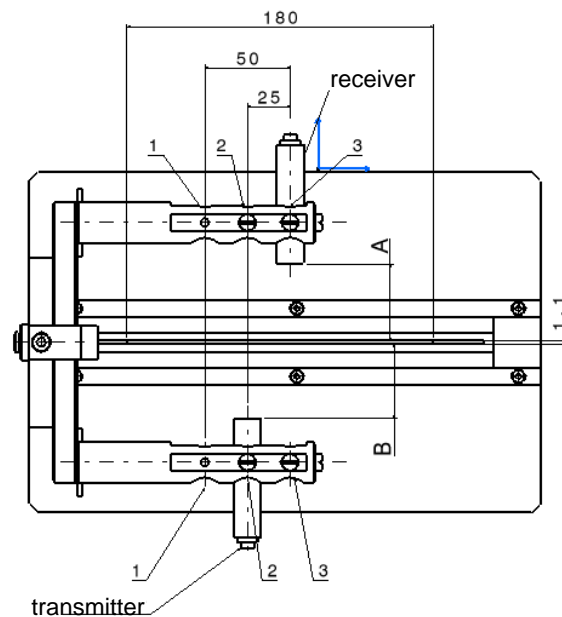


Figure 11. Non-coaxial placement of the non-contact ultrasonic transducers.

The transmitter was energized with rectangular pulses at a current voltage of 650 V using the ultrasonic system SITAU 32: 128: 2 LF at the frequency of 250 kHz and the receiver signal was amplified by 45 dB. The wheel (Figure 1, p. 1) was rotated step by step with 0.5° . The maximal amplitudes were obtained in an angular field from $+25^\circ$ till -25° with the adjustment of the values A , B , C , φ_i , φ_1 , and φ_2 . As a result, was obtained the angle of 15.5° , which is optimal angle of excitation of Lamb waves asymmetric mode A_0 (Figure 12):

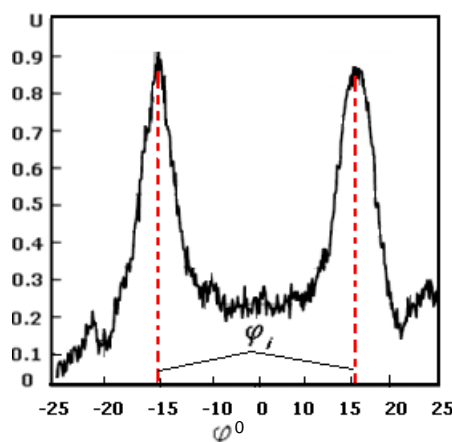


Figure 12. The optimal incidence angles for generating Lamb waves mode A_0 , the distance between the axes of the transducers 25mm, $f = 250$ kHz.

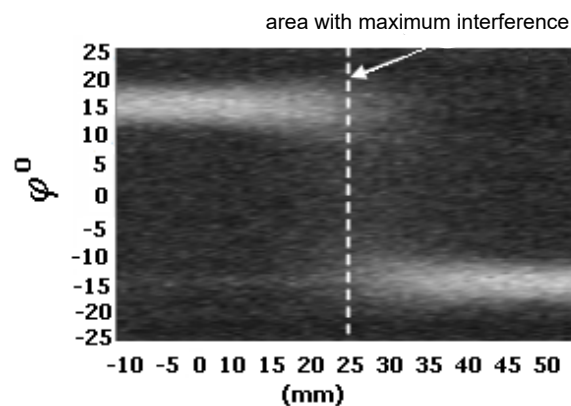


Figure 13. Type C image of received Lamb mode A_0 waves, $f = 250$ kHz.

Respectively, the phase velocity of the Lamb waves asymmetric mode is 1290 m/s. Subsequently, with the obtained signals was formed a type C image of the received waves (Figure 13) which shows the area with the maximal interference of Lamb waves when the distance between the axes of the transducers is 25 mm and respectively the angles of incidence φ_i is equal to 15.5° .

Another objective of the experiment was an attempt to move the axis of the transmitter transducer by 50 mm from the receiver axis, but no consistent results were obtained.

Conclusions

The paper addresses the issue of choosing the angles of incidence for the transmission and reception of Lamb ultrasonic waves during the control of plate-type parts by the non-contact ultrasound method. The experiment resulted with the design and manufacture of two devices: the first one was aimed to set the values of A , B , C , ϕ_i , ϕ_1 , and ϕ_2 , depending on the maximum amplitudes of the obtained signal; the second device was used to position the transducers with the obtained values and to control the plates of the same material and thickness with or without defects.

An observation of the experiment was that the asymmetric group speed increases with the frequency and the symmetric ones decreases with the frequency. The frequency of the non-contact ultrasonic transmitting transducer directly influences the angle of the incidence of Lamb waves in the plates. A better signal/noise ratio was obtained by moving the axis of the transmitting transducer with f equal to 250 kHz in relation to the axis of the receiver by 25 mm. Also, velocity phase of the Lamb waves decreased from 1353 m/s to 1290 m/s. Consecutively, the angle of incidence $\varphi_{1,2}$ of the Lamb waves generation increased from 14.7° to 15.5° .

Concerning materials with complex geometry, such as wings and propellers of the aircraft, the non-coaxiality of the non-contact transducers is not suitable for the control, because it may increase the rate of errors in data interpretation regarding the defect position and size.

Acknowledgments: I would like to express my special thanks of gratitude to Prof. Amza Gheorghe and his team from the University POLITEHNICA of Bucharest (Romania) for his help in the experimental and theoretical part of the research work and Acad. Ion Bostan from Technical University of Moldova who inspired me to publish these results.

References

1. Victor Giurgiutiu. „Boeing 787 Dreamliner” in „Structural Health Monitoring of Aerospace Composites” Published 2015.
2. Van Den Abeelen. „Spaceplane HERMES „Europe’s Dream of Independent Manned Spaceflight” Published 2017. pp. 417 - 433
3. F.C. Campbell. „ Structural Composite Materials” November 2010, ASM International, Materials Park, Ohio 44073-0002, ISBN-13:978-1-61503-037-8; ISBN-10:0-61503-037-9; SAN 204-7586
4. Maria Mrazova „ Advanced composite materials of the future in aerospace industry” September 2013, INCAS Bulletin 5(3):139 - 150
5. Robert E Green. Non-contact ultrasonic techniques. Ultrasonics 42 (1 - 9), May 2004: pp. 9 - 16
6. Mariusz Kaczmarek, Bogdan Piwakowski, Radosław Drelich. „Noncontact Ultrasonic Nondestructive Techniques” State of the Art and Their Use in Civil Engineering. Journal of Infrastructure Systems / Volume 23 Issue 1- March 2017
7. Gheorghe I. Gheorghe, Hacman Mihai, Florin Andrei, Alexandru Buga. „ Intelligent machine for dimensional control and marking “Power transfer unit” for the auto subassemblies in large-scale seriesproduction” IEEE International Conference on Mechatronics 13-15 April, 2011 Istanbul, Turkey, Pag: 933 – 936, Print ISBN: 978-1-61284-982-9.
8. Gheorghe I. Gheorghe, Hacman Mihal, Florin Andrei, Alexandru Buga. „Mechatronic intelligent unit for tightness checking reverse module TL8” – machined *IEEE International Conference on Mechatronics* 13-15 April, 2011 Istanbul, Turkey, pag. 930 – 932, Print ISBN: 978-1-61284-982-9.
9. Gheorghe I. Gheorghe, Vrabioiu Ion, Andrei Florin, Nineacă Dan, Alexandru Buga. „Intelligent mechatronic unit for tightness checking case timing H5 (machined)” E-newsletter „MECATRON” Octombrie 2012, pag. 7 - 8
10. Gholizadeh S. A review of non-destructive testing methods of composite materials / Procedia Structural Integrity 1 (2016) 050 – 057

11. B. Boro Djordjevic „Advancements in Ultrasonic Imaging for Materials Testing” Acoustical Imaging - book series ACIM, volume 26, pp. 289 - 296.
12. Petroni P, Revel Gm. „Non Contact Ultrasonic Techniques for Composite Material Diagnostics in Aeronautics Applications” ECNDT Conference at Berlin in 2006
13. Horace Lamb. „On waves in an elastic plate”, F.R.S.(1916, July 10)
14. Soleimanpour R. and NG CT., „Scatttering of the fundamental anti-symmetric Lamb wave at through thickness notches in isotropic plates” Journal of Civil Structural Health Monitoring 6(3) (July 2016): pp. 447 - 459
15. Sandeep Sharma, Abhijit Mukherjee. „Damage detection in submerged plates using ultrasonic guided waves” Indian Academy of Sciences, Sadhana Vol. 39, Part 5, October 2014, pp. 1009 – 1034
16. Kwan A., Dudley J., Lantz E. (2002) „ Who really discovered Snell’s law?” Physics World.15(4):64
17. Tomás Gómez Álvarez-Arenas, Jorge Camacho. „Air-coupled and resonant pulse-echo ultrasonic technique” published at 14 may 2019 in New methods and applications of nondestructive testing in close ranging)
18. Dixon P., Petcher Y., Fan D. Maisey and P. Nickolds. „Ultrasonic metal sheet thickness measurement without prior wave speed calibration” published 17 october 2013 at journal of physics: applied physics, volume 46, number 44.

[https://doi.org/10.52326/jes.utm.2021.28\(3\).03](https://doi.org/10.52326/jes.utm.2021.28(3).03)
CZU 621.887.002.5



DESIGN ASPECTS OF INSTALLATION DEVICES OF THE SUPPORT RINGS

Alexei Botez*, ORCID ID: 0000-0001-8357-076X,
Elena Rusu, ORCID ID: 0000-0002-2473-0353

Technical University of Moldova, 168 Stefan cel Mare Blvd, MD-2004, Chisinau, Republic of

**Corresponding author: Alexei Botez, alexei.botez@gddti.utm.md*

Received: 06. 23. 2021

Accepted: 08. 11. 2021

Abstract. The processes of manufacturing machines and appliances show a continuous tendency to increase the degree of automation. An important role in the automation of manufacturing processes is played by the constructive technologicality of the product. It is important to use a minimum number of components, which have a construction as technological as possible in terms of automation. In this context, the use of supporting rings as fasteners is welcome. The design of the installation devices of these rings requires the knowledge of their deformation forces, information that is missing in the profile literature. The authors set their goal to develop the method for calculating the forces required to deform the supporting rings with a rectangular transverse profile and their maximum allowable deformations. The calculation relationships were obtained by formalizing the supporting ring through a bar with a fixed end and studying its deformation using Mohr's integral. The article lists some types of the supporting rings used in the construction of machines and appliances, their advantages and disadvantages, aspects of their automatic installation: deformation and installation methods, precision of joint orientation, optimal design, calculation of forces required for deformation and the maximum permissible deformation value. As a result of the research carried out, recommendations were developed regarding the calculation of some constructive parameters of the devices for installing the supporting rings.

Keywords: *supporting ring, mounting process, deformation forces, accuracy of orientation.*

Introduction

Assembly is the final stage, but no less important of the manufacturing process, which integrates in itself the results of the previous stages and outlines the quality of the final product. The share of assembly constitutes about 40% of the total volume of works performed in the manufacture of the product, 80% of the assembly operations remaining manual [1]. Some of the causes of the delayed development of the automation of the assembly processes being studied in [2] are:

- Lack of systematic research on assembly processes, leading to intuitive methods of automatic tool design [3];
- Constructive inconvenience of the product for automatic assembly [4];

- Problems, related to ensuring the accuracy of the mutual orientation of the assembled parts [5];
- The low degree of unification of the component parts of the product [6].

An important role in increasing the degree of automation of assembly is played by the quantity of component parts [7] and the technologicality of the assembled object [8].

It should be noted that about 20% of the total number of components of the machine is occupied by the fasteners. According to the number of components, the fasteners are divided into four groups [9]:

- Assemblies without fixing parts (gluing, welding, etc.);
- Assemblies with a fixing piece (fixing with support ring, pin, etc.);
- Assemblies with two fixing parts (screw and washer);
- Assemblies with three fixing parts (screw, washer, nut).

Practice dictates the use of fasteners as simple and technological as possible [10].

Thus, designers rightly use widely support rings as fasteners in their constructions.

They are part of the second group of fasteners - with one piece.

The advantages of using supporting rings are [11]:

- - Constructive improvement;
- - The possibility of using the assembly equipment relatively cheaply;
- - Optimization of technological manufacturing processes;
- - Optimal operating characteristics.

1. Formulation of the Problem within the Study

The supporting rings are usually made of wires or sheets of spring steels as the material.

The supporting rings can be of the following types:

- with round transverse profile (Figure 1a);
- with a rectangular cross-section (eccentric (Figure 1b, c) or concentric (Figure 1d));
- exterior (installed only on shafts, Figure 1c);
- interiors (installed only in holes, Figure 1b);
- universal (Figure 1d).



Figure 1. Supporting rings.

Rings with round cross section are simple to manufacture, but their load capacity and positioning accuracy of fixed parts is low, therefore these are used only in places where they can meet its possibilities.

Rings with a rectangular transverse profile have better load-bearing and precision characteristics. In order to increase their deformability, they are made with eccentricity, but no information has been found in the literature to justify the value of eccentricity.

The deformation methods are the following:

- by applying a concentrated force, deposited at the ends of the ring (Figure 2a);
- by applying a distributed force, deposited on the entire perimeter of the ring (Figure 2b).

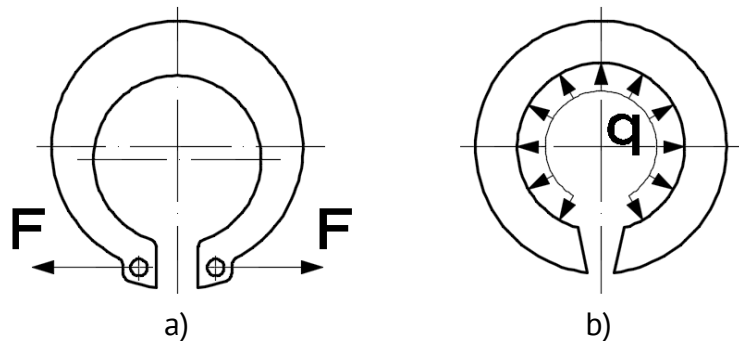


Figure 2. Deformation methods for rings.

With concentrated forces, the rings with special holes at the ends are usually deformed; with distributed forces, by propelling on conical surfaces, the rings that do not have such holes are deformed. No information was found in the literature on the calculation of the forces required to deform the supporting rings. The joining of the supporting rings takes place after deformation, so the joining process and the permissible positioning errors are similar to those when joining the bushing with a shaft (Figure 3).

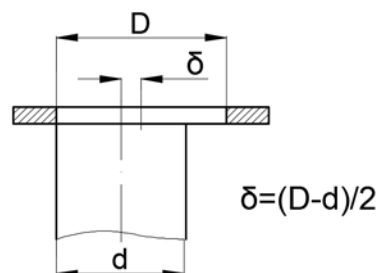


Figure 3. Permissible deviation when joining bushing to shaft.

It follows that a greater deformation of the supporting ring facilitates the joining, but its value should not exceed a certain allowable value, which would lead to damage to the supporting ring.

2. Determination of the deformation forces of the supporting rings with rectangular transverse profile

So, when joining the bearing rings are tightened or loosened, the difference being only in the direction of application of deformation forces.

Theoretically, eccentric rings in terms of deformation have more advantages than concentric ones. Due to their shape, the deformations in these rings are more evenly distributed, and, as will be shown below, such rings become more durable, especially at certain sizes. When mounting, the rings are deformed by the distributed force q or by two concentrated forces F , deposited tangentially. When installed in the hole, the rings are tightened and on the shaft are loosened. Depending on this, the deformation forces are deposited in one direction or another, so the formulas that are applied to the rings installed

on the shaft are equivalent to those that are applied to the rings installed in the hole, being different only the direction of forces and deformations.

The law of changing the cross section of the ring can be obtained in the following way: It follows from figure 4a that

$$AB = r_{\min} \cdot \cos \beta_1 \quad (1)$$

and from the other part we have

$$AB = r_{\max} - h - e \cdot \cos \varphi \quad (2)$$

At small eccentricities the angle β_1 is small and it can be supposed that $\cos \beta_1 \approx 1$. Connecting right-hand sides of equalities (1) and (2) we obtain:

$$h = r_{\max} - r_{\min} - e \cdot \cos \varphi \quad (3)$$

Let us denote the average height of the ring as follows:

$$r_{\max} - r_{\min} = \delta \quad (4)$$

and denote also the relative eccentricity by:

$$\frac{e}{\delta} = \chi \quad (5)$$

Let it be the height of the cross section

$$h = \delta \cdot (1 - \chi \cdot \cos \varphi) \quad (6)$$

The variation Δ_j can be established as the difference of the lengths of the middle circumference before and after deformation of the ring:

$$\Delta_j = 2 \cdot \pi \cdot r_2 - 2 \cdot \pi \cdot r'_2 \quad (7)$$

Within the limit of elastic deformations, the value Δ_j is directly proportional to the intensity of the distributed force q or concentrated force F . In both cases the proportionality coefficient between the given values can be found by means of the Mohr integral [12].

In order to do this we examine the half of the ring (Figures 4b, 4c), considering one end of it as fixed and the other one as free.

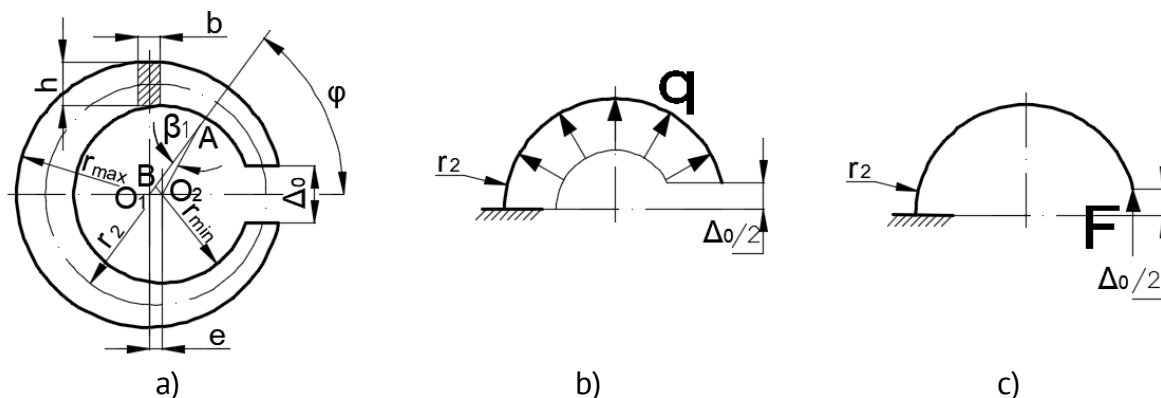


Figure 4. The constructive scheme and formalization of deformation of supporting ring.

The deformations of the second half of the ring will be symmetric to the deformations of the examined half of the ring.

Then in accordance to Mohr integral the move of the free end of the ring under the displacement of the free end from the force deposited tangent to the middle circumference of the ring will be:

$$\frac{\Delta_j}{2} = \int_0^{\pi} \frac{M \cdot M_1}{E \cdot I} \cdot r_2 d\varphi + \int_0^{\pi} \frac{k_{tr} \cdot Q \cdot Q_1}{G \cdot F_{tr}} \cdot r_2 d\varphi + \int_0^{\pi} \frac{N \cdot N_1}{E \cdot F_{tr}} r_2 d\varphi \quad (8)$$

where r_2 is the radius of the middle circumference of the ring;

M, Q, N are functions of bending moment, transverse and normal forces, occurring, occurring in the cross section of the ring from the given force;

M_1, Q_1, N_1 are the same functions from the unit force deposited instead of the cut, tangent to the middle circumference;

E, G is the modulus of elasticity of degree I and II of the material of the support ring;

$F_{tr} = b \cdot h$ is the cross-sectional area of the ring;

$I = \frac{b \cdot h^3}{12}$ is the moment of inertia of the ring at its deformation in the plane of curvature;

$k_{tr}=1.2$ is the coefficient, which depends on the transverse shape of the ring with a rectangular profile;

$\Delta_j = \Delta - \Delta_0$ is the change of play in the cut of the supporting ring, as a result of the actuation of the deformation force.

The functions of the internal factors are found using the section method. From the balance of the highlighted sector of the ring (Figure 4b, 4c) we find:

- when the ring is deformed with distributed force q :

$$\begin{aligned} M &= -2 \cdot q \cdot r_2^2 \cdot \sin^2 \frac{\varphi}{2} \\ Q &= -q \cdot r_2 \cdot \sin \varphi \\ N &= 2 \cdot q \cdot r_2 \cdot \sin^2 \frac{\varphi}{2} \end{aligned} \quad (9)$$

- at the deformation of the ring with concentrated forces F :

$$\begin{aligned} M &= -F \cdot r_2 \cdot (1 - \cos \varphi) \\ Q &= -F \cdot \sin \varphi \\ N &= -F \cdot \cos \varphi \end{aligned} \quad (10)$$

At the deformation of the bar with unit force (Figure 5) in the given direction, from the equilibrium condition we have:

$$\begin{aligned} M_1 &= -r \cdot (1 - \cos \varphi) \\ Q_1 &= -\sin \varphi \\ N_1 &= -\cos \varphi \end{aligned} \quad (11)$$

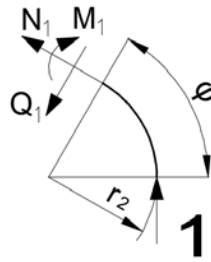


Figure 5. Deformation with unit force.

Substituting (9), (10), (11) in (8) and taking into account the already known F_{tr} , l , h we get:

a) when actuating the distributed force q :

$$\begin{aligned} \frac{\Delta_j}{2} = & \frac{24 \cdot q \cdot r_2^4}{E \cdot b \cdot \delta^3} \cdot \int_0^{\frac{\pi}{2}} \frac{\sin^2 \frac{\varphi}{2} \cdot (1 - \cos \varphi) d\varphi}{(1 - \chi \cos \varphi)^3} + \frac{1.2 \cdot q \cdot r_2^2}{G \cdot b \cdot \delta} \cdot \int_0^{\frac{\pi}{2}} \frac{\sin^2 \varphi d\varphi}{1 - \chi \cdot \cos \varphi} - \\ & - \frac{2 \cdot q \cdot r_2^2}{E \cdot b \cdot \delta} \cdot \int_0^{\frac{\pi}{2}} \frac{\sin^2 \frac{\varphi}{2} \cdot \cos \varphi d\varphi}{1 - \chi \cdot \cos \varphi} \end{aligned} \quad (12)$$

b) when actuating the concentrated force F :

$$\begin{aligned} \frac{\Delta_j}{2} = & \frac{12 \cdot F \cdot r_2^3}{E \cdot b \cdot \delta^3} \cdot \int_0^{\frac{\pi}{2}} \frac{(1 - \cos \varphi)^2}{(1 - \chi \cdot \cos \varphi)^3} d\varphi + \frac{1.2 \cdot F \cdot r_2}{G \cdot b \cdot \delta} \cdot \int_0^{\frac{\pi}{2}} \frac{\sin^2 \varphi}{1 - \chi \cdot \cos \varphi} d\varphi + \\ & + \frac{F \cdot r_2}{E \cdot b \cdot \delta} \cdot \int_0^{\frac{\pi}{2}} \frac{\cos^2 \varphi d\varphi}{1 - \chi \cdot \cos \varphi} \end{aligned} \quad (13)$$

After integration the change of variation Δ is determined accordingly:

a)

$$\begin{aligned} \Delta_j = & \frac{36 \cdot \pi \cdot r_2^4 \cdot q}{E \cdot b \cdot \delta^3 \cdot (1 + \chi^2) \cdot \sqrt{1 - \chi^2}} + \frac{2.4 \cdot \pi \cdot q \cdot r_2^2}{G \cdot b \cdot \delta \cdot \chi^2} \cdot \left(1 - \sqrt{1 - \chi^2} \right) + \\ & + \frac{2 \cdot \pi \cdot q \cdot r_2^2}{E \cdot b \cdot \delta \cdot \chi^2} \cdot \left(\sqrt{\frac{1 - \chi}{1 + \chi}} + (\chi - 1) \right) \end{aligned} \quad (14)$$

b)

$$\begin{aligned} \Delta_j = & \frac{18 \cdot \pi \cdot F \cdot r_2^3}{E \cdot b \cdot \delta^3 \cdot (1 + \chi^2) \cdot \sqrt{1 - \chi^2}} + \frac{1.2 \cdot \pi \cdot F \cdot r_2}{G \cdot \delta \cdot b} \cdot \frac{1 - \sqrt{1 - \chi^2}}{\chi} + \\ & + \frac{\pi \cdot F \cdot r_2}{E \cdot b \cdot \delta \cdot \chi^2} \cdot \left(\frac{1}{\sqrt{1 - \chi^2}} - 1 \right) \end{aligned} \quad (15)$$

In the rings used, the height of the cross section h is much smaller than the radius of the middle circumference r_2 . In this case the last two factors can be ignored without any major error for the accuracy of the calculation (the error does not exceed 0.3%).

Then:

$$q = \frac{E \cdot b \cdot \delta^3 \cdot (1 + \chi^2) \cdot \sqrt{1 - \chi^2}}{36 \cdot \pi \cdot r_2^4} \cdot \Delta_j \quad (16)$$

$$F = \frac{E \cdot b \cdot \delta^3 \cdot (1 + \chi^2) \cdot \sqrt{1 - \chi^2}}{18 \cdot \pi \cdot r_2^3} \cdot \Delta_j \quad (17)$$

Thus knowing the change of the variation Δ , from expressions (14) and (15) we can calculate the forces q and F , which will not exceed the permissible ones, which in turn depend on the durability of the ring:

$$\sigma_{\max} = \frac{M_{\max}}{W} = \frac{6 \cdot q \cdot r_2^2 \cdot (1 - \cos \varphi)}{b \cdot \delta^2 \cdot (1 - \chi \cdot \cos \varphi)^2} \leq [\sigma] \quad (18)$$

or

$$\sigma_{\max} = \frac{M_{\max}}{W} = \frac{6 \cdot F \cdot r_2 \cdot (1 - \cos \varphi)}{b \cdot \delta^2 \cdot (1 - \chi \cdot \cos \varphi)^2} \leq [\sigma] \quad (19)$$

where M_{\max} is the moment of bending in the dangerous section of the ring;

W is the moment to oppose bending in this section;

$[\sigma]$ are allowable stresses of the ring material.

The optimization of the dimensions of the support rings consists in determining the eccentricity χ at which the change of value Δ would be maximum. At the same time, changing the value of χ changes the place of the dangerous section in the ring. At low values of χ it is located opposite to the cut. With increasing χ the place of the dangerous section approaches the cut.

For this reason, when optimizing the dimensions of the support rings, first of all the angle ϕ at which the dangerous section in the ring is located must be determined and only then the dependence of this angle on the eccentricity χ .

In the dangerous section the stresses are maximum, therefore to find the place of this section it is necessary to study the extremes of the function σ_{\max} :

$$\frac{d \sigma_{\max}}{d \varphi} = \frac{6 \cdot q \cdot r_2^2}{b \cdot \delta^2} \cdot \sin \varphi \cdot \frac{(1 - \chi \cdot \cos \varphi) - 2 \cdot \chi \cdot (1 - \cos \varphi)}{(1 - \chi \cdot \cos \varphi)^3} = 0 \quad (20)$$

or

$$\frac{d \sigma_{\max}}{d \varphi} = \frac{6 \cdot F \cdot r_2}{b \cdot \delta^2} \cdot \sin \varphi \cdot \frac{(1 - \chi \cdot \cos \varphi) - 2 \cdot \chi \cdot (1 - \cos \varphi)}{(1 - \chi \cdot \cos \varphi)^3} = 0 \quad (21)$$

Equality to zero of the derivative of the function σ_{\max} is possible if $\sin \phi = 0$ or:

$$\frac{(1 - \chi \cdot \cos \phi) - 2 \cdot \chi \cdot (1 - \cos \phi)}{(1 - \chi \cdot \cos \phi)^3} = 0 \quad (22)$$

In the first case, the dangerous section is located opposite the cut and does not depend on the eccentricity χ , corresponding to rings with a constant profile ($\chi=0$).

For rings with variable profile, formula (22) enters into force, which represents a transcendent equation with respect to the variable ϕ . The solution of this equation in the interval $\chi = 0 \dots 1$ with step 0.01 is represented in Figure 6, from which follows that the dangerous section is located in the plane of symmetry of the ring ($\phi = 180^\circ$) at $\chi = 0 \dots 0.33$.

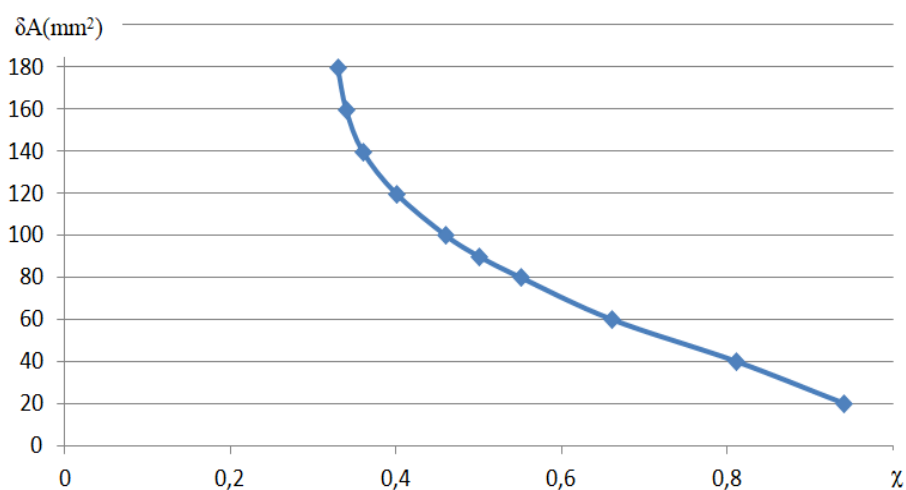


Figure 6. Location angle of the dangerous section ϕ° depending on the eccentricity χ .

Increasing the eccentricity moves the dangerous section to the cut of the ring. At $\chi = 1$ ϕ tends to zero.

The change of the eccentricity also leads to the change of the values of the forces necessary for the deformation and the maximum value of the variation Δ_j , respecting the condition of avoiding the plastic deformations of the deformed ring. These changes can be calculated by the formulas (16, 17, 18, 19). Figures 7, 8 show the graphs obtained as a result of the calculation of the change F and Δ_j depending on the change of eccentricity χ for rings with the dimensions:

$$r_2 = 24.3;$$

$$b = 1.5;$$

$$\delta = 4.1;$$

$$[\sigma] = 240 \text{ Mpa};$$

And step $\chi = 0.01$ in the interval from 0 to 1.

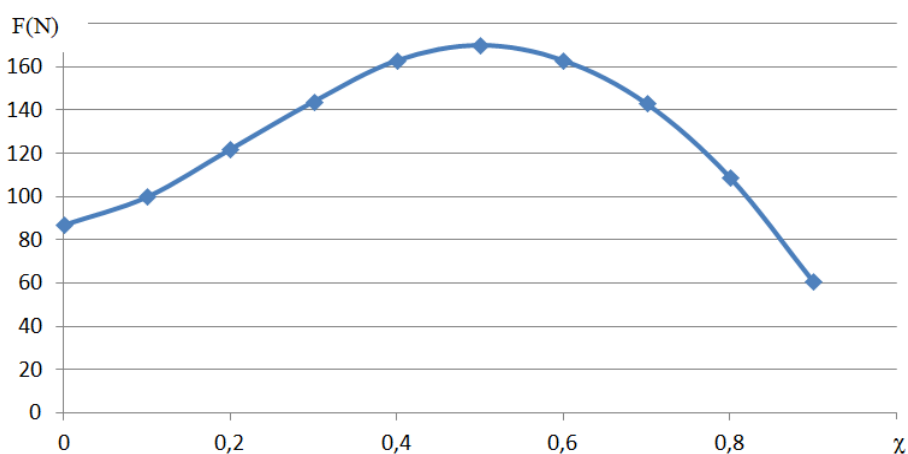


Figure 7. Dependence of the allowable force applied to the support ring $F \text{ (N)}$ as a function of eccentricity χ .

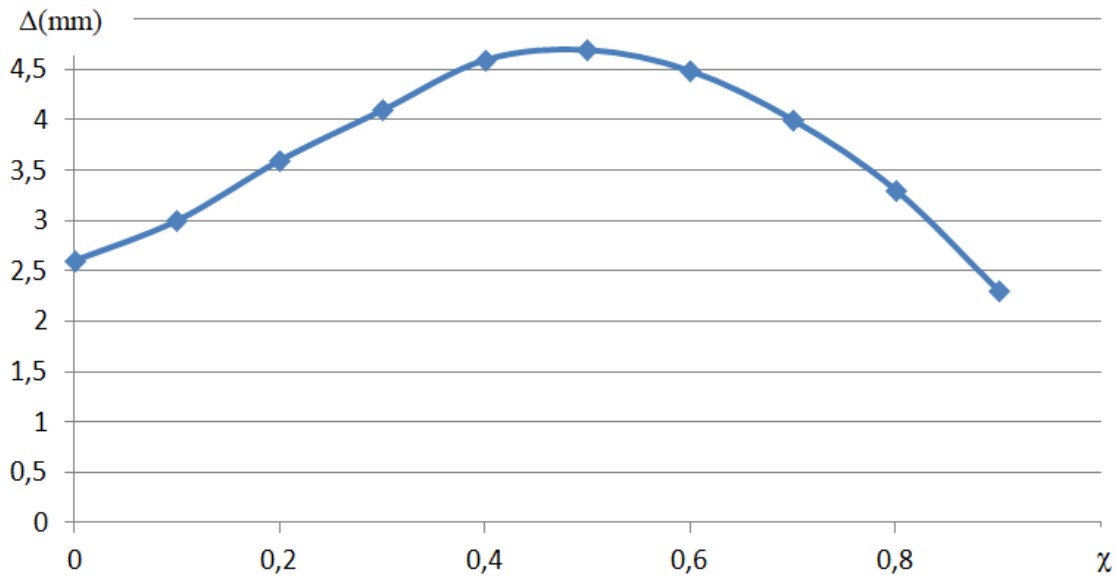


Figure 8. Dependence of the permissible deformation of the support ring Δ (mm) as a function of eccentricity χ .

The initial parameters of the supporting rings (sizes and material) do not influence the change of their deformation parameters; optimal eccentricity $\chi=0.49$, at which the permissible deformation acquires maximum values remains unchanged.

3. Optimizing the eccentricity of the rings and the angle of application of the deformation forces

The rings are deformed by the forces F , directed at a certain angle α to the tangents to the outer circumference of the ring (Figure 9). The change in the surface of the circle with radius r_2 can be taken as a parameter of the deformation of the rings.

When deforming, the ring deviates from the round shape, but this deviation can be neglected, being a variable value and difficult to appreciate.

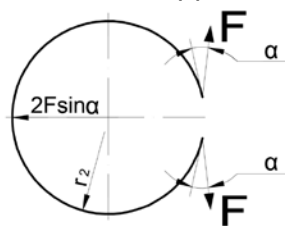


Figure 9. The scheme of application of deformation forces.

Mohr's integral for changing the surface of the circle with radius r_2 :

$$\delta A = 2 \cdot \int_0^\pi \frac{M_F \cdot M_1}{E \cdot I} d\phi + 2 \cdot \int_0^\pi \frac{N_F \cdot N_1}{E \cdot F_{tr}} d\phi + 2 \cdot \int_0^\pi \frac{k_{tr} \cdot Q_F \cdot Q_1}{G \cdot F_{tr}} d\phi \quad (3.423)$$

where $F_{tr}=bh$ is the cross-sectional area of the considered ring;

$I=bh^3/2$ – is the moment of inertia of the cross section;

R_{tr} – is the coefficient of the transverse shape of the ring.

Functions of internal factors occurring when actioning the force F : M_F , N_F and Q_F or by actioning the force q : M_1 , N_1 and Q_1 are determined by the method of sections (Figure 10):

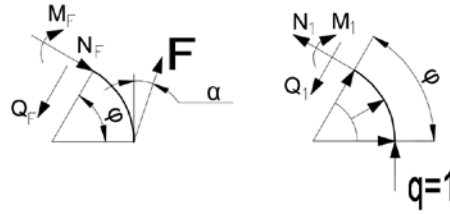


Figure 10. Formalization of the support ring deformation.

$$\begin{aligned}
 M_F &= -F \cdot r_2 \cdot \cos \alpha \cdot (1 - \cos \phi) - F \cdot r_2 \cdot \sin \phi \cdot \sin \phi; \\
 N_F &= -F \cdot \cos \alpha \cos \phi + F \cdot \sin \alpha \cdot \sin \phi; \\
 Q_F &= -F \cdot \cos \alpha \cdot \sin \phi - F \cdot \sin \alpha \cdot \cos \phi; \\
 M_1 &= -r_2^2 \cdot (1 - \cos \phi); \\
 N_1 &= r_2 \cdot (1 - \cos \phi); \\
 Q_1 &= -r_2 \cdot \sin \phi.
 \end{aligned} \tag{24}$$

Substituting the above values in (23) we get:

$$\begin{aligned}
 \delta A &= 24 \int_0^\pi \frac{\pi F \cdot \cos \alpha \cdot r_2^4 \cdot (1 - \cos \phi)^2}{E \cdot b \cdot \delta^3 (1 - \chi \cdot \cos \phi)^3} d\phi - \\
 &2 \cdot \int_0^\pi \frac{F \cdot \cos \alpha \cdot r_2^2 \cdot \cos \phi \cdot (1 - \cos \phi)}{E \cdot b \cdot \delta^3 \cdot (1 - \chi \cdot \cos \phi)} d\phi + \\
 &+ 2.4 \int_0^\pi \frac{\pi F \cdot \cos \alpha \cdot r_2^2 \cdot \sin^2 \phi}{G \cdot b \cdot \delta \cdot (1 - \chi \cdot \cos \phi)} d\phi + 24 \int_0^\pi \frac{\pi F \cdot \sin \alpha \cdot r_2^4 \cdot \sin \phi \cdot (1 - \cos \phi)}{E \cdot b \cdot \delta^3 \cdot (1 - \chi \cdot \cos \phi)^3} d\phi + \\
 &+ 2 \cdot \int_0^\pi \frac{F \cdot \sin \alpha \cdot r_2^2 \cdot \sin \phi \cdot (1 - \cos \phi)}{E \cdot b \cdot \delta \cdot (1 - \chi \cdot \cos \phi)} d\phi + 2.4 \cdot \int_0^\pi \frac{\pi F \cdot \sin \alpha \cdot r_2^2 \sin \phi \cdot \cos \phi}{G \cdot b \cdot \delta \cdot (1 - \chi \cdot \cos \phi)} d\phi
 \end{aligned} \tag{25}$$

and after integration we come to:

$$\begin{aligned}
 \delta A &= \frac{2 \cdot F \cdot \cos \alpha \cdot \pi \cdot r_2^2}{b \cdot \delta} \frac{18 \cdot r_2^2}{E \cdot \delta^2} \cdot \left[\frac{18 \cdot r_2^2}{E \cdot \delta^2} \cdot \frac{1}{\sqrt{1 - \chi^2} \cdot (1 + \chi)^2} + \frac{1}{E \cdot \chi^2} \cdot \left(\sqrt{\frac{1 - \chi}{1 + \chi}} - (1 + \chi) \right) \right] + \\
 &+ \frac{1.2}{G \cdot \chi^2} \cdot \left(1 - \sqrt{1 - \chi^2} \right) - \left[\frac{4 \cdot F \cdot \sin \alpha \cdot r_2^2}{b \cdot \delta} \cdot \left[\frac{12 \cdot r_2^2 \cdot (1 - \chi)}{E \cdot \delta^2 \cdot (1 - \chi^2)} + \frac{1}{E \cdot \chi^2} \cdot \left(\chi + \frac{1 - \chi}{2} \cdot \ln \frac{1 - \chi}{1 + \chi} \right) - \right. \right. \\
 &\quad \left. \left. - \frac{1.2}{G \cdot \chi^2} \cdot \left(\chi + \frac{1}{2} \ln \frac{1 - \chi}{1 + \chi} \right) \right] \right]
 \end{aligned} \tag{26}$$

This formula allows us to establish the influence of angle α and eccentricity χ on the deformation of the ring. The first factors in the square bracket play a key role in the formula. The rest of the factors can be neglected without losing the accuracy of the calculations.

Maximum elastic deformations of the ring, beware:

$$\sigma_{\max} = \frac{F \cdot r_2 \cdot (\cos \alpha \cdot \cos \phi)}{b \cdot h \cdot e_1} \cdot \frac{h/2 - e_1}{r_2 - h/2} \tag{27}$$

where e_1 is the eccentricity of the neutral line:

$$e_1 = h^2/12 \cdot r_2$$

Then:

$$\sigma_{\max} = \frac{2 \cdot F \cdot r_2}{b} \cdot \frac{\cos \alpha - \cos \varphi}{\delta^2 \cdot (1 - \chi \cdot \cos \varphi)^2} \cdot \frac{6 \cdot r_2 \cdot (1 - \chi \cdot \cos \varphi)}{2 \cdot r - \delta \cdot (1 - \chi \cdot \cos \varphi)} \quad (28)$$

The given formula suppose the knowledge of the angle φ , which depends on the angle α and the eccentricity χ .

If α and χ are known, the place of the dangerous section is calculated by studying the extremes of the function:

$$\begin{aligned} \frac{d \sigma_{\max}}{d \varphi} = \frac{2 \cdot F \cdot r_2}{b \cdot \delta^2} \cdot \sin \varphi \cdot \left[\frac{(1 - \chi \cdot \cos \varphi) - 2 \cdot \chi \cdot (\cos \alpha - \cos \varphi)}{(1 - \chi \cdot \cos \varphi)^3} \cdot \right. \\ \left. \cdot \frac{6 \cdot r_2 - \delta \cdot (1 - \chi \cdot \cos \varphi)}{2 \cdot r - \delta \cdot (1 - \chi \cdot \cos \varphi)} + \frac{\cos \alpha - \cos \varphi}{(1 - \chi \cdot \cos \varphi)^2} \cdot \frac{4 \cdot r_2 \cdot \delta \cdot \chi}{(2 \cdot r - \delta \cdot (1 - \chi \cdot \cos \varphi))^2} \right] = 0 \end{aligned} \quad (29)$$

This equality can take place for $\sin \varphi = 0$ or when the value of the square parenthesis is equal to zero. In the first case, the dangerous section is located opposite the ring cut ($\varphi = 180^\circ$) and corresponds to equality to zero of α and χ .

In the second case, the place of the dangerous section is found by solving the transcendental equation (in square brackets), equaling it with zero.

Thus the algorithm for studying the dependence of the ring deformation on the angle α and the eccentricity χ contains three stages:

1. Determining the angle φ having α and χ known;
2. Calculation of the maximum allowable force required for the deformation of the ring, based on the condition $\sigma_{\max} \leq [\sigma]$;
3. Determination of the parameter δA by changing α and χ .

In order to automate the process of optimizing the dimensions of the rings and determining the optimal angle α of actuation of the deformation forces, formulas 26, 28 and 29 were algorithmized, formula 29 being calculated by Ribacov's iteration method [13], because it is unsolvable mathematically.

The results of the calculations for the supporting rings with the parameters:

$$r_2 = 24.3;$$

$$b = 1.5;$$

$$\delta = 4.1;$$

$$[\sigma] = 240 \text{ Mpa};$$

are presented in the Figures 11 and 12.

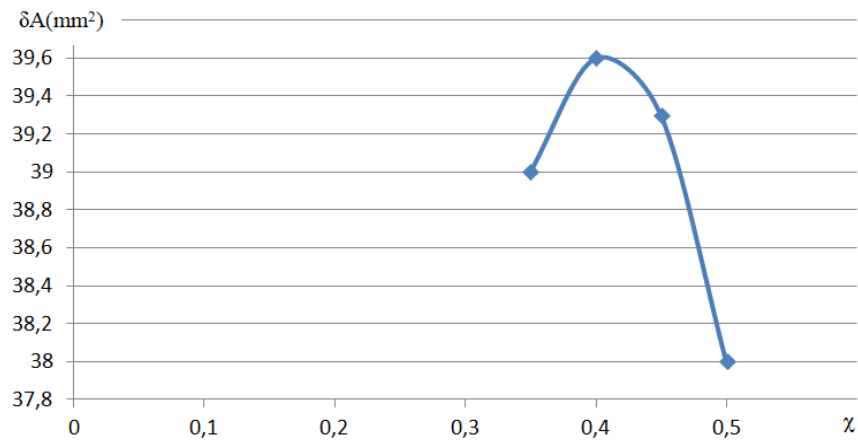


Figure 11. Dependence of the allowable deformation of the supporting ring $\delta A(\text{mm}^2)$ as a function of eccentricity χ with forces applied at an angle $\alpha=0^\circ$.

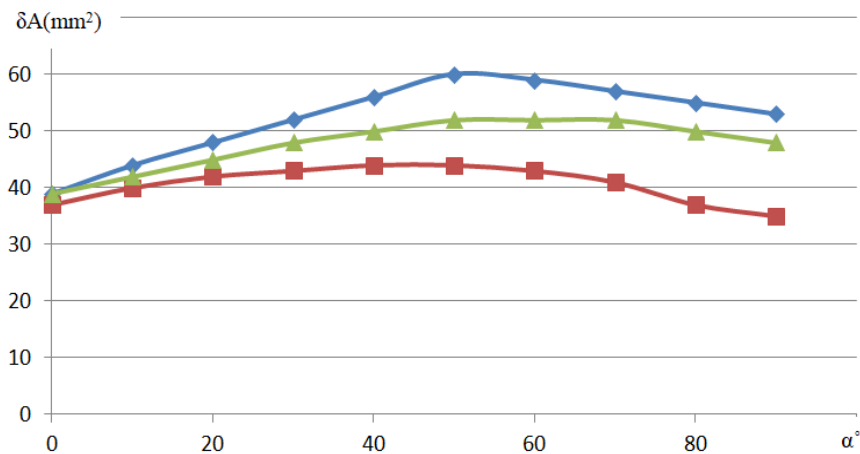


Figure 12. Dependence of the allowable deformation of the supporting ring $\delta A(\text{mm}^2)$ depending on the angle of application α of the deformation forces for eccentricity $\chi=0$ (graph with symbol \square), $\chi=0.33$ (graph with symbol Δ), $\chi=0.4$ (graph with symbol \diamond).

Conclusions

- 1) Eccentric rings create more pleasant conditions for deformation, due to the uneven location of the material in them;
- 2) The rings with the relative eccentricity 0.5, which was determined as optimal, possess an increased deformability by 20 ... 25% compared to those stipulated in the standards GOST 13942-83 and GOST 13943-86, which are executed with the relative eccentricity 0.2 ... 0.3;
- 3) The tightening and unwinding processes of the rings are equivalent, the calculation formulas in both cases are the same, only the deformation forces changing their sign;
- 4) When applying the deformation forces at an angle of 50 degrees, determined as optimal, the deformability of the eccentric rings increases by 25 ... 30% and of the concentric ones by about 20%;
- 5) The value of the optimal relative eccentricity is not influenced by the dimensions and the material of the rings, always remaining constant.

References

1. Jonson E. Automating assembly-A crucial step for day one. *Assemblymag.com*. 2020, November 5. <https://www.assemblymag.com/articles/95980-automating-assembly-a-crucial-step-for-day-one> - accessed 20.07.2021.
2. Abramova L.D., Salomatin N.A. Modern problems of production automation. *University Bulletin*, 2012, 7, pp. 42-49, ISSN 1816-4277 [in Russian].
3. Bozhko A.N. Automation of the design of assembly processes of complex products using virtual reality. *Intelligent IT in management*, 2018, N2, pp. 36-40, UDC.67.02, 004.942, 519 [in Russian].
4. Semenov A.N. Manufacturability of the design of the mechanical engineering product. Rybinsk, RGTAU, 2016, 217r., UDC.621 [in Russian].
5. https://studme.org/97106/tehnika/metodika_posledovatelnost_proektirovaniya_tehnologicheskikh_protsesov_sborki- accessed 20.07.2021.
6. Vorobiev E. I., Gavryushin S. S. New mechanisms in modern robotics. Moscow, Technosphere, 2018, 316p., ISBN: 978-5-94836-537-4.178 [in Russian].
7. Lorre B. L'automatisation industrielle, quel avenir pour les usines du futur?, 22.10.2020, iatranshumanisme.com- accessed 02.02.2021.
8. Costa M. J. R., Gouveia R. M., G. Silva F. J., Campilho R. D. S. How to Solve quality problems by advanced fully-automated manufacturing systems. *The international journal of Advanced Manufacturing Technology*, February 2018, 94(1), pp. 3041-3063, DOI: 10.1007/S00170-017-0158-8.
9. GOST 27017-86 (ISO 1891-79) Fasteners. Terms and Definitions [in Russian].
10. <http://www.smalley.ru/stati/stopornye-kolca>- accessed 20.07.2021.
11. <http://sibindustry.ru/engineering/stopornyje-kolca-vidy-kharaktjeristiki-sfjera-primjenjenija.html>- accessed 20.07.2021.
12. Feodosiev V.I. Resistance of materials. Moscow, MSTU im. N.E.Bauman, 2018, 544p., ISBN: 978-5-7038-4819-7 [in Russian].
13. Zhavoronkov L. Numerical Analysis in Pascal ABC: Studies in Applied Mathematics. Amazon.com Services LLC, 2020, 409p., ISBN: 978-5-906886-71-2.

[https://doi.org/10.52326/jes.utm.2021.28\(3\).04](https://doi.org/10.52326/jes.utm.2021.28(3).04)
CZU 544.45:546.27



IGNITION AND COMBUSTION OF SINGLE SOLID PARTICLES AS NON-ISOTHERMAL METHODS OF CHEMICAL KINETICS

Grigore Ambrosi*, ORCID ID: 0000-0001-7232-2998

Technical University of Moldova, 168 Ștefan cel Mare și Sfânt Blvd., Chisinau, Republic of Moldova

*Corresponding author: Grigore Ambrosi, grigore.ambrosi@tran.utm.md

Received: 06. 17. 2021

Accepted: 08. 12. 2021

Abstract. The ignition and combustion of single particles of crystalline boron continue to produce major scientific interest due to the particularities of the process and diversity of potential applications of boron compounds. The full valorization of boron energetic potential is a very current scientific challenge. The objective of the paper is to systematize the methodology for evaluating the kinetic parameters of boron ignition and combustion reactions in various oxidizing gaseous environments. Experimental dependencies between the ignition temperature and the particle size, as well as the combustion time as a function of oxidizing temperature are used for the calculation of the kinetic constants. As a main result, the kinetic parameters of the ignition and combustion reactions of boron in oxygen and water vapor are calculated.

Keywords: *boron, thermodynamics, reaction, oxidation, heterogeneous, calculation, parameter, experiment.*

Introduction

Initially approached by Wilhelm Nusselt, the issue of ignition and combustion of the solid particle still requires major attention. Despite an impressive amount of relevant information on this topic and the formulation of remarkable theoretical generalizations, currently there is no irrevocable analytical theory, which considers the complexity of physico-chemical phenomena specific to heterogeneous ignition and combustion processes. Usually, simplified models of chemical processes are applied or the similarity theory is used.

Chemical kinetics, developed from practical needs to clarify the picture of chemical transformations, especially for the determination of the speed and mechanism of reactions, contributes decisively to the study of ignition and combustion phenomena. Currently, the studies of chemical kinetics are combining two complementary directions, both of them having different paradigms and tasks [1].

The objective of the first direction is to identify the mechanism of the reaction. This objective is achieved by applying the modern methods of stoichiometry, chemical thermodynamics, theory of solid mechanics and theory of activated complex. Thus, the kinetic parameters of the sequence of elementary reactions are calculated theoretically and measured experimentally. The results are mainly of a qualitative nature. Consequently, the

intermediates and the sequence of transformation of the reactants into products are established [1].

The second direction of research is formal kinetics, which is methodologically analyzed in this paper. It consists in the phenomenological quantitative investigation of complex reactions, with sufficiently precise determination of kinetic parameters. The importance of these studies is growing due to the lack of accurate kinetic information needed in practice for model simulation and process optimization [2, 3].

The processes of ignition and combustion of the boron particle are characterized by a higher level of complexity than in the case of classical solid fuel particles. The main particularity is determined by the existence of the surface oxide layer, formed in the latent phase of the preliminary reaction, which substantially changes the picture of the interaction [2], [4], [8], [9].

The high calorific value and the distinctive physical-mechanical properties of some boron compounds are of increased interest, because these substances are less studied for energetic and technological applications [3, 4, 9, 10].

Until the development of non-isothermal theories in chemical kinetics, the self-heating of the reactant was qualified as an experimental error that deforms the kinetic curves. The theory of thermal explosion cardinally changed the approach to the problem, confirming the opportunity of kinetic study in non-isothermal conditions [2, 4].

The essence of this theoretical realization consists in the fact that the models of non-isothermal phenomena quantitatively relate the measurable characteristics of the processes with the kinetic parameters. If the conditions of chemical transformations are known, the physical parameters of the system being measured, then by solving the inverse problem the kinetic parameters of the chemical reaction can be determined: activation energy E , J·mol⁻¹ and the pre-exponential coefficient k_0 , m·s⁻¹ [2, 4, 7].

The defining characteristics are: the value of the oxidant temperature at ignition place of the sample (T_{ga} , °K), the duration of particle ignition under the respective conditions (t_{ap} , s) and the burning rate of the solid substance (t_{ar} , s). A wide variety of methods for calculating kinetic parameters from experimental ignition and combustion data are currently being developed and applied.

1. Evaluation of kinetic parameters for the ignition of solid particles

If the solid substance and the high temperature gaseous oxidant (700 - 2000°K) are separated by an oxide film, usually the speed of the chemical interaction is limited by the diffusion of the oxidant through the oxide layer to the reaction surface and depends not only on the temperature and the concentration of the oxidant, but also on the thickness of the increasing layer [2, 4, 5, 6].

Experimentally, different oxidation laws have been established [83]. The main laws states that the speed of the reaction R_{ox} (the rate of increase of the oxide layer) decreases with the increase of the thickness h of the film, inversely proportional to the thickness of the diffusion barrier raised to the power of n [2, 4]:

$$R_{ox} = \rho_{ox} \cdot \frac{dh}{dt} = \frac{C_{ox}^v}{h^n} \cdot k_0 \cdot e^{-\frac{E}{RT}}, \text{ mol} \cdot \text{m}^{-2} \cdot \text{s}^{-1} \quad (1)$$

where: ρ_{ox} is the density of the oxide surface layer (B_2O_3), mol·m⁻³;

C_{ox} - oxidant concentration in the gaseous environment, $\text{mol}\cdot\text{m}^{-3}$;

ν - reaction order for the given oxidant;

E - activation energy of the oxidation reaction in the ignition phase, $\text{J}\cdot\text{mol}^{-1}$;

k_0 - the pre-exponential coefficient of the oxidation reaction, $\text{m}\cdot\text{s}^{-1}$.

The exponent n defines the relationship between the reaction rate and the thickness of the oxide layer, having linear ($n = 0$), parabolic ($n = 1$) or cubic ($n = 2$) dependencies [2, 4].

Usually $n = 0$ for porous films or with very low protective properties. The oxidation process under these conditions coincides with the kinetics of the heterogeneous reaction on a clean surface. If $n = 1$, then the reaction rate is determined by the diffusion of the oxidant in the oxide layer, the dependence between the diffusion coefficient and the temperature being exponential.

For some substances, including boron, the combination of different oxidation mechanisms is noticed. In such situations the reaction takes place according to several mechanisms, each of one being predominant in distinct stages of the process. For example, if initially, at normal temperatures the oxidation is parabolic ($n = 1$), later, with the increase of the temperature due to various causes (polymorphic modification, melting, vaporization of the film) the reaction speed becomes linear ($n = 0$), the whole process being defined. as a parilinear.

For metals that interact with the oxidant according to formula (1), the system of equations that describes the process of ignition of the particle (neglecting the radiant energy exchange) has the following general form [4]:

$$\begin{aligned} \frac{1}{6} \cdot c_m \cdot \rho_m \cdot d_p \cdot \frac{dT_p}{dt} &= Q \cdot \rho_m \cdot \frac{dh}{dt} - \frac{\lambda \cdot Nu}{d_p} \cdot (T_p - T_g), \\ \frac{dh}{dt} &= \frac{C_{ox}^\nu}{h^n} \cdot k_0 \cdot e^{-\frac{E}{RT_p}} \end{aligned} \quad (2)$$

$$t = 0; \quad h = h_0; \quad T_p = T_{p0}.$$

where: c_m is the specific calorific value of the metal, $\text{J}\cdot\text{K}^{-1}\cdot\text{kg}^{-1}$;

ρ_m - metal density, $\text{kg}\cdot\text{m}^{-3}$; d_p - particle size, m; Q - thermal effect of the reaction, $\text{J}\cdot\text{kg}^{-1}$;

λ - thermal conductivity of the oxidant, $\text{W}\cdot\text{m}^{-1}\cdot^\circ\text{K}^{-1}$;

T_p, T_g - temperature of the particle and oxidizing environment, $^\circ\text{K}$; t - time, s,

Nu - Nusselt number.

The Nusselt number, the ratio between the temperature gradient of the gas oxide at the surface of single particles and the reference temperature gradient, is determined by the Ranz-Marshall criterion:

$$Nu = 2 + \text{Re}^{0.5} \cdot \text{Pr}^{0.33} \quad (3)$$

where: Re , Pr are the Reynolds and Prandtl numbers under the given experimental conditions.

The Reynolds number characterizes the flow regime of the oxidant around the particle and represents the ratio between the inertial forces and the viscosity forces. The Prandtl number characterizes the physical properties of the oxidant and represents the ratio between the molecular diffusivity of the impulse and the molecular diffusivity of the heat.

In the case of parilinear ignition reactions for $n = 0$, $\nu = 1$ and $Bi \ll 1$, the ratio between the system parameters in critical ignition conditions is determined according to the theory of heterogeneous ignition [48] with the following formula:

$$Q \cdot \rho_m \cdot c_{ox} \cdot \frac{E}{\lambda \cdot R} \cdot \frac{d_p}{Nu \cdot T_{ga}^2} \cdot k_0 \cdot e^{-\frac{E}{RT_{ga}}} = \frac{1}{e}, \quad (4)$$

where: T_{ga} is the temperature of the oxidant in the place of ignition of the solid particle, in °K;

Bi - Biot number.

When calculating the logarithm for relation (4), we obtain the following formula:

$$\ln\left(\frac{d_p}{Nu \cdot T_{ga}^2}\right) = \frac{E}{R \cdot T_{ga}} + \ln C_1, \quad (5)$$

If the experimental dependence $T_{ga} = f(d_p)$ is known, the graphical dependence $\lg(d_p / Nu \cdot T_{ga}^2) = F(T_{ga}^{-1})$ will result in a line from the slope of which the activation energy can be determined according to the relation:

$$E = 2,303 \cdot R \cdot |\operatorname{tg} \alpha| \cdot r, \text{ J} \cdot \text{mol}^{-1} \quad (6)$$

where: R is the universal gas constant, $\text{J} \cdot \text{mol}^{-1} \cdot \text{°K}$; θ - slope angle, degrees; r - the ratio of the axle scale.

The value of the pre-exponential coefficient k_0 will be determined by substituting in formula (3) the value E .

If radiation heat losses (relatively larger particles) are included in the analysis, then the thermal balance of the system of equations (2) can be represented as follows:

$$\frac{1}{6} \cdot c_m \cdot \rho_m \cdot d_p \cdot \frac{dT_p}{dt} = Q \cdot \rho_m \cdot \frac{dh}{dt} - \frac{\lambda \cdot Nu}{d_p} \cdot (T_p - T_g) - \varepsilon_p \cdot \sigma \cdot (T_p^4 - T_1^4), \quad (7)$$

where: ε_p is the emission coefficient of the particle surface;

σ - Stefan-Boltzmann constant, $\text{W} \cdot \text{m}^{-2} \cdot \text{°K}^{-4}$;

T_1 - temperature of the inner surface of the combustion chamber, °K.

When taking into account the effect of thermal radiation for parilinear ignition reactions, the ratio between the parameters in the critical ignition conditions is given by the following expression:

$$Q \cdot \rho_m \cdot c_{ox} \cdot \frac{E}{\lambda \cdot R} \cdot \frac{d_p}{Nu \cdot T_{ga}^2} \cdot k_0 \cdot e^{-\frac{E}{RT_{ga}}} \cdot e^{K_R \cdot (1-b)} = \frac{1}{e}, \quad (8)$$

where: K_R is the ratio of heat loss through radiation; b - ratio T_1^4 / T_{ga}^4 .

When calculating the logarithm for relation (8), we obtain:

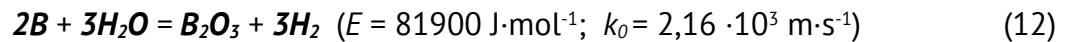
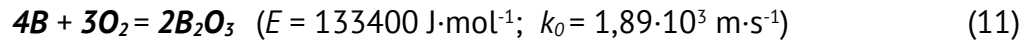
$$\ln\left(\frac{d_p}{Nu \cdot T_{ga}^2}\right) = \frac{E}{R \cdot T_{ga}} \cdot \left[1 + (1-b) \cdot \frac{\varepsilon_p \cdot \sigma \cdot T_{ga}^3}{\lambda \cdot Nu} \cdot d_p\right] + \ln C_2, \quad (9)$$

If the experimental dependence $T_{ga} = f(d_p)$ is known, then as a result of the graph:

$$\lg\left(\frac{d_p}{Nu \cdot T_{ga}^2}\right) = F(T^{-1} \cdot (1 + (1-b) \cdot \frac{\varepsilon_p \cdot \sigma \cdot T_{ga}^3}{\lambda \cdot Nu} \cdot d_p)), \quad (10)$$

a line will be obtained from the slope of which the activation energy E will be evaluated. Consequently, from the relation (8) the value of the pre-exponential coefficient k_0 can be evaluated.

In particular, the described methodology was used to determine the kinetic constants of the ignition of single particles of crystalline boron in air and water vapor, respectively, for the following two complex heterogeneous reactions:



2. Evaluation of kinetic parameters for the kinetic regime of combustion for solid particles.

For the kinetic combustion regime of single particles of crystalline boron the reaction rate is determined by the following formula:

$$R_B = k \cdot C_{ox} = \frac{k \cdot P_{ox}}{R \cdot T}, \text{ mol}\cdot\text{m}^{-2}\cdot\text{s}^{-1} \quad (13)$$

where: P_{ox} is the partial pressure of the oxidant in the gaseous medium, Pa.

If for the stationary combustion process, it is assumed that the density and temperature of the particle are constant as well as the combustion rate and the partial pressure of the oxidant, then for the combustion time of the particle can be calculated by the formula:

$$t_{ar} = -\frac{1}{2 \cdot M_B} \cdot \int_{d_p}^0 \frac{\rho_m}{R_B} \cdot d(d_p) = \frac{\rho_m \cdot R \cdot T}{2 \cdot M_B \cdot k \cdot P_{ox}} \cdot d_p = k \cdot d_p, \text{ s} \quad (14)$$

For the kinetic regime the combustion time of the boron particle, measured experimentally, is proportional to the diameter of the sample.

From relation (14) the following expression is obtained:

$$k_0 \cdot e^{\frac{E}{R \cdot T}} = \frac{\rho_m \cdot R \cdot T \cdot d_p}{2 \cdot M_B \cdot t_{ar} \cdot P_{ox}}, \text{ m}\cdot\text{s}^{-1} \quad (15)$$

By calculating the logarithm from equation (14), the following formula is obtained:

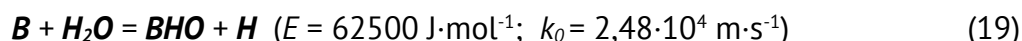
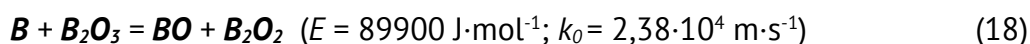
$$\ln\left(\frac{d_p \cdot T_{ox}}{t_{ar} \cdot P_{ox}}\right) = -\frac{E}{R \cdot T} - \ln\frac{R \cdot \rho_m}{2 \cdot M_B} \quad (16)$$

If the experimental dependence $t_{ar} = f(T_{ox})$ is known, then following the dependence:

$$\lg\left(\frac{d_p \cdot T_{ox}}{t_{ar} \cdot P_{ox}}\right) = F(T_{ox}^{-1}) \quad (17)$$

a straight line will result, from which the value of the activation energy of the complex combustion reaction in kinetic regime will be evaluated. Substituting the value E in formula (15), the value of the pre-exponential coefficient k_0 can be calculated.

For the kinetic combustion domain of the particle, the following constants of heterogeneous reactions were evaluated:



3. Conclusions

The ignition and combustion of single solid particles as non-isothermal methods of formal chemical kinetics contributes to obtaining unique information on the kinetics and thermodynamics of heterogeneous reactions at high temperatures, data that cannot be obtained otherwise, especially for dispersed systems.

Heterogeneous formal kinetics research is based on relatively simple experiments, with vast possibilities for varying experimental conditions.

Based on the principles of formal kinetics, which are a component of general methods of evaluating the kinetic parameters of chemical reactions, particular methods have been deducted for calculating the kinetic constants of complex reactions of ignition and combustion of single solid particles for different regimes of chemical reaction of oxidation.

The methodology for evaluating the kinetic parameters of heterogeneous oxidation reactions involves the use of some experimental data as initial data. The required experimental data is the following: the ignition temperature depending on the sample size and the combustion time of the sample depending on the oxidant temperature.

According to the theoretical formulas that describe the burning of single particles of crystalline boron, the kinetic regime of the interaction corresponds to the experimental domain in which the burning time of the sample is proportional to its size.

The procedures for evaluating the kinetic parameters of boron combustion, systematized in the paper, can be used to determine the kinetic vaporization rates of boron and boric anhydride in an inert atmosphere and the rate of gasification of anhydride in water-containing combustion products. The experimental parameter which is measured is the durations of those processes as a dependence of the temperature of the gaseous environment.

Acknowledgements: The research was conducted within the research according to scientific contracts no. 50 „Determination of gas dynamics and kinetic parameters in the combustion of metals-containing fuels for air-powered engines”, no. 159 „Processes of combustion of metals-containing fuels” and the budget state theme no. 111 „Hardening and reconditioning of parts by thermal and thermochemical methods”, running at Technical University of Moldova.

References

1. Gremyachkin V.M., Mihal'chuk M.V. *Some aspects in the theory of boron combustion*. In: *Physicochemical kinetics in gas dynamics*, 2014, pp. 1 – 8.
2. Yagodnikov D.A. *Vosplamnenie i gorenie poroshkoobraznykh metallov* [Ignition and combustion of powdered metals]. Moscow, Bauman MSTU Publ., 2009, 432 p. (in Russian).
3. Bakulin V.N., Dubrovkin N.F., Kotova V.N., Sorokin V.A., Frantsevich V.P., Yanovskiy L.S. *Energoemkie goryuchie dlya aviatsionnykh i raketnykh dvigateley* [Energy-intensive fuel for aircraft and rocket engines]. Moscow, Fizmatlit Publ., 2009, 400 p. (in Russian).
4. Hussman B., Pfitzner M. *Extended combustion model for single boron particles*. In: *Combustion and Flame*. 2010, 157, pp. 803 – 821.

5. Korotkih A.G., Arhipov V.A., Sorokin I.V., Selihova E.A. *Zajiganie i gorenje visokoenergheticheskikh materialov, sodержashchikh aliuminii, bor i diborid aliuminia* [Ignition and Combustion of high energy materials containing aluminium, boron and aluminium diboride], In: *Chemical physics and mesoscopy*, 2018, v. 20, No. 1, pp. 5 - 14.
6. Young G., Sullivan K., Zachariah M.R., Yu K., Zachariah M. R. *Combustion characteristics of boron nanoparticles*. In: *Combustion and Flame*. 2009, v.156, No 2, pp. 322 - 333.
7. Ao W., Yang W., Han Z., Liu J., Zhou J., Cen K. *Research on boron particles ignition and combustion model*. In: *Journal of solid rocket technology*, 2012, v.35, No 3, pp.361-366, (in Chinese).
8. Jain A., Joseph K., Anthonysamy S., Gupta G.S. *Kinetics of oxidation of boron powder*. In: *Thermochimica Acta*, 2011, v.514, No. 1 - 2, pp. 67 - 73.
9. Chintersing K.A. *Improving boron for combustion applications*, Ph.D. Dissertations, New Jersey Institute of Technology, 2019, 337 p.
10. Potanin A.I. *Polucenie keramicheskikh materialov v sistemah Mo-Si-B i Cr-Al-Si-B metodom samorasprostraneaiuscegosea visokotemperaturnogo sinteza* [Production of ceramic materials in the Mo-Si-B and Cr-Al-Si-B systems by the self-propagating method high temperature synthesis], Ph.D. Dissertations, National Research Technological University "Moscow Institute of Steel and Alloys", 2014, 143 p.
11. Pawan K.O., Srinibas K. *Boron for liquid fuel Engines-A review on synthesis, dispersion stability in liquid fuel, and combustion aspects*, *Progress in Aerospace Sciences*, 2018, XXX, pp. 1 – 28.
12. Yagodnikov D.A., Papirin P.V., Sukhov A.V. *Matematicheskaya modeli vosplamneniya odinocnoi ciastiti diborida aliuminia* [A Mathematical Model of the Single Aluminium Diboride Particle Ignition], *Science and Education of the Bauman MSTU*, 2014, no. 12, pp. 452 – 462, (in Russian).

[https://doi.org/10.52326/jes.utm.2021.28\(3\).05](https://doi.org/10.52326/jes.utm.2021.28(3).05)
CZU 621.314.25



ENERGY CHARACTERISTICS OF PHASE REGULATING DEVICE BASED ON "STAR" CIRCUIT

Lev Kalinin, ORCID: 0000-0003-1894-5734,
Dmitrii Zaitsev, ORCID: 0000-0001-7207-1754,
Mihai Tirsu*, ORCID: 0000-0002-1193-6774,
Irina Golub, ORCID: 0000-0001-8053-9329,
Danila Kaloshin, ORCID: 0000-0001-7194-2175

Institute of Power Engineering, 5 Academiei str., Chisinau, Republic of Moldova

**Corresponding author: Mihai Tirsu, tirsu.mihai@gmail.com*

Received: 05. 12. 2021

Accepted: 06. 28. 2021

Abstract. The electric power industry development mean increases the electric grids flexibility through the use of various devices type (FACTS) controlled by means of power electronics and being an element of the Smart Grid. This type of device includes a phase-shifting transformer (PST), which redistributes power flows in the branches of electrical networks. In connection with the relevance of this topic, new technical solutions appear that implement similar functions, which entails the need for a comparative analysis of such developments in order to optimize the energy characteristics of this kind of equipment. The aim of the work is to develop schematic version of the PST made according to the "star" scheme and analyze its operation in typical modes. During the study, the energy characteristics of the device were determined. The possibility of reducing the typical power of the phase-shifting device due to the use of capacitive compensation is analyzed.

Keywords: *phase-shifting transformer, angle of phase shift, electronic power switches, control strategy, rated capacity.*

Introduction

In the process of SMART GRID concept development and implementation in the electric power industry, the role of FACTS devices, which makes it possible to control the parameters of the power system mode in accordance with the chosen strategy significantly increases. The tasks of ensuring effective control of steady-state and transient modes of electric power systems can be solved by various means, one of which is phase-shifting transformer (PST).

Currently, there is a significant global experience in the use of PST [1 - 12]. Also, considerable attention is paid to the development of various technical solutions and the study of the operation modes of phase-shifting devices [13 - 19].

This work is devoted to the development and study of a two-transformer circuit version of a phase-shifting transformer made according to the "star" scheme.

General characteristics of the research object

The work purpose is to study the energy characteristics of new technical solution of the PST made according to the "star" scheme when adjusting the phase shift angle using power electronics, as well as the use of capacitive compensation to reduce the installed power of the transformer device. During research, methods of mathematical, structural and simulation modeling were used based on the SPS-models of the object built in the Simulink (Matlab) environment.

The main elements of the investigated device are two power transformers, one of which performs the functions of parallel (or magnetizing) element, the other - the functions of series (or phase-shifting) element. The subscript " p " denotes the windings and the corresponding electrical values characterizing the magnetizing transformer mode, the subscript " q " denotes the windings and the electrical values of the phase-shifting transformer.

The schematic diagram of the PST technical solution considered in the work is shown in Figure 1.

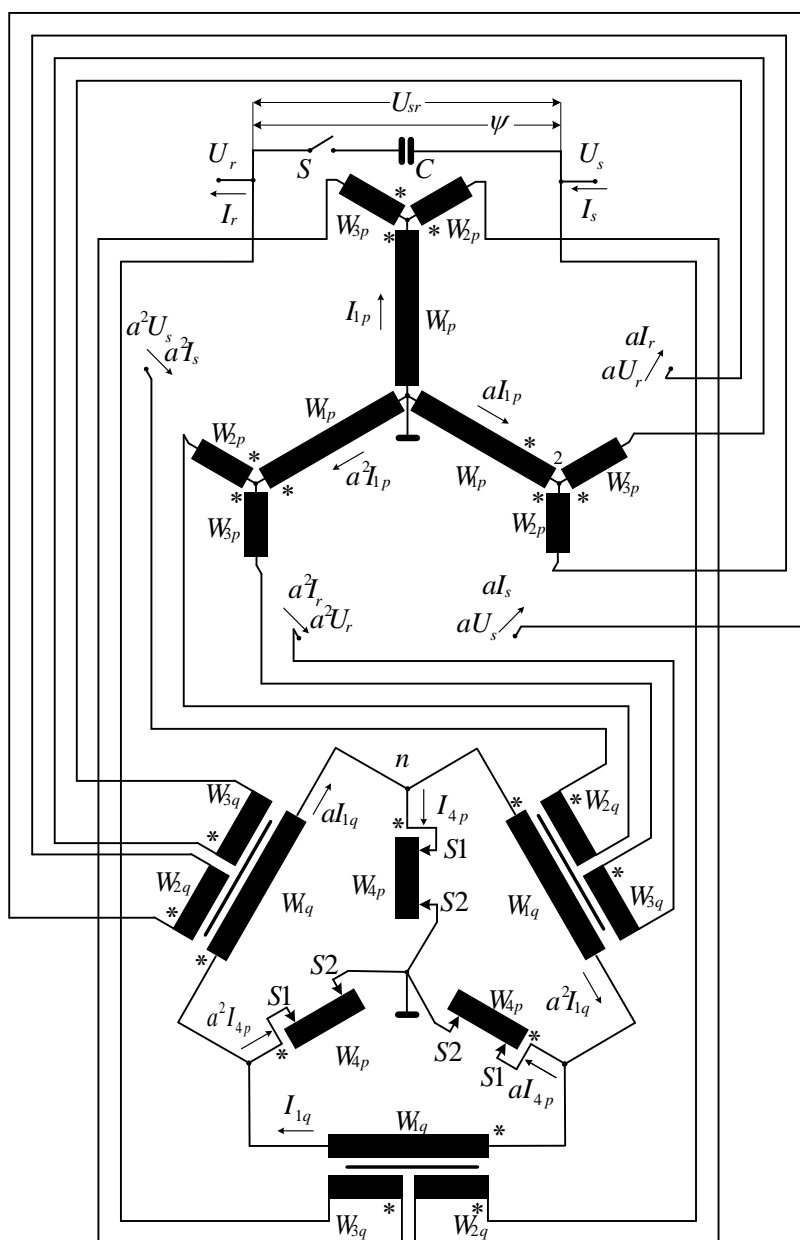


Figure 1. Technical solution of new proposed PST.

On Figure 1 next designations are accepted:

W_{1p}, W_{2p}, W_{3p} - magnetizing transformer windings;

W_{4p} - regulating winding of magnetizing transformer;

W_{1q}, W_{2q}, W_{3q} - phase-shifting transformer windings;

C - capacitor bank used to reduce the installed power of PST;

S - Power key switching capacitor bank;

$SI, S2$ - switch mechanism contacts.

The primary windings W_{1p} of the magnetizing transformer are "star-to-zero" connected. Secondary W_{2p} and tertiary W_{3p} windings of the corresponding phases are connected to the ends of the primary windings, providing a 120° shift relative to each other. The primary windings W_{1q} of the phase-shifting transformer are connected according to the "triangle" scheme, to the vertices of which the control windings W_{4p} of the magnetizing transformer assembled into a "star - to- zero" are connected. The windings W_{2q}, W_{3q} of the phase-shifting transformer are connected in series with the corresponding windings W_{2p}, W_{3p} of the magnetizing transformer.

Input electrical values are labeled "*s-sending*" and output electrical values are labeled "*r-receiving*", where:

U_s, I_s - input voltage and current of PST;

U_r, I_r - output voltage and current of PST;

ψ - the phase shift angle between the input and output currents (or between the input and output voltages) provided by the voltage U_{sr} .

To adjust the phase shift angle between the input and output voltage of the device, it is proposed to section the control winding W_{4p} as shown in Figure 2.

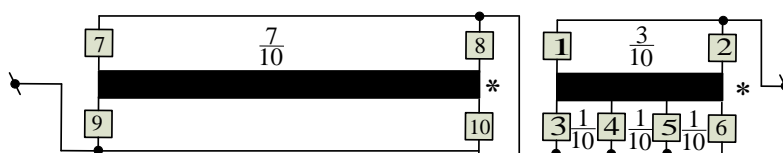


Figure 2. Control winding scheme.

Partitioning in given proportions made it possible to reduce the number of electronic keys and, when using the developed control law (Figure 3) and reversing the control winding, provide control angle ψ in the range of $0^\circ \div 60^\circ$.

Switch number	10																				
	9																				
	8																				
	7																				
	6																				
	5																				
	4																				
	3																				
	2																				
	1																				
Position	+10	+9	+8	+7	+6	+5	+4	+3	+2	+1	0	-1	-2	-3	-4	-5	-6	-7	-8	-9	-10

Figure 3. Working diagram of power keys.

Device simulation

For technical solution presented on Figure 1 in the Simulink (Matlab) software a structural-simulation model of the device was created, which was used for research and analysis of various modes of device operation.

Each PST element was modeled as a group of single-phase transformers. The parameters of the each transformer phase elements are determined for conditions $U_s = U_r = 230V$ and nominal load power of the device $10kVA$ in order to have possibility of comparative analysis and manufacture of laboratory sample. Table 1 shows the calculated currents and voltages of the magnetizing and phase-shifting transformers windings.

Table 1

Currents and voltages of windings of transformer elements							
	Magnetizing transformer windings p				Phase-shifting transformer windings q		
	W_{1p}	W_{2p}	W_{3p}	W_{4p}	W_{1q}	W_{2q}	W_{3q}
$U(V)$	190.67	78.66	78.66	78.66	136.6	68.02	68.02
$I(A)$	10	12	12	12	12	11.87	11.87

Based on the data in Table 1, the parameters of SPS - models of the phase-shifting and magnetizing elements are calculated and presented in Table 2.

Table 2

Parameters of transformers SPS – models	
Magnetizing transformer	Phase-shifting transformer
Normal power and frequency[Pn(VA) fn(Hz)]: [1633.92 50] Winding nominal voltages [U1 U2...Un] (Vrms): [136.16 68.02 68.02] Winding resistances [R1 R2...Rn] (Ohm): [0.07392 0.04004] Winding leakage inductances [L1 L2...Ln] (H): [0.48062e-3 0.12015e-3 0.12015e-3] Magnetization resistance Rm (Ohm) 1134.67 Magnetization inductance Lm (H) 1.8068 Saturation characteristic [i1(A), phi1(Vs); i2(A), phi2;...] [0,0;0.5931,0.6747;14.8286,0.7564;29.6573, 0.7769;59.3146,0.7973;177.9437,0.8178]	Normal power and frequency[Pn(VA) fn(Hz)]: [1906.7 50] Winding nominal voltages [U1 U2...Un] (Vrms): [190.67 78.66 78.66 78.66 78.66 78.66 55.062] Winding resistances [R1 R2...Rn] (Ohm): [0.1195 0.0445 0.0445 0.0025 0.0025 0.0025 0.0192] Winding leakage inductances [L1 L2...Ln] (H): [0.8724e-3 0.14849e-3 0.14849e-3 0.14849e-3 0.14849e-3 0.14849e-3 0.07276e-3] Magnetization resistance Rm (Ohm) 1906.7 Magnetization inductance Lm (H) 3.0361 Saturation characteristic [i1(A), phi1(Vs); i2(A), phi2;...] [0 0;0.4577 0.9448;11.4392 1.0593;22.8783 1.0879;45.7567 1.1165;137.27 1.1452]

The rated power of the phase-shifting device can be decreased by a capacitor bank in parallel with the magnetizing transformer. To select the required value of the capacitor bank, the power keys are set to the position corresponding to the maximum value of the phase shift angle in the load mode. The value of the capacitor bank is selected so that the current flowing through it is equal to the current flowing through the PST. The resulting value of the capacitor bank of $C = 97,39 \text{ mkF}$ allows you to obtain the maximum effect of reducing the installed transformer device power by transferring part of the power through the capacitor.

Results of modelling

To determine the operating characteristics of the PST, made according to the "star" scheme, in accordance with the developed program of design experiments, the device was studied in no-load and short-circuit modes. Based on the calculated experiments results, the parameters dependences of the PST equivalent circuit on the value of the phase shift angle ψ and the adjustment position were obtained, shown in Figures 4, 6 and 5, 7, respectively, for options without and with the use of a capacitor bank.

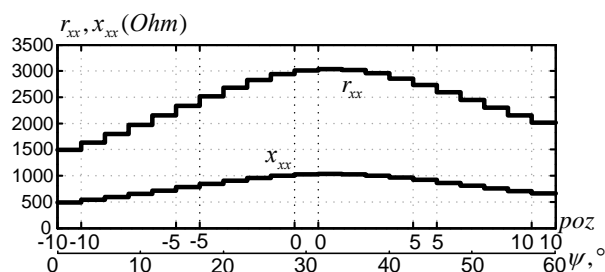


Figure 4. The characteristics of PST active (r_{nl}) and reactive (x_{nl}) components of resistance (Z_{nl}) in no-load mode.

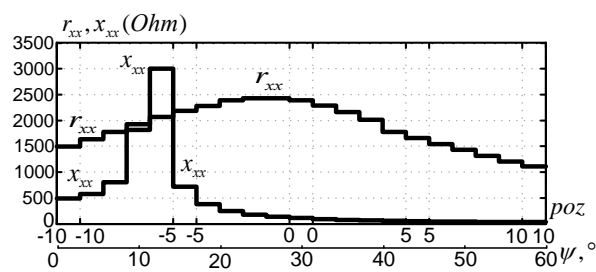


Figure 5. The characteristics of PST active (r_{nl}) and reactive (x_{nl}) components of resistance (Z_{nl}) in no-load mode with capacitor bank.

The analysis of the dependencies presented in Figure 4 shows that the no-load resistances change smoothly and have maximum values during phase shift $\psi = 30^\circ$ (zero position) and symmetrically decrease in the process of both decreasing and increasing the angle for the option without capacitance. The range of active resistance variation is $1500 \div 3000 \text{ Ohm}$, and the reactance is $500 \div 1000 \text{ Ohm}$. When using a capacitor bank (Figure 5), the nature of the change in active resistance remains the same, with the only difference that the maximum value becomes slightly less (2500 Ohm). Inductive resistance, when using a capacitor bank, has a pronounced maximum (3000 Ohm) at a control angle of about 12° .

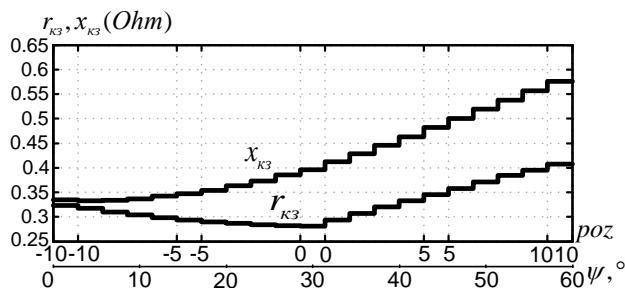


Figure 6. The characteristics of PST active (r_{sc}) and reactive (x_{sc}) components of resistance (Z_{sc}) in short-circuit mode.

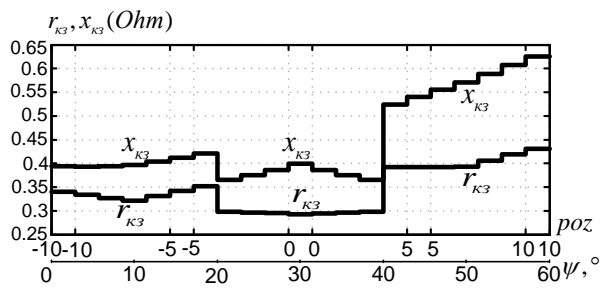


Figure 7. The characteristics of PST active (r_{sc}) and reactive (x_{sc}) components of resistance (Z_{sc}) in short-circuit mode with capacitor bank.

Figures 6 and 7 show the characteristics of the active r_{sc} and reactive x_{sc} components of the short-circuit resistance of the device Z_{sc} , without and with the use of a capacitor bank, respectively.

Evaluating the obtained curves (Figure 6), it can be concluded that the reactive component of the short-circuit resistance grows exponentially with increasing angle ψ . The minimum value of the active component falls on the angle $\psi = 30^\circ$. The maximum values are observed at the limits of the regulation range. When using a capacitor bank (Figure 7), the dependences have a complex shape with pronounced minima in the range $20^\circ \div 40^\circ$. In addition, the graphs are located slightly higher compared to the characteristics of Figure 6.

Figures 8, 9 show the characteristics of changes in active power losses obtained as a result of open-circuit and short-circuit tests. The maximum values of active losses occur at the boundaries of the regulation range. When using a capacitor bank (Figure 9), the ΔP_{sc} graph has a complex shape with minima in the range of $20^\circ \div 40^\circ$.

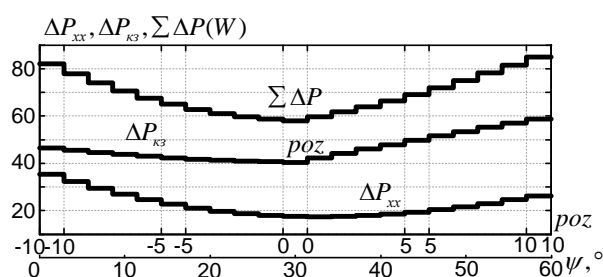


Figure 8. Dependences of PST active losses for no-load and short circuit tests.

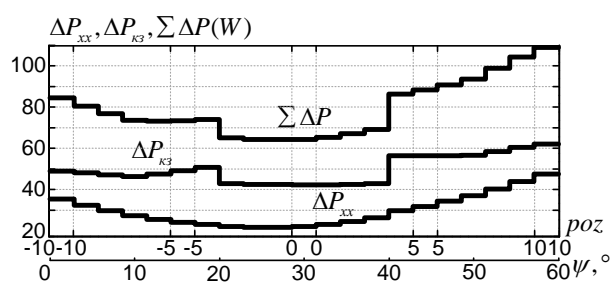


Figure 9. Dependences of PST active losses for no-load and short circuit tests with capacitor bank.

The characteristics of voltage change of the magnetizing and phase-shifting transformer windings during regulation under load are presented in Figure 10 and completely coincide with the voltage curves when using a capacitor bank.

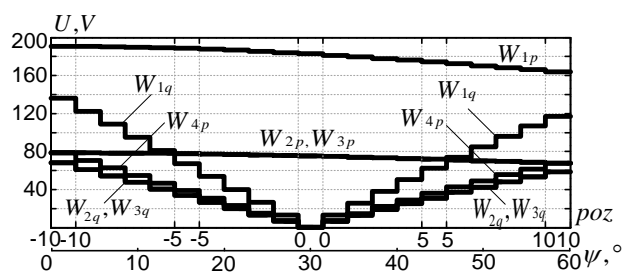


Figure 10. Voltage curves in PST windings for load mode.

As it can be seen from Figure 10, the voltages on the windings W_{2p} and W_{3p} during the angle adjustment are practically unchanged. The voltage across the winding W_{1p} decreases slightly as the angle changes $\psi = 0^\circ \div 60^\circ$.

The voltage on the remaining windings of the device varied symmetrically, taking the minimum values at $\psi = 30^\circ$ (zero regulation step), and the maximum values at $\psi = 0^\circ$ and $\psi = 60^\circ$, respectively.

The graphs of the device windings currents change are shown in Figures 11, 12, respectively, for modes without and with the use of a capacitor bank.

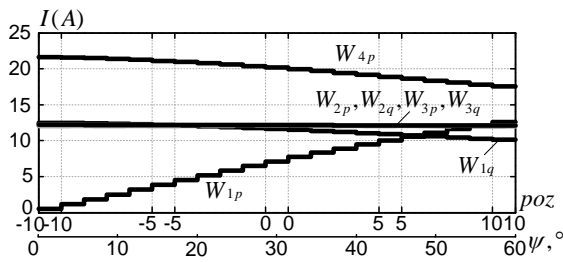


Figure 11. Currents curves of PST windings in load mode.

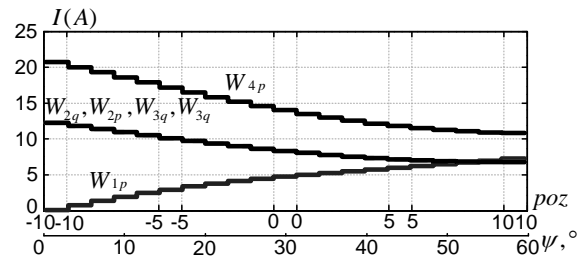


Figure 12. Currents curves of PST windings in load mode with capacitor bank.

The analysis of the presented graphs (Figure 11) shows that the currents in the windings W_{2p} , W_{2q} , and W_{3p} , W_{3q} , practically do not change during the regulation process and are equal to each other. The currents in the windings W_{1q} and W_{4p} tend to decrease exponentially with increasing angle ψ , while the current in the winding W_{1p} increases.

When using a capacitor bank (Figure 12), the current load of the windings is lower. The nature of the currents change in the windings W_{2p} , W_{2q} , and W_{3p} , W_{3q} is changes (are exponential). The rest of the characteristics have similar shapes to Figure 11.

Based on the study, the energy characteristics of the research object were determined, the analysis of which made it possible to conclude about the effectiveness of the use of a capacitor bank, which made it possible to reduce the installed power of the device in relation to the throughput power from 1.64 - the original PST circuit, to 1.45 - the PST circuit with capacitor.

Comparison of the research results with the previously proposed circuit variants of the device

To determine the technical efficiency of the considered device, a comparative analysis was carried out with the previously proposed technical solution of the PST when using a capacitor bank to reduce rated power. For this, the following characteristics were used:

$\frac{S_{pst}}{S_r}$ – coefficient characterizing the device rated power in relation to the throughput power;

$\frac{S_{re}}{S_r}$ – coefficient characterizing the power keys capacity of the control system.

The comparative analysis results are presented in the histogram form on Figure 13 for the following PST circuit options:

- 1 – “triangle” [13,14];
- 2 – “delta connection” [15];
- 3 – “two-transformers PST” [16];
- 4 – “double-core polygon” [17];
- 5 – “multi-polygon” [18];
- 6 – “single-transformer PST with neutral regulation” [19];
- 7 – “star” – researched device.

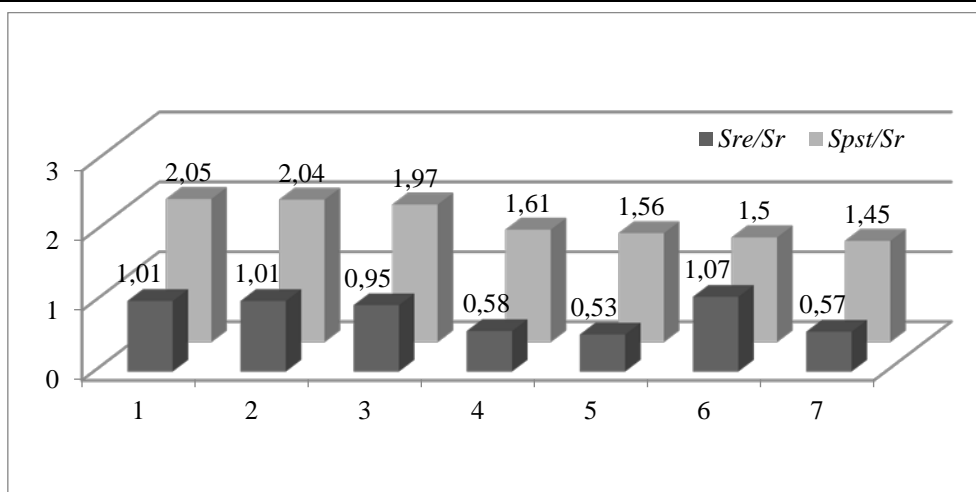


Figure 13. Histogram of the comparative analysis results of different PST solutions.

The presented histogram shows that the investigated PST solution can significantly reduce the transformer installed power, which in turn will reduce the cost of constructing devices of this type and their operating costs. Consequently, the proposed circuit variant has a competitive advantage over other PST schemes.

Conclusions

Based on the study results, the following conclusions can be drawn:

1. On the basis of the proposed PST technical solution, an analysis of the equivalent circuit parameters is carried out. The energy characteristics of the device have been determined.
2. The proposed method for reducing the installed power of investigated PST, based on the capacitor bank use connected between the input and output terminals. The optimal parameters of the capacitor bank have been determined.
3. The results analysis was carried out, which made it possible to draw a conclusion about the effectiveness of the proposed method (capacitive transmission of a part of the power), using the example of the research object.
4. The energy characteristics comparative analysis of investigated and previously developed PST technical solution showed its advantages, allowing it to be considered as an active element of modern Smart Grid systems.
5. The study results can be used for a comparative analysis of the technical solution of transformer PST developed in the future.

Acknowledgment: The results were obtained in the frame of State Program project no. 20.80009.7007.18: Eco-friendly technical solutions for efficient energy consumption in buildings and development of smart grid options with advanced renewable energy integration in Moldova.

References

1. Brochu J., Beaugregard F., Cloutier R., Bergeron A., Garant L., Sirois F. Innovative applications of phase-shifting transformers supplemented with series reactive elements. Cigre 2006, A2-203
2. Dorian O. Sidea., Constantin Bulac, Valentin A. Boicea. Power engineering education toolbox for active power flow control using the phase-shifting transformer; Year: 2017; page: 177 - 183
3. Fang Z. Peng. Flexible AC Transmission Systems (FACTS) and Resilient AC Distribution Systems (RACDS) in Smart Grid; Proceedings of the IEEE; Year: 2017; page: 2099 - 2115

4. Gopiram Maddela. Quantifying Losses in Power Systems Using Different Types of FACTS Controllers; Year: 2013.
5. Karim Shaarbafi. Transformer Modelling Guide; Year: 2017; Page: 192 - 196
6. Leonardo-Geo Mănescu, Denisa Ruşinaru, Marian Ciontu, Cosmin Buzatu, Radu Dinu, Paul Stroică. Congestion management using dispatch or phase shifting transformers; Year: 2016; Page: 1 - 6
7. Makoto Kadowaki - Hitachi LTD., Kazuhito Dobashi. Japanese Experience with the use of Phase-Shifting transformers.- Tohoku Electric Power Company ID074. Switzerland, 8 -14 september 2013
8. Mircea Eremia, Chen-Ching Liu, Abdel-Aty Edris. Phase Shifting Transformer: Mechanical and Static Devices; Advanced Solutions in Power Systems: HVDC, FACTS, and Artificial Intelligence; Year: 2016
9. Gellings C. W. The Smart Grid. Enabling Energy Efficiency and Demand Response. – CRC Press, 2010.
10. Belivanis, M.; Bell, K.R.W., Use of phase-shifting transformers on the Transmission Network in Great Britain, Universities Power Engineering Conference (UPEC), 2010 45th International. Publication Year: 2010 , Page(s): 1 – 5.
11. Djordje M. Dobrijević and Jovica V. Milanović. Contribution of Phase Shifting Transformers to Improvement of the Security of Power Transfer from the Power Plant; Agia, Napa, Cyprus; 7 - 10 November 2010.
12. Hossein Nasir Aghdam. Analysis of Phase-Shifting Transformer (PST), on Congestion management and Voltage Profile in Power System by Matlab/Simulink Toolbox; Maxwell Scientific Organization, 2011.
13. Dobrusin L. Tendencii primeneniya fazopovorotnyh transformatorov, [Trends in the use of phase-shift transformers] [Power Electronics] Silovaya elektronika, № 4'2012 (In Russian) Available at: http://power-e.ru/pdf/2012_04_60.pdf, date of access 20.12.2017
14. Golub I.V., Zaitsev D.A., Zubareva I.G. Modified Two-core Phase-shifting Transformer Based on the Classical «Delta Connection» Problemele energeticii regionale 1(30) 2016 pp. 25 - 30.
15. Kalinin L., Golub I., Zaitsev D., Tîrşu M. [Osnovnye tekhnicheskie harakteristiki dvuhtransformatornogo fazoreguliruyushchego ustrojstva.] The technical characteristics of the two-core phase-shifting device.. Forumul regional al energiei pentru Europa Centrala si de Est – FOREN 201415-19 Iunie 2014, Romania.
16. Tîrşu M., Calinin L., Zaitsev D., Berzan V. Phase-shift transformer with improved characteristic 9th World Energy System Conference, June 28 - 30 2012 Suceava, Romania <http://www.agir.ro/buletine/1417.pdf>.
17. Kalinin L., Zaitsev D., Tirshu M., Golub I. The characteristics of the phase-turn transformer, made according to the scheme "polygon". Problemele Energeticii Regionale 3 (35) 2017 Electroenergetica, pp. 1 - 8.
18. Calinin L., Zaitsev D., Tîrşu M., Golub I. Regulator de fază trifazat cu transformator Institutul de Energetică al Academiei de Ştiinţe a Moldovei, MD; C/BIRregistru Patent MD, No 4397, 2016.
19. Calinin L., Zaitsev D., Tirshu M., Golub I., Moraru L. Transformator trifazat de reglare a decalajului de fază cu reglare în punctul neutru. Problemele energeticii regionale 1 (27) 2015 pp. 11 - 18

[https://doi.org/10.52326/jes.utm.2021.28\(3\).06](https://doi.org/10.52326/jes.utm.2021.28(3).06)
CZU 685.34.017.8



FITNESS AND COMFORT ASSESSMENT OF FOOTWEAR: AN ANTHROPOMETRIC APPRAISAL

Adinife Patrick Azodo^{1*}, ORCID ID: 0000-0002-2373-1477,
Olasunkanmi Salami Isamaila^{1,2}, ORCID ID: 0000-0002-9875-8594,
Sampson Chisa Owzor², ORCID ID: 0000-0003-2126-7903

¹Department of Mechanical Engineering, Federal University of Agriculture Abeokuta, Nigeria

²Department of Mechanical Engineering, Federal University Wukari, Taraba state, Nigeria

*Corresponding author: Adinife Patrick Azodo, azodopat@gmail.com

Received: 06. 04. 2021

Accepted: 07. 12. 2021

Abstract. Suitability determination of any product designed for specific types of consumers is possible through the effective use of anthropometric information. This study assessed anthropometric data utilization in footwear designs and patterns as an indicator of fitness and comfort in footwear production. The data collected for analysis were the length and the breadth dimensions of footwear design pattern from eighteen footwear cottage shops and the foot anthropometric parameter from a total of four hundred and thirty-three (433) (males (226) and females (207)) subjects. The instrumentation design for the data collection was a digital vernier caliper (model Mitutoyo 500-506-10). The analysis of the foot anthropometry dimension and the design footwear pattern data obtained showed a lack of bilateral symmetry for the male and female gender. The fitness and comfortable foot support function of the footwear analyzed using a paired samples t-test between the footwear design pattern dimensions, and the foot anthropometric parameters disclosed $p > 0.05$ in all cases – not significant. This study concluded that tailoring a product design to the users' population reduces the mismatch challenges, grants fitness, and comfort to the users.

Keywords: *foot anthropometry, footwear, fitness, production, cottage firm.*

Introduction

Footwear production, either hand-crafted or produced through the use of high-end machines, follows a sequential and progressive process route, starting with the dimension. The measurement of the size and proportion of the foot parameters for footwear productions is called foot anthropometry. The physical feature of the human foot, in most cases, is the linear dimensions of the foot length and foot breadth [1]. In the developing nation, the footwear fabrication in the cottage sector is with the use of simple tools. The local production in this sector serves the footwear need of a specific population, either on-demand or produced for sales. The basic fundamental in the design and construction of footwear involves quantitative analysis of the physical differences that exist in linear measurements of the foot for comfortable and functional foot support [1]. While walking, running, or

working, footwear prevents the foot from injuries, offers fitness and comfortable foot support, and protects it against variations of ground surfaces texture and temperature adversities of the environment. It also facilitates the proper functioning of the foot for daily activities [1]. However, this is only guaranteed when the footwear fit with the shape of the foot as it is an essential determinant factor [1]. Beyond the aesthetically pleasing, stylish, and great-looks of footwear, the best choice lies either in the proper foot function or the overall health. Wearing poorly fitting footwear is painful in the ankles, hips, knees, and lower back, and it is debilitating. The aching effect of the feet can zap the energy of a person. Other poorly fitting footwear effects are blisters, bunions, calluses, hammertoes, and blood circulation problems. The foot support offered by the footwear in standing position, walking and accommodation to variations of surfaces can cause change to the skeletal system and the muscular structure that it supports. It can also change a person's posture and the way the person walks if poorly fitted. It then means that for a desired fit and comfort of footwear, foot anthropometry is necessary.

Anthropometric data accommodates a wide range of biological variation of the human body characteristics that uniquely distinguishes individuals [2, 3]. The diversity in anthropometric of the human body characteristics cut across age, gender, tribe, geographical location, occupation, and nationality [4]. The defining factors that make for the classification and identification of the physical geometry of the human body of a group are cover in the body anthropometry. It guides in the development and establishment of the standards that are specific for effective product design, and enhance product usability and suitability for the user population [5, 6, 7]. Studies revealed that the development of standard anthropometric data helps to solve the significant variations of the human body dimensions through the provision of vital database information applicable to the design of products [8]. Ismaila [3] emphasized that for product design to suit specific types of consumers, anthropometry data is needed as it varies from person to person and between nations. In practice, garment makers, clothes, and footwear measure their customers to design the wears that fit the individuals. Garment production for easy and short time accessibility, as well as the relatively inexpensive products, requires consultation of anthropometry database. This phenomenon has a significant effect on the development of garment industries. Anthropometry positively affects the desired economies of scale conditions in the development of product design sector. Also, it reduces setup-time and stoppages in the mass production of readymade products [8].

The understanding of the importance of anthropometry values, according to Musa et al. [9], lies in its application. This is because an individual's body anthropometry for fitness and comfortable garment needs to capture the variations as the human foot shows a range of variation in length, breadth, and height due to genetic, natural, and environmental factors [10]. The challenge with the user population and the anthropometric data for Nigerians is in the sparse nature, mostly found from individual researchers and skewed to a particular state, region, gender, age, or ethnicity [3, 11]. Tackling these ranges of variations in the human body anthropometry by accommodating to the extreme deviation to the 5th and 95th percentiles of a population across age, gender, tribe, and nationality gives a significant suitability determination of a product targeted for a particular people [5, 12, 13]. Most foot anthropometry research studies found in the works of literature covered foot shape under different weight-bearing conditions [1, 14], and foot dimensions evaluation [3, 15]. Similar studies such as [16, 17, 18], considered gender and tribe. In other studies, anthropometry of

the foot was used in the estimation of the body standing height [19, 20, 21]. Monye and Omotehinse [22] developed a model of foot anthropometric descriptors for the design of prosthesis and footwear in Nigeria. Likewise, Nacher et al. [23] developed a model for predicting footwear fit based on user data. However, the application of anthropometry data for the design for a target user's population as guidelines for designers of commercial products, necessary for product usability and suitability for the user population, is still scarce. Therefore, this study assessed the anthropometry of footwear designs and patterns as an indicator of fitness and comfort for sandals and chappals production.

Materials and method

This study was conducted in the Ukum local government area of Benue state Nigeria with study site locations at Jootar and Zarki-ibaim areas. The data sampling of this study covered the physical measurement of the footwear design patterns used in eighteen (18) footwear making shops. The sampled footwear making shops were those that locally design the straps and the soles of the footwear for sale. The foot anthropometric data measurements were from a total of four hundred and thirty-three (433) participants, males (226) and females (207) contacted at the footwear making shops. The footwear design pattern dimensions (Figure 1) and the foot anthropometric parameter (Figure 2) measurements were the foot length and the foot breadth dimensions using a digital vernier caliper (model Mitutoyo 500-506-10, Mitutoyo Corporation, Japan).

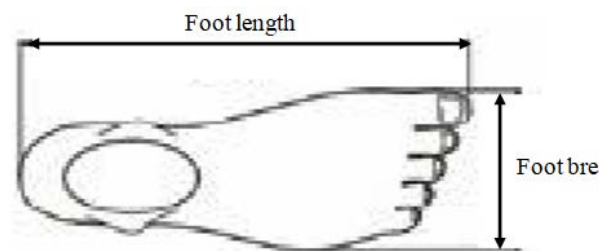
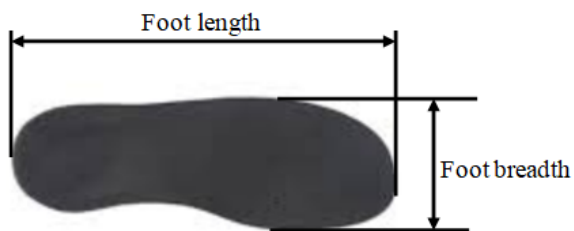


Figure 1. Footwear design pattern dimensions. **Figure 2.** Foot anthropometric parameter.

As this study is a forensic study, the measurement precision and reliability were ensured as only one of the researchers did the data collection. The foot lengths and foot breadths measurements were carried out when the participant is in a seated position barefooted with the foot flat on the ground making an angle ninety degrees at the talocrural (ankle) joint. Foot breadth measurement is the distance across the metatarsal region of the foot from the lateral to the medial side. Foot length measured the maximum distance between the most anterior part of the heel and the posterior projecting end of the foot. The measurements on the footwear design pattern were the corresponding positions and dimensions for the foot lengths and foot breadths for each of the participants' foot anthropometry. The subjects agreed to participate in this study verbally. The recruitment was after an explanation of the purpose of the study was communicated to the participants. Data analyzed was only from those who gave their permission and with no physical deformities on their feet. The data obtained were descriptive and inferential statistical analyses. The comparison of the foot anthropometric data of the subjects and design footwear pattern for the significant difference was with the use a 2-tailed paired samples t-test on the SPSS 20.0 Statistical package. The value considered for the significant difference between the foot anthropometric data and footwear design pattern is less than 0.05.

Results and Discussions

Table 1 shows the descriptive statistics of the foot anthropometry variables for the males and the female genders. From the table, the average mean value for the right foot length (27.45 cm) and the right foot breadth (10.17 cm) were longer than the left foot length (27.44 cm) and the left foot breadth (10.16 cm) (Table 1). For the female participants, the average mean value for the right foot length (25.29 cm) was higher than the left foot length (25.28 cm). The average mean value of right foot breadth (8.83 cm) is lower than the right foot breadth (8.85 cm) (Table 1). This study observed a lack of bilateral symmetry in both the foot anthropometry dimension of the participants for both the male and female gender. The lack of bilateral symmetry in the foot anthropometry dimension for both gender found in this study in line with observation in previous similar studies [24-29].

Table 1

Descriptive statistics of foot anthropometry dimension for gender

Descriptive statistics	Male = 226				Female = 207			
	Right FT	Left FT	Right FB	Left FB	Right FT	Left FT	Right FB	Left FB
Min (cm)	24.04	24.11	9.00	9.01	22.23	22.00	8.04	8.04
Max (cm)	30.00	29.98	11.78	11.43	28.44	28.96	9.98	10.02
Mean (cm)	27.45	27.44	10.17	10.16	25.29	25.28	8.83	8.85
SD (cm)	1.68	1.69	0.55	0.56	1.08	1.15	0.52	0.54

The design footwear pattern used in the cottage firm for the sandals and chappals footwear production followed a different order (Table 2). The measured dimension of the design footwear pattern used in the cottage firm for the female subjects' footwear production showed that average the right foot length and left foot length are of the same dimension (25.15 cm). The foot breadths have variation as the left foot breadth (8.88 cm) was found higher than the right foot breadth (8.86 cm) (Table 2). The design footwear pattern also observed a lack of bilateral symmetry in the male and female design footwear pattern. The variation in the footwear design dimension implies that both sides of the pairs are not equal.

Table 2

Descriptive statistics of footwear pattern dimension for gender

Descriptive statistics	Male = 226				Female = 207			
	Right FT	Left FT	Right FB	Left FB	Right FT	Left FT	Right FB	Left FB
Min (cm)	24.7	24.9	9.43	9.45	22.7	22.5	8.18	8.52
Max (cm)	29.4	29.6	11	10.9	27.9	28.1	9.64	9.54
Mean (cm)	27.3	27.28	10.22	10.16	25.15	25.15	8.86	8.88
SD (cm)	1.58	1.53	0.38	0.38	1.05	1.14	0.38	0.32

Table 3 compares the average mean of the foot anthropometry variables with the corresponding variable on the design footwear pattern dimension for both genders. The result obtained showed that for the males, the average mean value of the right foot length anthropometry parameter had a higher mean value (27.45 (SD = 1.68) compared to the right foot length of the design footwear pattern parameter that had 27.30 (SD = 1.58), $t(225) = -$

1.07, $p = 0.28$ (Table 3). The result obtained means that the right foot length anthropometry variables and the corresponding right foot length of the design footwear pattern dimension were not significantly different as the p -value was higher than 0.05. The high p -value obtained from the paired t -test indicated that the design footwear pattern parameters used for the right foot length anthropometry parameter for the male subjects gave the desired fits. Similarly, the paired samples t -test for the left foot length ($p = 0.27$), right foot breadth ($p = 0.25$), and left foot breadth ($p = 0.89$) between the foot anthropometry and design footwear pattern were not significantly different as the values were higher than 0.05 (Table 3). The result obtained implies that the basis adopted for designing footwear at the cottage firm assessed gave the desired fit need for comfort. This study established that guided anthropometry developed and used at the cottage firms for the footwear design and production in this study matched the studied population fitness and comfort. This finding is in agreement with the postulations in several other similar studies [5 - 7].

Table 3

Paired sample t-test for the foot anthropometry variables and design footwear pattern dimension for the male subjects

Anthropometry variables		Descriptive statistics t-test for equality of means					
		Mean	SD	SEM	t	Df	p-value
Right FT	Foot anthropometry variables	27.45	1.68	0.11			
	Design footwear pattern	27.30	1.58	0.11	1.07	225	0.28
Left FT	Foot anthropometry variables	27.44	1.69	0.11			
	Design footwear pattern	27.28	1.53	0.1	1.1	225	0.27
Right FB	Foot anthropometry variables	10.17	0.55	0.04			
	Design footwear pattern	10.22	0.38	0.03	-1.16	225	0.25
Left FB	Foot anthropometry variables	10.16	0.56	0.04			
	Design footwear pattern	10.16	0.38	0.03	-0.14	225	0.89

Table 4 shows the comparison of the average mean of the foot anthropometry parameters and the foot design pattern for the female participants. The paired samples t -test comparison made between the foot anthropometry parameters and the foot design pattern for the foot length and foot breadth on both legs showed that there was a significant difference in all cases.

The p -value obtained for each was higher than 0.05.

The result obtained demonstrated that the foot anthropometry data used in the cottage shops is suitable for the study population.

This study also showed that the product design specific to a group of people helped in the achievement of footwear fitness and comfort. Therefore, the finding in this study buttressed Cooper et al. [30] statement that the anthropometry data must be appropriate to the design of a product and must be descriptive to the target users' population for the product design to be effective. As such, it forms the guidelines for footwear designers for the commercial production of footwear.

Table 4

Paired sample t-test for the foot anthropometry variables and design footwear pattern dimension for the female subjects

Anthropometry variables		Descriptive statistics			t-test for equality of means		
		Mean	SD	SEM	T	Df	p-value
Right FT	Foot anthropometry variables	25.29	1.08	0.07			
	Design footwear pattern	25.15	1.05	0.07	1.64	206	0.10
Left FT	Foot anthropometry variables	25.28	1.15	0.08			
	Design footwear pattern	25.15	1.14	0.08	1.40	206	0.16
Right FB	Foot anthropometry variables	8.83	0.52	0.04			
	Design footwear pattern	8.86	0.38	0.03	-0.84	206	0.40
Left FB	Foot anthropometry variables	8.85	0.54	0.04			
	Design footwear pattern	8.88	0.32	0.02	-0.83	206	0.41

Conclusion

The anthropometry assessment of the human body or any part of the human body through physical measurements is a means of identification of the body characteristics. This physical measurement exposes any deformities or impaired integrity and provides useful information on the measured part. The fitness of the footwear design pattern used in the production of footwear in the cottage firms in Nigeria assessed in this study showed that there no significant difference between the foot anthropometry variables and footwear design pattern dimension for the male and the female gender. This study has demonstrated that tailoring a product design to the users' population reduces the mismatch challenges, grant fitness, and comfort to the users. However, this study only covered two-foot anthropometry variables, foot length and foot breadth, applicable in sandals and chappals production. Further studies are recommended that will consider other parameters of the foot anthropometry. As well data collection should be extended to more population and classified according to ages.

References

1. Oladipo G., Bob-Manuel I., Ezenatein G. Quantitative comparison of foot anthropometry under different weight bearing conditions amongst Nigerians. In: *The Internet Journal of Biological Anthropology*, 2008, 3(1).
2. Osunwoke E.A., Vidona W.B., Atulegwu G.C. Anthropometric study on the anatomical variation of the external ear amongst Port Harcourt students, Nigeria. In: *International Journal of Anatomical Variations*, 2018, 11(4), pp. 143 - 146.
3. Ismaila S.O. Anthropometric data of hand, foot and ear of university students in Nigeria. In: *Leonardo Journal of Sciences*, 2009, 15(8), pp. 15 - 20
4. Kaankuka T.K. Ikyaator, M.T. Umogbai V.I. Development of anthropometric data for Benue state Nigeria agricultural workers. In: *International Journal of Engineering and Technology*, 2016, 6(8), pp. 271 - 276.
5. Agrawal K.N., Singh R.K.P., Satapathy K.K. Anthropometric considerations of farm tools/machinery design for tribal workers of Northeastern India. In: *Agricultural Engineering International: CIGR Journal*, 2010, 12(1), pp. 143 - 150.
6. Caragliu B. Fitness for drivers. In: *Italian Journal of Occupational Medicine and Ergonomics*, 2006, 28 (1), pp. 82-84.
7. Muzammil M., Rizvi S., Hassan F. Hassan S.N. Anthropometric data with special reference to the indian needs-an overview. In: *Journal of the Institution of Engineers (India) Part PR, Production Engineering Division*, 2007, 87, pp. 14 - 19.

8. Beshah B., Belay B., Tilahun S., Tizazu B., Matebu A. Anthropometric data of Bahirdar City's adult men for clothing design. In: *International Journal of Vocational and Technical Education*, 2014, 6(1), pp. 51 - 57.
9. Musa A., Ismaila S., Adejuyigbe S., Akinyemi O. Abolarin M. Comparison of biomechanical and anthropometrical data of Nigeria tertiary institution students with some selected countries. In: *Management Science Letters*, 2012, 2(6), pp. 1885 - 1894.
10. Amitava P., Sujaya D., Piyali S., Payel M., Prakash C.D. Estimation of stature from hand dimensions in Bengalee population, West Bengal, India. In: *Egyptian Journal of Forensic Sciences*, 2016, 6(2), pp. 90 - 98.
11. Muhammad A.U., Abdullah K.A., Faris W.F. Automotive seat fit parameters based on representative Nigerian anthropometric data. In: *Malaysian Journal of Public Health Medicine*, 2018, 2, pp. 32 - 40.
12. Ismaila S.O., Akanbi O.G., Adekunle N.O., Adetunji O.R., & Kuyue S.I. An ergonomics assessment of passenger seats in buses in South Western Nigeria. In: *Sigurnost: časopis za sigurnost u radnoj i životnoj okolini*, 2010, 52(4), pp. 329-334.
13. Ashby P. *Ergonomics handbook 1: Human factors design data: Body size and strength*. Pretoria: Tute Publication. 1978
14. Tsung B.Y.S. Quantitative comparison of planter foot shapes under different weight bearing conditions. In: *Journal of Rehabilitation Research & Development*, 2003, 40(6), pp. 517 - 526.
15. Obikili E.N., Didia B.C. Foot dimensions of a young adult Nigerian population. In: *Anatomical Society of Eastern Nigeria*, 2006, 1, pp. 22 - 24.
16. Danboro B., Elukpo A. Sexual dimorphism in hand and foot length, indices, stature ratio and relationship to height in Nigerians. In: *Forensic Science International - Journal*, 2008, 3(1), pp. 1-5.
17. Reena S., Minu B., Mrinal B. Sex estimation from foot anthropometry in Haryanvijats and North Indian mixed population. In: *Journal of Punjab Academy of Forensic Medicine & Toxicology*, 2012, 12 (1), 13-16.
18. Ekezie J. Foot Anthropometry; A forensic and prosthetic application. In: *International Journal of Science and Research (IJSR)*, 2013, 4(6), 738 - 746
19. Ozden H., Balci Y., Demirüstü C., Turgut A., Ozden E.M. Stature and sex estimate using foot and shoe dimensions. In: *Forensic Science International - Journal*, 2005, 147(2 - 3), pp. 181 -184
20. Jitender K.J. Estimation of height from measurement of foot length in Haryana region. In: *Journal of Indian Academy of Forensic Medicine*. 2010, 32(3), pp. 231 - 233.
21. Sonali K., Ashish R. Estimation of stature from the measurement of foot length, hand length and head length in Maharashtra region. In: *Indian Journal of Basic and Applied Medical Research*, 2012, 2(1), pp. 77 - 85.
22. Monye I.S., Omotehinse S.A. Developing a model for foot anthropometric descriptors for the design of prosthesis and footwear in Nigeria. In: *Journal of Applied Sciences and Environmental Management*, 2019, 23(12), pp. 2165-2170.
23. Nacher B., Alemany S., Gonzalez J.C., Alcantara E., Garcia J., Hernanadez S., Heras Juan A. A footwear fit classification model based on Anthropometric Data. DHM. 2006, pp. 01 - 2356.
24. Igbigbi P.S., Ominde B.S., Adibeli C.F. Anthropometric dimensions of hand and foot as predictors of stature: A study of two ethnic groups in Nigeria. In: *Alexandria Journal of Medicine*, 2018, 54(4), pp. 611 - 617.
25. Nirenberg M.S., Krishan K., Kanchan T. A metric study of insole foot impressions in footwear of identical twins. In: *Journal of Forensic and Legal Medicine*. 2017, 52, pp. 116 - 121.
26. Saka O. S., Alamu O.A., Olayode A.A., Akinjisola A.A., Ogundipe J.O. Studies on the estimation of stature from hand and foot length of an individual. In: *Journal of Krishna Institute of Medical Sciences University*, 2016, 5, pp. 73 - 80.
27. Kanchan T., Sinha S., Krishan K. Is there a correlation between footstep length, lower extremities, and stature? In: *Journal of Forensic Sciences*, 2015, 60(5), pp. 1337 - 1340.
28. Ishak N.I., Hemy N., Franklin D. Estimation of stature from hand and handprint dimensions in a Western Australian population. In: *Forensic Science International*, 2012, 216, pp. 1 - 3.
29. Krishan K., Kanchan T., Menezes R.G. Ghosh A. Forensic anthropology case work essential methodological considerations in stature estimation. In: *Journal of Forensic Nursing*, 2012, 8, pp. 45 - 50. 10.1111/j. 1939-3938. 2011.01122. x Epub 2012 ja.
30. Cooper R.A. Bedi J., Gross F. Mechanical efficiency of training wheelchair racers. In: *the Proceedings of the 11th Annual IEEE-EMBS Conference*, Philadelphia PA: IEEE-Press, 1990, 12(5), pp. 2311 - 2312.

[https://doi.org/10.52326/jes.utm.2021.28\(3\).07](https://doi.org/10.52326/jes.utm.2021.28(3).07)
CZU 623.4.021+004.42



MULTIPLE CLASSIFICATION ALGORITHMS UNIMODAL AND MULTIMODAL TARGET RECOGNITION SYSTEMS

Veaceslav Perju*, ORCID ID: 0000-0002-7755-4277

Agency for Military Science and Memory, 47 Tighina Str., Chisinau, Republic of Moldova

*Corresponding author: Veaceslav Perju, vlperju@yahoo.com

Received: 06. 11. 2021

Accepted: 08. 12. 2021

Abstract. Target recognition is of great importance in military and civil applications – object detection, security and surveillance, access and border control, etc. In the article the general structure and main components of a target recognition system are presented. The characteristics such as availability, distinctiveness, robustness, and accessibility are described, which influence the reliability of a TRS. The graph presentations and mathematical descriptions of a unimodal and multimodal TRS are given. The mathematical models for a probability of correct target recognition in these systems are presented. To increase the reliability of TRS, a new approach was proposed – to use a set of classification algorithms in the systems. This approach permits the development of new kinds of systems - Multiple Classification Algorithms Unimodal and Multimodal Systems (MAUMS and MAMMS). The graph presentations, mathematical descriptions of the MAUMS and MAMMS are described. The evaluation of the correct target recognition was made for different systems. The conditions of systems' effectiveness were established. The modality of the algorithm's recognition probability maximal value determination for an established threshold level of the system's recognition probability was proposed, which will describe the requirements for the quality and, respectively, the costs of the recognition algorithms. The proposed theory permits the system's design depending on a predetermined recognition probability.

Keywords: *target, recognition, system, unimodal, multimodal, algorithm, probability.*

Introduction

Target recognition is of great importance in military and civil applications – object detection [1], image classification [2], security and surveillance [3], access control [4], border control [5], medicine [6], etc. Actual target recognition systems can be divided into two main groups – unimodal and multimodal systems [7]. The unimodal systems are based usually on one processing module and one recognition algorithm [8]. The multimodal systems consist of a set of sensors and processing modules, every of which realizes one target recognition algorithm [9].

In many unimodal and multimodal target recognition systems, the operations of the data acquisition and processing are realized as separated tasks. As a result, the accuracy and robustness of the target recognition may be insufficient, especially if the data are found to

be incomplete or ambiguous during processing and there are no available supplementary data to mitigate those deficiencies [10]. Active multimodal sensor systems have been elaborated to overcome this problem. For example, a multisensory system for moving object detection and tracking was proposed [11] in which were used Radar, LIDAR, and vision sensors.

The system could actively control all the sensors to collect or supplement target information and effectively detect and track target movement, and obtained good performance results in actual driving conditions. The multimodal sensing system was elaborated [12], using a PTZ camera and a laser Doppler vibrometer, which can improve the performance and efficiency in automatic remote applications. This class of systems is based on the combination of multimodal hardware data collection. Subsequent data processing permits improvement of the accuracy of recognition and tracking systems, to expand the application range, and increase the system's flexibility. In other surveillance systems, the hardware data collection and software data processing are two completely separate and independent parts [13]. In these systems, the software data processing algorithms are used to improve the targets' detection and tracking rate, and the hardware sensor is used only for data collection and does not consider the interaction with the sensor to supplement the data and eliminate ambiguous judgments.

In the article [14] an active multimodal sensor system for target recognition and tracking was proposed. Different from the passive multi-modal sensor system, the active multi-modal system can adjust sensors' attitudes to get supplementary information during data processing. This system consists of a visible sensor, an infrared sensor, and a hyperspectral sensor, working together to collect supplementary data from the target to eliminate ambiguous recognition.

Unfortunately, in many applications, the described systems do not ensure the necessary level of identification probability, accuracy, and robustness of the target recognition may be insufficient.

In this article new classes of the systems are described – multiple classification algorithm unimodal and multimodal systems and results of a comparative analysis of the proposed and existing systems regarding their recognition probability are presented. In section 2 the general structure and main components of a target recognition system are presented. The characteristics such as availability, distinctiveness, robustness, and accessibility are described, which influence the reliability of a TRS. In sections 3 and 4 the graph presentations and mathematical descriptions of a unimodal and multimodal TRS are given. The mathematical models for a probability of correct target recognition in these systems are presented. It was determined that the unimodal systems are characterized by a disadvantage - a vulnerability of the sensor to bad or noisy data as a result of the imperfect acquisition of captured features. In section 5 the new classes of the systems are described – multiple classification algorithm unimodal and multimodal systems (MAUMS and MAMMS). The graph presentations, mathematical descriptions of the MAUMS and MAMMS are described. In section 6 the evaluation of the correct target recognition was made for different systems: the unimodal system (UMS); multimodal systems with one algorithm and 2 and 3 sensors (MMS-1A2S and MMS-1A3S); multi-algorithm unimodal systems with 2 and 3 algorithms and one sensor (MAUMS-2A1S and MAUMS-3A1S), multi-algorithm multimodal systems with 2 algorithms and 2 sensors (MAMMS-2A2S), with 3 algorithms and 2 sensors (MAMMS-3A2S) and with 3 algorithms and 3 sensors (MAMMS-3A3S). The conditions of

systems' effectiveness were established. The modality of the algorithm's recognition probability p_{AM} maximal value determination for an established threshold level of the system's recognition probability P_{ST} was proposed. The values of p_{AM} will describe the requirements for the quality and, respectively, the costs of the recognition algorithms.

1. General structure of a target recognition system

A target recognition system (TRS) acquires the data of an object, extracts a feature set from the data, compares this feature set against the feature sets stored in the database, and provides the results of the comparison [15]. A TRS consists of the next main components (Figure 1) [16]: sensor unit, which acquires the data of an object by scanning; quality assessment and feature extraction unit, which is used for further processing of the input data; local decision-making unit, in which the extracted templates are then matched against the stored templates and a matching score is given; output decision-making unit, in which the data from one or more local decision-making modules are processed and the final identity of the target is made; system database unit; the basic software, intended for general management of the processes in the system; the algorithmic software, used to realize the target recognition tasks.

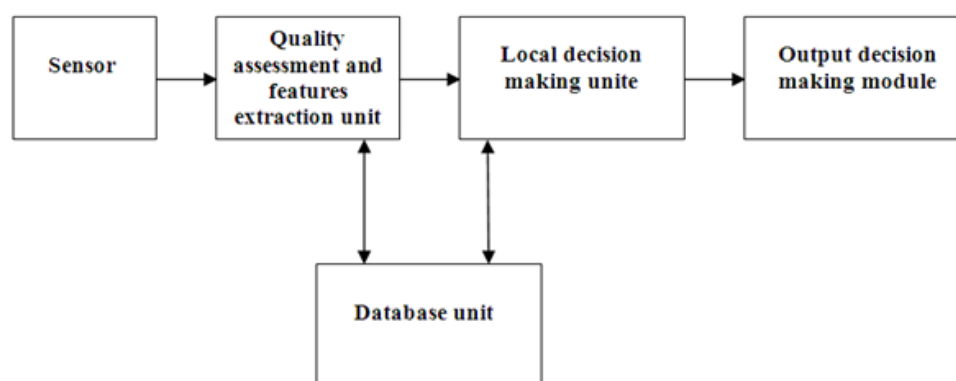


Figure 1. The structure of the target recognition system.

A target recognition system can consist of one or more sensors and processing modules, which include the units described previously. The reliability of a TRS depends on the following characteristics [17]. Availability - indicates that a target should have distinct characteristics. Distinctiveness - this asserts that two targets should have adequately different characteristics. Robustness - it declares that characteristics should be constant over some time concerning matching characteristics. Accessible - it asserts that the features can be measured using a quantitative method, and can also be easy to image with electronic sensors.

Unfortunately, not all the described requirements can always be achieved at the different stages of the target image acquisition and processing, which is reflected in the probability level of the target's recognition.

2. Model of the unimodal target recognition system

The unimodal target recognition system consists of one sensor for target image acquisition, one processing module, in which is realized one recognition algorithm, and one output decision-making unit [18]. The processing module includes a quality assessment and feature extraction unit, local decision-making unit, and database unit. The unimodal system can be presented in the form of a graph shown in Figure 2.

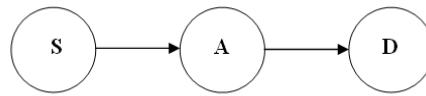


Figure 2. The graph presentation of the unimodal system: S – sensor, A – algorithm, D – output decision-making module.

Let $T(x,y)$ be the function that describes the input target. Following algorithm A of target recognition, at the first stage will be extracted the features $F_A = \{f_{Ai}\}$, $i=1 \div I$ from the function $T(x,y)$. At the second stage will be determined the matrix $D_A = \min\{W[F_A, F_{Aj}]\}$, were $F_{Aj} = \{f_{Aj}\}$ – features of the reference targets, $j=1 \div J$. At the next stage, the input target will be identified. The probability of correct recognition of the target $T(x,y)$ in the system will be:

$$P_{UMS} = p_A \quad (1)$$

where p_A is the probability of correct recognition of the target based on algorithm A.

In article [19] the recognition system, based on the Image Moments Features algorithm, principal component analyses algorithm, and correlation algorithm. The software application captures the target's images via a video camera, creates the database, and realizes different recognition algorithms. The probability of correct target recognition varies from 0.6 for the IMF algorithm to 0.85 for the correlation algorithm.

The unimodal systems are characterized by a disadvantage - a vulnerability of the sensor to bad or noisy data as a result of the imperfect acquisition of captured features. This limitation can influence the results of the correct recognition.

3. Model of the multimodal target recognition system

The multimodal systems consist of a set of sensors and processing modules, every one of which realizes one algorithm for target recognition [20]. Multimodal TRS is more reliable than a unimodal system because many independent recognition modalities are used [21].

Let the functions $T_k(x,y)$, $k=1 \div K$, describe the patterns generated by different sensors (Figure 3). For every function, $T_k(x,y)$ the respective recognition algorithm A_k will be used which will permit the recognition of the target with a probability p_{Ak} .

In this case, the probability of correct target recognition in the multimodal system can be described as:

$$P_{MMS} = 1 - \prod_{k=1}^K (1 - p_{Ak}) \quad (2)$$

where Π is the product function.

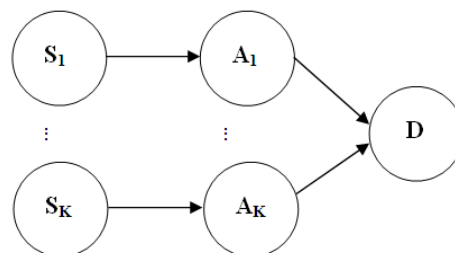


Figure 3. The graph presentation of the multimodal recognition system.

4. Multiple classification algorithm recognition systems

To increase the reliability of TRS a new approach was proposed – to use a set of classification algorithms in the systems. This approach will permit the development of new kinds of systems - Multiple Classification Algorithms Unimodal and Multimodal Systems.

4.1. Multiple classification algorithms unimodal system

In the Multiple Classification Algorithms Unimodal System (MAUMS) one sensor is used and a set of the recognition algorithms is employed (Figure 4). Let $T(x,y)$ describe the input target, to which will be applied a set of the recognition algorithms $\{A_q\}$, $q=1 \div Q$. As a result will be obtained a set of matrixes $\{D_{Aq}\}$, $q=1 \div Q$, each of which will be characterized by a probability of correct target recognition p_{Aq} .

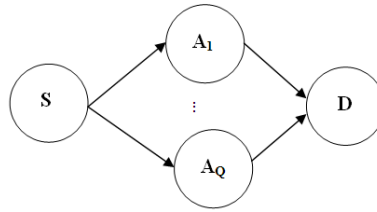


Figure 4. The graph presentation of the MAUMS system.

In this case, the correct recognition probability of the target $T(x,y)$ in the system can be evaluated as:

$$P_{MAUMS} = 1 - \prod_{q=1}^Q (1 - p_{Aq}) \quad (3)$$

4.2. Multiple classification algorithms multimodal system

In the Multiple-Algorithm Multimodal System (MAMMS) a set of the sensors $\{S_i\}$, $i=1 \div L$ is used and the data from them are processed by different recognition algorithms (Figure 5). Let the functions $T_l(x,y)$, $l=1 \div L$, describe the input targets. For every function $T_l(x,y)$ a set of the recognition algorithms $\{A_{lz}\}$, $z=1 \div Z_l$ will be applied, which will permit the recognition of the target with a probability p_{Alz} . In this case, the probability of correct target recognition in the system can be described as:

$$P_{MAMMS} = 1 - \prod_{l=1}^L \{ \prod_{z=1}^{Z_l} (1 - p_{Alz}) \} \quad (4)$$

5. Analysis of the systems' target recognition probabilities

The probability of the correct target recognition evaluation was made in the different systems based on the formulas (1), (3), (5), and (7). For evaluation there were selected the unimodal system (UMS); multimodal systems with one algorithm and 2 and 3 sensors (MMS-1A2S and MMS-1A3S); multi-algorithm unimodal systems with 2 and 3 algorithms and one sensor (MAUMS-2A1S and MAUMS-3A1S), multi-algorithm multimodal systems with 2 algorithms and 2 sensors (MAMMS-2A2S), with 3 algorithms and 2 sensors (MAMMS-3A2S) and with 3 algorithms and 3 sensors (MAMMS-3A3S). For simplicity, it was supposed that the recognition probability p_A of different algorithms is the same. The results of the calculations are presented in Table 1 and Figure 6, and show the following. The most effective are the

multi-algorithm multimodal systems (MAMMS). The recognition effectiveness of the system MAMMS-3A3S is equal to 1.0 starting from the algorithm's identification probability $p_A = 0.7$. The recognition effectiveness of the systems MMS-1A2S and MAUMS-2A1S, of the MMS-1A3S and MAUMS-3A1S, of the MAMMS-3A2S and MAMMS-2A3S is the same.

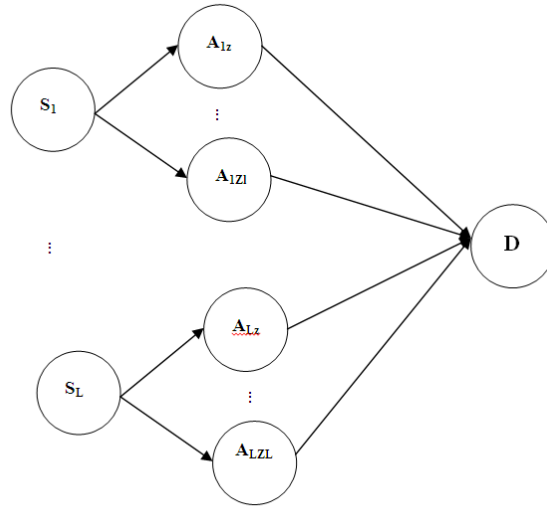


Figure 5. The graph presentation of the MAMMS system.

The maximal value of the algorithm's recognition probability p_{AM} is proposed to determine for an established threshold level of the system's recognition probability P_{ST} . The values of p_{AM} will describe the requirements for the quality and, respectively, the costs of the recognition algorithms used in the systems. In the last row of Table 1 and Figure 7, the values p_{AM} are presented for $P_{ST} \geq 0.99$. It is evident, that in the MAMMS systems the requirements for recognition algorithms are lowest – $p_{AM} = 0.5-0.55$.

Table 1

Recognition probability of the systems, P_S									
p_A	UMS-1A1S	MMS-1A2S	MMS-1A3S	MAUMS-2A1S	MAUMS-3A1S	MAMMS-2A2S	MAMMS-3A2S	MAMMS-2A3S	MAMMS-3A3S
0.5	0.5	0.75	0.875	0.75	0.875	0.9375	0.98438	0.98438	0.99805
0.55	0.55	0.7975	0.90887	0.7975	0.90887	0.95899	0.9917	0.9917	0.99924
0.6	0.6	0.84	0.936	0.84	0.936	0.9744	0.9959	0.9959	0.99974
0.65	0.65	0.8775	0.95713	0.8775	0.95713	0.98499	0.99816	0.99816	0.99992
0.7	0.7	0.91	0.973	0.91	0.973	0.9919	0.99927	0.99927	0.99998
0.75	0.75	0.9375	0.98438	0.9375	0.98438	0.99609	0.99976	0.99976	1.00
0.8	0.8	0.96	0.992	0.96	0.992	0.9984	0.99994	0.99994	1.00
0.85	0.85	0.9775	0.99663	0.9775	0.99663	0.99949	0.99999	0.99999	1.00
0.9	0.9	0.99	0.999	0.99	0.999	0.9999	1.00	1.00	1.00
0.95	0.95	0.9975	0.99988	0.9975	0.99988	0.99999	1.00	1.00	1.00
p_{AM}	-	0.9	0.8	0.9	0.8	0.7	0.55	0.55	0.5

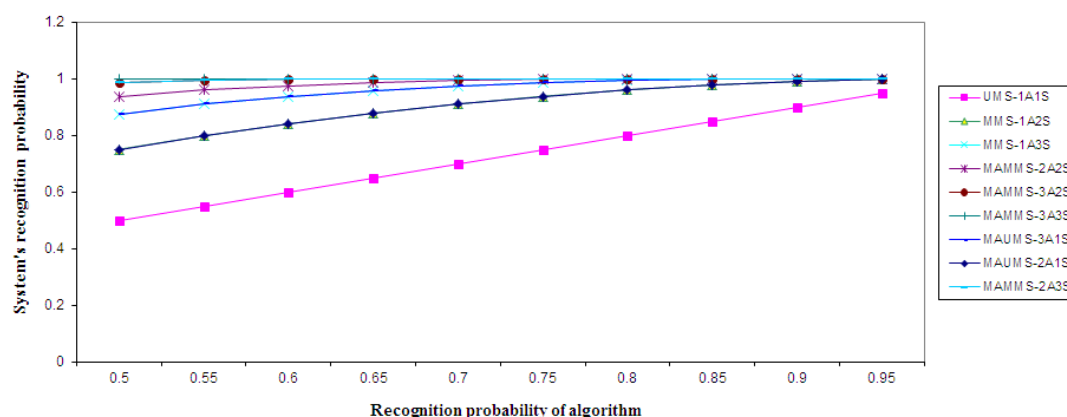


Figure 6. Recognition probability of systems.

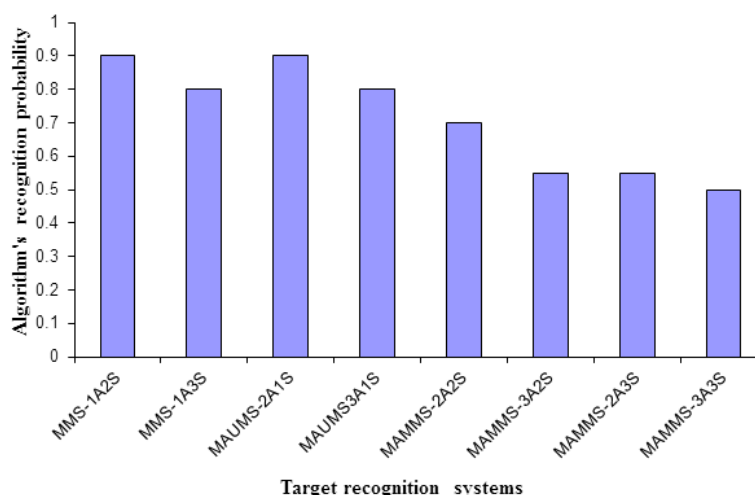


Figure 7. Algorithm's recognition probability p_{AM} values at the system's recognition probability threshold level $P_{ST} = 0.99$.

6. Conclusions

The general structure and main components of a target recognition system are presented. The characteristics such as availability, distinctiveness, robustness, and accessibility are described, which influence the reliability of a TRS.

The graph presentations and mathematical descriptions of a unimodal and multimodal TRS are given. The mathematical models for a probability of correct target recognition in these systems are presented. The unimodal systems are characterized by a disadvantage - a vulnerability of the sensor to bad or noisy data as a result of the imperfect acquisition of captured features.

To increase the reliability of TRS, a new approach was proposed – to use a set of classification algorithms in the systems. This approach permits the development of new kinds of systems - Multiple Classification Algorithms Unimodal and Multimodal Systems (MAUMS and MAMMS).

The graph presentations, mathematical descriptions of the MAUMS and MAMMS are described. The evaluation of the correct target recognition was made for different systems: the unimodal system (UMS); multimodal systems with one algorithm and 2 and 3 sensors (MMS-1A2S and MMS-1A3S); multi-algorithm unimodal systems with 2 and 3 algorithms and one sensor (MAUMS-2A1S and MAUMS-3A1S), multi-algorithm multimodal systems with 2

algorithms and 2 sensors (MAMMS-2A2S), with 3 algorithms and 2 sensors (MAMMS-3A2S) and with 3 algorithms and 3 sensors (MAMMS-3A3S).

It was established that the most effective are the MAMMS systems. The recognition effectiveness of the system MAMMS-3A3S is equal to 1.0 starting from the algorithm's identification probability $p_A = 0.7$. The recognition effectiveness of the systems MMS-1A2S and MAUMS-2A1S, of the MMS-1A3S and MAUMS-3A1S, of the MAMMS-3A2S and MAMMS-2A3S is the same.

The conditions of systems' effectiveness were established. For $p_A < 0.55$ the system MAUMS-2A1S is more effective than other systems. For $p_A < 0.7$ the system MAUMS-3A1S is more effective than the system MMS-1A2S and the system MAMMS-2A2S is more effective than the system MMS-3S. The system MAMMS-3A2S is more effective in comparison with the system MAMMS-2A3S.

The modality of the algorithm's recognition probability p_{AM} maximal value determination for an established threshold level of the system's recognition probability P_{ST} was proposed. The values of p_{AM} will describe the requirements for the quality and, respectively, the costs of the recognition algorithms. It was determined that in the MAMMS systems the requirements for recognition algorithms are lowest for $P_{ST} \geq 0.99$.

It was established that the proposed target recognition systems of the MAMMS kind ensure higher recognition probability in comparison with other systems, and they can use more simple and, respectively, cheaper recognition algorithms.

The proposed theory permits the system's design depending on a predetermined recognition probability. In the future, computer modeling and simulation of the proposed systems will be made and testing on the different kinds of targets.

References

1. Khan M., Yousaf A., Javed N. Automatic Target Detection in Satellite Images using Deep Learning. *Journal of Space Technology*, Vol. 7, No 1 (2017).
2. Hussain M., Bird J., Faria D. A Study on CNN Transfer Learning For Image Classification. 18th Annual UK Workshop on Computational Intelligence, Nottingham (2018).
3. DOAA, M., HASSANEIN, A., HASSANIEN, E. An Automatic Detection of Military Objects and Terrorism Classification System Based on Deep Transfer Learning. *Proc. of Intern. Conf. on Artificial Intelligence and Computer Vision*, p. 594 - 603, (2020).
4. Uribe-Hurtado A., Orozco-Alzate M. Acceleration of Dissimilarity-Based Classification Algorithms Using Multi-core Computation. *Proc. Intern. Conf. on Practical Applications of Agents and Multi-Agent Systems*, p. 231 - 233 (2017).
5. Ebbutt G., Thales R. New Intelligence, Surveillance, and Reconnaissance Concepts. *Janes*, 23 Sept. 2019. <https://www.janes.com/defence-news/news-detail/thales-reveals-new-isr-concepts>.
6. Jagruti J., Mehzebabeen A. Object Recognition Using CNN. *Intern. Journal of Advanced Research, Ideas, and Innovations in Technology*. Vol. 4, Issue 2, p. 1987 - 1991 (2018).
7. Schachter B. Automatic Target Recognition. *Proc. SPIE TT118*, (2018).
8. Clemente, C., Pallotta, L., Gaglione, D. Automatic Target Recognition of Military Vehicles with Krawtchouk Moments. *IEEE Trans. on Aerospace and electronic systems*. Vol. 53, Issue 1, p. 493 - 500 (2017).
9. Gurbuz A. C., Robiulhossain M., Bedri C. A Cognitive Radar Target Detection and Tracking With Multifunctional Reconfigurable Antennas. *IEEE Aerospace and electronic systems magazine*. Vol. 35, Nr. 6 p. 64 - 76 (2020).
10. Qu Y., Wang T., Zhu Z. Vision-aided Laser Doppler Vibrometry For Remote Automatic Voice Detection. *IEEE/ASME Trans. Mechatron*. p. 1110 - 1119 (2011). DOI: 10.1109/TMECH.2010.2077678.
11. Cho H., Seo Y.W., Kumar B.V., Rajkumar R. A Multi-Sensor Fusion System For Moving Object Detection And Tracking In Urban Driving Environments; *Proceedings of the 2014 IEEE International Conference on Robotics and Automation (ICRA)*; Hong Kong, China. 31 May - 7 June 2014; pp. 1836 - 1843.

12. Makantasis K., Protopapadakis E., Doulamis A., Matsatsinis N. Semi-supervised Vision-Based Maritime Surveillance System Using Fused Visual Attention Maps. *Multimed. Tools Appl.* Vol. 75, p. 1– 28. (2016). DOI: 10.1007/s11042-015-2512-x.
13. Yufu Q., Guirong Z., Zhaofan Z. Active Multimodal Sensor System for Target Recognition and Tracking. *Sensors*. Vol. 17, Issue 7. (2017). Published online 2017 Jun 28. DOI: 10.3390/s17071518. <https://www.ncbi.nlm.nih.gov/pmc/articles/PMC5539591/>
14. Qu Y., Wang T., Zhu Z. Vision-aided Laser Doppler Vibrometry for Remote Automatic Voice Detection. *IEEE/ASME Trans. Mechatron.* Vol. 16, p.1110 – 1119. (2011). DOI: 10.1109/TMECH.2010.2077678.
15. Gao Z., Dai J., Xie C. Dim and Small Target Detection Based On Feature Mapping Neural Networks. *Journal of Visual Communication and Image Representation*. Vol. 62. p. 206 - 216. (2019).
16. Woollard M., Bannon A., Ritchie M., Griffiths H. Synthetic Aperture Radar Automatic Target Classification Processing Concept. *Electronics Letters*. Vol. 55, Nr. 24, p. 1301 - 1303. (2019).
17. Correll B., Beard J., Swanson C. Cost as Array Waveforms for Closely Spaced Target Detection. *IEEE Trans. on Aerospace and electronic systems*. Vol. 56, Nr. 2, p. 1045 - 1076. (2020).
18. Geng Z., Deng H., Himed B. Ground Moving Target Detection Using Beam-Doppler Image Feature Recognition. *IEEE Trans. on Aerospace and electronic systems*. Vol.54, Nr. 5, p. 2329 - 2341. (2018).
19. Perju V., Casasent D., Ciubotaru O. The Systems for Persons' Identification and Verification Based On Face Correlation Recognition. *Proc. SPIE* 6245 (2006).
20. Shuang Y., Xiaoran S., Feng Z. Automatic Target Recognition for Low-Resolution SAR Images Based on Super-Resolution Network. *Proc. of the 6th Asia-Pacific Conference on Synthetic Aperture Radar Conf.* November (2019). DOI: 10.1109/APSAR46974.2019.9048251.
21. Silva H., Rad P., Beebe N., et all. Cooperative Unmanned Aerial Vehicles With a Privacy-Preserving Deep Vision For Real-Time Object Identification And Tracking. *Journal of parallel and distributed computing*. Vol. 131, p. 147 - 160. (2019).

[https://doi.org/10.52326/jes.utm.2021.28\(3\).08](https://doi.org/10.52326/jes.utm.2021.28(3).08)
CZU 336.76:004.8



ARTIFICIAL INTELLIGENCE IN STOCK MARKET INVESTMENT

Badri Narayan Mohapatra*, ORCID ID: 0000-0003-1906-9932,
Bhagwat Nagargoje, Prajwal Zurunge, Suraj More

Savitribai Phule Pune University, AISSMS IOIT, Pune, INDIA

*Corresponding author: Badri Narayan Mohapatra, badri1.mohapatra@gmail.com

Received: 06. 28. 2021

Accepted: 08. 11. 2021

Abstract. This study investigates the selection of stock from huge stock markets and by using good selection tools so that it will give a good return value. It helps investor to find an easy decision regarding their investment in stock market individually with effective collection of trading activities. Many artificial intelligence (AI) techniques are untested in the financial crisis scenario. This research really helpful to the investor in the stock selection and stock purchase decision. AI is also a one of the hottest topic for most industries, researchers and investors. The financial market is easy to analyze with multiple charts, due to the application of artificial intelligence.

Keywords: *stock market, artificial intelligence, trading, investment, financial.*

Introduction

Stock forecasting is very important because based on this one should have to decide his/her financial decision [1]. However stock market fluctuations may change the mood of the person's investment. Rate of risk also effect the investor's mind. But stock market plays in the mobilization of capital as well as it returns interesting results like low risk in long run investment.

Even though no sure-shot formula has discovered yet but few tools with certain rules give more chances for getting good return. Proper investigation with proper decision should refine to achieve the target amount [2]. For this proper research work should require with investing different stocks. Proper knowledge and understanding are highly recommended before taking any investment in the stock and also involves regularly through the market cycle. One should also look of investing money in a very systematic approaches with a disciplined investment will give good return for a long term plan [3]. Emotions never make the judgment beginners may start with low risk and making diversification of portfolio [4 - 5]. Also each time same kind of return is not possible, so one should think realistic expectation and each time one should monitor the growth of the investment by proper use of risk tolerance with different goals and timelines [6].

Strategies in stock market

Before going to think any strategies there should be require of depth knowledge and sufficient research should require to get good return from stock market.

Strategies like fundamental analysis, technical analysis, growth investing, qualitative analysis, buy and hold, averaging down, any one strategies may be best for the stock market [7]. One should have to know how to avoid risk and will get the benefits from stock market. Even one have small amount of money but can start investing in share market. Diversifying strategies simple means that investor money will not be in a single basket, but that money is spreading for different sectors. Daily basis technical analysis and for long term fundamental analysis are good.

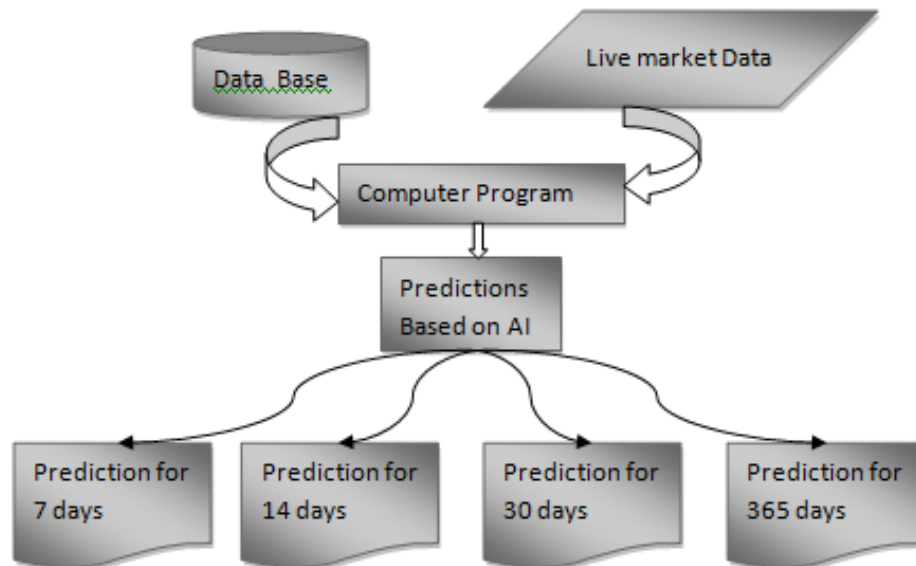


Figure 1. Prediction based on AI.

AI Tools

In today's market so many tools which will give indication of stock market like on-balance volume, accumulation, aroon indicator, RSI, MACD, Etrade, Trade station, Market gear, meta stock, stock charts and many more [8].

Simulations tool like trade station, TD Ameritrade, Invest opedia and virtual stock exchange which helps the capitalizes for analysis in the market.

Risk–Reward Ratio is a non linear approach to access the risk/reward, by divide the net profit with by the price of your highest risk [9]. Some interesting analysis can be possible through MACD, Moving average and parabolic sar [10 - 12]. Machine learning also plays a important parameter [13]. AI based prediction can be visualize from figure 1.

AI in stock market

In artificial intelligence analysis it helps to provide results for each and every milliseconds. AI have started the magical role in trading. It gives information with accurate and quick by prediction of stock prices by using the previous historical data. Basically it combines the community of trading and by scanning all the trading as a result it perform better.

Even if many companies use AI to make benefit for the economies like Amazon uses AI for product recommendation to customer. Through AI Netflix make different content creation based on this artificial Intelligence and make an huge demand on the current scenarios. Companies are adopting AI for different sectors like low AI adoption for travel/

Tourism, education and health care system. basically retail and media, entertainment uses medium AI adoption. For automation and for finance services uses high AI adoption.

In financial for portfolio management AI techniques can help and improve the performance. Now a day's the ability of AI make it as essential for trading. AI helps in model validation, back testing, trading, portfolio composition also helps to finding the fraud detection in financial services.



Figure 2. Moving average.



Figure 3. Parabolic Sar.

Different type moving average can be calculate by using tool, figure 2 shows for moving average strategies and figure 3 represents parabolic sar. Parabolic sar signals when close crossing buy or close crossing below sell.

Trading decision can be success especially when there will be a technical analysis. Technical analysis also help to understanding the core concept of trading.



Figure 4. Moving average convergence divergence.

Profitable trading set up can be made by MACD (Moving average convergence divergence). All the figures 2, 3 and 4 represents the reliance industries ltd India NSE, so all type of analysis can be performed within few seconds through the analysis tool.

By using artificial intelligence, smart trading can be possible, which is very fast and accurate to analyze different pattern with high speed. It does not need any human intervention. Even in millisecond it gives result without require of human inputs.

Comparing between two stocks can be easily predicted. For an example considering two shares comparison of reliance and Larsen, which is shown in figure 5.



Figure 5. Easy comparison of two shares.

Now companies like Google, Microsoft and Netflix and many more uses AI to improve product design and gain strategies.

Now a days AI and ML play a key factor behind the existing stock. It is also started helping chatbot trading. Tt really helps to analyze massive data.

Conclusions

One should get good foundation before starting any investment to the stock market. The research may be informative for the readers. Readers should take interest by proper understanding the theory of stock market and make theory into action. So one should start investing and make profits from stock market. AI actually becomes smarter and smarter. Huge analytical power can be possible when AI along with big data. Still many AI techniques are untested in financial crisis scenario. More educator trainers require to give awareness to people. AI and ML are moving faster which makes the regulatory framework to financial industry. It is easy to see the market situation and make require changes in portfolio management. Due to AI ,it is easy to analyze financial market with multi chart layouts.

References

1. Chen L., Qiao, Z., Wang M., Wang C., Du R., & Stanley H. E. (2018). Which artificial intelligence algorithm better predicts the Chinese stock market?. *IEEE Access*, 6, 48625 - 48633.
2. Santana E. J., Mastelini S. M., & Barbon Jr S. (2019). Stock portfolio prediction by multi-target decision support. *iSys-Revista Brasileira de Sistemas de Informação*, 12(1), 05 - 27.
3. Al Qudah I., & Rabhi F. A. (2019, December). Systematic Approach to Quantify Impact of News Sentiment on Financial Markets. In 2019 International Conference on Computational Intelligence and Knowledge Economy (ICCIKE) (pp. 60-65). IEEE.
4. Baker H. K., Nofsinger J. R., & Spieler A. C. (2020). Designing Your Portfolio: The Role of Asset Allocation, Diversification, and Rebalancing. In *The Savvy Investor's Guide to Building Wealth Through Traditional Investments*. Emerald Publishing Limited.
5. Yavas B. F., Grave K., & Vardiabasis D. (2019). Diversification strategies and equity market performances. *Review of International Business and Strategy*.
6. Nti I. K., Adekoya A. F., & Weyori B. A. (2019). A systematic review of fundamental and technical analysis of stock market predictions. *Artificial Intelligence Review*, 1 - 51.
7. Shrier, D., Canale, G., & Pentland, A. (2016). *Mobile money & payments: Technology trends*. Massachusetts Inst. Technol, 27.
8. O'Halloran S., & Nowaczyk N. (2019). An artificial intelligence approach to regulating systemic risk. *Frontiers in Artificial Intelligence*, 2, 7.
9. Vaidya R. (2020). Moving Average Convergence-Divergence (MACD) Trading Rule: An Application in Nepalese Stock Market" NEPSE". *Quantitative Economics and Management Studies*, 1(6), 366 - 374.
10. Ostrovska K. Y. (2019). MACD technical indicator study and software implementation of decision function. *System technologies*, 4(123), 155 - 168.
11. Mohapatra R. K., Mohapatra B. N., & Panda P. P. (2019). Application and security in internet of things (IOTs). *International Journal of Technology*, 9(1), 1 - 4.

[https://doi.org/10.52326/jes.utm.2021.28\(3\).09](https://doi.org/10.52326/jes.utm.2021.28(3).09)

CZU 697.34:621.311.2



REGRESSION ANALYSIS OF THE ENERGY PRODUCED IN COGENERATION AND SUPPLIED TO DISTRICT HEATING SYSTEMS

Corina Chelmenciu*, ORCID ID: 0000-0002-5126-8539,

Constantin Borosan, ORCID ID: 0000-0003-1975-4577

Technical University of Moldova, 168 Stefan cel Mare Blvd., Chisinau, MD-2004 Republic of Moldova

*Corresponding author: Corina Chelmenciu, corina.chelmenciu@tme.utm.md

Received: 07. 15. 2021

Accepted: 08. 14. 2021

Abstract. Currently, the district heating systems (DHSs) are intensively promoted both nationally and globally. The advantages of using these systems in urban areas compared to individual heating systems are practically indisputable. Still, it is essential that the calculation underlying the assessment of the economic profitability of the projects to connect the new heat consumers to DHS be made correctly by taking into account all the necessary investments and the benefits obtained from the additional amount of energy sale. The article presents the methodology for the optimal regression model selection that can be applied to predict the additional electricity produced in cogeneration mode in case of the new heat consumer connection to the DHS, based on the actual data of the thermal and electrical energy supplied to network from a CHP in the Republic of Moldova. At the same time, it is demonstrated that between the thermal energy supplied to a new consumer connected to DHS and the additional electricity produced in the cogeneration mode, there is a direct and linear correlation.

Keywords: *cogeneration, equation of a straight line, heating season, new consumer's connection to the DHS, regression analysis.*

Introduction

The main purpose of the current projects on the district heating systems development in the Republic of Moldova is to provide for the heat consumers a high quality, reliable and affordable service. The success of a heat supply company depends much on the consumers' satisfaction degree and its profit - on the consumers' number connected to the DHS.

At first glance, it would seem that any new consumer connected to the DHS would brought profit to the company, but this may not always be feasible, given that the new consumer connection involves making investments, such as constructing new networks (sometimes with pumping stations), acquiring and installing the heating agent regulation equipment; thermal energy measuring equipment, etc.

In many DHS, the thermal energy is produced from cogeneration. For example, of the total thermal energy supplied to consumers connected to Chisinau DHS, about 80% is produced in cogeneration mode by the combined heat and power (CHP) plants. In this case,

in calculating of economic profitability of connecting the new heat consumer, it is necessary to consider both gains due to additional sales of heat and those related to the sale of electricity produced in cogeneration when assessing revenues.

The amount of thermal energy supplied to the new consumer can be easily determined from the thermal load for space heating, depending on the rooms/buildings volume to be heated. The calculation temperatures of indoor and outdoor air, while the amount of electricity to be additionally produced with the production of thermal energy for the new consumer, cannot be determined by applying a calculation formula. This problem can be solved by using regression analysis.

The regression analysis theory

A linear regression model is a statistical tool used for the propose to determine a dependency relationship between two variables [1]. The statistical methodology is focused on the regression function with the aim of determining the parameters that express to what extent one or more factors influence a particular process [2].

The regression analysis can be quickly done using the personal computer by applying the *Regression* function in the *Microsoft Excel* tool.

The linear regression analysis showed promising results among the statistical models due to its reasonable accuracy and relatively simple implementation compared to other methods [3].

The linear regression method can be successfully applied in the energetics analysis and is used when for a data set represented by the pairs of values (x_i, y_i) , the line must be found that best approximates their placement in a diagram $y = f(x)$.

The advantage of the method is that it generates an equation applicable to the entire range of the variable x and even performing extrapolations within a specific limit. The equation will allow making predictions on energy consumption, being a valuable tool in the energetics analysis.

At the same time, the regression analysis method, applied by using the Excel calculation tool, has other advantages such as the speed and simplicity of calculation and reduced possibility of the results influence by the user [4].

The linear regression method can be used in the DHS domain to determine dependencies such as:

1. the fuel consumption for the thermal energy production for space heating according to the heating degrees-days or the consumers' thermal load [5];
2. heat losses at the thermal agent distribution depending on the outdoor air temperature or the heating distribution networks length;
3. the additional electricity supplied once the thermal energy is delivered to the new heat consumer;
4. the needed investments for the new consumers' connection (i.e., for the individual heat substations) depending on the thermal load for space heating and domestic hot water preparation;
5. the thermal agent temperature supplied to the consumers depending on the outdoor air temperature, etc.

The linear regression technique must be used with caution, as it can lead to erroneous conclusions. If the data participating in the analysis are lacking, conclusions drawn

based on an insufficient data set have a low degree of credibility. The more data we have available, the higher the degree of trust.

The linear regression method application is focused on the heuristic reasoning based on which there is a linear dependence between two variables such as, for example, fuel consumption for building heating and the heating degree-days (HDD) during a month or a heating season. If the data collected over a long period are available, they can be graphically represented in a fuel consumption diagram = $f(\text{HDD})$.

The points thus obtained are arranged approximately linearly and must determine the line that best approximates the sequence of points, i.e., to find the equation of the form $y = bx + c$, which describes a dependence between discretely represented data. In the considered example, the independent variable x is the heating degrees-days during each month of 2020. The dependent one y , is the fuel consumption (natural gas) for each month (Figure 1).

By applying Eq. (1), the corresponding natural gas consumption can easily be determined for any value of the heating degree-days.

$$y = -17,443x + 35745. \quad (1)$$

Thus, in energetics analysis, the straight-line equation can be used to predict energy consumption for any variable value (driver):

$$\text{Energy}(y) = \text{Factor} \cdot \text{Driver}(x) + \text{Constant} \quad (2)$$

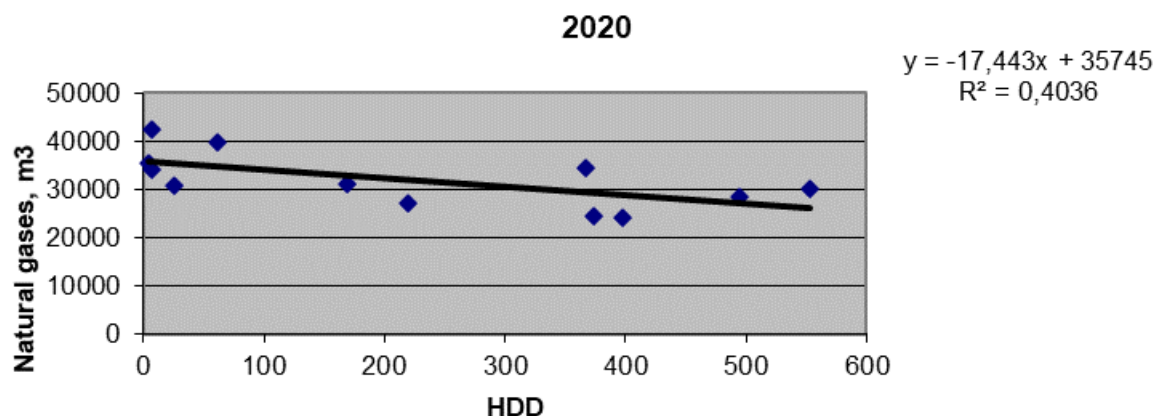


Figure 1. The natural gas consumption regression analysis based on heating degree-days.

The R^2 value is also significant in determining the dependence intensity of the correlation between the two variable values. The closer to 1 the R^2 value is, the more the variation of the value x explains the interpretation of the value y . The $R^2 = 0,4036$ (Figure 1) analysis results that the heating degree-days influenced the natural gas consumption for space heating in 2020 insignificantly.

Therefore, another driver that influenced the gas consumption in 2020 must be identified (for instance: possible thermal agent leaks in the distribution networks, heat supply with a higher temperature than it is required following the outdoor air temperature, increase the number of thermal energy consumers, etc.).

It should be borne in mind that the regression model obtained from the analysis of fuel consumption data for a given building should not be generalized and applied for the fuel

consumption prediction for any other type of building [6], especially in cases where the structure and dimensions of the building differ significantly from those of the model for which the regression model was made.

The research methodology

The methodology of regression analysis applying for the establishment of the correlation between two values (simple regression analysis), or even between three and more values (multiple regression analysis), both in the field of economics and energetics, is described in detail by authors in the cited papers. For instance, in the article [7], the doctors' number evolution in Romania in the period after accession to the European Union is modeled using the regression analysis depending on three variables: the population in this country, the wage in the health field, and the number of doctors who operates in the private sector.

In the article [8], by applying the regression method, the correlation between the supermarkets' energy consumption in Great Britain and two variables is deduced: the outside air temperature and its relative humidity, to predict the energy consumption evolution in these types of buildings depending on the climate change.

The same regression method can also be successfully applied for the energy consumption prediction for cooling needs, for instance, in fruits cold storages depending on the fruits amount stored and the outdoor air temperature [9].

The article [10] presents the methodology of the regression analysis applying to predict the energy consumption in China depending on some variables less characteristic for energy analyses: the GDP value and the population number in that country.

Daily data of the heat and electricity supplied into the network from a CHP plant located in the Republic of Moldova will be used to develop the linear regression model related to the correlation between the electricity supplied to the network in addition to the heat supplied to the new consumer connected to the DHS, which is produced at the CHP plant.

Also, the heating degree-days during three consecutive heating seasons (2018 - 2019, 2019 - 2020 and 2020 - 2021), lasting 166 days each, will be used to assess the correlation between these two values.

Table 1 presents the data for the 2018 - 2019 heating season.

Similar data were used for the other two heating seasons, specific to the 2019 - 2020 and 2020 - 2021 heating seasons.

In the first stage, the hypothesis regarding the correlation between the resultant variable - the electricity produced and the variable considered as an influencing factor - the supplied heat, separately for each heating season, will be verified.

Suppose there are different correlation degree results for each heating season. In that case, the regression analysis will be carried out to establish the correlation between the thermal energy produced and HDD, separately for each heating season.

The supplied heat in the DHS should depend on how cold the weather outside is. HDDs were collected from [11].

In the second stage, the most appropriate model will be established that can be recommended for application to predict the volume of additional electricity produced in case of connecting the new consumer to the DHS.

Table 1

The amount of heat and electricity supplied into the network by CHP and HDD

Day	Heat (Gcal)	Electricity (kWh)	HDD	Day	Heat (Gcal)	Electricity (kWh)	HDD	Day	Heat (Gcal)	Electricity (kWh)	HDD
1	1743,7	1184272	3,8	57	7982,8	4830608	16,9	113	6895,8	3576304	14,3
2	1969,4	1256624	7,9	58	8155	4855312	17,4	114	6937,6	3573376	12,2
3	2494,5	1534432	6	59	8150,9	4838240	19,4	115	6845,4	3547344	12,1
4	2668,6	1818544	5,6	60	7993,9	4752240	18	116	6505,1	3633024	11,2
5	3113,1	2188432	1,3	61	7710,8	4609008	17,5	117	6372,2	3556848	7,5
6	2514	1917392	1,5	62	7685,8	4596256	15,8	118	6285,6	3529408	8,5
7	2486,8	1978592	1,6	63	7714,2	4635408	11	119	6062,6	3489888	10,2
8	2742,7	1983232	0,4	64	7690,7	4605584	14,2	120	6047,7	3485184	9,2
9	3286,7	2064704	2,6	65	7497,8	4444112	14,9	121	6081,1	3595472	9,2
10	3957,9	2406512	2,8	66	7284	4319952	14	122	6531,2	4056496	14,9
11	4490,5	2706272	4	67	7356,7	4428112	11,6	123	6953,6	4199440	20,4
12	4450,4	2680640	4,9	68	7391	4445664	11,1	124	6988,7	4211488	19,1
13	4651,7	2817664	6,5	69	7518,9	4537008	11,5	125	6937	4162640	14,5
14	4953,3	2959664	6,7	70	7423,7	4437520	13,3	126	6623,5	4072320	10,6
15	5224,6	3049840	10	71	7250,6	4318656	14,8	127	6628,3	4104176	11,8
16	5234,2	3088272	11,1	72	7443	4493008	14	128	6462,3	3937392	6,9
17	5482,5	3298640	10,5	73	7828,7	4728992	14,8	129	6299,9	3868368	8
18	5569,1	3349968	9,5	74	7960,8	4746512	16	130	6434,7	4012640	14,6
19	5601,9	3359920	10,3	75	7952,9	4745808	18,3	131	6469	3990624	15,4
20	5950,1	3486544	10,5	76	8186,4	4887840	18,5	132	6071,9	3773680	8,1
21	6229	3592480	14,4	77	8279,1	4930880	19	133	5602,3	3412352	5,9
22	6321,7	3688224	16,7	78	8482,8	4997824	19,5	134	5621,5	3437056	10,8
23	6157,8	3581392	12,8	79	8351,7	4922352	22,1	135	5637	3414896	9,8
24	5841,4	3467840	14,8	80	8393,6	4972960	23,5	136	5454,3	3307536	3,7
25	5877,6	3478640	15,1	81	8674,4	5142416	17,9	137	4939,9	3094912	3
26	6402,7	3697376	14,8	82	8532,4	5070800	17,5	138	5210,3	3240736	5,4
27	6932,4	4097600	14,4	83	8420,3	5010880	19,3	139	4915,1	3226976	4
28	7280,3	4409376	14,5	84	8269,3	4820528	18,4	140	5076,9	3243344	9,9
29	7516,8	4584992	15,1	85	8237,1	4813904	18,2	141	5222,1	3262032	12,1
30	7668,9	4674784	18,2	86	8134,7	4822000	16,6	142	5327,5	3259040	10,1
31	7792,5	4754752	19,6	87	7941,6	4680432	17,9	143	5239,6	3224640	8,3
32	7816,8	4768192	18,3	88	7878,3	4649088	16,8	144	5146,3	3131920	8,1
33	7778,3	4719440	14,1	89	7941,3	4710336	14,6	145	5065	3008816	5,4
34	7711,9	4628848	13,1	90	8028,2	4749920	15,5	146	4645,8	2906096	5
35	7711,5	4618944	13,6	91	8076,9	4768080	16,6	147	4528,2	2913760	5,3
36	8048,6	4793904	18,1	92	8039,7	4735728	16,6	148	4803,3	2980480	7,6
37	8287,2	4907344	19,8	93	7880,0	4669168	18,9	149	4890	3017504	7,5
38	8572,1	5111792	21,8	94	8092,4	4804656	15,3	150	4713,7	2935280	3,7
39	8491,8	5039248	21,2	95	8042,5	4743216	17,7	151	4783,6	2926560	7,5
40	8572,1	5086864	22,3	96	7962,7	4698608	21	152	4799,1	2954192	8,2
41	8270,9	4863808	17,4	97	7954,5	4697072	19	153	4691,3	2914496	6
42	7692,7	4631792	12,3	98	7466,6	4426864	20,2	154	4793,3	2967664	9,1
43	7644,5	4624112	13,3	99	7365,1	4387648	15,4	155	5275,2	3324688	11,8
44	7737,7	4686992	14,1	100	7159,8	4279120	12,3	156	5429,6	3248288	11,5
45	7902,2	4800512	17,3	101	7093,2	4285232	11,3	157	5315,2	3093648	9,7
46	7715,3	4624960	14,3	102	7004,4	4287616	12,5	158	4968,5	2934096	6,1
47	7618,5	4540816	13,1	103	6709,4	4213600	12,4	159	4333,7	2861856	5,3
48	7525,6	4519952	14,8	104	6624,2	4286704	11,8	160	3967,9	2869104	4,7
49	7273,6	4363904	13,6	105	6689,3	4291920	7,9	161	4233	2791072	7,3
50	7313	4405312	14	106	6845	4247920	8,9	162	4358,6	2819328	10,3
51	7412,3	4490064	14,2	107	6851,9	4272160	12,1	163	4296,5	2784240	9,1
52	7406,3	4493136	15,3	108	6840,5	4275936	12,3	164	4123,8	2765856	7,8
53	7631,4	4612368	17,3	109	6932,6	4361072	15,9	165	3969,6	2682432	6,8
54	7688,6	4606496	16	110	6935,7	3899920	14,3	166	3520	2631696	4,4
55	7812	4711024	16,9	111	7005,8	3601776	10,5				
56	7868	4761776	17,4	112	6669,3	3618880	11,9				

The results of the regression analysis: produced electricity - supplied heat

The corresponding graphs for each heating season were drawn to verify the correlation between the electricity produced and the thermal energy supplied into the network. The straight-line equation was generated, and the influence degree of the variables over the R^2 value was determined (Figures 2, 3 and 4). The R^2 value must obtain values higher than 0,5 to consider the thermal energy supplied into the network as a determining factor for the produced electricity.

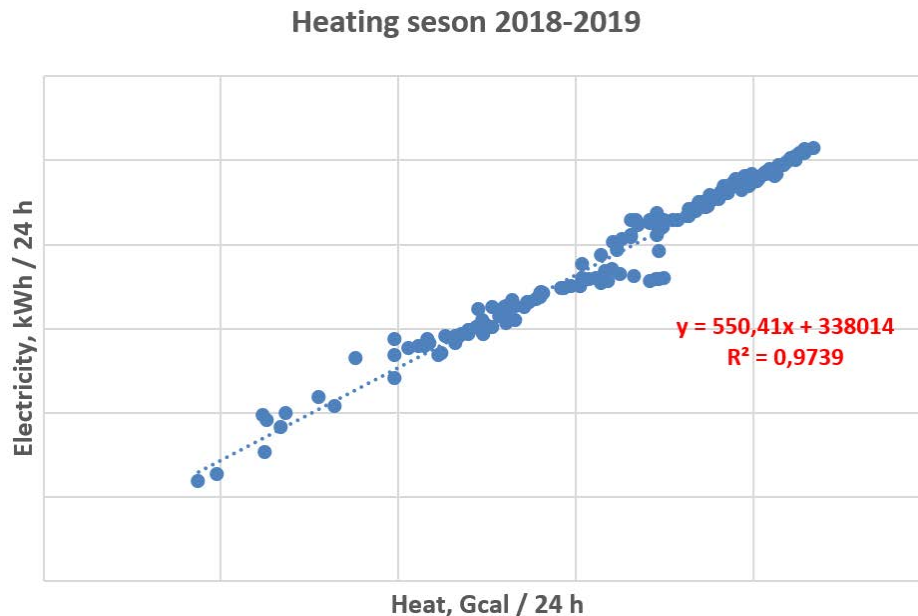


Figure 2. The regression analysis of produced electricity depending on the supplied thermal energy for the 2018 - 2019 heating season.

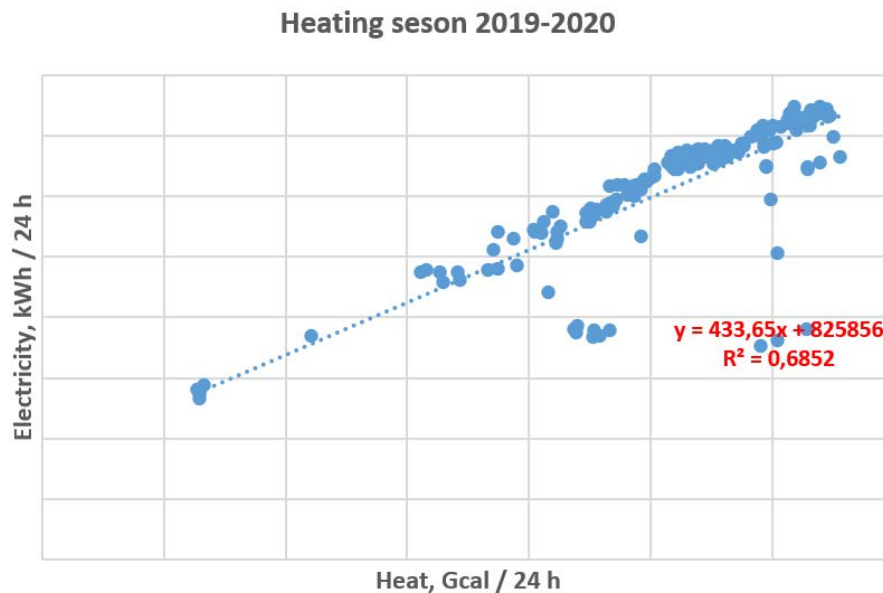


Figure 3. The regression analysis of produced electricity depending on the supplied thermal energy for the 2019-2020 heating season.

When analysing the graphs in Figures 2, 3, and 4, the graphical representation of the two variables is a straight line. Thus, it can be stated that there is a direct correlation between the electricity produced and the heat supplied, including the fact that $R^2 > 0,5$.

At the same time, it can be observed that for the three heating seasons, different values of the variable R^2 were obtained, the best value - $R^2 = 0,9739$ was obtained for the 2018 - 2019 heating season, and the weakest value - $R^2 = 0,6852$ - for the one from 2019 - 2020.

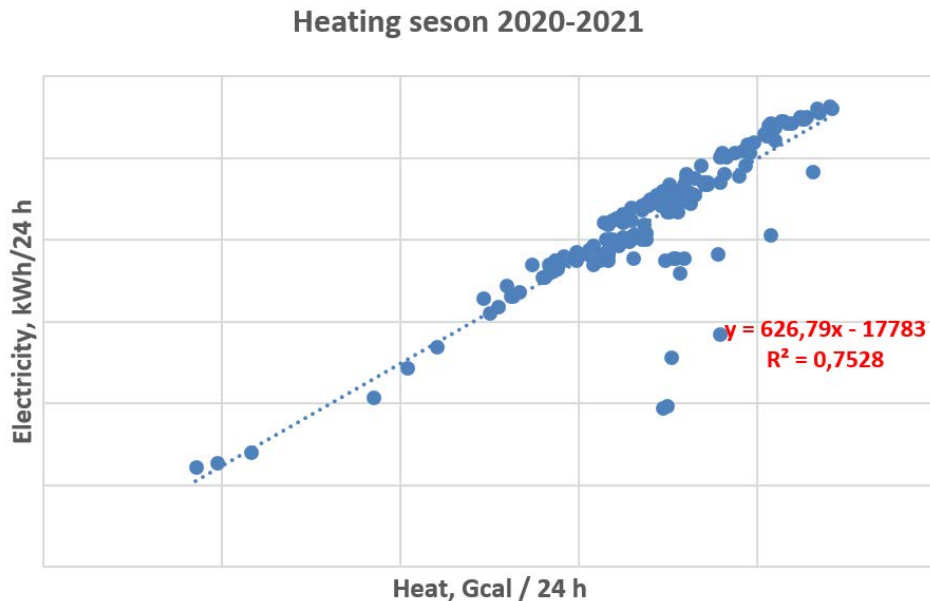


Figure 4. The regression analysis of produced electricity depending on the supplied thermal energy for the 2020-2021 heating season.

The results of the regression analysis: supplied thermal energy - HDD

Different correlation degrees between the produced electricity and the supplied heat was obtained in this article for different heating seasons. Therefore, it is necessary to perform the regression analysis for the thermal energy produced depending on the HDD to recommend the linear regression model for application to predict the additional produced electricity in case of the new consumer connection to the DHS.

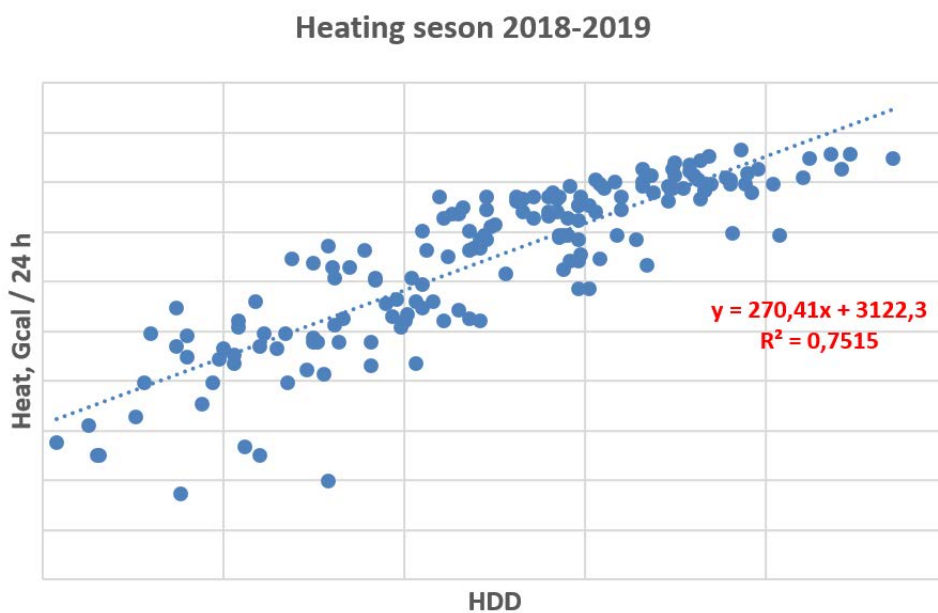


Figure 5. The regression analysis of supplied heat depending on HDD for the 2018-2019 heating season.

When analysing the graphs in Figures 5, 6, and 7, the graphical representation of the two variables is a straight line. Thus, it can be stated that there is a strong correlation between heat supplied into the network and HDD, including the fact that $R^2 > 0,5$.

Heating seson 2019-2020

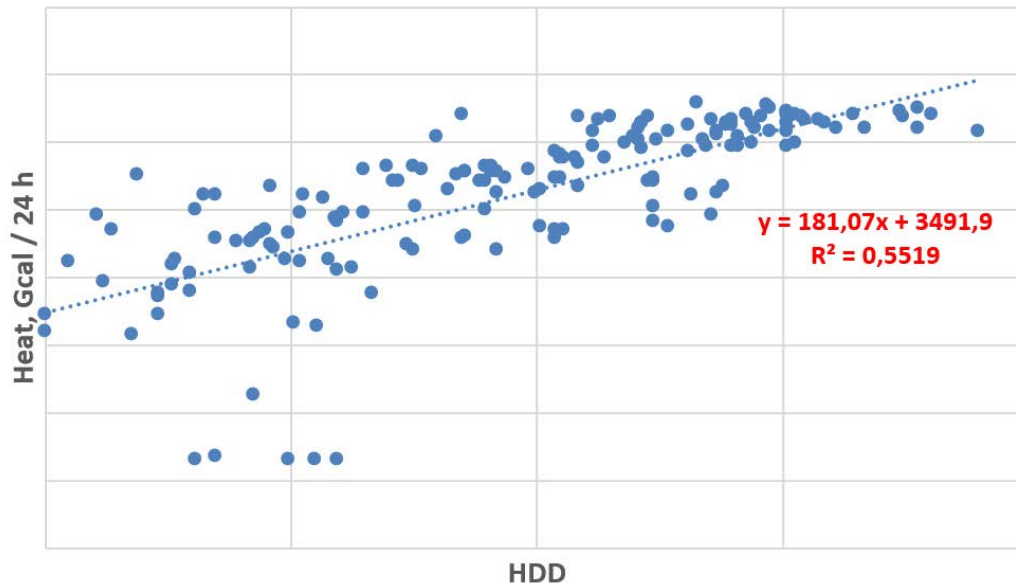


Figure 6. The regression analysis of supplied heat depending on HDD for the 2019 - 2020 heating season.

Heating seson 2020-2021

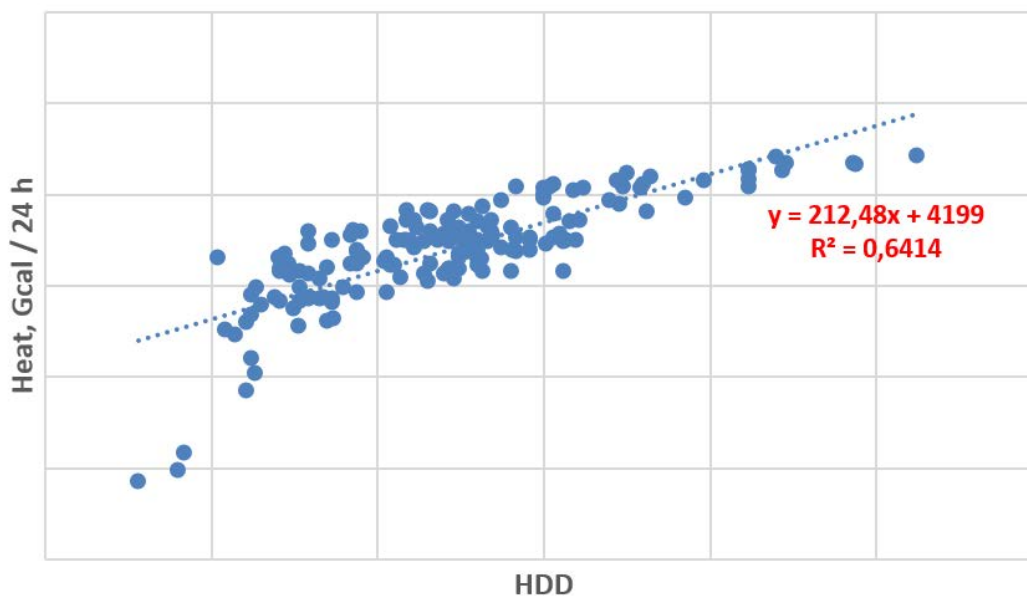


Figure 7. The regression analysis of supplied heat depending on HDD for the 2020 - 2021 heating season.

It can be observed that for the 2018-2019 heating season, the best correlation was obtained between the supplied thermal energy and the heating degree-days, namely $R^2 = 0,7515$. For the other two heating seasons, weaker correlation degrees were obtained.

Thus, taking into account the fact that the volumes of supplied thermal energy for the consumer's buildings heating should be dependent on the outdoor air temperature, it can be concluded that in the 2018-2019 heating season, to a greater extent, this condition was met.

The regression model

As a result of the performed analysis, the best correlation degree was obtained between the electricity produced and the heat supplied into the network ($R^2 = 0,9739$) and between the heat supplied into the network and HDD ($R^2 = 0,7515$) in the 2018-2019 heating season. As a result, it is recommended to use the obtained linear regression model for the dependence of produced electricity - heat supplied into the network in the 2018-2019 heating season, to predict the additional electricity produced in cogeneration mode in case of the new heat consumer connection to the DHS, used as a model in this article, namely:

$$y = 550,41 \cdot x + 338014, \quad (3)$$

where: y - the additional annual electricity produced, x - the thermal energy yearly supplied to the new consumer connected to the DHS.

Conclusions

The regression model use, having as variables the thermal energy supplied to the new consumer connected to the DHS and the additional electricity produced in cogeneration mode, demonstrated a direct and linear correlation between these two variables.

Thus, it is recommended to use the described method in this article to predict the additional quantity of the produced electricity, along with the heat supplied to the new consumer connected to any DHS in which these two forms of energy are produced in cogeneration mode. The regression model choice will be made carefully, selecting the one corresponding to the heating season for which the highest correlation degree was obtained both between the pairs of variables electricity produced - thermal energy supplied into the network and the thermal energy supplied into the network - HDD.

The obtained results will be used in the pre-feasibility studies to connect the new thermal energy consumer to the DHS by considering the income due to the production and supply of the additional electricity.

References

1. Sfetcu M., Marinescu I.: Using the linear regression model in order to analyse the correlation between the gross domestic product and the household effective individual final consumption. In: Romanian Statistical Review, 2016, Supplement nr.12, pp. 69 - 73.
2. Anghelache C, Radu I.: Construction of the regression model for the economic risk analysis. In: Romanian Statistical Review, 2020, Supplement nr.7, pp.4 - 22.
3. Fumo N., Biswas M.A. *Regression analysis for prediction of residential energy consumption*, [online]. Renewable and Sustainable Energy Reviews, 2015, Volume 47, pp.332 - 343.
4. Vesterberg J. *A regression approach for assessment of building energy performance*. Umea: Print&Media, 2014.
5. Moletsane P. P., Motlhamme T. J., Malekian R., Bogatinoska D. C. Linear regression analysis of energy consumption data for smart homes. In: International Convention on Information and Communication Technology, Electronics and Microelectronics (MIPRO), 2018, pp. 433 - 437.
6. Leigh S-B., Won J-S., Bae J-I.: An energy management process and prediction of energy use in an office Building. In: Journal of Asian Architecture and Building Engineering, 2005, pp. 501 - 507.
7. Mărcăine L., Poșircă I. Using the regression method in the factorial analysis of the evolution of the number of medicines in Romania in the post-accession period to the EU. In: ECOSTUDENT – Revistă de cercetare științifică a studenților economiști, 2017, nr. 10, pp. 4 - 11[in Romanian].

8. Braun M.R., Altan H., Beck S.B.M. *Using regression analysis to predict the future energy consumption of a supermarket in the UK*, [online]. 2014, Volume 130, pp. 305 - 313. [accessed 20.05.2021]. Available: <https://www.sciencedirect.com/science/article/pii/S0306261914005674>
 9. Safa M., KC B., Safa M.: Linear model to predict energy consumption using historical data from cold stores. In: International Journal of Advances in Science Engineering and Technology, 2015, Spl. Issue 3, pp. 146 - 150.
 10. Li Y. Prediction of energy consumption: variable regression or time series? A case in China. In: Energy Science & Engineering, 2019, pp. 2510 - 2518.
 11. Regression Analysis of Energy Consumption and Degree Days in Excel. <https://www.degree-days.net/regression-analysis> [accessed 28.05.2021].
-

[https://doi.org/10.52326/jes.utm.2021.28\(3\).10](https://doi.org/10.52326/jes.utm.2021.28(3).10)

CZU 693.54:666.972



DEVELOPMENT ULTRA-HIGH STRENGTH CEMENTITIOUS CHARACTERISTICS USING SUPPLEMENTARY CEMENTITIOUS MATERIALS*

Ameer Baiee*,** ORCID ID: 0000-0001-5393-7022

Babylon University, Babylon, Iraq

*Corresponding author: Ameer Baiee, eng.ameer.tuama@uobabylon.edu.iq

**According to the author's PhD thesis, University of Brighton, research.brighton.ac.uk

Received: 06. 22. 2021

Accepted: 08. 12. 2021

Abstract. For sustainability purposes, supplementary cementitious materials (SCMs) are considered essential components for gaining ultra-high strength properties of concrete and mortar. This study experimentally investigates the influence of single, binary, and ternary partial cement replacements of the SCMs on the performance of ultra-high-strength mortar. The investigated SCMs were included ground granulated blast furnace slag (GGBS), densified silica fume (DSF), un-densified silica fume (UDSF), and Fly ash (FA). Three replacements ratios were implemented; 10%, 20%, and 30% in addition to mortar without SCMs to work as a control mix for comparison reasons. 27 mixes were designed to quantify the replacement ratio that explains the best performance, through examining the workability, compressive and tensile strength of each mix. In addition, XRD test was carried out to identify the various decomposition phases of the hardened mortar. The results indicated that binary replacement of 15% GGBS and 15% UDSF exhibited the best performance among all other replacements ratios.

Keywords: *binary replacement, supplementary cementitious materials, single replacement, ternary replacement, ultra-high strength, XRD patterns.*

Introduction

Currently, there is a growing demand for high-strength cementitious materials in the field of structural constructions. Production such as these materials involves a high amount of cement which leading to resource consumptions and increases carbon dioxide emissions. Ernst Worrell et al. (2001) [1] stated that the production of one ton of cement releases about one ton of carbon dioxide. Moreover, in many cases, it might be a challenging to obtain a cementitious matrix with high-performance properties without incorporation SCMs.

The role of the SCMs in enhancing the strength mainly attributes to their pozzolanic reaction with the calcium hydroxide (Ca(OH)_2) that resulted from cement hydration to produce supplementary calcium-silicate-hydrate (C-S-H) gel which is the source of the strength [2]. Generally, many studies reported that the addition of SCMs significantly improves the mechanical properties of cementitious materials. However, the improvement depends on the type, properties, and replacements configuration [3 - 9].

GGBS is a waste by-product of steel industries, which has similar chemical and physical properties to Portland cement. Using GGBS in the field of concrete production leads to improve the strength and durability through pore refinement as a result of the pozzolanic reaction. Many studies investigated high replacement of GGBS, more than 50% by weight of cement, for concrete and mortar [6, 10 - 15]. However, it was found that higher than 20% of GGBS might adversely affect the strength of the cementitious matrix despite the enhancement in workability and durability. That could be attributed to the low development strength in early ages due to the insufficient amount of calcium hydroxide (Ca(OH)_2) that resulted from cement hydration [12, 16, 17].

Silica fume is also a waste by-product of the production of silicon metal or silicon alloys. It contains a high amount of silicon dioxide (SiO_2) in an amorphous phase. Numerous researchers indicated the effectiveness of silica fume in enhancing the mechanical properties of concrete and mortar [3, 5, 7, 19, 11, 22]. Otherwise, it was reported that silica fume as a partial replacement of cement increases the water demand that significantly reduces the workability [3, 5, 6, 8, 11]. Most researchers confirmed the effectiveness of silica fume in the pore refinement in the hardened structure of concrete, which reduces the permeability and controls the volumetric changes [18, 20]. Other studies found a slight enhancement in the drying shrinkage behavior of matrices with silica fume [3, 20]. The most productive replacement ratio of silica fume was ranged between 5 and 10 percent of cement [5, 6, 10, 19, 21, 23 - 26].

Similarly, the effectiveness of fly ash in enhancing the workability and durability of concrete and mortar was stated by many studies [8, 18, 28, 30]. However, other studies indicated adversely influences on the mechanical properties due to the low content of amorphous SiO_2 in the composition of FA [7, 10, 11, 20, 27, 28]. The binary replacements of silica fume and fly ash were examined to gain high strength without reducing the workability [7, 27, 20, 29]. The obtained enhancement was limited within cementitious matrices that have normal strength. Additionally, some studies found a drop in strength due to the presence of FA compared with matrices with a single replacement of silica fume [7, 10]. Also, it was reported that binary replacement of silica fume with GGBS improves the performance of cementitious matrix especially for durability aspects [6, 11, 20]. On other hand, the GGBS was found less effective in enhancing the cementitious matrix that contains FA [20, 29].

In the same field, ternary replacements of GGBS, SF and FA were observed improving the workability and strength of the cementitious matrix as reported by Rashad et al. 2014 [29]. It was found that addition 10 percent replacement of SF and GGBS to concrete contains FA exhibited higher improvement in strength compared with binary replacement of GGBS or SF with FA. Similarly, Dave et al. 2017 [30] found that the ternary replacement of 30% of FA, 10% of SF and 10 % of GGBS explained the highest improving in strength to about 16% compared with control. It can be stated that most of the previous investigations of the replacement of supplementary materials (SCMs) were conducted on cementitious materials with normal strength properties. However, limited studies concerning high-strength properties were conducted. Moreover, there are controversial data about the influences of SCMs on the performance of concrete and mortar. Therefore, the main objective of this study aims to investigate the effect of different amounts and configurations of the SCMs on the performance of ultra-high-strength cementitious materials. This investigation is part of comprehensive study of a PhD study at Brighton University for developing cementitious materials with ultra-high strength properties.

2. Experimental program

2.1 Materials

In all investigated mixes, high strength cement type CEM 52.5N was used for casting the high strength mortar. Table 1 demonstrates the physical and chemical properties provided by the manufacturer (Hanson UK Company). Ground-granulated blast-furnace slag (GGBS) satisfying BS EN 15167-1:2006 [31] obtained from Hanson Heidelberg Cement group was utilized. The chemical compositions and physical properties of GGBS are listed in Table 1 (as supplied by the manufacturer). X-ray analysis of the GGBS demonstrates a high peak of SiO_2 at 2θ equal to 21° . However, the peak had less intensity comparing the silica fume peak, which indicates a lower content of SiO_2 in GGBS mineral content, as shown in Figure 1. In addition, no frequent peaks were observed that state an amorphous phase [32]. The chemical composition and physical properties of the densified (DSF) and un-densified silica fume (UDSF) obtained from the manufacturer (Elkem A Bluestar Company) are presented in Table 1. The X-ray patterns of a powder of both type of silica fume explained a peak at 2θ equal to 22° , which refers to a high characteristic of amorphous SiO_2 [22], as shown in Figure 1. Fly ash type 450-S satisfying BS EN 450-1:2012 [33] was adopted in the mixes of high-strength mortar. This class of fly ash was used because of its high pozzolanic activity, and it has a constant fineness and carbon content. It was supplied from the Drax Power Station, North Yorkshire, UK under the CEMEX brand. The chemical and physical properties of the FA are listed in Table 1. The X-ray diffraction analysis of fly ash (Figure 1) explained that the most crystalline constituents of the fly ash are quartz (SiO_2) at 2θ equal to 26° . However, the amorphous SiO_2 appeared at 2θ of 21° at less intensity.

Fine silica sand satisfying BS EN 12620:2002+A: 2008 [34] obtained from Sibelco UK was utilized in casting all investigated mixes. It contains a high proportion of silica in quartz configuration with a colour of yellow/brown. The grain distribution ranges between 0.5 to 0.1 mm. Table 1 lists the chemical composition of silica sand (as supplied by the manufacturer). To achieve the desired workability, Fosroc Auracast 200 high-performance concrete superplasticizer based on polycarboxylate polymers (obtained from Resapol UK company) was used. It has a pH of 4 ± 1 with a specific gravity of 1.050 – 1.070.

Table 1

The chemical and physical properties of cement, SCMs, and silica sand

Characteristics	CEM52.5N	Silica fume	GGBS	Fly ash	Silica sand
CaO	63.8	0.1	40	2.38	--
SiO_2	19.9	92	35	59	99.73
Al_2O_3	4.8	0.7	12	23	0.1
Fe_2O_3	3.1	0.8	0.2	8.8	0.05
MgO	1.1	--	10	1.39	1.0
SO_3	3.3	--	--	0.27	--
Na_2O	0.7	0.33	--	0.74	<0.05
K_2O	0.6	1.45	--	2.81	0.01
L.O.I	2.7	4.6	2.8	1.61	0.09
Specific gravity	3.18	2.20	2.90	2.20	2.6
Specific surface area (mm^2)	--	15-30	--	--	--
Mean particle size (μm)	--	0.15	9.2	--	--

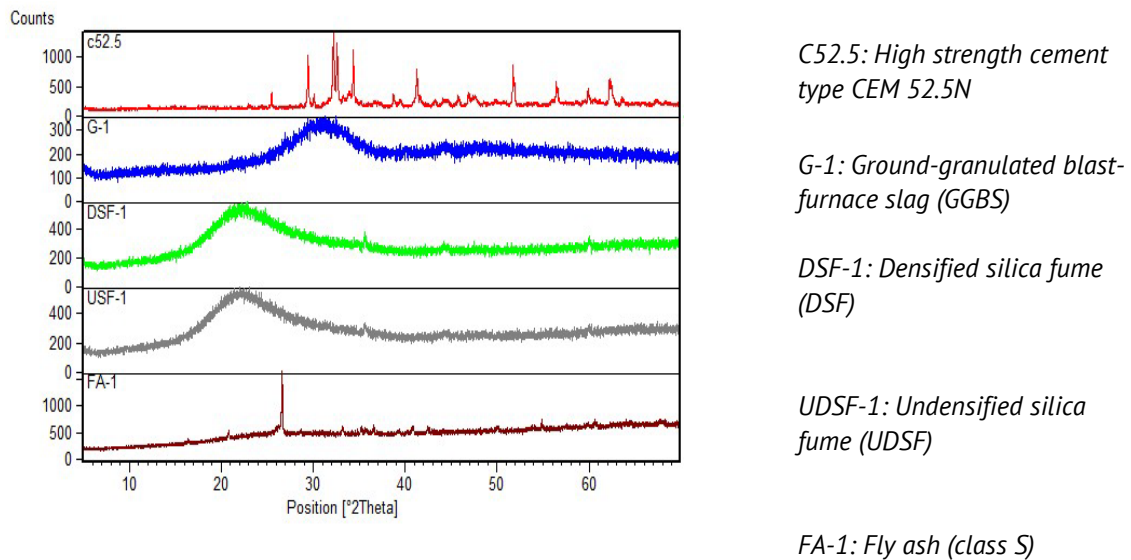


Figure 1. X-Ray patterns of cement and SCMs.

2.2 Mix proportions

Several mixes were designed to achieve the desired compressive strengths of high-strength mortar.

The absolute volume method was applied to determine the proportions of the cement, aggregates, superplasticizer, and water [2].

The designed quantities by mass of the constituent materials for the cubic meter were determined according to the following equation:

$$\frac{C}{1000 \times \rho_C} + \frac{S.S}{1000 \times \rho_{S.S}} + \frac{S.P}{1000 \times \rho_{S.P}} + \frac{W}{1000} = 1.0 \quad (1)$$

Where: C, S.S, S.P and W are the amount of cement, silica sand, superplasticizer and water in kg, respectively, ρ_C , $\rho_{S.S}$ and $\rho_{S.P}$ is the specific gravity of cement, silica sand and superplasticizer, respectively.

After establishing the mix proportions of the control mix, 26 mixes that contain SCMs were designed. In these mixes, all the mix proportions of the control mix were kept constant except the amount of cement and the SCMs.

The SCMs were included in the control high-strength mortar mix as a volumetric replacement of cement according to equation (1), as listed in Table 2.

The absolute volume method was adopted in the calculation of the mix proportions of the mix. The mixing procedure included firstly dry mixing for about 5 minutes of cementitious materials (cement and SCMs) then added silica sand. After that, during mixing, the water which previously mixed with the superplasticizer was added, and the mixing was continued for 10 minutes.

The designed mixes included three main groups. The first group comprised a single replacement of each SCMs with three replacement ratios, 10%, 20%, and 30% of cement. Another replacement ratio of 40% was investigated for GGBS based on the observed enhancement of the literature review.

The investigated replacement for binary replacements were 5% GGBS+5% SCM, 10% GGBS+10%SCM and 15% GGBS+15% SCM. The ternary replacement included 5% and 10% of each type of SCMs.

Table 2

Mix proportions of ultra-high strength mortar including SCMs

Mix	C (kg/m ³)	S.S (kg/m ³)	W (kg/m ³)	S.P (kg/m ³)	GGBS (kg/m ³)	DSF (kg/m ³)	UDSF (kg/m ³)	FA (kg/m ³)
Control (M105)	1100	1100	200	30	--	--	--	--
10 GGBS	990	1100	200	30	100	--	--	--
20 GGBS	880	1100	200	30	200	--	--	--
30 GGBS	770	1100	200	30	300	--	--	--
40 GGBS	660	1100	200	30	400	--	--	--
10 DSF	990	1100	200	30	--	76	--	--
20 DSF	880	1100	200	30	--	152	--	--
30 DSF	770	1100	200	30	--	228	--	--
10 USF	990	1100	200	30	--	--	76	--
20 USF	880	1100	200	30	--	--	152	--
30 USF	770	1100	200	30	--	--	228	--
10 FA	990	1100	200	30	--	--	--	76
20 FA	880	1100	200	30	--	--	--	152
30 FA	770	1100	200	30	--	--	--	228
5GGBS+5DSF	990	1100	200	30	51	39	--	--
10GGBS+10DSF	880	1100	200	30	102	78	--	--
15GGBS+15DSF	770	1100	200	30	153	117	--	--
5GGBS+5UDSF	990	1100	200	30	51	--	39	--
10GGBS+10UDSF	880	1100	200	30	102	--	78	--
15GGBS+15UDSF	770	1100	200	30	153	--	117	--
5GGBS+5FA	990	1100	200	30	51	--	--	39
10GGBS+10FA	880	1100	200	30	102	--	--	78
15GGBS+15 FA	770	1100	200	30	153	--	--	117
5GGBS+5DSF+5FA	935	1100	200	30	51	39	--	39
10GGBS+10DSF+10FA	770	1100	200	30	102	78	--	78
5GGBS+5UDSF+5FA	935	1100	200	30	51	--	39	39
10GGBS+10UDSF+10FA	770	1100	200	30	102	--	78	78

C : cement, S.S: silica sand, W: water, S.P: superplasticizer, GGBS: ground granulated blast furnace slag, DSF: densified silica fume, UDSF: undensified silica fume, FA: fly ash.

2.3 Test methods

2.3.1 Workability

Flowability of the fresh cementitious material is an essential property to assure compatible mixing, casting, and adequate consolidation as a homogenous mass.

The amount of water within the mix has a crucial role in controlling workability.

A large amount of water improves the workability but impairs the strength by increasing the voids inside the hardened mortar. In addition, the presence of voids reduces the durability by increasing the gas and liquid permeability of the hardened structure. In this research, the workability of the mortar was measured using the flow table test based on the BS-EN 1015-3:1999 [35], as shown in Figure 2.



Figure 2. Flow table test setup of high strength fresh mortar.

2.3.2 Compressive and tensile strength

Usually, a compressive strength test was used to explore the behaviour of materials under compressive stresses. This behaviour is essential to gain an inclusive picture of the quality of mortar because the strength of mortar is directly related to the structure of the hydrated cement [2]. Compressive strength tests at ages 7, 28, and 90 days were carried out for cube mortar samples with dimensions 50×50×50 mm based on BS EN 12390-3:2009 [36]. Three specimens of each mix were tested, and the average strength was reported. A universal testing machine was used based on a constant rate of displacement-based loading of 0.01 mm/sec, as shown in Figure 3.a.

The tensile strength of mortar is also vital in determining the load causing the cracking of the hardened mortar. The tensile strength of the hardened structure is controlled by the chemical adhesion bond between the results of cement hydration and the aggregates [2]. A direct tensile test of three dog bone specimens of each mix was implemented to determine the effect of SCMs on the tensile strength of high strength mortar (HSM). The dog bone specimen has 78mm length and 25.5×25.5mm² cross sectional area at the midspan. A universal testing machine with a rate of displacement-based loading of 0.02 mm/sec was used, as shown in Figure 3.b.



a)



b)

Figure 3. a) Compression test setup, b) tensile test setup of mortars.

2.3.2 X-RD patterns

To analysis the composition of the main components of the mortar matrix, an X-ray diffraction test of powder samples was performed using an X'Pert diffractometer with CuK

radiation ($\lambda = 1.5418 \text{ \AA}$) operating at 40 kV, 30 mA. This test is adopted to identify the variation of the amount of calcium hydroxide (Ca(OH)_2) in the sample. The Ca(OH)_2 variation demonstrates the reactions between the SCMs with the Ca(OH)_2 to produce supplementary C-S-H. The peaks at 2θ equal to 34° were adopted to refer to the amount of Ca(OH)_2 based on previous studies [11, 14, 28, 36]. The test includes preparing a powder of the sample that tested under compression load at 28 days and then measures the reflection of the X-ray. The results of the test were analysed using the provided software with the X-ray machine.

3. Results and discussion

3.1 Influence of SCMs on the workability

The effect of the addition SCMs on the workability of high-strength mortar (HSM) is demonstrated in Figure 4. Single replacements of all replacement ratios of GGBS and FA displayed higher workability as the replacement ratio increases. The effectiveness of GGBS in improving the workability was due to the surface characteristics of the GGBS particles, which are smooth and absorb little water during mixing [2]. Similarly, most FA particles are spherical and solid which reduces the water demand for a particular workability [2]. Megat Johari et al. (2011) [11] reported a similar observation of enhancing the workability of FA and GGBS with high-strength concrete. In the same field, Dave et al. (2017) [30] observed that the addition of FA was significantly increasing the workability of concrete.

In contrast, mixes with DSF and UDSF explained a reduction in workability. That could be attributed to the particles patterns of silica fume which have a high surface area that absorbs a high amount of water during mixing, which led to increasing the water demand of the mix. A similar reduction in workability due to silica fume was observed by previous studies [5, 7, 8]. However, in binary replacement, the addition of GGBS combined with DSF enhanced the workability for all replacement ratios. Similarly, to less extent, the workability of mortar with UDSF increased as the replacement ratio increased in the presence of GGBS. However, the addition of GGBS with FA reduced the workability comparing with the single replacement of FA counterparts. The workability of ternary replacements of all ratios proportional increasingly with the replacement ratios. Also, it can be observed that mixes with SCMs contain UDSF explained higher workability than DSF counterparts. These results agree with the findings observed by Dave et al. (2017) [30].

In summary, the results demonstrated the effectiveness of addition GGBS in improving the workability of mortar in all forms of replacements (single, binary and ternary). Moreover, regardless of the type and amount of SCMs replacement, binary and ternary replacement explained a higher enhancement of the workability of high-strength mortar.

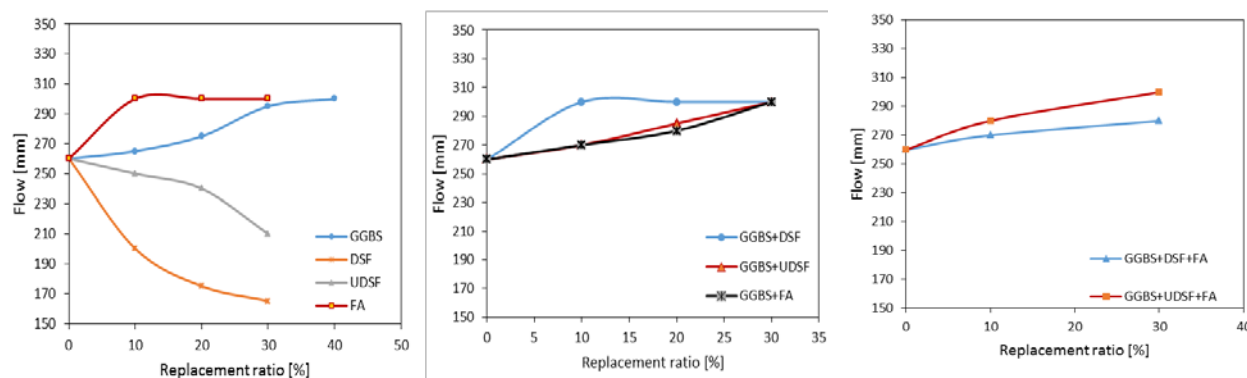


Figure 4. Effect of SCMs replacements of on workability of HSM.

3.2 Influence of SCMs on the compressive strength

Figure 5 demonstrates the enhancement in the compressive strength for 28 days age respecting to the control mix (M105). The obtained compressive strength at all ages increased comparing with the control mortar for all mixes with 10% of single replacement of all types of SCMs as illustrated in Figure 6. However, the enhancement was continued for GGBS and UDSF up to a 20% replacement ratio and a reduction in the enhancement was observed for higher single replacement. At 28 days, the compressive strength was increased to about 28% comparing with the control mix. The highest compressive strength was observed for 20% of UDSF, while the lowest strength was found for the 30% replacement ratio of densified silica fume. That may be due to the low workability of mixes with DSF, which leads to a decrease in the compaction of the mix during casting, see Figure 4. The results also explained that mixes with a single replacement of GGBS explained higher compressive strength than mixes with FA despite both pozzolanic materials improve the workability. That could be because most of the silica in the mineral composition of FA has a crystalline structure as observed in the X-Ray patterns.

Figure 7 illustrates the variation of the effect of binary replacement of SCMs. The compressive strength at 28 days ranged between 92.2MPa and 135.2MPa. The GGBS and UDSF explained the highest compressive strength comparing to other SCMs. In addition, it was observed increasing in compressive strength as the replacement ratio increased. However, the compressive strength of binary replacement consists of 5%GGBS, and 5%DSF explained better performance than binary replacement of UDSF. That may be due to the higher reactivity of densified silica fume, which led to rapid consumption of the available Ca(OH)_2 . This assumption can be proven by the results at the age of 90 days. All replacement ratios of binary replacement of GGBS and DSF explained the same compressive strength due to the availability of Ca(OH)_2 as a result of cement hydration. Binary replacement of FA was ineffective on the compressive strength at the initial stage, and compressive strength was lower than control beams. At 90 days, binary replacement of GGBS and FA up to 20% improved the compressive strength compared to the control mix. The reason could be due to the availability of Ca(OH)_2 that is required for the pozzolanic reaction which is agreed by literature findings [30,37]. Overall, it can be stated that the enhancement of binary replacements of SCMs was higher than single replacement which is compatible with the observation of Gesoglu et al. (2009).

The effect of ternary replacements is illustrated in Figure 8. Ternary replacement of GGBS, DSF, and FA at initial stages exhibited negligible enhancement, but at 90 days the enhancement was obvious. 5% of UDSF increases the compressive strength, while 10% reduced the strength for all ages. That may be due to the segregation of mixed components which can be noted from the high workability (flow excess 300mm). This segregation refers to a high content of fluids that leaving voids in the hardened structure of mortar [2]. The compressive strength at 28 days of the ternary replacements ranged between 93.5MPa and 119.6MPa, which indicates that binary replacement is more effective, and these results agree with the findings of Gesoglu et al. (2009) [20].

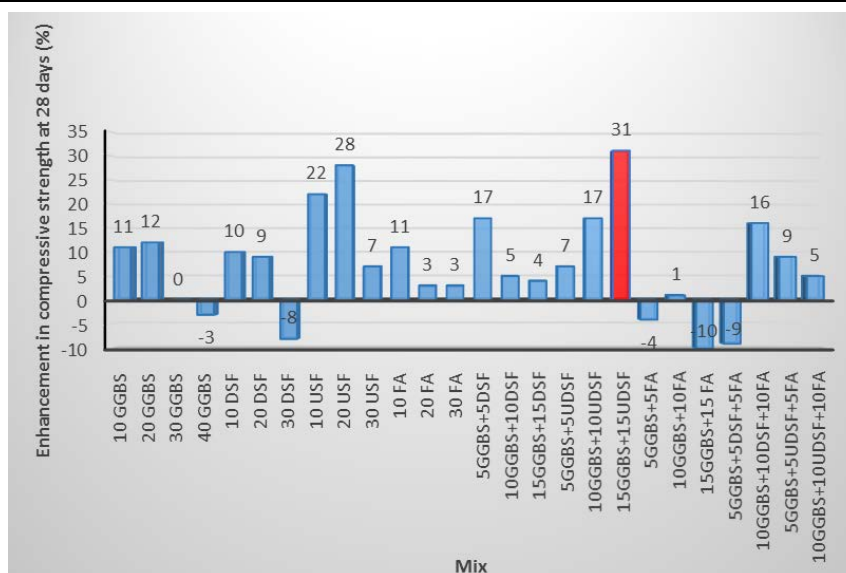


Figure 5. Effect of SCMs on compressive strength of HSM.

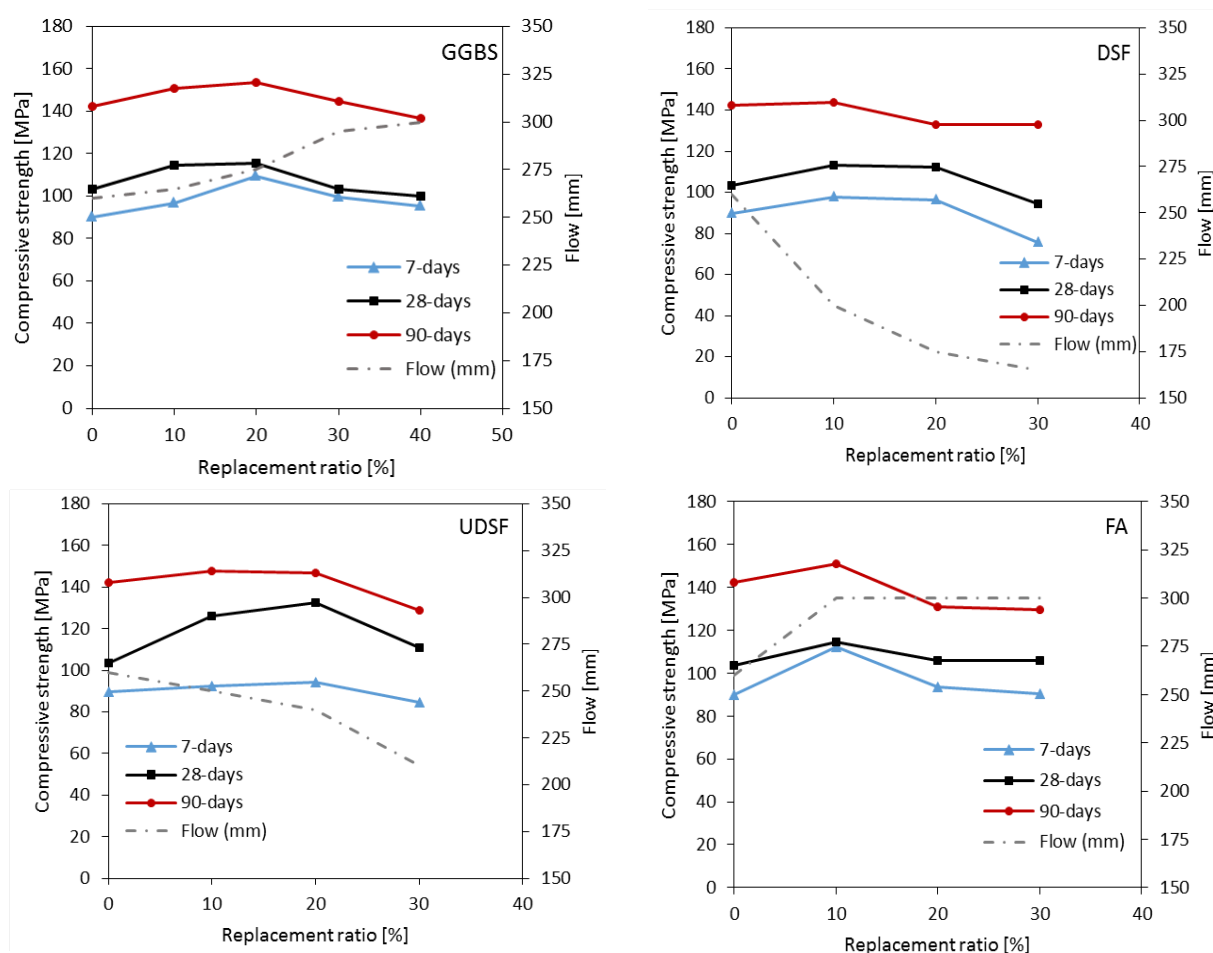


Figure 6. Effect of single replacement of SCMs on compressive strength of HSM.

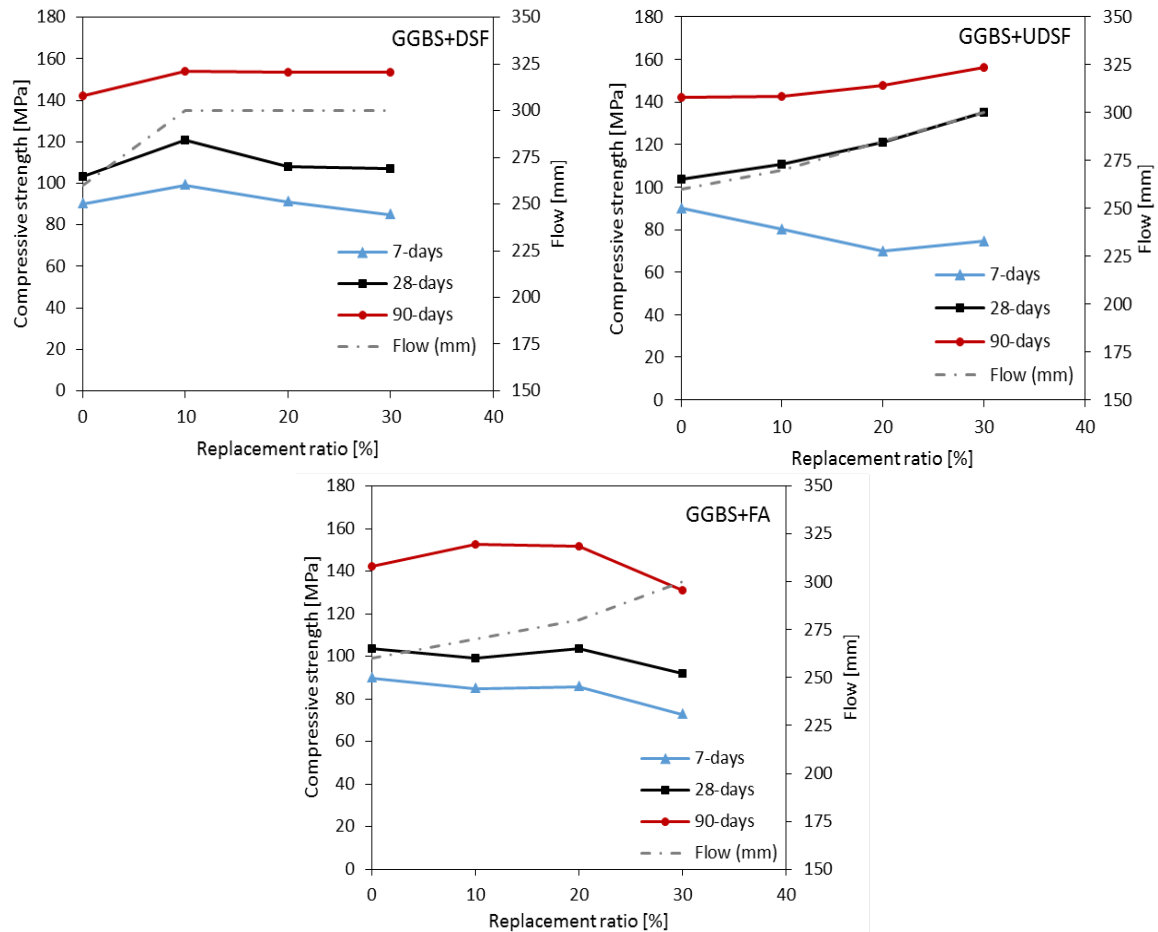


Figure 7. Effect of binary replacement of SCMs on compressive strength of HSM.

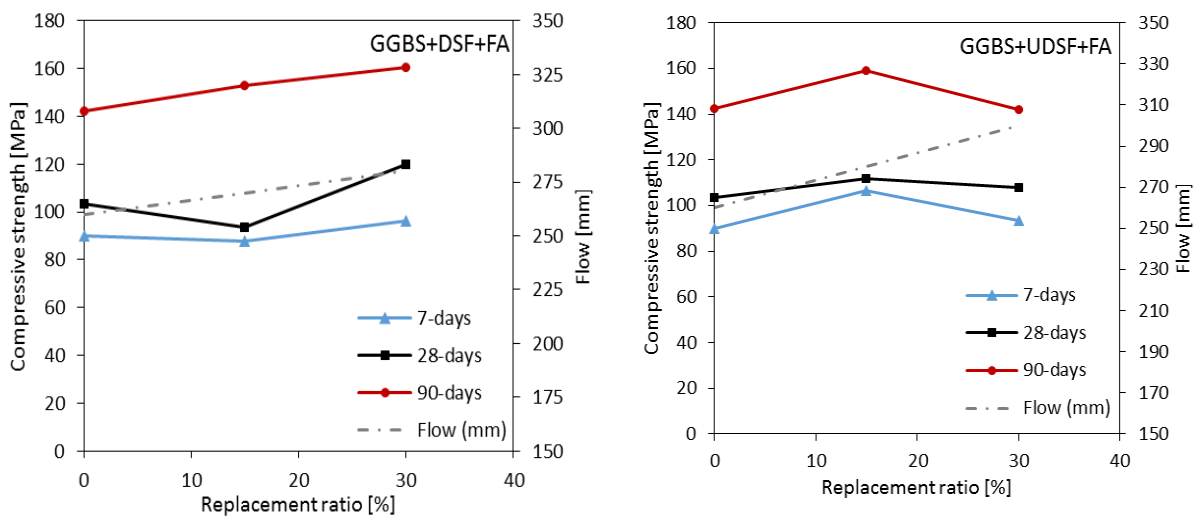


Figure 8. Effect of ternary replacement of SCMs on compressive strength of HSM.

3.3 Influence of SCMs on the tensile strength

The single replacement explained the disadvantage of addition GGBS and FA on the tensile strength as shown in Figure 8. However, the addition of UDSF and DSF improves the tensile strength, which could be attributed to the lower silica content of FA and GGBS. A similar reduction was observed by Dave et al. (2017) [30] with 30% replacement of FA. The single replacements of SCMs explained tensile strength ranged between 4.3 MPa and 6.7 MPa depending on the type of SCMs. The UDSF exhibited a continuous increase in tensile strength

for all replacement ratios. However, DSF presented an optimum replacement ratio of 10% which could be due to a decrease in the compactness of the mix as a result of reducing the flowability of mixes.

The best performance was observed for binary with tensile strength ranged between 5.3 MPa and 6.7 MPa. The maximum tensile strength was reported for a replacement ratio of 15% GGBS and 15% UDSF with 6.7 MPa. The lowest tensile strength was found for binary replacement of GGBS and FA. That could be because of less silica in the chemical composition of FA in comparison with silica fume.

Figure 9 demonstrated a negligible effect of DSF and FA in enhancing the tensile strength. However, UDSF exhibited enhancement in the tensile strength with a replacement ratio equal to 15%. Above this replacement ratio, a reduction in tensile strength was observed. The tensile strength of ternary replacements mixes was ranged between 4.5 MPa and 6.3 MPa which explains less effectiveness comparing to binary replacement.

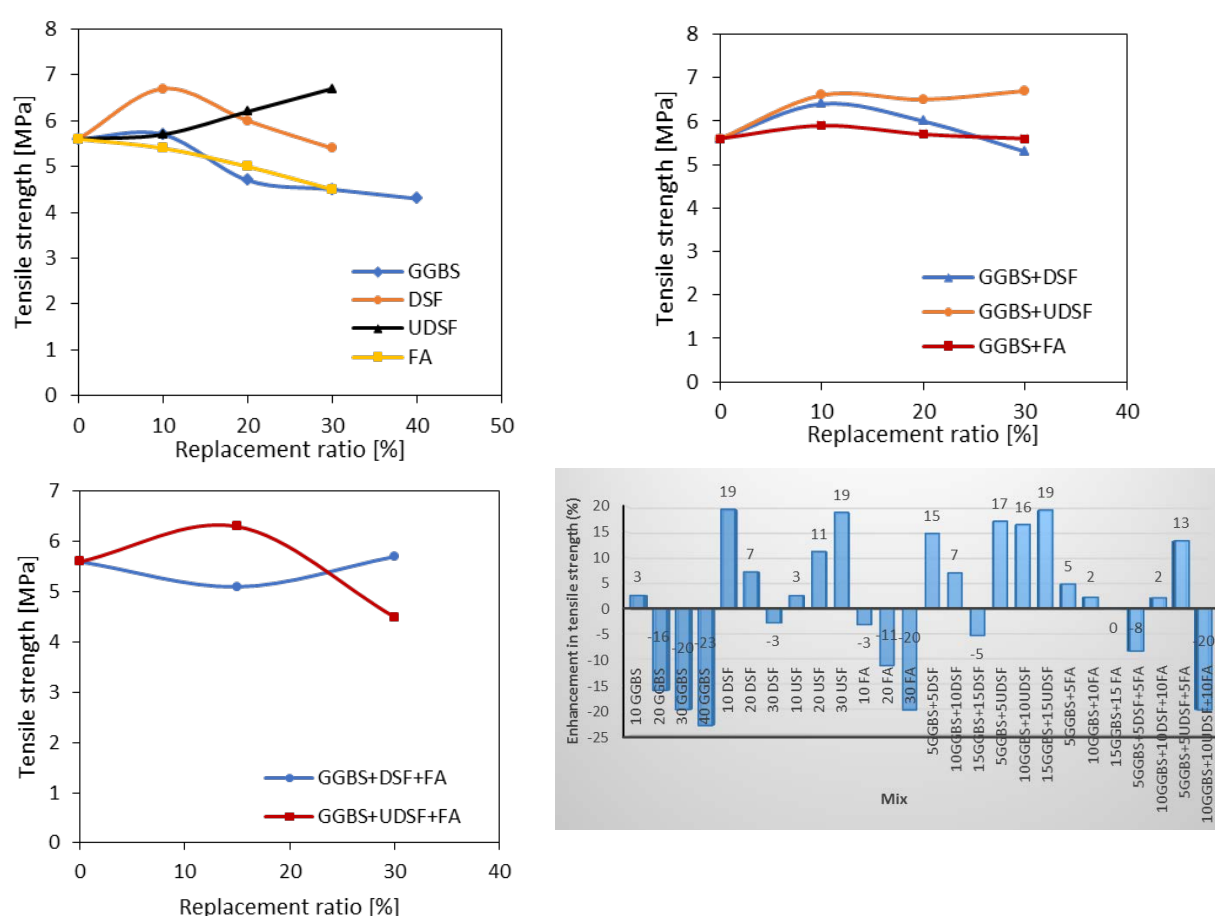


Figure 9. Effect of SCMs replacement on tensile strength of HSM.

Figure 10 demonstrates a consistency of the general behaviour between the tensile and compressive strength of high-strength mortar with SCMs. However, there is no direct proportionality between the two types of strength. In addition, in some cases, particularly of high replacement ratio, the increase in compressive strength did not accompany with increasing in tensile strength. That could be due to the lack of calcium hydroxide for a high replacement ratio, and the SCM works as a filler rather than cementitious material. That will be effective in resisting the compressive stresses by friction, while it has a negligible

influence in resisting the tensile stresses. The figure also indicated the superiority of binary replacements among single and ternary replacements.

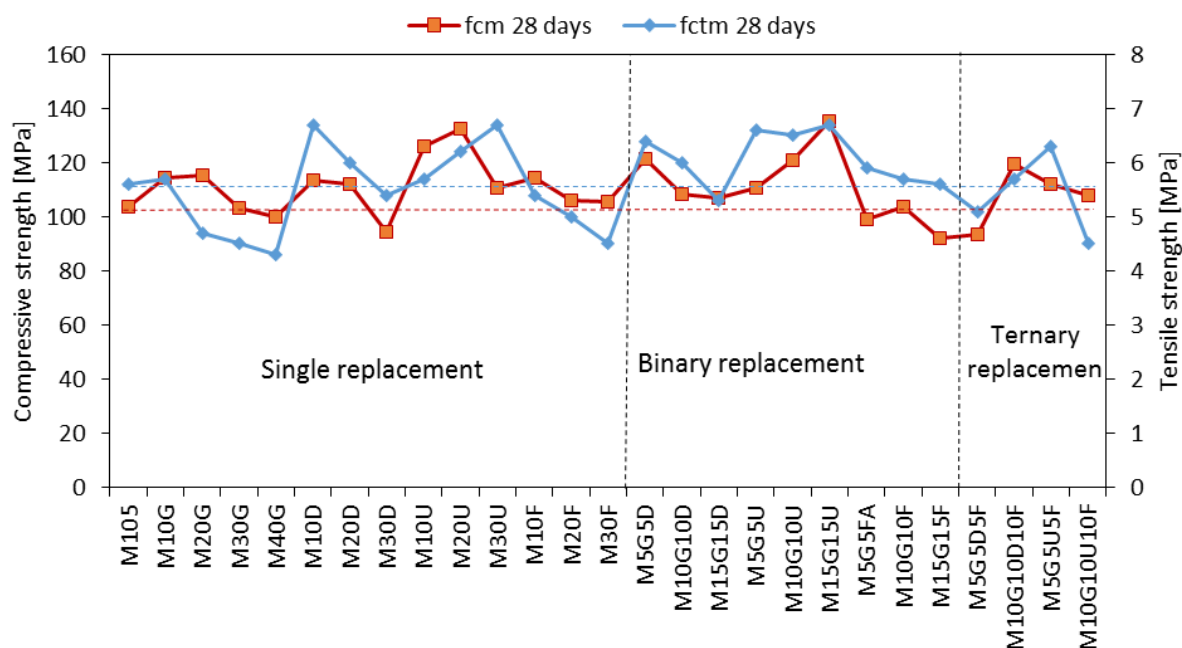


Figure 10. Mechanical properties of single, binary and ternary replacement of SCMs.

3.5 XRD patterns

Figure 11 presents the intensity peaks of $\text{Ca}(\text{OH})_2$ obtained from the analysis of the X-Ray diffraction test of high strength mortar with SCMs. As shown in the figure, the SCMs reduced the amount of calcium hydroxide for control mix (M105). This reduction increased as the replacement ratio increases which indicates to the consumption of calcium hydroxide in the pozzolanic reaction of SCMs. The results also demonstrated higher content of amorphous SiO_2 , such as DSF and UDSF were more effective in contributing the pozzolanic reaction products which present higher strength enhancement. These findings consistent with the observation of Supit et al. (2014) [28].

High consistency between the obtained compressive strength and the intensity peaks of $\text{Ca}(\text{OH})_2$ was observed. For the same replacement ratio, as the intensity peaks decrease, the compressive strength increases. However, the addition of DSF with replacement ratio 20% and 30% exhibited a reduction in intensity peaks of $\text{Ca}(\text{OH})_2$ without a considerable contribution to the strength. That could be attributed to the low flowability of the matrix, which in turns decrease the compaction of the mix during casting and increase the voids inside the hardened mortar.

The best performance in consumption $\text{Ca}(\text{OH})_2$ was observed for mixes UDSF because of the high content of amorphous SiO_2 . In contrast, mixes contain fly ash explained the highest intensity peaks of $\text{Ca}(\text{OH})_2$ among all SCMs mixes. That stated the low compressive strength that was observed of mortar with FA in comparison with control mortar. Overall, binary replacement of 15% GGBS and 15% UDSF explained the lowest intensity peak of $\text{Ca}(\text{OH})_2$ which refers to high activity in the pozzolanic reaction that led to enhance the strength of mortar. This finding coincides with the highest compressive and tensile strength of this mix proportion.

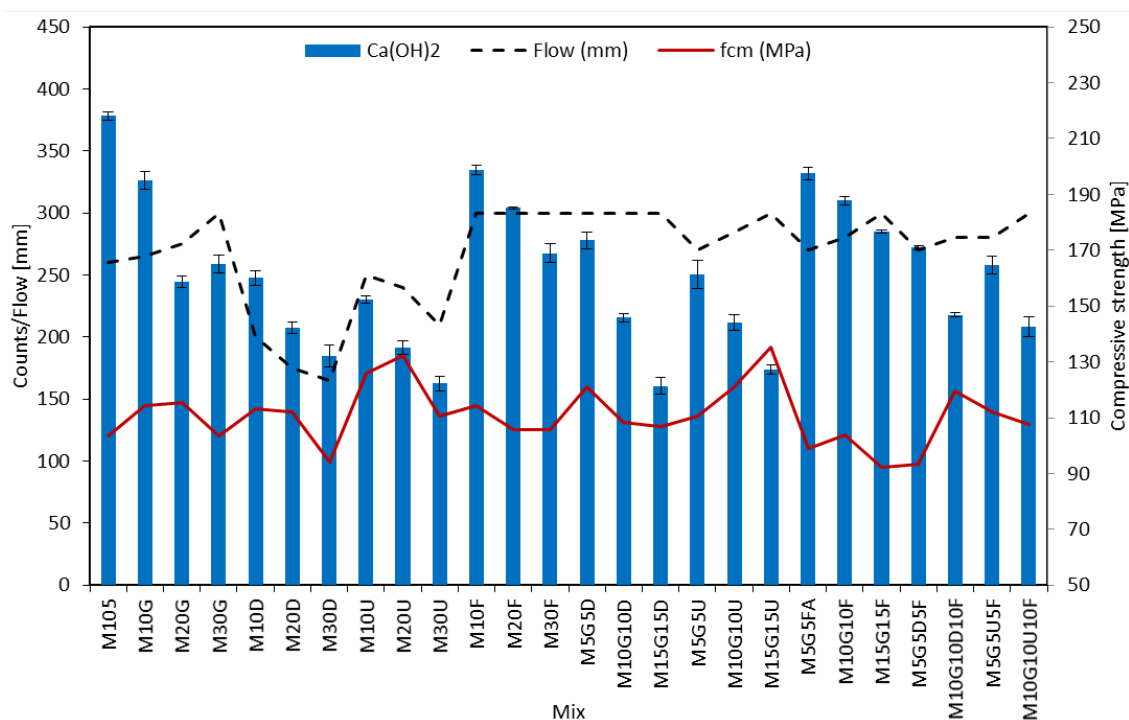


Figure 11. XRD of calcium hydroxide peaks of HSM with SCMs.

4. Conclusions

Based on the result of the investigated SCMs, the following conclusions can be drawn:

- Apart from both types of silica fume, all replacement of the SCMs improved the workability of the fresh mixes depending on the type and ratio of replacement. In addition, the most considerable improvement in workability was observed for mixes with fly ash.
- Both types of silica fume reduced the workability of mortar. However, the un-densified form explained better fresh mortar properties.
- Fly ash demonstrated a relatively low enhancement in the mechanical properties of high strength mortar compared with other SCMs.
- Regarding the mechanical properties, both types of silica fume exhibited approximately similar behaviour up to 10% replacement. Higher replacement indicated the superiority of unidentified silica fume in increasing the strength.
- GGBS explained enhancement in workability as well as in the mechanical properties.
- Binary replacement of 15% of un-densified silica fume and 15% of GGBS presented the highest mechanical properties. Moreover, the effect of enhancing the strength of mortar was evident from the low intensity of the Ca(OH)_2 that determined from the X-Ray diffraction analysis compared with mixes with lower strength.
- Despite of the obvious consistency between the compressive and tensile strength, a direct relationship between them is unavailable due to the variation in the hardened structure on mortar due to flowability.

Acknowledgements: The author would like to thank the University of Brighton for providing the required equipment for the investigation. Thank is also continued to the Elkem A Bluestar Company and Hanson UK Company for supplying the SCMs.

References

1. Ernst Worrell, Lynn Price, Nathan Martin, CHRIS HENDRIKS & MEIDA, L. O. 2001. Carbon dioxide emissions from the global cement industry. *Annual Review of Energy and the Environment*, 26, 303 - 329.
2. Neville A.M. 2011. Properties of concrete, Edinburgh Gate Harlow Essex, Pearson Education Limited.
3. Mazloom M., Ramezani-pour A. A. & Brooks J. J. 2004. Effect of silica fume on mechanical properties of high-strength concrete. *Cement and Concrete Composites*, 26, 347-357.
4. Megat Johari M. A., Brooks J. J., Kabir S. & Rivard p. 2011. Influence of supplementary cementitious materials on engineering properties of high strength concrete. *Construction and Building Materials*, 25, 2639 - 2648.
5. Inan Sezer G. 2012. Compressive strength and sulfate resistance of limestone and/or silica fume mortars. *Construction and Building Materials*, 26, 613 - 618.
6. Bagheri A. R., Zanganeh H. & Moalemi M. M. 2012. Mechanical and durability properties of ternary concretes containing silica fume and low reactivity blast furnace slag. *Cement and Concrete Composites*, 34, 663 - 670.
7. Bagheri A., Zanganeh H., Alizadeh H., Shakerinia M. & Marian M. A. S. 2013. Comparing the performance of fine fly ash and silica fume in enhancing the properties of concretes containing fly ash. *Construction and Building Materials*, 47, 1402 - 1408.
8. Jalal M., Pouladkhan A., Harandi O. F. & Jafari D. 2015. Comparative study on effects of Class F fly ash, nano silica and silica fume on properties of high performance self compacting concrete. *Construction and Building Materials*, 94, 90 - 104.
9. Hossain M. M., Karim M. R., Hasan M., Hossain M. K. & Zain M. F. M. 2016. Durability of mortar and concrete made up of pozzolans as a partial replacement of cement: A review. *Construction and Building Materials*, 116, 128 - 140.
10. Elahi A., Basheer P. A. M., Nanukuttan S. V. & Khan Q. U. Z. 2010. Mechanical and durability properties of high performance concretes containing supplementary cementitious materials. *Construction and Building Materials*, 24, 292 - 299.
11. Seleem H. E.-D. H., Rashad A. M. & El-Sabbagh B. A. 2010. Durability and strength evaluation of high-performance concrete in marine structures. *Construction and Building Materials*, 24, 878 - 884.
12. Megat Johari M. A., Brooks J. J., Kabir S. & Rivard P. 2011. Influence of supplementary cementitious materials on engineering properties of high strength concrete. *Construction and Building Materials*, 25, 2639-2648.
13. Barnett S. J., Soutsos M. N., Millard S. G. & Bungey J. H. 2006. Strength development of mortars containing ground granulated blast-furnace slag: Effect of curing temperature and determination of apparent activation energies. *Cement and Concrete Research*, 36, 434 - 440.
14. Alhozaimey A., Al-Negheimish A., Alawad O. A., Jaafar M. S. & Noorzaei J. 2012. Binary and ternary effects of ground dune sand and blast furnace slag on the compressive strength of mortar. *Cement and Concrete Composites*, 34, 734 - 738.
15. Li K., Zeng Q., Luo M. & Pang X. 2014. Effect of self-desiccation on the pore structure of paste and mortar incorporating 70% GGBS. *Construction and Building Materials*, 51, 329 - 337.
16. Zhang W., Hama Y. & Na S. H. 2015. Drying shrinkage and microstructure characteristics of mortar incorporating ground granulated blast furnace slag and shrinkage reducing admixture. *Construction and Building Materials*, 93, 267 - 277.
17. Özbay E., Erdemir M. & Durmuş H. İ. 2016. Utilization and efficiency of ground granulated blast furnace slag on concrete properties – A review. *Construction and Building Materials*, 105, 423 - 434.
18. Mardani-Aghabaglou A., Inan Sezer G. & Ramyar K. 2014. Comparison of fly ash, silica fume and metakaolin from mechanical properties and durability performance of mortar mixtures view point. *Construction and Building Materials*, 70, 17 - 25.
19. Canpolat F. 2012. Sulfate resistance of mortars containing silica fume and pozzolan. *Proceedings of the Institution of Civil Engineers - Construction Materials*, 165, 65 - 72.
20. Gesoğlu M., Güneyisi E. & Özbay E. 2009. Properties of self-compacting concretes made with binary, ternary, and quaternary cementitious blends of fly ash, blast furnace slag, and silica fume. *Construction and Building Materials*, 23, 1847 - 1854.
21. Zelić J., Krstulović R., Tkalčec E. & Krolo P. 2000. The properties of Portland cement-limestone-silica fume mortars. *Cement and Concrete Research*, 30, 145 - 152.

22. Qing Y., Zenan Z., Deyu K. & Rongshen C. 2007. Influence of nano-SiO₂ addition on properties of hardened cement paste as compared with silica fume. *Construction and Building Materials*, 21, 539 - 545.
23. Zhang Z., Zhang B. & Yan P. 2016a. Hydration and microstructures of concrete containing raw or densified silica fume at different curing temperatures. *Construction and Building Materials*, 121, 483 - 490.
24. Borosnyói A. 2016. Long term durability performance and mechanical properties of high performance concretes with combined use of supplementary cementing materials. *Construction and Building Materials*, 112, 307 - 324.
25. Zhang Z., Zhang B. & Yan P. 2016b. Comparative study of effect of raw and densified silica fume in the paste, mortar and concrete. *Construction and Building Materials*, 105, 82-93.
26. Motahari Karein S. M., Ramezani-pour A. A., Ebadi T., Isapour S. & Karakouzian M. 2017. A new approach for application of silica fume in concrete: Wet granulation. *Construction and Building Materials*, 157, 573 - 581.
27. Wongkeo W., Thongsanitgarn P. & Chaipanich A. 2012. Compressive strength and drying shrinkage of fly ash-bottom ash-silica fume multi-blended cement mortars. *Materials & Design (1980 - 2015)*, 36, 655 - 662.
28. Supit S. W. M., Shaikh F. U. A. & Sarker P. K. 2014. Effect of ultrafine fly ash on mechanical properties of high volume fly ash mortar. *Construction and Building Materials*, 51, 278 - 286.
29. Rashad A. M., Seleem H. E.-D. H. & Shaheen A. F. 2014. Effect of Silica Fume and Slag on Compressive Strength and Abrasion Resistance of HVFA Concrete. *International Journal of Concrete Structures and Materials*, 8, 69 - 81.
30. Dave N., Misra A. K., Srivastava A., Sharma A. K. & Kaushik S. K. 2017. Study on quaternary concrete micro-structure, strength, durability considering the influence of multi-factors. *Construction and Building Materials*, 139, 447 - 457.
31. BS EN 15167-1. 2006. Ground granulated blast furnace slag for use in concrete, mortar and grout.
32. Teng S., Lim T. Y. D. & Sabet Divsholi B. 2013. Durability and mechanical properties of high strength concrete incorporating ultra fine Ground Granulated Blast-furnace Slag. *Construction and Building Materials*, 40, 875 - 881.
33. BS EN 450-1. 2012. Fly ash for concrete. Definition, specifications and conformity criteria. London. BSI Standards Publication.
34. BS EN 12620. 2013. Aggregates for concrete. London. BSI Standards Publication.
35. BS EN 1015-3 .1999. Methods of test for mortar for masonry. Determination of consistence of fresh mortar (by flow table). London. BSI Standards Publication.
36. Liu S., Han W. & Li Q. 2017. Hydration Properties of Ground Granulated Blast-Furnace Slag (GGBS) Under Different Hydration Environments. *Materials Science*, 23.
37. Yazici H. 2007. The effect of curing conditions on compressive strength of ultra high strength concrete with high volume mineral admixtures. *Building and Environment*, 42, 2083 - 2089.

[https://doi.org/10.52326/jes.utm.2021.28\(3\).11](https://doi.org/10.52326/jes.utm.2021.28(3).11)
CZU 628.17:681.515



PERFORMANCE STUDIES ON WATER FLOW CONTROL USING P, PI AND PID CONTROLLERS

Ramesh Babu Aremanda*, ORCID ID: 0000-0002-6609-8640,
Nahom Yohannes, ORCID ID: 0000-0001-8926-5141,
Yosief Ghezae, ORCID ID: 0000-0001-9602-3546

*Department of Chemical Engineering, Mai Nefhi College of Engineering & Technology (MCOETEC), P.O. Box 344,
Asmara, Eritrea.*

*Corresponding author: Ramesh Babu Aremanda, ramesh.nitrkl@gmail.com

Received: 05. 28. 2021

Accepted: 08. 11. 2021

Abstract. The main purpose of this study is to revitalize the concept of wise and controlled supply of water for domestic, industrial and agricultural applications which facilitate sustainable usage of fresh water resources. As Eritrea is striving to manage its water resources, attention paid primarily to enable water flow control mechanisms in municipal water distribution systems. A table top process control trainer (PCT) was tested through proportional(P), integral (I) and derivative (D) control mechanisms using Ziegler-Nichols second method to evaluate the tuning variables. Applying exclusively P control action, critical period of oscillation (P_{cr}) was estimated as 1.4 sec at proportional band value of 9. P, PI and PID controller performance studies were conducted with tuned variables on the water flow control system at different step disturbances between 20 – 50 % and their corresponding responses were characterized. P controller exhibited faster responses with consistent increments in offset, PI controller recorded highest overshoot values with negligible offset and prolonged settling times. PID controller showed less overshoot values and faster response times than PI but it increased chatter on the control output signal. The study revealed that the system can be safely controlled between 0-80 LPH. If the offset is not a major concern, P controller would be reflected suitable with simple design and minimum expenditure, else PI controller makes offset to zero though it possesses higher settling times. In other words, PID controller is complex using more tuning parameters, need expensive maintenance, and has resulted an intermittent noise in the output signal.

Keywords: *Control System, Flow controllers, Step Disturbances, Sustainable Supply of Water, Tuning of PID Controllers, Water Flow control, Ziegler and Nichols Method.*

Introduction

Freshwater supply is the main pillar for sustainable economic activities of humankind and an essential element of human life. Currently, scarcity and quality of water have become prior concerns in many developing countries. Of the 3% of freshwater on earth, only one third is of drinking water quality available in streams, rivers and lakes that can support human's

daily activities and other usage [1]. Globally, water use has been increasing by 1% every year and expected to rise 20 – 30 % by 2050 [2]. Population growth and urbanization are prominent reasons for water scarcity everywhere in the world [3, 4]. Eritrea, a northeast African country mainly relies on seasonal rainfalls usually happens every year for short period from July to September. However, Government of Eritrea (GOE) has made significant progress in water and sanitation service delivery since its independence. Despite progress, water scarcity and poor water quality are increasingly common across Eritrea, demand for freshwater in rural and urban areas is expected to increase as a result of rapid climate change, population growth, rapid urbanization, economic activity, competition for water and improved standards of living. Hence, in 2019, with the support of UNICEF, the GOE has developed a One WASH (Water, Sanitation and Hygiene) Strategy and Investment Plan (OWSIP) that integrates resilience considerations, climate change mitigation and adaptation [5]. Therefore, the study of water supply control systems and their design strategies would be on prior to ensure deterministic supply with improved safety.

Flow controllers are designed to measure and control the flow of liquids and gases in domestic, industrial and agricultural applications. Water flow control in process industries is essential for precise supply in manufacturing operations, perhaps it may decide the end product specification. An effective fluid control equipment can also help in the prevention of hazardous substances into the working environment. Flow controllers, which need modulating electronically to enable a closed process loop are installed to speed up and improve the processes whilst lowering the cost. Applications that benefit from this include the sampling systems in petrochemical plants, gas and chemical control in manufacturing processes and in off-shore oil rigs. Solenoid valves are a good performer in these environments; however, it is important to consider the power requirements and the environment they are being used in. A standard solenoid would potentially pose great risk without being upgraded, due to the electricity needed to operate them. A simple and more reliable method of flow control within these environments are pneumatic valves. The removal of electricity from its process of delivery, removes fire and explosion hazards [6, 7]

Three types of controllers, proportional, integral and derivative (PID) were developed in 1930s, still the most widely applied industrial controllers. This succeed is a result of many good features of this algorithm such as simplicity, robustness and wide applicability [8]. Transfer function (G_C) of PID Controller generally expressed as

$$G_C(s) = K_C(1 + \frac{T_I}{s} + T_D s)$$

where K_C , is proportional gain T_I is integral time and T_D is derivative time [8, 9]. Many different tuning methods have been proposed from 1942 to the present day for gaining better and more acceptable control system response based on desirable control objectives such as percent of overshoot, offset, settling time, manipulated variable behavior etc. PID controller tuning methods are classified into closed loop methods such as Ziegler-Nichols method, Tyreus-Luyben method and Damped Oscillation method etc., and Open loop methods like open loop Ziegler Nichols methods, Cohen and Coon method, Minimum error criteria methods etc. [8, 10]

Nevertheless, there exist very few literatures [11 - 13] about PID tuning of flow control system, in this study, attention paid mainly to evaluate the parameters of PID controller applied for turbine flow control of water assembled in a table top process control trainer

(PCT) system. Since the Ziegler-Nichols models are simple and most popular in industrial applications, closed loop Ziegler-Nichols tuning method was adopted to estimate PID controller parameters. Tuned variables were set for proportional (P), proportional integral (PI), and proportional integral derivative (PID) control mechanisms and several experiments were performed at different set values to identify the system overall performance.

Closed Loop Ziegler-Nichols Tuning Method

This is a heuristic trial and error tuning process based on sustained oscillations that was proposed by Ziegler and Nichols in 1942. This is probably the most widely used method for tuning of PID controllers, is also known as *online* or *continuous cycling* or *ultimate gain* tuning method [8, 14].

Table 1

Closed loop calculations PID controller parameters, K_C , T_I and T_D

Controller/Parameter	Proportional Gain (K_C)	Integral Time (T_I)	Derivative Time (T_D)
P	$0.5K_{cr}$	∞	0
PI	$0.45K_{cr}$	$P_{cr}/1.2$	0
PID	$0.6K_{cr}$	$0.5 P_{cr}$	$0.125P_{cr}$

It applies only proportional gain (K_P) in a feedback control loop by neglecting integral and derivative actions.

The process usually begin with low values of gain, K_P followed by gradual increase until a steady state oscillation occurs.

The gain corresponding to sustained oscillation period, P_{cr} can be evaluated as $K_{cr} = 100/P_b$, where P_b is the proportional band of the system. After that PID controller parameters can be calculated as in Table 1. [15 - 17].

Materials & Methodology

Materials: Ambient air passed through compressor followed by oil catch filter was used as fluid to provide pressure for differential pressure flow sensor and also to serve in I to P Converter.

Water fetched from municipal water supply lines of Mai-Nefhi was utilized as process fluid.

Experimental Setup:

A table top process control trainer (PCT) system, originally supplied by Matrix Global Pvt. Ltd. India but accessed from the Process Control lab, Department of Chemical Engineering, Mainefhi College of Engineering & Technology (MCOETEC). Water was taken as process fluids, and the air served as utility in differential pressure flow sensor.

PCT mainly composed of a sump tank of 70 liters, mounted horizontally, ½ HP centrifugal pump to drive water from sump tank to the process, a compressor that compress air up to 10 bar with automatic on/off operation, an oil catch filter to purify air that comes into the process, a process tank of 70 liter mounted vertically, control valve and computer loaded with PID controller software.

All these hardware elements were connected with auxiliary fittings such as pipelines, pressure dials, inline valves and transmission lines as shown in Figure 1.

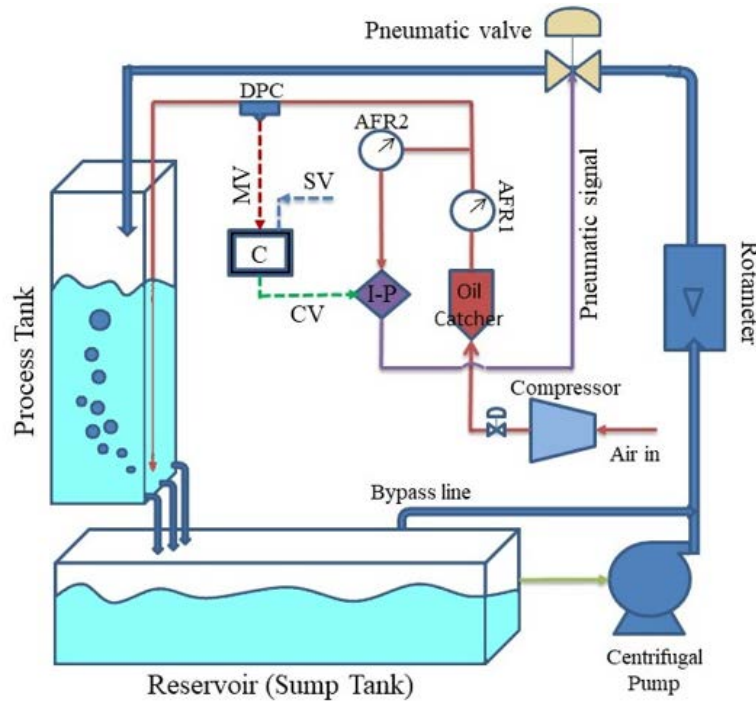


Figure 1. Schematic diagram of process control trainer (PCT) system.

Methodology

To configure flow control system into a closed loop control, the connections were made according to the wiring sequence shown in the text box below prior to conduct experiments. As a primary phase, a set of experiments were performed to evaluate PID controller parameters by using Ziegler-Nichols method.

Tuning of PID controller of Water flow control system:

According to Ziegler Nichol's Second method, a closed loop setup was arranged as shown in Figure 2 through accomplished wiring sequence. Initially the system intake pressure was arranged at 1 bar by watching on pressure dial AFR1. Prior to switch on the pump, all the necessary parameters as shown in Figures 3 & 4 were set on main window and on settings window of PID controller software installed on PC. As the pump capacity is quite high, a bypass line was provided, and the inflow valve was kept open, and also two of the exit valves of process tank were also kept open. The pump made on and for a set value of 30 %, the responses of the system in Figure 1 were noted by changing proportional band (P_b) values in ascending order, from 3 to 11 manually in the main window of PID Controller application until a sustained wave with constant amplitude was recorded. The data generated from the different sets of experiments were collected and analyzed clearly to identify a perfect wave with a constant amplitude.

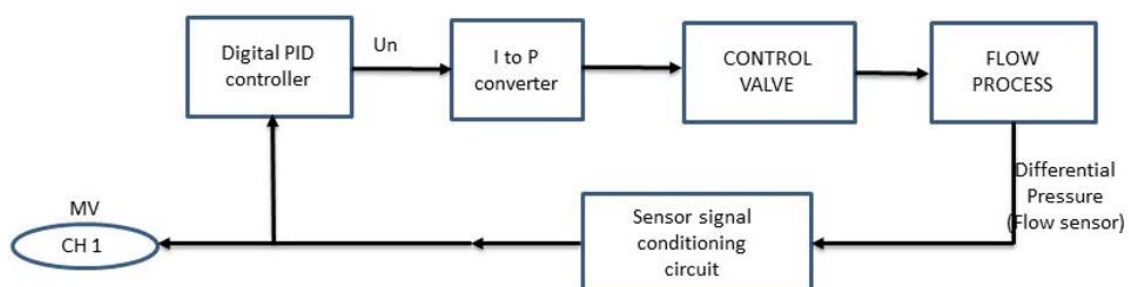


Figure 2. Block diagram of closed loop control of flow control.

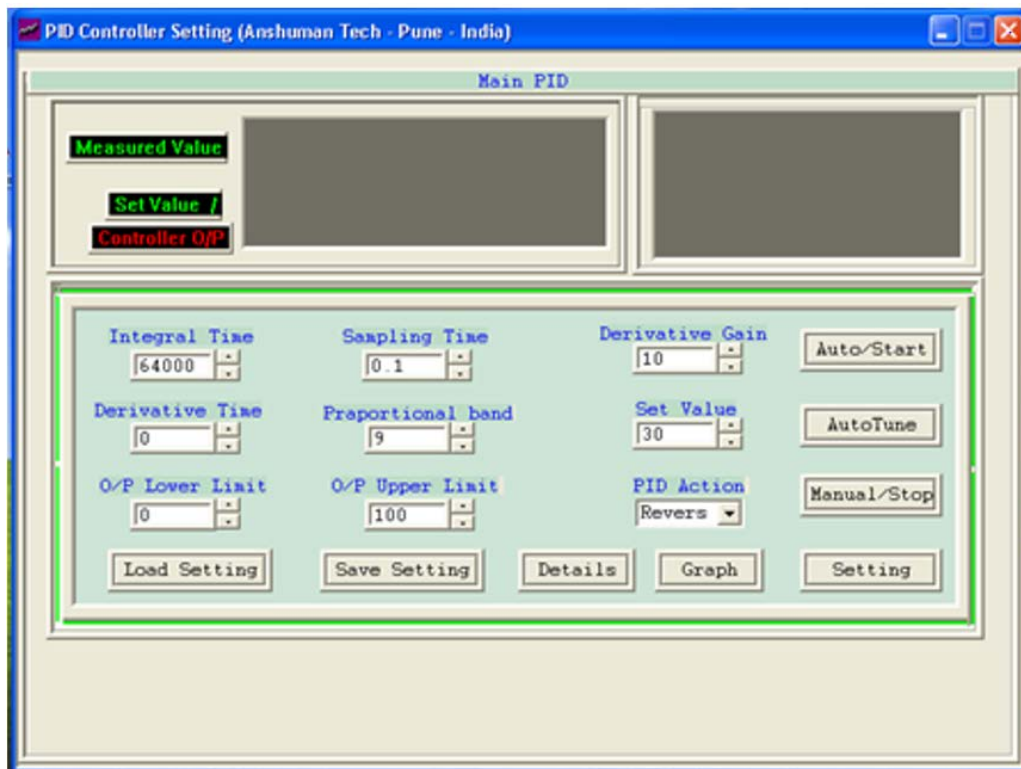


Figure 3. Parameters Set on Main window of PID controller software.

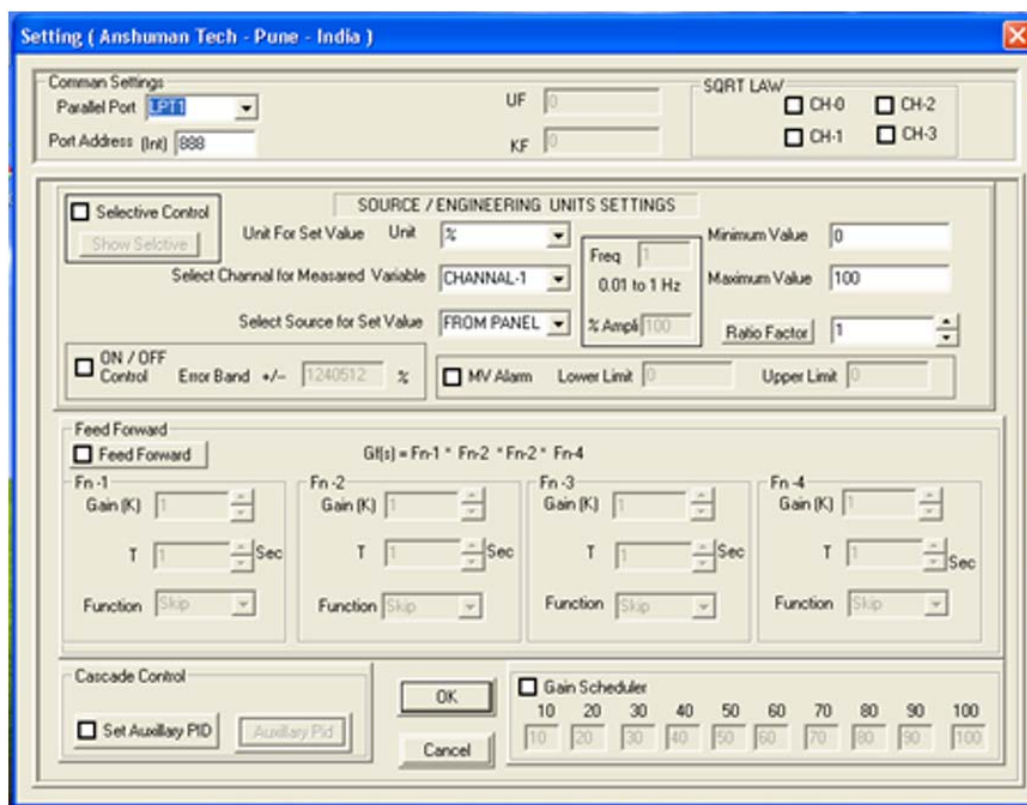


Figure 4. Parameters Set on Setting window of PID controller application.

Wiring Sequence: Pump - L14 on EMT8, Pump - N15 on EMT8, FLOW O/P (14 of Signal conditioning panel) – Computer interface panel (CIP) CH1, CIP 6 – CIP 9, CIP 10 – (+ve) of I to P converter, (-ve) of I to P converter – CIP 20, FLOW O/P (14 of SCP) – (+ve) of DPM, (-ve) of DPM – GND on SCP.

Performance Studies on Step responses of water flow control system

Estimated Ziegler-Nichols parameters of P, PI and PID controllers were employed on physical system through PID controller application and a range of step values starting from 20 % to 50 % were applied to identify the system response. Produced data with a sampling time of 0.1 sec from all the experiments were examined independently for the comparison of variables such as overshoot, decay ration, settling time and offset.

Results & Discussion

To evaluate Ziegler-Nichols tuning parameters of single loop flow control system, experiments were conducted on a closed loop system with P controller by changing proportional band (P_b) gradually from 3 to 11 for a set value of 30 % of flow rate and their responses were plotted as shown in Figures 5 & 6. Response of the system in the wave form were notified at lower P_b values and wave structured response was totally disappeared at $P_b = 11$ as shown in Figure 7. Most of the cases, total number of samples in a cycle were equal but the position of amplitude was shifted to the right, counted 8 samples in the left and 6 on the right as shown in figures 5 & 6. But a constant value of amplitude measured exactly at middle of the cycle was clearly seen with equally distributed samples in case of experiments at proportional band (P_b) of 9 and its corresponding gain was evaluated as $K_{cr} = 100/P_b$. Measured value (MV) verses time (t) was plotted and the period of oscillation (P_{cr}) was calculated as

$$P_{cr} = \text{Number of Samples in a cycle}(N) \times \text{Sampling time}(t_s)$$

$$P_{cr} = 14 \times 0.1 = 1.4 \text{ sec}$$

Other tuning parameters of P, PI and PID controllers were estimated as given by Table 2.

Table 2

Estimated Ziegler-Nichols tuning parameters of P, PI and PID controllers

Controller/Parameter	Proportional Gain (K_p)	Proportional Band (P_b)	Integral Time (T_I)	Derivative Time (T_D)
P	5.55	18	64000	0
PI	4.99	20	1.167	0
PID	6.67	15	0.7	0.175

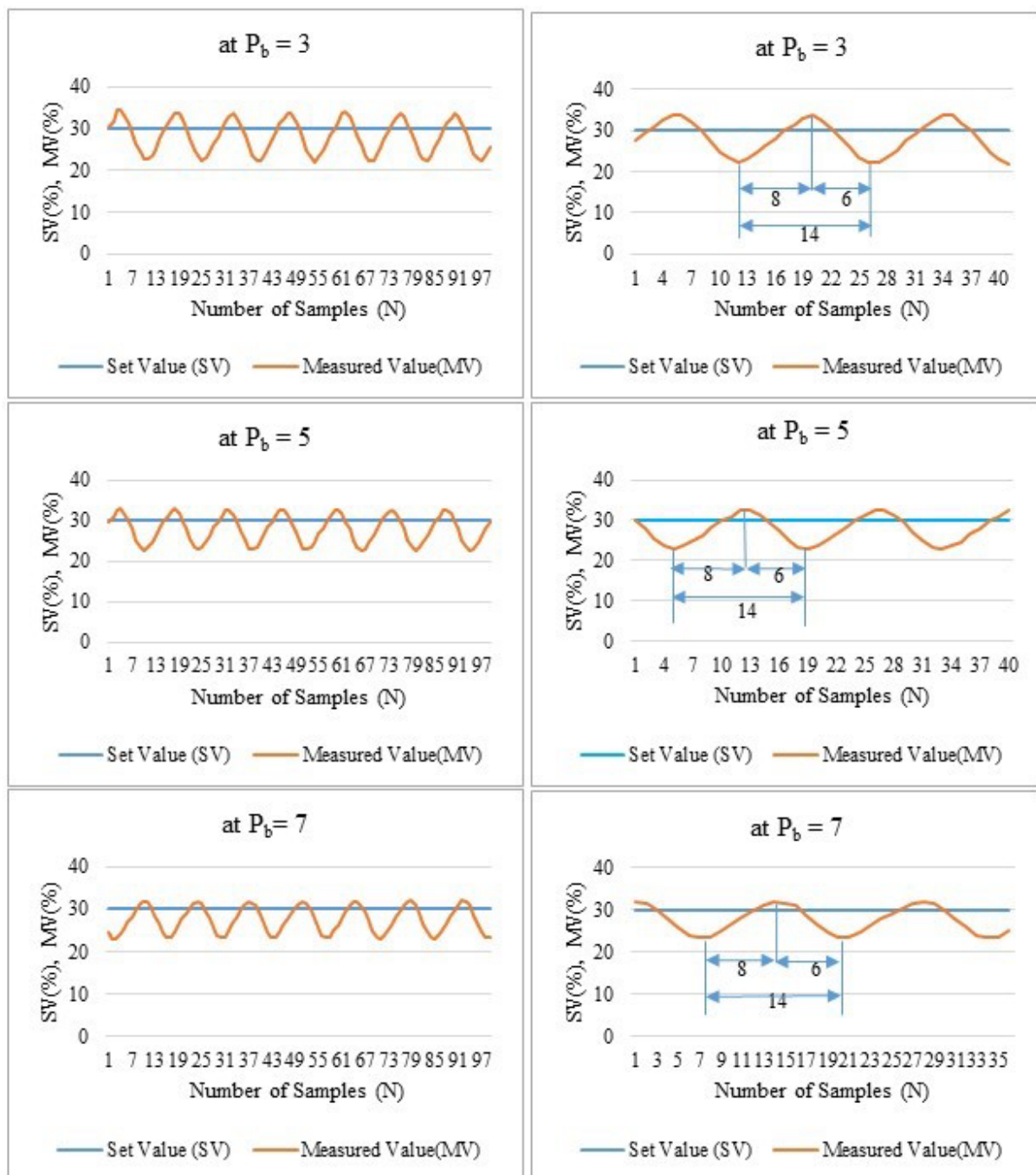
Effect of Tuned Parameters on Step Response of the System

Performance studies on water flow control system at different step shifts, 20 %, 30 %, 40 % and 50 % were conducted with Ziegler-Nichols tuning variables of P, PI and PID controllers and corresponding data was generated with a sampling time of 0.1 sec. It was noticed that there wasn't further change in the output for set values higher than 50 %. In fact, the system could able to attain the maximum flow rates of 40.39 %, 40.78 % and 41.17 % with P, PI and PID control mechanisms respectively for 50 % of set value as shown in Table 3. It was clearly observed that Pi and PID controllers eliminated offset at lower flow rates as set values and the system could able to attain a maximum flow rate of 82.34 LPH though the set values were taken to further higher. Set values (SV) and measured values (MV) were opted as ordinates and time (t) taken as abscissa and their resultant responses were plotted for P (figure 8), PI (figure 9) and PID (figure 10) controllers to analyze the system characteristics.

Table 3

Ultimate flow rates attained by P, PI and PID Controllers for different set values

Set value (SV)	20 %			30 %			40 %			50 %		
Controller	P	PI	PID	P	PI	PID	P	PI	PID	P	PI	PID
Flow rate in % (MV)	18.82	20	20	25.49	29.8	29.8	34.5	39.61	39.61	40.39	40.78	41.17
Flow rate in LPH	37.64	40	40	50.98	59.6	59.6	69	79.22	79.22	80.78	81.56	82.34
Offset	1.18	0	0	4.51	0.2	0.2	5.5	0.39	0.39	9.61	9.22	8.83

**Figure 5.** Response of P controller of water flow system for 30 % of Set Value at different P_b values of 3, 5 and 7.

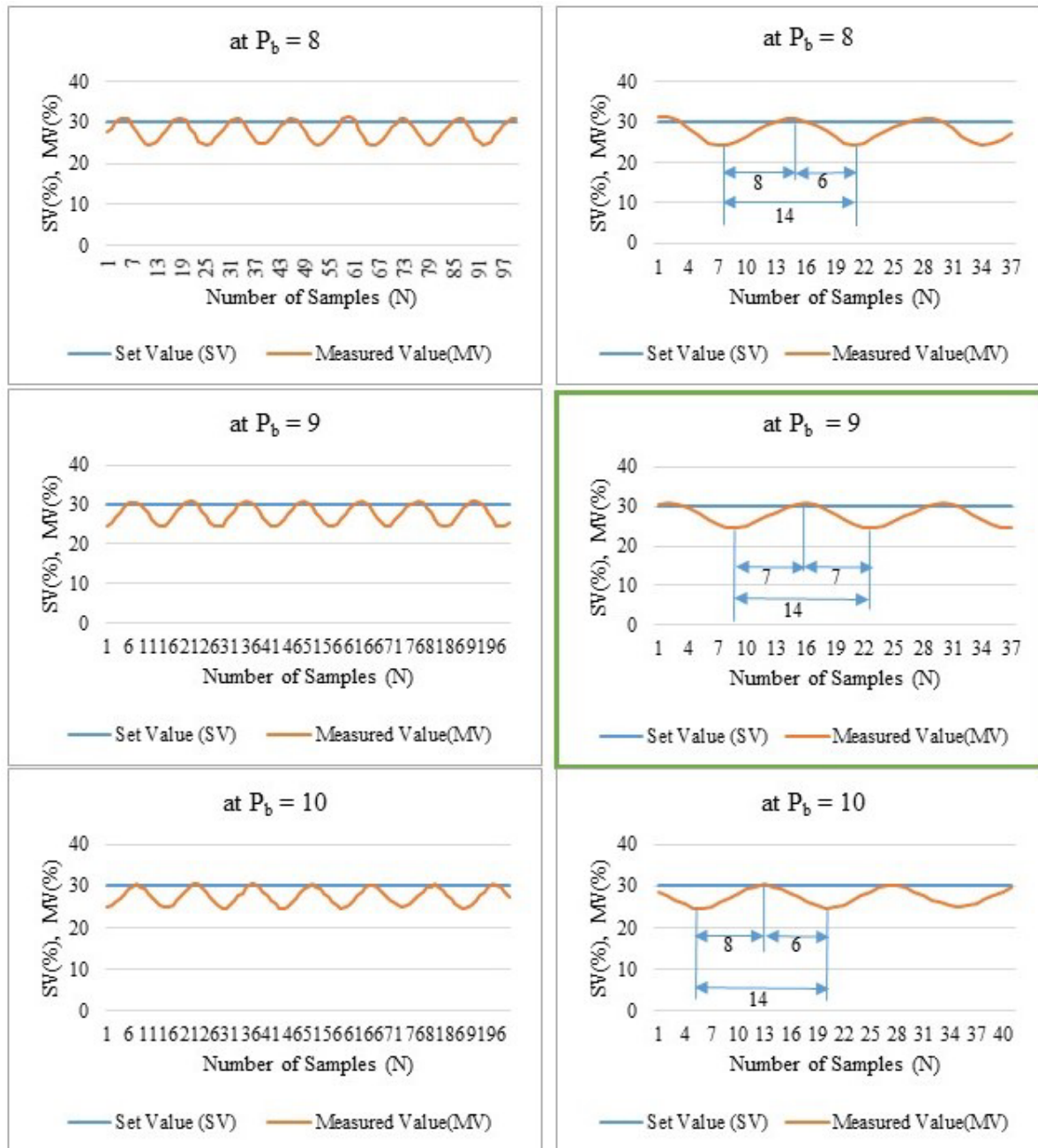


Figure 6. Response of P controller of water flow system for 30 % of Set Value at different P_b values of 8, 9 and 10.



Figure 7. Step response of closed loop control of water flow system for 30 % set value at $P_b = 11$.

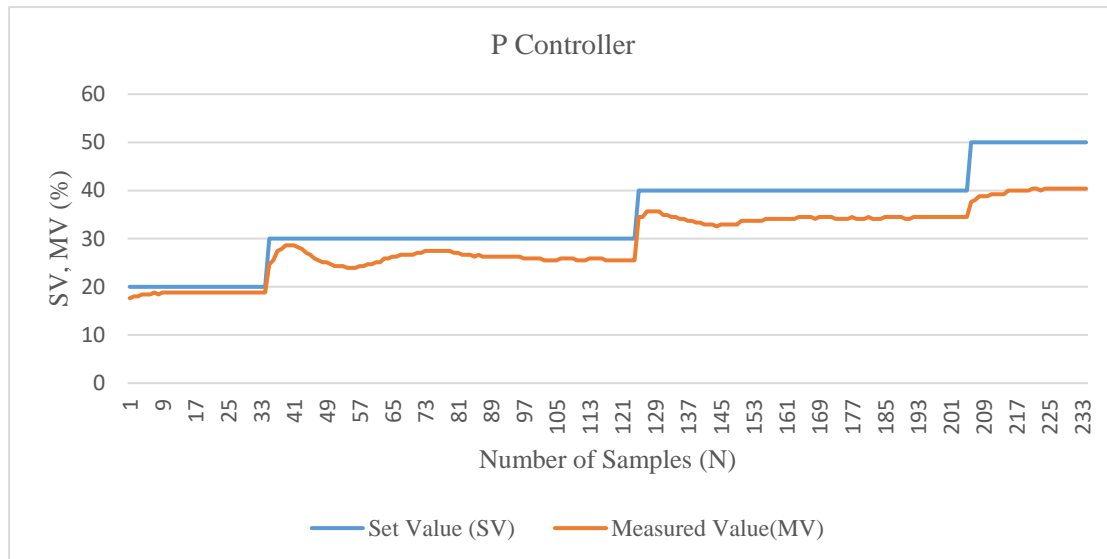


Figure 8. Step responses of water flow control system with P controller.

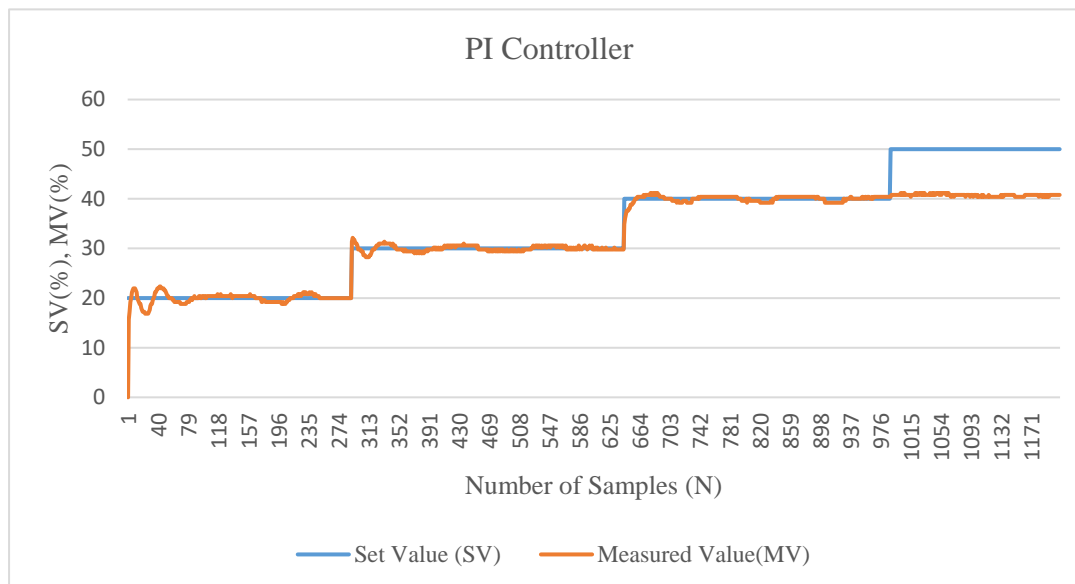


Figure 9. Step responses of water flow control system with PI controller.

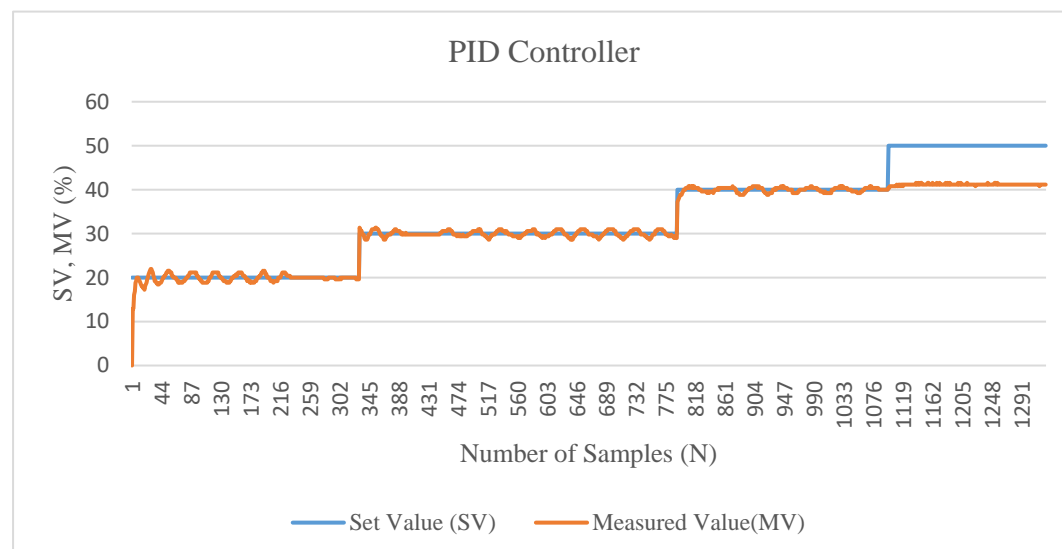


Figure 10. Step responses of water flow control system with PID controller.

Characterization of P, PI and PID controllers of Water flow control system

For different step disturbances, the system response plots were developed to evaluate the characteristic parameters of P, PI and PID control mechanisms. Overshoot, Decay ratio, settling time and Offset values were calculated and the results are furnished in Table 4. When the system facilitated exclusively only P control through setting estimated proportional band value of 18, and applied different step changes, system performed with faster settling times than PI and PID controllers, especially at 20 % and 50 % set values as shown in Figure 11 whereas PI controller of tuned parameters, has recorded with higher settling times than other two modes. In other words, P controller has led to consistent steady state errors which is called as offset.

Table 4

Estimated characteristic parameters of step response of water flow control system with P, PI and PID control mechanisms

Set value (SV)	20 %			30 %			40 %			50 %		
Controller	P	PI	PID	P	PI	PID	P	PI	PID	P	PI	PID
Overshoot	NA	11.75	9.8	NA	3.27	4.57	NA	1.95	1.95	NA	0	0
Decay Ratio	NA	16.6	79.6	NA	59.2	71.5	NA	50	50	NA	0	0
Settling time	9	250	232	83	326	69	68	324	62	18	175	23
Offset	1.18	0	0	4.51	0.2	0.2	5.5	0.39	0.39	9.61	9.22	8.83

With increasing step changes, offset values also increased and recorded higher values for P controllers than PI and PID controllers as depicted in Figure 12. As the purpose of integral action is to provide lower or zero offset value, it was observed that the PI controllers holds zero offset at 20 % step disturbance, and very close to zero at 30 and 40 % step changes but it is high at 50 % step change because the physical design of the specific system was identified as it doesn't support flow rates greater than 41.56 % of its capacity.

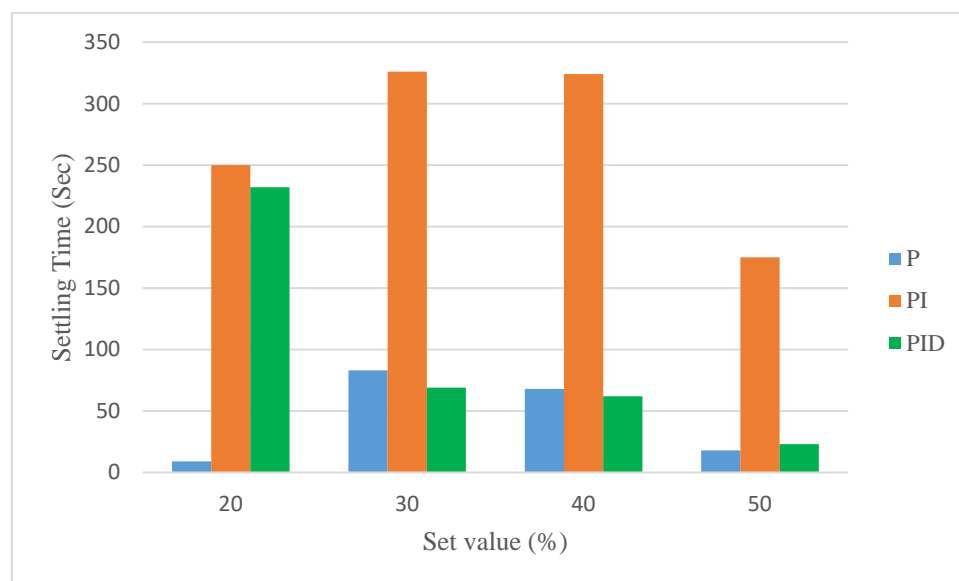


Figure 11. Settling times of P, PI and PID controllers at different set values.

Overshoot is defined as the ratio of amplitude of the peak to the set value and the ratio of two successive amplitudes is known as decay ratio [18, 19]. Overshoot and decay ratios of PI and PID controllers were compared in figures 13 and 14, and notified the values are significant for step changes of 20, 30 and 40 % but not at 50 % as it beyond the range of the system. PI controller has recorded higher overshoots than PID with lower decay ratios. As the integral term integrates or continually sums up error over time even a small error amount of persistent error calculated in the process will aggregate to a considerable amount of over time [20], therefore higher response times were observed for PI Controllers.

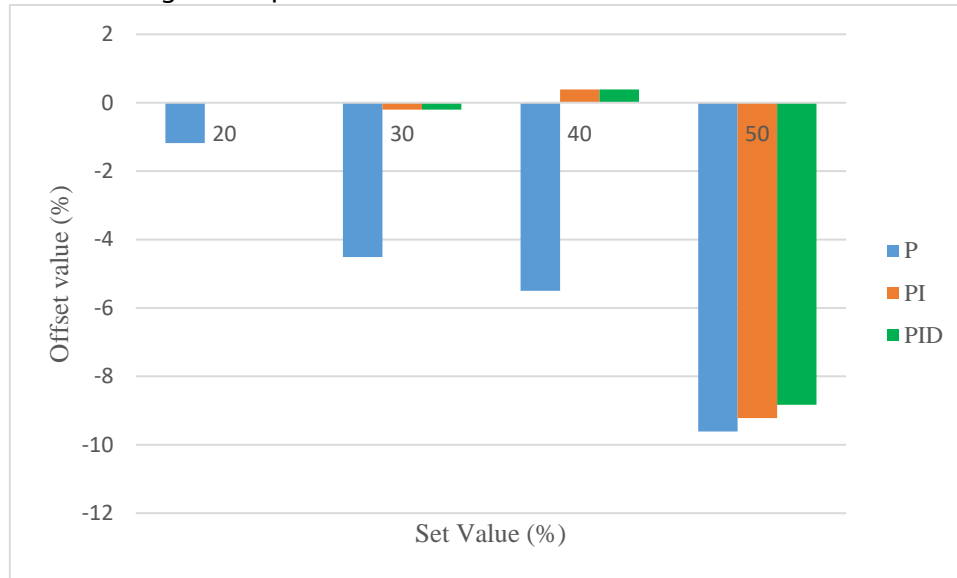


Figure 12. Offset values recorded for P, PI and PID controller at different set values

The configuration of PID control has used full set of tuned parameters, proportional, integral and derivative variables and it exhibited aggressive response with lower overshoot values but it increased chatter on the control output signal. Thus, PID control is preferable for use in steady state processes or processes that either respond slowly or have little-to-no noise [20]. Flow control in general possess low sampling time between 1 - 5 sec [20], therefore because of faster and stable responses, P controller could be a better choice for water flow control if offset to be zero is not a constraint. Else, PI controller would provide zero offset although it consumes longer time to settle with moderate maintenance.

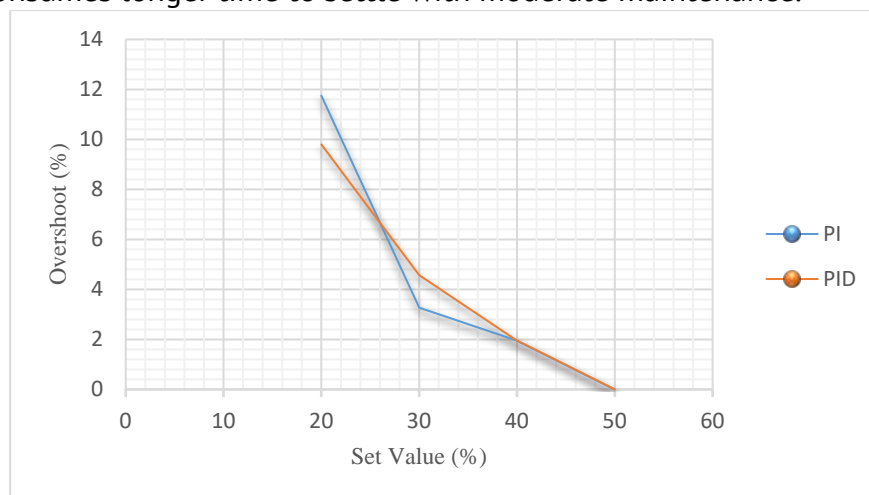


Figure 13. Comparison of overshoot values of PI and PID controllers.

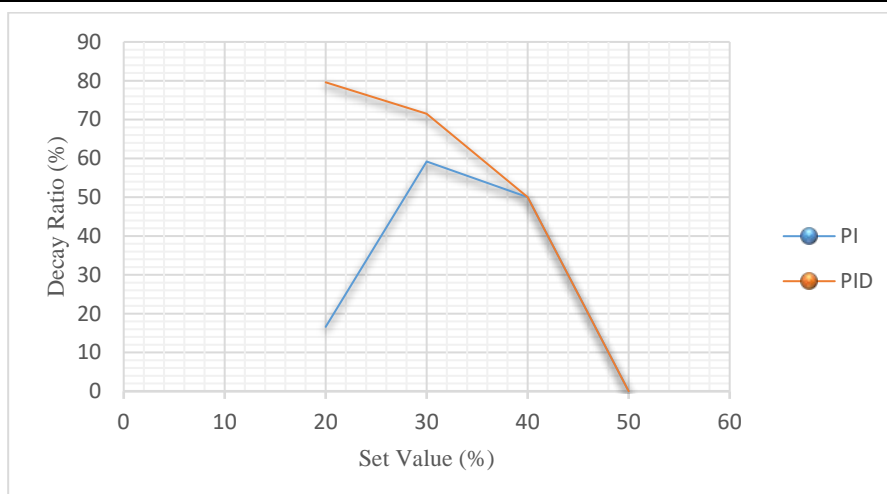


Figure 14. Comparison of decay ratios of PI and PID controllers.

Conclusions

As Eritrea is striving to manage its limited water resources, application of flow controllers to improve water distribution system in the country addressed for the first time in this work. A table top process control trainer (PCT) was tested through proportional (P), integral (I) and derivative (D) control mechanisms. Applying exclusively P control action, critical period of oscillation (P_{cr}) was estimated as 1.4 sec at proportional band value of 9. Tuning parameters of PID controller for water flow control system were evaluated using Closed loop Ziegler-Nichols method. Setting sample time at 0.1 sec, P, PI and PID controller performance studies were conducted with tuned variables on the water flow control system at different step disturbances between 20 – 50 % and their corresponding responses were characterized. P controller exhibited faster responses with consistent increments in offset, PI controller recorded highest overshoot values with negligible offset and prolonged settling times. PID controller showed less overshoot values and faster response times than PI but it increased chatter on the control output signal. The study revealed that the system could attain maximum controlled flow rates of 83.12 LPH (Litre Per Hour) with a set value of 50%, and it retained there for further higher set values. Therefore, the system can be safely controlled between 0-80 LPH. Since flow control systems possess shorter sampling times between 1-5 sec, if the offset is not a major constraint, P controller could be reflected suitable with simple design and minimum expenditure, else PI controller makes offset to zero though it possesses higher settling times. In other words, PID controller is complex using more tuning parameters, need expensive maintenance, and has resulted an intermittent noise in the output signal.

Acknowledgements: Authors would like to express their deepest gratitude to HOD, Department of Chemical Engineering Mr. Abraham Yohannes, for his untiring endeavour in establishing Chemical Engineering laboratories at Mai Nefhi College of Engineering and Technology (MCoET). Authors also want to convey their thankfulness to Dr. Sujana Ramesh for her consistent patronage in proof reading and editing the document. They enhance their thankfulness to Staff of Process Control laboratory, and to all the Faculty and technical staff of the Chemical engineering, MCoET for their persistent support. Authors would like to extend their inmost gratefulness to the Dean of MCoET, Dr. Kahsay Neguse for his diligent effort to encourage earnest research from the college.

References

1. Grace Kam Chun Ding. Wastewater Treatment and Reused -The Future Source of Water Supply. In: *Encyclopedia of Sustainable Technologies*, 2017, vol 4, pp. 43 - 52. <http://dx.doi.org/10.1016/B978-0-12-409548-9.10170-8>
2. A. Ramesh babu, Samsom K., Samuel M. Experimental Studies on Step Response of Water Level Control System with P, PI and PID Control Mechanisms, In: *International Research Journal of Engineering and Technology (IRJET)*, 2020, 10(7), pp. 1504 - 1509.
3. Ranade V.V., Bhandari V.M. Industrial Wastewater Treatment, Recycling and Reuse. Amsterdam: Elsevier Ltd, 1st ed, 2014.
4. UNESCO, 2015. The United Nations World Water Development Report: water for a sustainable world. United Nations Educational, Science and Cultural Organization, France.
5. UNICEF, WASH/FN/27/2019 Prioritizing Climate Resilience, Sustainability and Equity: OneWASH Programming in Eritrea. In: *UNICEF's WASH field note*. Available online https://www.researchgate.net/profile/David-Tsetse/publication/338710232_Prioritizing_Climate_Resilience_Sustainability_and_Equity_-_One_WASH_programming_in_Eritrea/links/5e2653d692851c89c9b5a584/Prioritizing-Climate-Resilience-Sustainability-and-Equity-One-WASH-programming-in-Eritrea.pdf
6. Technology Zones. How Important is Flow Control in Hazardous Environments, In: Fluid Control Ltd articles, 2019. Available at the following weblink. <https://fluidhandlingpro.com/how-important-is-flow-control-in-hazardous-environments/#:~:text=Flow%20controllers%20are%20designed%20to,they%20are%20being%20used%20in.>
7. Fujikin Corp Group, Flow Control Systems, Catalogue No.712-01E-H, 2013.
8. Mohammad S., Alireza Z. Comparison of PID Controller Tuning Methods, In: Computer Science, 2012. Online Source to access http://ie.itcr.ac.cr/einteriano/control/clase/Zomorodi_Shahrokhi_PID_Tunning_Comparisn.pdf
9. Thomas E. Marlin. Process Control-Design processes and Control systems for Dynamic response, New York: McGraw Hill, Inc. 2nd ed, 2000.
10. P.Sathishkumar, N. Selvaganesan. Tuning of Complex Coefficient PI/PD/PID controllers for a universal plant structure, In: *International Jurnal of Control*, 2020, <https://doi.org/10.1080/00207179.2020.1755726>
11. Philip R. Page., Enrico Creaco. Comparison of Flow Dependent Controllers for Remote Real-Time Pressure control in Water Distribution System with Stochastic Consumption, In: *Water*, MDPI, 2019, 11, pp. 422 doi:10.3390/w11030422
12. Sina R., Cristobal V.J., Raheleh J., Alexander G. Flow Control of Fluid in Pipelines Using PID controller, In: *IEEE Access*, 2019, 7, pp. 25673 - 25680. DOI 10.1109/ACCESS.2019.2897992
13. Hakki U.U., Altug. I. Performance and Robustness of Flow Controllers Designed Using Non-Casual Uncertainty Blocks, In: *Asian Journal of Control*, Wiley Online Library, 2013, 15(1), pp. 214 - 224. doi: 10.1002/asjc.488
14. Jietae Lee. On-line PID controller tuning from a single, closed-loop test, In: *AIChE Journal*, 1989, 35(2), pp.329 <https://doi.org/10.1002/aic.690350221>
15. Matrix Global Private Limited. User's Guide of Process Control Trainer (PCT), Noida: *Matrix Global Pvt.Ltd., version 1.5*, 2009.
16. Robert Ziff. Chemical Process Dynamics and Control, Book-I, In: University of Michigan, 2007, pp. 693 - 694
17. Stephanopolous G. Chemical Process Control, New Jersey: Prentice-Hall Inc., 1984, pp. 352 - 354
18. Donald.R. Coughanowr. Process Systems Analysis and Control, New York: McGraw Hill Publications, 2nd ed, 1991, pp. 96 - 98
19. D.E.Seborg, T.F.Edgar,D.A. Mellichampt. Process Dynamics and Control, New Jersey: John Wiley & Sons Inc., 2004, 2nd Ed.
20. Robert.C.Rice. PID Tuning Guide-Yokogawa,Control station Inc., 2010, pp. 20 - 23. https://web-material3.yokogawa.com/Yokogawa_PID_Tuning_Guide_-_csTuner.pdf

[https://doi.org/10.52326/jes.utm.2021.28\(3\).12](https://doi.org/10.52326/jes.utm.2021.28(3).12)
CZU 663.1:[637.146+663.81]



MICROENCAPSULATION OF FUNCTIONAL COMPONENTS IN THE FOOD TECHNOLOGY: PARTIALLY OPTIMISTIC VIEW

Alexei Baerle*, ORCID ID: 0000-0001-6392-9579

Technical University of Moldova, 168 Stefan cel Mare Blvd., MD-2004,
Chişinău, Republic of Moldova

*Corresponding author: Alexei Baerle, alexei.baerle@chim.utm.md

Received: 07. 03. 2021

Accepted: 08. 16. 2021

Abstract. This work deals with the use of microencapsulation of biologically active compounds (BAC) as an alternative method of protection and prolongation of their functional properties in the food products. The main methods for the formation of microcapsules (MC) are considered. Biopolymer materials, suitable for MCs production, are outlined. Some technological solutions, suitable for microencapsulation and successfully used in other industries, present interest only for laboratory researches in the food science, but are not suitable for industrial scale food production. It is discussed why the methods of simple and complex coacervation, liposomal entrapment are thermodynamically advantageous for obtaining microcapsules in comparison with others. To achieve further progresses of microencapsulation in food technologies, the direct integration of the microencapsulation into the food production technological cycle is necessary. Products should initially have a texture and consistency that allow microcapsules to be resistant to premature aggregation. MCs should not exfoliate or break down, while execute their functions of protection and targeted delivery of biologically active compounds. Only high viscous colloidal systems, as traditional fermented dairy products (kefir, yoghurts, ice cream, curd and cheese) and fruit juices with pulp, are mostly suitable for supplementation of them by BACs using microencapsulation.

Keywords: *biopolymers, biologically active compounds (BAC), coacervation, complex coacervation, fermented dairy products, microencapsulation's thermodynamic.*

Protection of biological activity: necessity of alternative “SMART” methodology

Over the past decades, there have been fundamental changes in the field of nutritional science and in the way quality food is produced. The scientific concepts of optimal nutrition, based on functional foods of a new generation, have been developed in response to the consumers' needs of the foods with functional properties. These trends should have forced manufacturers to develop new technologies for the functional foods production [1]. The modern concept of nutrition suggests that in addition to nutritional and energy value, functional food products must have their own biological activity. It was found that the consumption of foods containing biologically active substances, promotes and really affects the maintenance of consumer's health, prevents the occurrence of various diseases [2].

However, until now, the food industry produces mainly traditional food products, which correspond in their properties to the traditional concept of a balanced diet. Despite the constant growth in food production in general, the share of functional food products is still relatively small. It seems that manufacturers are not ready to introduce functional ingredients into food, because they generate additional legal, technological, and economic problems. Functional ingredients or Biologically Active Compounds, BAC, interact with the main “stable” components of food (proteins, fats, carbohydrates and bio-metals). In traditional food cultures, the biological activity and functionality of nutrition is achieved using various fermented, mainly dairy products [3]. Unfortunately, these products have short shelf-life. It also seems at least absurd from the point of view of common sense to actively use synthetic antioxidants in order to protect the functional properties of biologically active substances introduced into the product. In order to run away from this (techno)logical error, attempts are being made to reduce the total quantity of the antioxidants used to protect the biological activity of various food components, at least, using effects of their synergistic interaction [4, 5].

One of the relatively new methods of stabilizing biologically active substances in food is their isolation from contact with other active food components by means of microencapsulation. Microencapsulation is a directed process of forming a thin, sufficiently strong, low-permeability shell with desired properties around small solid particles or their aggregates (granules), or around the liquid droplets of microencapsulated agent. The main goals of the microencapsulation are the reversible isolation of the biologically active content, its targeted delivery and controlled release. Thus, the main role of the microcapsules inclusion in the food products composition is to exclude direct contact of biologically active food components with the main composition, that is, with an aggressive environment for biologically active substances. Various high-molecular compounds are used as a building material for the shells of microcapsules. As part of a microcapsule, it is called a membrane, shell, carrier material, wall material, external phase, or matrix. The shell of the microcapsule separating the biologically active substance from the corrosive environment of the food product should be stable in the composition of the food product, but easily release its biologically active content when it enters the human gastrointestinal tract [6].

High-tech solutions as microencapsulation: why a food manufacturing is an exception?

Over the 70 years passed since the introduction of the term of “microencapsulation” into scientific circulation. Thousands of research papers with excellent experimental results, many thematic reviews and books have emphasized the potential of this method for creating functional food products [7 - 10]. However, a much larger number of works and patents are devoted to the microencapsulation of drugs, cosmetic components, and even ingredients that improve the functional properties of forages.

Why the microencapsulation, a smart technology for the engineering of products with desired properties, finds its place with great difficulty in modern food technology? There are enough reasons for this “paradox”:

✓ The principle “The benefits of medicines outweigh the risks of treatment” opens the way for the use of a wide variety of modified or synthetic materials in the manufacture of medicines, inclusive using microencapsulation [11]. This trend is indirectly reflected in many experimental studies and analytical reviews [12 - 14]. However, this principle is completely

inapplicable to food products of daily consumption, which should be tasty and absolutely safe without any amendments, involved by the probability theory;

✓ At the legislative and consumers level, there are much higher quality and safety requirements for food than for cosmetic products and, of course, for animal feed. At the same time, there are practically no “aesthetic” requirements for the appearance, texture and taste of veterinary drugs and feeds [15];

✓ Also, there are less restrictions on the addition of synthetic polymers, crosslinking or surface-active agents, good for the production of microcapsules for cosmetics, veterinary medicine and in animal nutrition. Majority of these chemical agents cannot be used in food manufacturing;

✓ A significant increase in the price of the final product caused by microencapsulation will hardly be accepted by the food industry with high risks and relatively low incomes, also will be hardly tolerated by the mass consumers [7];

✓ Food industry is generally characterized by high inertia of the and its adherence to traditions, which is supported by consumer mistrust not only for new food products, but to manufacturers and new technologies [16].

The combination of all mentioned factors leads to the fact that microencapsulation of functional food ingredients is perhaps the area of microencapsulation, which is most difficult for development (Figure 1).

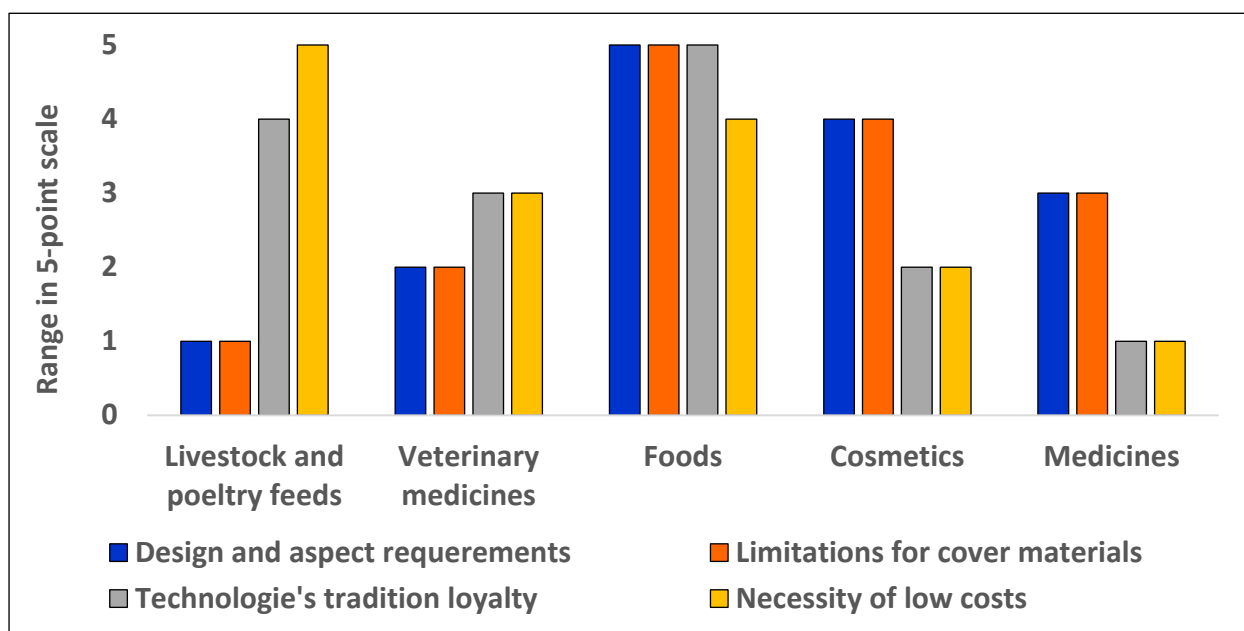


Figure 1. The uphill road: why is so difficult to incorporate microencapsulation into food technology?

Expectations regarding the MCs properties and benefits of are quite high and ambitious:

- They must immobilize the active substance during technological processes of food manufacturing by changing its state of aggregation, for example, converting liquids into a solid free-flowing form.
- They must prevent the degradation of biologically active substances as a result of interaction with the active components of the food product and oxygen, increase their stability during processing and in the final food product.

- They should improve the safety of production, reduce odor and reduce the loss of volatile substances, flavors, mixtures containing volatile components.
- They should create the desired visual and texture effects, but not to create unwanted ones;
- Should regulate the properties of active ingredients: particle size, fat solubility or water solubility, mask their undesirable taste; change color;
- Should provide controlled release of the contents under specified conditions, including by regulating the permeability of the shell.

From the requirements and features, mentioned above, the super-goal of microencapsulation of food functional ingredients becomes clear:

Encapsulated food ingredients must not to add significantly values to the food costs - this way is not expected by consumers. The technologies used must ensure compliance with the requirements regarding the functional properties and food safety of microcapsules, their assimilation by the human organism, while not impairing the sensorial properties (taste, aspect and odour) of the product.

This overarching super-task is difficult to solve because its parts contradict each other. It is possible to create a science-intensive high-tech product only with resorting to a multilateral and multidisciplinary systematic approach. The solution of the microencapsulation tasks which are associated with the prevention of biologically active compounds degradation in food can be achieved through a targeted combination of scientific researches with ingeniously engineering innovations. But some of the ways which at first seems like breakthrough solutions are doomed to failure, because of “unfortunate” combination of different factors, given below.

Structure and functional properties of microcapsules

In function of particles diameter, the nano-capsules ($1\mu\text{m} > d < 1000\text{nm}$) and microcapsules ($1...1000\mu\text{m}$) are mentioned in majority of references. Some of them, however, indicate that the size of microcapsules can reach up to 3-8 millimeters in diameter [17 - 19].



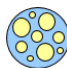





It should be emphasized that if the capsules are larger than 1 mm ($1000\mu\text{m}$), they can no longer be considered “micro”, even if they are obtained by microencapsulation methods. And it's not just because of the non-corresponding to formal size: the dimensions of capsules larger than 1mm are not “negligible” in any way, significantly affecting the texture and sensory perception of any food product.

There are two main types of microcapsules: reservoir-type, **R**, and matrix-type, **M**. Reservoir-type microcapsules contain an external cover, surrounding the entire encapsulated content, in different sources named as “shell”, “wall” or “membrane”. Capsules of this type are also called “single-core”, “mono-core” or “core-wall”. The external cover of such microcapsules can be destroyed by the application of external physical, mechanical, or chemical action, leading to the release of the contents.

In the matrix type microcapsules, microencapsulated content is distributed over the carrier material, in the form of small particles or droplets, and represent discontinuous phase - suspension or emulsion of active compound in the carrier material. In the case of matrix type MCs and in the contrast to MCs of the reservoir type, the encapsulated active compound can be present on the surface of microcapsules if they do not have an additional “reservoir” coating.

Table 1

The main types of nano- and microcapsules

Particles	Type	Definition	Scheme	Refer.
Biopolymer-based				
Micro- and nanoparticles	R	Particles containing solid cores are covered with other solid materials with protective properties		12,13, 20,21
Micro- and nanocapsules	R	Spherical particles containing a liquid core and a solid or gel-like elastic cover		23,23
Multicore microcapsules	M	Liquid droplets are distributed in a polymer matrix representing three-dimensional baffles net		24,25
Porous and gel-like matrix	M	Porous solid particles or gels, fulfilled with active compounds		26
Lipid- and Surfactant-based nano- and microparticles*				
Liposomes	M	Single-layer or multilayer phospholipid membranes with hydrophilic content		13,27
Phytosomes	R	Active compounds are chemically bonded with polar phospholipid parts, covered with non-polar		28,29
Niosomes	R	Particles with hydrophilic core, covered with non-ionic surfactants and lipids		30
Colloidosomes	R	Particles formed by hydrophilic core and by shell from solid nanoparticles (colloidal shell)		31,32

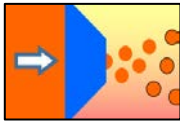
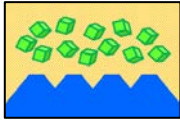
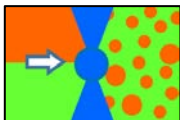
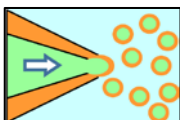
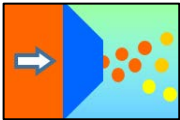
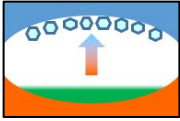
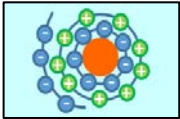
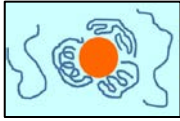
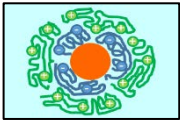
A very detailed graphical analysis of the different types of lipid-based particles construction can be found in a recently published reviews [12, 13, 33]. Mixed type, reservoir-matrix, **RM** microparticles also exist; for example, polynuclear matrices, additionally wrapped in a continuous shell [24]. Such group as “multiwall microcapsules” are also mentioned [25]. Conventionally, in this group it should be attributed liposomes and phytosomes, and “classical” MCs, with the shells obtained from charged biopolymers using Layer-by-Layer (Table 2). Sometimes **dendrimers** and **micelles** are mentioned as a nano-particles [13]. But these *de facto* high-molecular structures don't contain any clear boundary between two phases. Therefore, such monophasic colloidal formations are not be considered nano-capsules in unambiguous mode.

Common encapsulation methods

Microencapsulation of biologically active compounds in order to protect their biological activity is possibly using various technological solutions, more or less universal for various industries (Table 2). Emulsification is not strictly an independent method of microencapsulation. However, obtaining a stable BAC emulsion is the most important stage in preparation for Layer-by-Layer, (Simple) Coacervation or Complex Coacervation, both assisted or not by cross-linking.

Table 2

Microcapsule structure formation: basic methods

Briefly describing of nano- and microencapsulation method	Graph	Refer.
Spray Drying (SD). A mixture containing BAS, biopolymers and surfactants is spraying in a hot chamber. A thin film is formed on the droplets surface because of evaporation of solvent.		17, 34 - 36
Fluidized Bed Coating (FB). The finely dispersed solid covered with a film former by spraying, is "liquefied" with a stream of air. Surface film formation occurs as a result of solvent evaporation.		37, 38
Emulsification (EM). Relatively stable emulsions are obtained using high-speed homogenizers and surfactants. To obtain monodisperse emulsions, their fractionation is necessary, which is not easy.		26, 39 - 43
Extrusion (EX). A continuous process in which molten components are dosed by pushing through an extrusion die, after which the mixture solidifies, sometimes the product is portioned after solidification.		44, 45
Spray Cooling (SC). Liquid systems containing thermic unstable BAS or cell cultures are sprayed by injector in a chilled chamber, which leads to their solidification in the form of small particles.		24, 36, 46
Freeze-Drying (FD) = Lyophilization, Sublimation. Removal of water by freezing and sublimation to obtain a highly porous dispersed structure. Large amounts of cryoprotectants sometimes required.		18, 47
Layer-by-Layer (LL). Sequentially covering of emulsion drops or solid particles by several layers of oppositely charged polyelectrolytes: pectins and polyuronic acid salts, (-); proteins, chitosan (+), etc.		20, 48
(Simple) Coacervation (C). Spontaneous or induced condensation of a biopolymer or several biopolymers from a solution as a new solid phase on the surfaces of encapsulated material droplets.		49
Complex Coacervation (CC) – formation of a two-phase shell by electrostatic forces, H-bonds or cross-linking between two different polymers, rather induced in stringent conditions, than spontaneous		41, 50, 51

Complex coacervation should not be confused with the layer-by-layer method: in CC two thick layers, presenting different phases are formed, but in LL – several pairs (3 - 7) of thin layers, but which form only one common phase. It's also not Layer-by-Layer, when one or both phases in Complex Coacervation, are formed by oppositely charged polyelectrolytes [49, 52]. Finally, it is no coacervation, if shell is formed from different initially solid materials [53].

Some methods, as electro-spray assisted extrusion [54, 55], represent a way to control microcapsules' size and to obtain monodisperse *samples*, but application of such method in food-industrial scale should be very expensive.

Common edible biopolymeric materials for mc membranes (walls, shells) construction

The shells of microcapsules used in the food industry must be edible and safe for humans. The shell material and other accompanying components of microcapsules should not disintegrate with the formation of harmful metabolites. They should create a barrier between the active content of microcapsules and an aggressive external environment, thus preventing premature degradation of biologically active substances and the formation of derivatives without functional value. Ideally, the membranes themselves can have their own biological activity [56, 57].

These sometimes-conflicting requirements significantly reduce the variety of materials that can be used to obtain edible microcapsule shells. In order to form microcapsules, cover materials based on various natural and modified biopolymers are used (Table 3).

Table 3

Edible natural biopolymers as covering materials for microencapsulation

Biopolimer	Code	Natural source	BP Peculiarities	References
Polysaccharides				
Dextran		Glucose, <i>Lactobacillus</i>	branched	14,58-60
Dextrin ²	E1400	Starch (potato, corn, rise)	short-chain	61
Cyclodextrin ^{3,4}	E459	Starch (potato, corn, rise)	cyclic with 4-10 rings	62
Arabic gum	E414	Several species of <i>Acacia</i>	contain glycoproteins	35,63,64
Xanthan gum	E415	<i>Xanthomonas Campestris</i> ³	branched polyglucans	52,65,66 ⁵
Chitosan		Chitin (<i>Crustacea</i> , <i>Fungi</i>) ⁶	polycation at pH < 7	43,50,67
Mucilage		<i>Salvia Hispanica</i> ; <i>Linum</i> ⁷	2D, very wet-retaining	65,68
Alginates	E401	<i>Laminaria Japonica</i>	Polyanion at pH > 5	22,53,69
Carrageenan		<i>Rhodophyta</i>	Polyanion at pH > 3	59,70
Proteins				
Gelatin	E441	Livestock's and fish skin	Triple-helix amphoteric	23,41,50
Lactoproteins		Milk; whey powder	Caseinates, globulins	36,71
Legume protein		<i>Glucine Max</i>	Globulin	72
Modified Polysaccharides				
Hypromellose	E464	linear, esterified with 1-metilpropane-1,2-diol		38,61
OSA Starches	E1450	esterified by octenyl succinate, 2D, 3D-structured		73,74

² Thermically hydrolysis, or enzymatically

³ Enzymatic conversion of glucose

⁴ Not in the list of starches, being one of them

⁵ Diacylated

⁶ Chemical treatment

⁷ Our preliminary results

It should be noted that although dextrin (E1400) and cyclodextrin (E459) are modified starch derivatives, in Table 3 they are classified as natural, since they can be obtained from starch by hydrolysis or microbiological method [75, 76].

Exotically biopolymers, also common proteins and carbohydrates, actively interact with biologically active compounds [72]. Therefore, the kinetic incompatibility of the microencapsulated ingredient with the microcapsule shell is not at all excluded. Such incompatibility should not appear either immediately or during the microcapsules use in the foods. Incompatibility may be expressed either by the interaction with the shell content, or by gradual unwanted diffusion of the ingredient from the shell. Another possible reason for incompatibility may be the diffusion of destructive agents, for example, oxygen or catalytic enzymes, through the shell into the inner cavity of the microcapsule.

Table 4

Application areas for microencapsulated food ingredients

Class: Examples	Methods	Expected microencapsulation results	Ref.
Minerals: Ca^{2+} , Mg^{2+} , Fe^{2+} or salts of Fe^{3+} , Zn^{2+}	SD, FB	Isolation of bio-metals (or minerals) in order to reduce vitamins' degradation	77,78
Acidity Regulators / Agents: Weak acids and bases	SD, FB	Delivery to the intestine, bypassing the receptors in the oral cavity (taste masking)	79
Aroma: Oils, oil extracts, aromatic resins.	EX, SD	Solid powders which are activated during cooking or in the mouth cavity	19,58, 62
Sweet Taste Agents: Natural sugars, artificial sweeteners	FB, SD	Reducing hygroscopicity, improving distribution, prolonging taste	80,81
Food Dyes: Carotenoids, anthocyanins	CC, EX	Dosage, uniform distribution, protection over oxidation during storage.	10,67
Lipids: PUFA ω_3 - ω_6 , fish oil, phospholipids, lecithin	SD, EM, LE ⁸	Prevention of redox destruction during storage, undesirable taste masking (fish oil)	40-42, 82
Vitamines: liposoluble A, D, E, hydrosoluble (B, C...)	LE,	Control of release time, exclusion of contact with the food matrix	71,72
Polyphenols	SD, LL	Prevention of redox destruction during storage, undesirable taste masking	30,58, 59,83
Antibodies, Enzymes IgY, amilase	CC, LL	Stabilization in food matrix, targeted delivery to the intestine, release control	76,84
Microorganisms and cells Bacteria, Fungi, Cyanophyta	C, SA ⁹	Isolation from food environment, targeted delivery, controlled release	33,46,60,67 ,78

⁸ Liposome Entrapment – a promising nanoencapsulation method, based on the formation of liposomes (phospholipidic spheres) and the capture of polar and non-polar substances by them

⁹ Self-assembly - a group of methods, characterized by relatively low enthalpy and entropy of MCs production

Contradictory influence of the sample's geometry on mcs properties and stability

The process of microencapsulation of liquid oils can be defined as the coating of an O/W emulsion droplets with a layer or several layers of a shell-forming material. It is generally

known that the aggregate stability of colloidal systems increases with a decrease of particle size. However, no less important for the stability of the colloidal system is its polydispersity, that is, the profile characterizing the presence of particles of different diameters.

Microcapsules obtained from emulsions by any of the known methods will inherit the emulsions polydispersity.

The effect of polydispersity on the rheological properties of emulsions and, respectively, microcapsules, is ambiguous and contradictory, and, moreover, is closely related to the values of many other factors, one of which is the concentration of particles of the dispersed phase. The most chaotic and unpredictable seems to be a polydisperse emulsions, those that are formed during direct dispersion. Monodisperse emulsions and suspensions of microcapsules should have much lower entropy. At the same time, the geometry of a concentrated monodisperse system resembles a foam, and the process of adhesion of microcapsules, in turn, should repeat the mechanism of foam destruction [85]. Finally, concentrated mono- and bi-dispersed emulsions are most prone to coalescence (Figure 5).

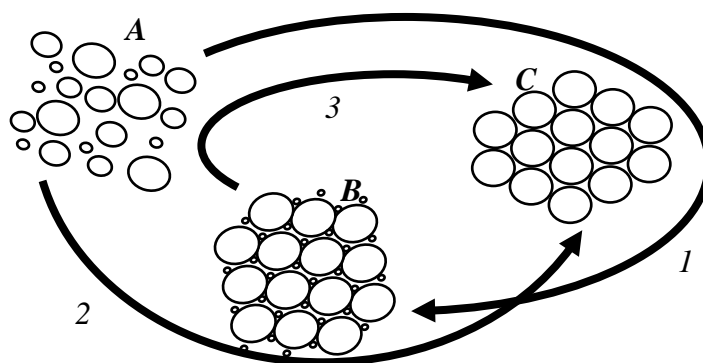


Figure 5. Effect of dispersion on the characteristics of emulsions and microcapsules:

- A – diluted polydisperse emulsion; B – concentrate bi disperse emulsion;
- C – concentrate monodisperse emulsion. Arrows show growth of the: 1 – density;
- 2 – structural organisation (negentropy); 3 – anti-coalescence stability.

How to form stable mcs shell?

The formation and strengthening of the shell around the microencapsulated substance occurs according to the thermomechanical, physicochemical and mixed mechanisms. Strengthening of the microcapsule shell is achieved in various ways:

Shell thickness increasing is not possible anytime, but if it is possible, leads to an overconsumption of the encapsulating agent or requires an increase in the number of microencapsulation cycles in the case of the LL process.

Increasing the MC-shell strength by removing of water excess from it. Coacervate shells of lipid-containing microcapsules can be viewed as a water-based gel that forms on the surface of a lipid droplet [31]. Various compounds can lead to syneresis of the coacervate layer. Necessity of a desiccant use to strengthen coacervate shells is fraught with the fact that the desiccant will perform its function only as long as it is part of the shell itself. Most widely used desiccant sodium sulfate - allowed food additive (E514), which has its own bitter taste.

To achieve the edibility of the coacervate casing (and of MC as a whole), the desiccant must be partially or completely removed. Relative rarely used (due to information from accessible sources) dialysis and electrodialysis can serve as one of the promising methods of removing a desiccant excess from the microcapsules [86]. Though, any attempts to

completely remove the desiccant from pure-Gelatin simple coacervation shells lead to shells destabilization and release of active content [69].

Cross-linking. Cross-linking is the strengthening of MCs polymeric membranes at the molecular level by means of bi- or polyfunctional agents. There are physical (ionic) and chemical cross-linking. Ionic cross-linking involves the interaction of polymer ions with oppositely-charged polyions. The allowed food additives tripolyphosphates (E451) and citrates (E331) can be used as polyanions. Such a mechanism may seem similar to Layer-by-Layer, but this is not entirely true. In the LL technique, several oppositely charged layers of biopolymers or more or less the same thickness are successively applied [20]. The cross-linking technique involves a one-time creation of a consistent shell, which is then exposed to a binding agent. Effective results can be achieved by a combination of ionic cross-linking and the addition of agents that promote the formation of intermolecular hydrogen bonds [57]. Chemical cross-linking involves the covalent binding of linear biopolymer molecules and the formation of a three-dimensional net structure. For proteins, in particular, gelatin, this method is the binding of glutamine and lysine by amide “bridges” under the action of the enzyme trans-glutaminase [40]. Various types of cross-linking, i.e. ionic and covalent, if they are used separately, all other conditions being equal in similar systems, do not significantly affect the shell thickness and the microcapsules size. However, in the case of a combination of ionic and chemical crosslinking, microcapsules may become more unstable in presence of an excess of ionic crosslinking agent, for example, Na-TPP [87].

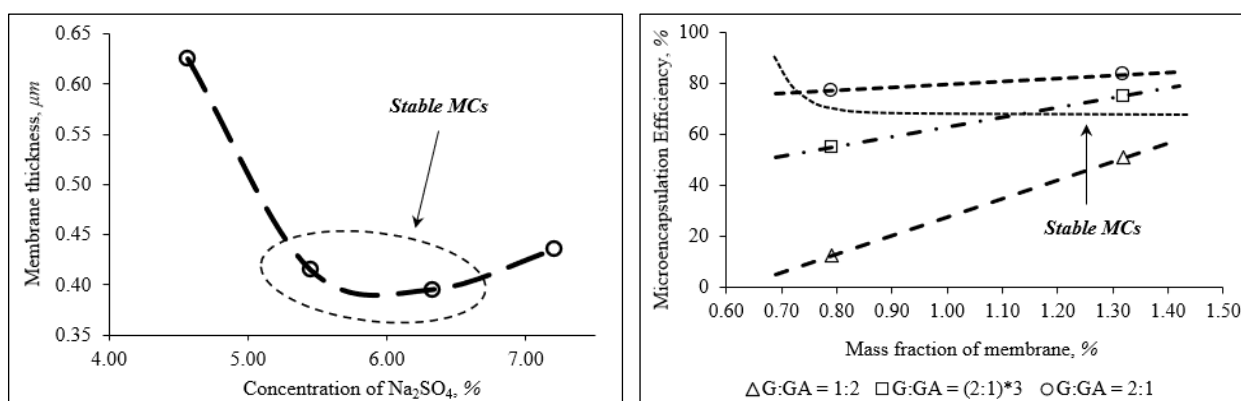


Figure 6. Influence of different Factors to MC stability: Left: Reduction of membrane thickness by influence of sodium sulphate – [69]; Right: Influence of wall material (Gelatin: Gum Arabic) relationship and quantity - recalculated from data, published in [63].

The influence of various factors on the stability of microcapsules and the efficiency of microencapsulation does not always correspond to “natural” expectations. For example, we have found that only certain average concentrations of sodium sulfate lead to the formation of stable gelatinous alginate shells around the walnut oil droplets [69]. Detailed studies of the gelatin: gum arabic system in microencapsulation of olive oil show that an increase in the amount of wall material does not always lead to an increase in the efficiency of microencapsulation [63]. In other words, for a microcapsule containing liquid oil, both a thin and too thick shell are harmful. Even double reduction of tension on the Oil/Water interface in the emulsions formed in the biopolymer solutions [88], is able to maintain on surface only a thin monomolecular biopolymeric layer; a thick layer, possible, is destroyed by gravitational stratification [85].

On the thermodynamics and efficiency of the microencapsulation process

Direct energy consumption for food production is 4 - 7 MJ/kg, and for some products it reaches 10-17 MJ/kg [89]. Therefore, according to actual trends, in the manufacturing of any new food products, energy consumption should not increase significantly in comparison with traditional processes [90]. Spray Drying, SD, and Fluid Beds, FB, require elevated temperatures; Freeze Drying, FD, and Spray Cooling, SC, on the other hand, require cooling energy. Another energy-consuming vector is a large number of stages of the process, which will lead to an increase systems negentropy, that is, to increase a work, time and energy spent on the MCs production.

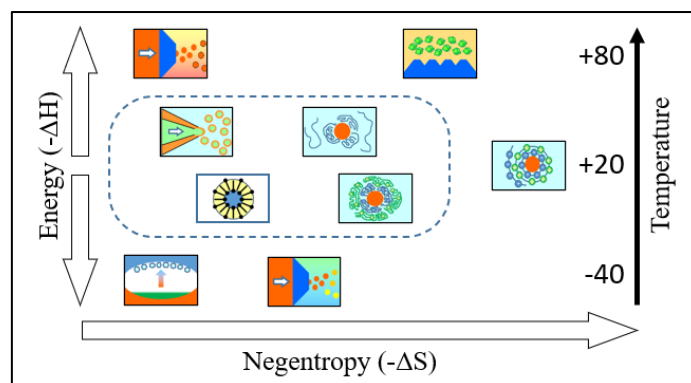


Figure 7. Thermodynamic, hence, energetic and economic restrictions for obtaining of edible microcapsules. BAC-friendly, relative energetic low methods, are dotted.

As is shown in the Figure 4, extrusion refers to the category of low energy microencapsulation methods. But then another problem arises. It is easy to extrude large capsules, which is done industrially very successfully. The reducing the linear dimensions (cm, mm) to microns (μm) practically does not reduce the time, required for the production of *one unit*. Thus, the production by extrusion of 1cm^3 of microcapsules with a diameter of 100 microns will require... **nothing at all, 1909859, $\approx 2 \cdot 10^6$ time longer**, than the production of single big pharmaceutical capsule with a volume of 1cm^3 . Recently, very significant advances have been made in the development of technologies for obtaining monodisperse emulsions and microcapsules based on them [91]. One-piece matrix, containing up to 1000 dispensing nozzles, can be produced by 3D printing techniques. But nevertheless, even such truly revolutionary solutions are still laboratory, but not industrial. In order to obtain 2000000 microcapsules per unit of time (with a total volume of only 1 cm^3), you will need to have 2000 such matrices with 1000 nozzles each...

Thus, from all existing microencapsulation methods, it seems that only liposomal entrapment (LE) and both types of coacervation: simple (C), and complex (CC), are **realistically** suitable for use in the manufacturing of relative available food-grade microcapsules.

Controlled release of biologically active compounds: how not to open the mc-shells at the wrong time and place, but to open it in the correct ones?

As was already noted, the food industry is strictly limited in the use of related materials, due to which developments in microencapsulation in the production of innovative drugs are ahead of those in the food manufacturing field. For example, methods of nano-capsulation of chemotherapeutic drugs in elastin-like membranes are being developed, the opening of which is activated by components built into the membrane; encapsulated content

release take place predominantly by cancer cells [92]. However, the engineering of microcapsules at a similar level is quite possible for functional food products, when, for example, the active substance is released only under the combined action of factors (pH, temperature and enzymes) corresponding to the conditions of the human intestine and even its specific zones [55, 93, 94]. Another interesting example of MC engineering is the technology of cheese production, in which a controlled release of microencapsulated bixin occurs in a ripening product due to the sequential action of proteases and lipases on microcapsules containing this food coloring [10].

Mathematical modelling of microcapsules properties

If microcapsules were obtained by simple or complex coacervation only from edible compounds, is not always possible, and most importantly, is always not rationally to isolate them from the supernatant and to obtain them in solid state. Isolation from the supernatant involves additional filtration, energy-intensive spray drying or sublimation steps. Also, the attempts to isolate edible microcapsules in dry form fails, because is impossible to avoid their sintering [23]. These microcapsules (especially, those obtained by simple coacervation) are relatively stable as long as they stay in their own supernatant environment. This limits the possibilities for the direct instrumental determinations of some food microcapsules parameters. For the numerical estimation of microencapsulation parameters, it is reasonable to resort to a combination of possible direct measurements and indirect evaluative methods.

Microencapsulation yield, also called **recovery** [51], is the practical percentage of obtained microcapsules (m_{MC}^p), formed from the total initial mass of microencapsulated core material ($m_{c.m.}^0$), and of initial mass of shell materials used ($m_{s.m.}^0$):

$$Y_{MC} = \frac{m_{MC}^p}{m_{s.m.}^{in.} + m_{c.m.}^{in.}} \cdot 100\%$$

Microencapsulation efficiency, E_{MC} [83], also named **Loading Capacity, LC** [52], is the percent ratio of the practically microencapsulated core material ($m_{c.m.}^p$) vs initial mass of active core material (biologically active compounds) introduced into microencapsulation process:

$$E_{MC} = LC = \frac{m_{c.m.}^p}{m_{c.m.}^{in.}} \cdot 100\%$$

Core material volumetric fraction [93], $\varphi_{c.m.}$, in the microcapsules of radius r (diameter d) with a known thickness h , may be calculated by the equation:

$$\varphi_{c.m.} = \frac{V_{c.m.}^0}{V_{MC}^0} = \frac{(r-h)^3}{r^3} = \frac{(d-2h)^3}{d^3}$$

Distribution width (Span). The distribution width can be estimated as:

$$Span = \frac{D_{90\%} - D_{10\%}}{D_{50\%}}$$

in which $D_{i\%}$ is diameter, below which $i\%$ of sample is contained [6, 95].

Polydispersity characterizes the size distribution of microcapsules in much more detail than the distribution width. In a test sample containing microcapsules with a total volume $\sum V$, polydispersity can be expressed by a distribution curve, in which the volumetric fraction of microcapsules, φ_i is a function of their radius r_i [22]

$$\varphi_{r_i} = \frac{V_{r_i}}{\sum V}$$

Experimental values of radius or diameter can be obtained by counting of representative samples consisting of not less than 100-150 microcapsules in magnified microscopic images [22, 88].

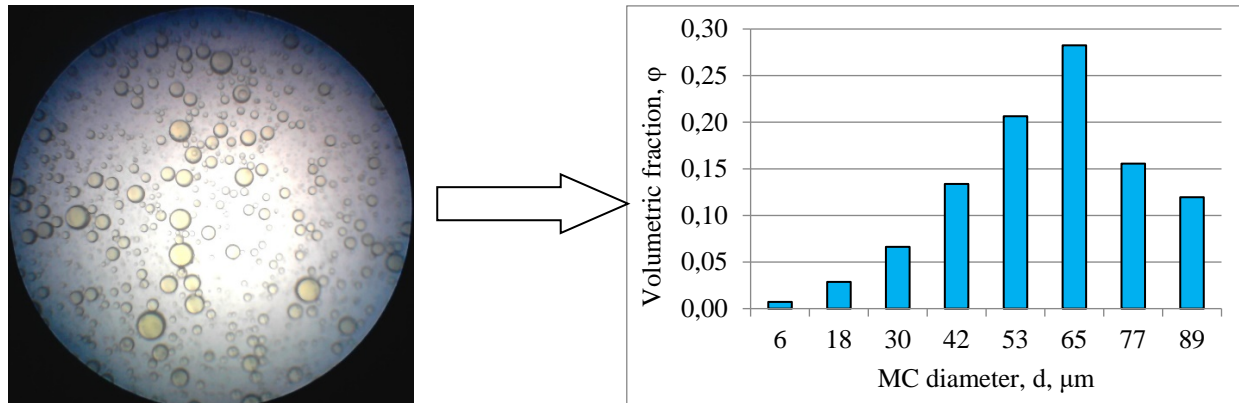


Figure 8. Transformation of MC image into “normal distribution”.

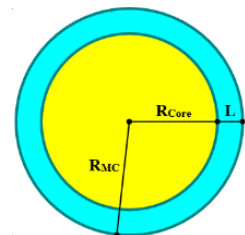
On the effect of microcapsules on foods sensory perception

Appearance and consistency of food systems are of great importance to the consumer. Therefore it is important that the microcapsules be distributed evenly throughout the food product without forming a separate phase. One of the factors of such a uniform distribution is the equal density of microcapsules and the food environment in which they are located, $\rho_{MC} = \rho_{env}$.

$$\frac{V_{shell}}{V_{core}} = \frac{m_{shell} \cdot \rho_{core}}{m_{core} \cdot \rho_{shell}} = \frac{R_{MC}^3 - R_{core}^3}{R_{core}^3}$$

$$(\rho_{MC} - \rho_{core}) \cdot R_{core}^3 + 2L(\rho_{MC} - \rho_{shell}) \cdot R_{core}^2 + \\ + 2L^2(\rho_{MC} - \rho_{shell}) \cdot R_{core} + (\rho_{MC} - \rho_{shell}) \cdot L^3 = 0$$

$$(\rho_{env} - \rho_{core})R_{core}^3 + 2LR_{core}R_{MC}(\rho_{env} - \rho_{shell}) + (\rho_{env} - \rho_{shell})L^3 = 0$$



The solution of the last third-order equation using the Cardano algorithm [96] makes it possible to mathematically calculate the practical values of the MC size at which the processes of their sedimentation or stratification in model or real systems are minimized.

About the foods, suitable for mcs introduction

The introduction of microcapsules into milk and cream led to their uneven distribution in the volume of the product, and even to the formation of separate layers and clots consisting of microcapsules. Dairy products, obtained from fermented milk (fat-reached kefir and sour

cream), turned out to be friendlier to the microcapsules, introduced into them [97]. The consistency of kefir and sour cream allowed the microcapsules to be distributed evenly throughout the volume of these products, at the same time, without changing their sensorial characteristics. Using various nanoencapsulation techniques, it is possible to obtain a wide range of food products enriched with encapsulated BACs, including yoghurts, fruit juices, and some bread and meat products [98].

Recently, it seems, gradually comes the understanding that the success of microencapsulation of biologically active substances specifically for food products is closely related to the thermodynamic characteristics of the corresponding methods. It is not accidentally mentioned, that the coacervation process (also named “phase inversion”) - is predominantly isothermal [99]. The use of already existing working technological lines, taking into account the thermodynamics of the innovative processes introduced into them, allows the creation of innovative food products with low negentropy [100]. A similar approach should finally bring microencapsulation to the level of mass industrial use.

Conclusion

Microencapsulation technologies, which have proven themselves in the production of convenient dosage forms, in cosmetology and many other fields, still remain mostly only “promising” for the food industry.

Scientific and technological still require a solution for number of challenges. The kinetic instability and solubility of natural biopolymer casings in food environments limits the scope of application of microcapsules in food products. The search for new edible compositions based on natural polymers and fibers for stable microcapsule shells should be continued. Ideally, all accompanying ingredients should have a status “*quantum satis*” for use in food manufacturing.

The possibilities of BAC microencapsulation will always be limited by the temperature regimes acceptable for working with biologically active compounds and with useful microflora, because these are often existing in a narrow temperature range. An increase in the cost of a product during the modernization of its production technology is most sensitive for the consumer. The multistage process of microencapsulation, the practical impossibility of making it continuous, and therefore additional costs, reduce the possibilities of application of known technological solutions for the MCs production for foods. Serious questions are also raised by the possibility of sterilization of microcapsules and their long-term storage as such, as a separate product.

It has been shown by using thermodynamic functions, that such methods of MC production as simple coacervation, complex coacervation and liposomal entrapment are thermodynamically reasonable for BACs nano- and microencapsulation.

The implementation of these three basic methods is a big challenge for equipment developers: these three methods still exist in the form of laboratory solutions, and their elegant embodiment in the form of working industrial technology has not been realized yet.

Food-grade microcapsules should release biologically active compounds or beneficial microflora only in the desired sector of the digestive tract, that is, the release should not occur in the composition of food, but should be activated only by certain digestive enzymes.

The real ways of using microcapsules in food technologies are associated with the direct integration of the microencapsulation process into the technological cycle of the production of specific food products. Moreover, these products should initially have a texture

and consistency that allow microcapsules to be aggregation resistant, not to exfoliate or break down prematurely, while maintaining their functions of protection and targeted delivery of biologically active compounds. Such products should be highly viscous colloidal systems. Thereby, the traditional fermented milk products and yoghurts, ice cream and juices with pulp, curd and cheese, are mostly suitable for supplementation of them by BAC using microencapsulation.

Acknowledgements: We express our gratitude to the National Research and Development Council of the Republic of Moldova for the funding of Postdoctoral Grant 20.00208.1908.02 – “Prolongation of biologically active compounds functionality and its protection in food compositions”, within which this work was developed. Heartful gratitude to Prof. Pavel Tatarov and Prof. Rodica Sturza – Technical University of Moldova.

References

1. FAO: Draft Vision and Strategy for FAO's work in Nutrition. [online, accessed 03.08.2021] - <http://www.fao.org/3/ne699en/ne699en.pdf> - accessed 25.07.2021
2. Ortega A.M.M., Campos M.R.S. Bioactive Compounds as Therapeutic Alternatives. In: CAMPOS, M.R.S., ed. *Bioactive Compounds*. Cambridge, Woodhead Publishing, 2019, pp. 247 - 264.
3. Singh V.P. Recent approaches in food bio-preservation - a review. *Open Vet. J.*, 2018; 8(1), pp. 104 - 111.
4. Baerle A., Popovici C., Radu O., Tatarov P. Effect of Synthetic Antioxidants on the Oxidative Stability of Cold Pressed Walnut Oil. *Journal of Food and Packaging Science, Techniques and Technologies*, 2016 (9), p. 19 - 24.
5. Radu O. Food compositions based on walnut oil (*Juglans regia* L.), resistant to oxidative degradation. *PhD Thesis in Biological and Chemical Technologies in the Food Industry*. Chişinău, Technical University of Moldova, 2020, 150p. – in Romanian.
6. Guedes Silva K.C., Bourbon A.I., Pastrana L., Kawazoe Sato A.C. Emulsion-filled hydrogels for food applications: Influence of pH on emulsion stability and a coating on microgels protection. *Food & Function*, accepted paper, 2020. DOI: 10.1039/D0FO01198C
7. Amaral P.H.R., Andrade P.L., De Conto L.C. Microencapsulation and Its Uses in Food Science and Technology: A Review. In: SALAÜN F., ed. *Microencapsulation – Processes, Technologies and Industrial Applications*. IntechOpen, 2019, <https://www.intechopen.com/chapters/67432> - accessed 03.08.2021
8. Ferreira S., Nicoletti V.R. Use of a tubular heat exchanger to achieve complex coacervation in a semi-continuous process: Effects of capsules curing temperature and shear rate. *Journal of Food Engineering*. Vol. 310, 2021. [online, accessed 03.08.2021] – <https://doi.org/10.1016/j.jfoodeng.2021.110698>.
9. De Matos F.E., Thomazini M., Trindade M.A., Favaro-Trindade C. Application of free or encapsulated Vitamin C to chicken frankfurter sausage by spray chilling: Physicochemical characteristics, stability and sensory acceptance. *Braz. J. of Food Technology*, 2015, 18(4), pp. 322 - 331 – in Portuguese
10. Sharma P., Segat A., Kelly A.L., Sheehan J.J. Colorants in cheese manufacture: Production, chemistry, interactions and regulation. *Comp. Review in Food Science and Food Safety*, 2020 (19), pp. 1220 - 1242.
11. Raynor T. The benefits of medicines outweigh the risks of treatment – says who? *The Pharmaceutical Journal*, 2013, Vol. 290, p. 616.
12. Mahato R. Multifunctional Micro- and Nanoparticles - In: MITRA, A.K., CHOLKAR, K., MANDAL, A. Eds: *Micro and Nano Technologies Emerging Nanotechnologies for Diagnostics, Drug Delivery and Medical Devices*. Elsevier, 2017, pp. 21-43.
13. Ciucă A.G., Grecu C.I., Rotărescu P., Gheorghe I., Bolocan A., Grumezescu A.M., Holban A.M., Andronescu E. Nanostructures for drug delivery: pharmacokinetic and toxicological aspects – IN: Andronescu E., Grumezescu A.M. Eds. *Micro and Nano Technologies, Nanostructures for Drug Delivery*. Elsevier, 2017, pp. 941-957.
14. Vasile C., Pamfil D., Stoleru E., Baican M. New Developments in Medical Applications of Hybrid Hydrogels Containing Natural Polymers. *Molecules*, 2020, 25 (7), 1539.
15. Codex (Alimentarius) general standard for contaminants and toxins in food and feed. www.fao.org/fileadmin/user_upload/livestockgov/documents/1_CXS_193e.pdf - accessed 05.08.2021
16. Nunes K. Consumers continue to mistrust food and beverage manufacturers. Accessed 03.08.2021 - <https://www.foodbusinessnews.net/articles/12058>

17. Parvathy U., Jeyakumari A. Microencapsulation and Spray Drying Technology. In: *Protocols for the production of high value secondary products from industrial fish and shellfish processing*. Bindu J., Sreejith S., and Sarika K. Eds. Central Institute of Fisheries Technology. Cochin, 2018, pp. 140 - 147.
18. Da Silva P.T., Fries L.L.M., De Menezes C.R., Holkem A.T., Schwan C.L., Wigmann É.F., De Oliveira Bastos J., De Bona Da Silva C. Microencapsulation: concepts, mechanisms, methods and some applications in food technology. *Ciência Rural*, 2014, 44(7), pp. 1304 - 1311.
19. Gupta S., Khan S., Muzafar M., Kushwaha M., Yadav A.K., Gupta A.P. Encapsulation: entrapping essential oil/flavors/aromas in food. In: Grumezescu A.M., ed.: *Nanotechnology in the Agri-Food Industry, Encapsulations*. Academic Press, 2016, pp. 229 - 268.
20. Kalaycioglu G.D., Aydogan N. Layer-by-layer coated microcapsules with lipid nanodomains for dual-drug delivery. *Colloids and Surfaces A: Physicochemical and Engineering Aspects*. 2020, 584, 124037.
21. Radulova G.M., Slavova T.G., Kralchevsky P.A., Basheva E.S., Marinova K.G., Danov K.D. Encapsulation of oils and fragrances by core-in-shell structures from silica particles, polymers and surfactants: The brick-and-mortar concept. *Colloids and Surfaces A: Physicochemical and Engineering Aspects*, 2018, 559, pp. 351 - 364.
22. Baerle A., Dimova O., Zadorojnai L., Tatarov P., Zenkovich A. Electrophoresis of Oil-Containing Edible Microcapsules with Protein-Polyuronic Shells. *Ukrainian Food J.*, 2014, 3(2), pp. 211 - 217.
23. Baerle A., Dimova O., Urumoglova I., Tatarov P., Zadorojnai L. Phase Diagram of Gelatine-Polyuronate Colloids: its Application for Microencapsulation and Not Only. *Chemistry Journal of Moldova*. 2016, 16 (1), pp. 97 - 105.
24. Favaro-Trindade C., Okuro P.K. Encapsulation via Spray Chilling / Cooling / Congealing. In: MISHRA, M. ed. *Handbook of Encapsulation and Controlled Release*. CRC Press, 2015, pp. 71 - 86.
25. Bakry A.M., Abbas S.H., Ali B., Majeed H., Abouelwafa M.Y., Mousa A.H., Liang L. Microencapsulation of Oils: A Comprehensive Review of Benefits, Techniques, and Applications. *Comprehensive Reviews in Food Science and Food Safety*. 2015, 15(1), pp. 143 - 182.
26. Dabija A., Nechifor I. Study regarding the microencapsulation of food ingredients in alginates. *Annals. Food Science and Technology*. 2015, 16, (1), pp. 20 - 26.
27. Tsai W.Ch., Rizvi S.S.H. Liposomal microencapsulation using the conventional methods and novel supercritical fluid processes. *Trends in Food Science & Technology*, 2016, 55, pp. 61 - 71.
28. Babazadeh A., Jafari S.M., Shi, B. Encapsulation of food ingredients by nanophytosomes. In: Jafari S.M. ed. *Nanoencapsulation in the Food Industry. Lipid-Based Nanostructures for Food Encapsulation Purposes*. Academic Press, 2019, pp. 405 - 443.
29. Awasthi R., Kulkarni G., Pawar V. Phytosomes: An Approach to Increase the Bioavailability of Plant Extracts. *International Journal of Pharmacy and Pharmaceutical Sciences*. 2011, 3, pp. 1 - 3.
30. Rashidinejad A., Boostani S., Babazadeh A., Rehman A., Rezaei A., Akbari-Alavijeh S., Shaddel R., Jafari S.M. Opportunities and challenges for the nano-delivery of green tea catechins in functional foods. *Food Research International*, 2021, 142(2), 110186.
31. Lengyel M., Kállai-Szabó N., Antal V., Laki A.J., Antal I. Microparticles, Microspheres, and Microcapsules for Advanced Drug Delivery. *Sci. Pharm.* 2019, 87 (3), 20.
32. Purkayastha M., Manhar A., Mandal M., Mahanta Ch. Industrial Waste-Derived Nanoparticles and Microspheres Can Be Potent Antimicrobial and Functional Ingredients. *Journal of Applied Chemistry*, 2014, pp. 1 - 12.
33. Kyriakoudi A., Spanidi E., Mourtzinis I., Gardikis K. Innovative Delivery Systems Loaded with Plant Bioactive Ingredients: Formulation Approaches and Applications. *Plants*, 2021, 10, 1238.
34. Mohammed N.K., Tan C.P., Manap Y.A., Muhialdin B.J., Hussin ASM. Spray Drying for the Encapsulation of Oils – a Review. *Molecules*. 2020, 25(17), 3873.
35. Corrêa-Filho L.C., Lourenço M.M., Moldão-Martins M., Alves V.D. Microencapsulation of β -Carotene by Spray Drying: Effect of Wall Material Concentration and Drying Inlet Temperature. *International Journal of Food Science*, 2019, 8914852.
36. Mis-Solval K.E., Jiang N., Yuan M., Joo K.H., Cavender G.A. The Effect of the Ultra-High-Pressure Homogenization of Protein Encapsulants on the Survivability of Probiotic Cultures after Spray Drying. *Foods*. 2019, 8(12) : 689.
37. Mohylyuk V., Patel K., Scott N. Richardson C., Murnane D., Liu F. Wurster Fluidized Bed Coating of Microparticles: Towards Scalable Production of Oral Sustained-Release Liquid Medicines for Patients with Swallowing Difficulties. *AAPS PharmSciTech*, 2020, 21 (3).

38. Zhang R., Hoffmann T., Tsotsas E. Novel Technique for Coating of Fine Particles Using Fluidized Bed and Aerosol Atomizer. *Processes*, 2020, 8, 1525.
39. Colucci G., Santamaria-Echart A., Silva S.C., Fernandes I., Sipoli C.C., Barreiro M.F. Development of Water-in-Oil Emulsions as Delivery Vehicles and Testing with a Natural Antimicrobial Extract. *Molecules*, 25 (9), 2105.
40. Gharibzadeh S.M.T., George S., Greiner R., Estevinho B.N., Frutos Fernández M.J., McClements D.J., Roohinejad S. New Trends in the Microencapsulation of Functional Fatty Acid-Rich Oils Using Transglutaminase Catalyzed Crosslinking. *Comprehensive Reviews in Food Science and Food Safety*. 2018, 17(2), p. 274 - 289. doi: 10.1111/1541-4337.12324.
41. Ferreira S., Nicoletti V.R. Complex coacervation assisted by a two-fluid nozzle for microencapsulation of ginger oil: Effect of atomization parameters. *Food Research International*, 2020, 138 (Pt B):109828.
42. Amran M., Zulfakar M.H., Danik M.F., Abdullah M., Shamsuddin A.F. A new alternative for intravenous lipid emulsion 20% w/w from superolein oil and its effect on lipid and liver profiles in an animal model. *Journal of Faculty of Pharmacy, Tehran University of Medical Sci.*, 2019, 27 (1), pp. 191 - 201.
43. Vidal R.R.L., Desbrières J., Borsali R., Guibal E. Oil removal from crude oil-in-saline water emulsions using chitosan as bio sorbent. *Separation Science and Technology*, 2020, 55 (5), pp. 835 - 847.
44. Harrington J., Schaefer M. Extrusion-Based Microencapsulation for the Food Industry. In: eds. GAONKAR A.G., Vasisht N., Khare A.R., Sobel R. *Microencapsulation in the Food Industry*, Academic Press, 2014, pp. 81 - 84.
45. Seth D., Mishra H.N., Deka S.C. Effect of microencapsulation using extrusion technique on viability of bacterial cells during spray drying of sweetened yoghurt. *International Journal of Biological Macromolecules*, 2017, 103, pp. 802 - 807.
46. Bampi G.B., Backes G.T., Cansian R.L., Matos F.E., Araldi-Ansolin I.M., Poletto B.C., Corezzolla L.R., Favaro-Trindade C.S. Spray Chilling Microencapsulation of *Lactobacillus acidophilus* and *Bifidobacterium animalis* subsp. *lactis* and its Use in the Preparation of Savory Probiotic Cereal Bars. *Food Bioprocess Technology*, 2016, 9, 1422 - 1428.
47. Nogueira M., Prestes C.F., Burkert J.F. Microencapsulation by lyophilization of carotenoids produced by *Phaffia rhodozyma* with soy protein as the encapsulating agent. *Food Science and Technology International*, 2017, 37, 1 - 4.
48. Piccinino D., Capecchi E., Botta L., Bizzarri B.M., Bollella P., Antiochia R., Saladino R. Layer-by-Layer Preparation of Microcapsules and Nanocapsules of Mixed Polyphenols with High Antioxidant and UV-Shielding Properties. *Biomacromolecules*, 2018, 19(9), pp. 3883 - 3893.
49. Lu T., Spruijt E. Multiphase Complex Coacervate Droplets. *Journal of American Chemical Society*, 2020, 142, pp. 2905 - 2914.
50. Ang L.F., Darwis Y., Por L.Y., Yam M.F. Microencapsulation Curcuminoids for Effective Delivery in Pharmaceutical Application. *Pharmaceutics*, 2019, 11 (9), pp. 451.
51. Justi P.N., Sanjinez-Argandoña E.J., Macedo M.L.R. Microencapsulation of Pequi pulp oil by complex coacervation. *Revista Brasileira de Fruticultura*, 2018, v. 40, n. 2: (e-874).
52. Shu G., He Y., Chen L., Song Y., Meng J., Chen H. Microencapsulation of *Lactobacillus Acidophilus* by Xanthan-Chitosan and Its Stability in Yoghurt. *Polymers*, 2017, 9(12), 733.
53. Lombardo S., Villares A. Engineered Multilayer Microcapsules Based on Polysaccharides Nanomaterials. *Molecules*, 2020, 25, 4420.
54. Gasperini L., Mano J.F., Reis R.L. Natural polymers for the microencapsulation of cells. *Journal of the Royal Society Interface*, 2014, 11: 20140817.
55. Coghetto C.C., Brinques G.B., Siqueira N.M., Pletsch J., Duarte Soares R.M., Záchia Ayub M.A. Electro-spraying microencapsulation of *Lactobacillus plantarum* enhances cell viability under refrigeration storage and simulated gastric and intestinal fluids. *Journal of Functional Foods*, 2016, 24, pp. 316 - 326.
56. Duan Ch., Meng X., Jingru Meng Khan M.I.H., Dai L., Khan A., An X., Zhang J., Huq T., Ni Y. Chitosan as A Preservative for Fruits and Vegetables: A Review on Chemistry and Antimicrobial Properties, *Journal of Bioresources and Bioproducts*, 2019, 4 (1), pp. 11 - 21.
57. Correa R.F., Colucci G., Halla N., Pinto J.A., Santamaria-Echart A., Blanco S.P., Fernandes I.P., Barreiro M.F. Development of Chitosan Microspheres through a Green Dual Crosslinking Strategy Based on Tripolyphosphate and Vanillin, *Molecules*, 2021, 26, 2325.
58. Ferreira S., Piovanni G.M., Malacrida C.R.O., Nicoletti V.R. Influence of emulsification methods and spray drying parameters on the microencapsulation of turmeric oleoresin. *Emirates Journal of Food and Agriculture*, 2019, 31 (7), pp. 491 - 500.

59. Dewi E.N., Kurniasih R.A., Purnamayanti L. Physical Properties of Spirulina Phycocyanin Microencapsulated with Maltodextrin and Carrageenan. *Philippine J. of Science*, 2018, 147 (2), pp. 201 - 207.
60. Batista De Oliveira T.T. Microencapsulation of spirulina platensis by spray drying method as a promising alternative for the development of new products. *Brazilian Journal of Development*, 2020, 6 (4), p. 2017 - 20186.
61. Prakash A., Soni H., Mishra A., Sarma P. Are your capsules vegetarian or nonvegetarian? - An ethical and scientific justification. *Indian Journal of Pharmacology*, 2017, 49 (5), pp. 401 - 404.
62. Perinelli D.R., Palmieri G.F., Cespi M., Bonacucina G. Encapsulation of Flavours and Fragrances into Polymeric Capsules and Cyclodextrins Inclusion Complexes: an Update. *Molecules*, 2020, 25 (24) : 5878.
63. Marfil P.H.M., Paulo B.B., Alvim I.D., Nicoletti V.R. Production and characterization of palm oil microcapsules obtained by complex coacervation in gelatin/gum Arabic. *Journal of Food Process Engineering*, 2018, 41 (4): e12673.
64. Atgie M. Composition and structure of gum Arabic in solution and at oil-water interfaces. PhD Thesis, 2018, 161p, [accessed 05.08.2021], https://oatao.univ-toulouse.fr/20871/1/ATGIE_Marina.pdf - in French.
65. Hernandez-Nava R., Lopez-Malo A., Palou E., Ramírez-Corona N., Jimenez-Munguía M.T. Encapsulation of Origanum vulgare essential oil by complex coacervation between gelatin and chia mucilage and its properties after spray drying. *Food Hydrocolloids*, 2020, 109: 106077, 8p.
66. Boudoukhani M., Yahoum M.M., Lefnaoui S., Moulai-Mostefa N., Banhobre M. Synthesis, characterization and evaluation of deacetylated xanthan derivatives as new excipients in the formulation of chitosan-based polyelectrolytes for the sustained release of tramadol. *Saudi Pharmaceutical Journal*, 2019, 27 (8), pp. 1127 - 1137.
67. Enache I. M., Vasile A. M., Enachi E., Barbu V., Stănciuc N., Vizireanu C. Co-Microencapsulation of Anthocyanins from Black Currant Extract and Lactic Acid Bacteria in Biopolymeric Matrices. *Molecules*, 2020, 25 (7), 1700.
68. Hernández-Nava R., López-Malo A., Palou E., Ramírez-Corona N. and Jiménez-Munguía M.T. Complex Coacervation Between Gelatin and Chia Mucilage as an Alternative of Encapsulating Agents. *Journal of Food Science*, 2019, 84 (6), pp. 1281 - 1287.
69. Dimova O., Baerle A. Formation of Microcapsule's Biopolymeric Shells: Electrochemical Aspects. *Journal of Engineering Science*, 2018, 2 (1), pp. 90 - 94.
70. Mitchell G.R., Hiremath Ch., Heggannavar G. Biopolymers in Drug Delivery. Applications. In: *Green Polymer Composites Technology: Properties & Applications*, Taylor & Francis, 2015, pp. 551 - 525.
71. Mujica-Álvarez J., Gil-Castell O., Barra P.A., Ribes-Greus A., Bustos R., Faccini M., Matiacevich S. Encapsulation of Vitamins A and E as Spray-Dried Additives for the Feed Industry, *Molecules*, 2020, 25 (6): 1357.
72. Benetti J.V.M., Nicoletti V.R. Carotenoid stability in spray dried microspheres based on soybean protein isolate microgels. CIPCA 2020. VIII-th International Conference of Food Proteins and Colloids. At: Campinas/SP – Brazil. p. 1
73. Malacrida C.A., Ferreira S, Cireli Zuanon L.A., Nicoletti Telis V.R. Freeze-drying for microencapsulation of turmeric oleoresin using modified starch and gelatin. *Journal of Food Processing and Preservation*, 2014, 39(6), DOI:10.1111/jfpp.12402
74. Li J. The Use of Starch-Based Materials for Microencapsulation. In: eds. Gaonkar A.G., Vasisht N., Khare A.R., Sobel R. *Microencapsulation in the Food Industry*. Academic Press, 2014, pp. 195 - 210.
75. Gamboa-Carballo J.J., Rana V.K., Levalois-Grützmacher J., Gaspard S., Jáuregui-Haza U. Structures and stabilities of naturally occurring cyclodextrins: a theoretical study of symmetrical conformers, *Journal of Molecular Modeling*, 2017, 23 (11): 318.
76. De Souza I.A., Orsi D.C., Gomes A.J., Lunardi C.N. Enzymatic hydrolysis of starch into sugars is influenced by microgel assembly. *Biotechnology Reports*, 2019, 22 : e00342.
77. Jeyakumari A., Zynudheen A.A., Parvathy U. Microencapsulation of bioactive food ingredients and controlled release-a review. *MOJ Food Processing & Technology*, 2016, 2 (6), pp. 214 – 224.
78. Li Y.O., Dueik González V.P., Diosady L.L. Microencapsulation of Vitamins, Minerals, and Nutraceuticals for Food Applications. In: eds. Gaonkar A.G., Vasisht N., Khare A.R., Sobel R. *Microencapsulation in the Food Industry*. Academic Press, 2014, pp. 501 - 522.
79. Callegari M.A., Novais A.K., Oliveira E.R., Dias C.P., Schmoller D.L., Pereira J.M., Nagi J.G., Alves J.B., Silva C.A. Microencapsulated acids associated with essential oils and acid salts for piglets in the nursery phase. *Semina Ciências Agrárias*, 2016, 37 (4), pp. 2193 - 2208.

80. Zorzenon M., Hodas F., Milani P., Formigoni M., Dacome A., Monteiro A., Costa C., Costa S. Microencapsulation by Spray-drying of Stevia Fraction with Antidiabetics Effects. *Chemical Engineering Transactions*, 2019, 75, pp. 307 - 312.
81. Favaro-Trindade C.S., Rocha-Selmi G.A., Dos Santos M.G. Microencapsulation of Sweeteners. In: ed. Sagis L.M.C. *Microencapsulation and Microspheres for Food Applications*. Academic Press, 2015, pp. 333 - 349.
82. Sanjay Ch., Jasjeet K., Sandeep K. Liposome Entrapment of Bacteriophages Improves Wound Healing in a Diabetic Mouse MRSA Infection. *Frontiers in Microbiology*, 2018, 9, p. 561.
83. Pacheco C., González E. Paz R., Parada J. Retention and pre-colon bio accessibility of oleuropein in starchy food matrices, and the effect of microencapsulation by using inulin. *Journal of Functional Foods*, 2018, 41, pp. 112 - 117.
84. Bortoloti Fernandes T.A., Emerson J.V. Sakanaka L.S., Ueno C.T. Development of immunoglobulin-Y antibody encapsulation process for maintenance viability. In: eds. OLIVEIRA A.F., SHIRAI M.A. *Topics in Food Science and Technology: Results of Academic Research*. 2020, 5, pp. 115 - 134. - in Portuguese
85. Sturza R., Verejan A., Subotin Iu., Haritonov S., Munteanu D., Covaci E. et al. *Applied Chemistry for Engineers*. Chişinău, Tehnica-UTM, 2021, 356p. - in Romanian
86. Baerle A., Tatarov P., Dimova O., Cojohari C. Process for microencapsulation of food and cosmetic oil compositions. Patent MD-557, BOPI 2012-11-30, p. 32 - 33.
87. Correa R., Colucci G., Noureddine H., Pinto J., Santamaria-Echart A., Monte Blanco S., Fernandes I., Barreiro M. Development of Chitosan Microspheres through a Green Dual Crosslinking Strategy Based on Tripolyphosphate and Vanillin. *Molecules*, 2021, 26, 2325.
88. Kawazoe Sato A.C., Zagatto Polastro M., De Figueiredo Furtado G., Lopes Cunha R. Gelled Double-Layered Emulsions for Protection of Flaxseed Oil. *Food Biophysics*, 2018, 13, pp. 316 - 323.
89. Ladha-Sabur A., Bakalis S., Fryer P.J., Lopez-Quiroga E. Mapping energy consumption in food manufacturing. *Trends in Food Science & Technology*, 2019, 86, pp. 270 - 280.
90. Monforti-Ferrario F., Dallemand J., Pinedo Pascua I., Motola V., Banja M., Scarlat N. et al. Energy use in the EU food sector: State of play and opportunities for improvement. EUR 27247. Publications Office of the European Union, 2015, JRC96121.
91. Schroen K., Berton-Carabin C., Renard D., Marquis M., Boire A., Cochereau R., Amine C., Marze S. Droplet Microfluidics for Food and Nutrition Applications. *Micromachines*, 2021, 12 (8), 863.
92. Vallejo R., Gonzales-Valdivieso J., Santos M., Rodriguez-Rojo S., Arias F.J. Production of elastin-like recombinamer-based nanoparticles for docetaxel encapsulation and use as smart drug-delivery systems using a supercritical anti-solvent process. *Journal of Industrial and Engineering Chemistry*, 2021, 93, pp. 361 - 374.
93. Ghaffarian R., Herrero E.P., OH, H., Raghavan S.R., Muro S. Chitosan-Alginate Microcapsules Provide Gastric Protection and Intestinal Release of ICAM-1-Targeting Nanocarriers, Enabling GI Targeting In Vivo. *Advanced Functional Materials*, 2016, 26 (20), pp. 3382 - 3393.
94. Dimova O. Behavior of microcapsules containing $\omega 3$ - and $\omega 6$ - polyunsaturated acids from walnut oil in the model of digestive tract environment. *Journal of Food and Packaging Science, Technique and Technologies*, 2016, 9, pp. 44 - 48.
95. Silva J., Munari Benetti J., Alexandrino T., Assis O., De Ruiter J., Schroën K., Nicoletti V. Whey Protein Isolate Microgel Properties Tuned by Crosslinking with Organic Acids to Achieve Stabilization of Pickering Emulsions. *Foods*, 2021, 10 (6), 1296.
96. <https://www.dpmms.cam.ac.uk/~wtg10/cubic.html> - accessed 10.07.2021.
97. Dimova O.V., Baerle A.V., Tatarov P.G., Kiritsa E.N. Fortification of fermented milk products with microencapsulated beta-carotene – Dairy Industry, 2013, 9, pp. 42 - 43. - in Russian.
98. Pateiro M., Gómez B., Muneke P.E.S., Barba F.J., Putnik P., Kovačević D.B., Lorenzo J.M. Nanoencapsulation of Promising Bioactive Compounds to Improve Their Absorption, Stability, Functionality and the Appearance of the Final Food Products. *Molecules*, 2021, 26, 1547.
99. Trojanowska A., Nogalska A., Valls R.G., Giamberini M., Tylkowski B. Technological solutions for encapsulation. *Physical Sciences Reviews*, 2017, 2 (9), 20170020.
100. Radu O. Baerle A., Tatarov P., Popescu L. Factors, that determine the shelf life of a butter-like spread, based on walnut oil. *Journal of Engineering Science*, 2019, XXVI (3), pp. 119 - 124.

[https://doi.org/10.52326/jes.utm.2021.28\(3\).13](https://doi.org/10.52326/jes.utm.2021.28(3).13)
CZU 637.146.34:634.7



THE ROLE OF BERRIES IN QUALITY AND SAFETY ENSURING OF GOAT'S AND COW'S MILK YOGHURT

Tatiana Cușmenco*, ORCID ID: 0000-0001-6628-0752,
Elisaveta Sandulachi, ORCID ID: 0000-0003-3017-9008,
Viorica Bulgaru, ORCID ID: 0000-0002-1921-2009,
Artur Macari, ORCID ID: 0000-0003-4163-3771

Technical University of Moldova, 168 Stefan cel Mare blvd., Chisinau, Republic of Moldova

*Corresponding author: Tatiana Cușmenco, tatiana.cusmenco@sa.utm.md

Received: 06. 27. 2021

Accepted: 08. 25. 2021

Abstract. The yogurt was obtained from a combination of 50% goat's milk and 50% cow's milk with the inclusion of scald fruits of aronia (*Aronia melanocarpa*), raspberries (*Rubus idaeus*), strawberry (*Fragaria xanassa*). Physico-chemical and microbiological indices were determined, according to standard methods, after manufacture and storage, after 1, 5, 10, 15 days. Compared to other samples, yogurt with aronia showed the best values of the dynamics specific to the development of microorganisms: $2.93 \cdot 10^7$ cfu/ml; the growth rate of lactic acid bacteria at fermentation 0.95μ ; physico-chemical indices: titratable acidity $85 \pm 0.078^\circ\text{T}$, pH 4.28 ± 0.002 , water activity 0.875 ± 0.025 ; total dry matter $18.45 \pm 0.31\%$, viscosity 2500 ± 0.023 mPa s, ash content $0.89 \pm 0.10\%$ and the optical density 2.531 ± 0.054 nm. Yeasts and molds were not detected in any of the samples. From a physico-chemical point of view, in storage, in all fruit yogurt samples the titratable acidity showed increasing values, pH remaining in the range of permissible values. In storage fruits formed an association to control the microbiological risk and stability of yogurt. Fruit yogurt shows a synergism with *Streptococcus thermophilus*, *Lactobacillus delbrueckii subsp. bulgaricus*, *Lactococcus lactis subsp. lactis biovar diacetylactis*. The overall Pearson coefficient ($P_c = f(\text{pH and MC})$) for all fruit yogurt samples is -0.95066.

Keywords: fermentation, growth curve, lactic acid, lactic acid bacteria, metabolic process, microbial counts (MC), starter culture, synergism.

Introduction

Nutritionists call yogurt a food product that has a high nutritional value, especially due to its low lactose content and high calcium content, as well as positive bioactive effects, due to prebiotic ingredients and probiotic bacteria contained [1].

Yogurt is obtained by lactic acid fermentation of milk under the action of lactic acid bacteria, which has a significant impact on health because in the fermentation process bioactive peptides are released [2].

Consumption of yogurt reduces blood cholesterol levels [3], has an antihypertensive and protective effect on the bone system [4]. The balance of lactic acid bacteria contained in yogurt are important in maintaining intestinal health and could help protect against cancer and coronary heart disease [5]. Yogurt has higher antioxidant properties compared to milk, by releasing biopeptides that monitor the hydrolysis of α -casein, α -lactalbumin and β -lactoglobulin [6].

The fermentation process helps to break down large organic molecules into simpler ones by the action of microorganisms [7, 8] and obtaining a safer yogurt [9, 10]. The activity of microorganisms plays a significant role in fermentation, showing changes in physicochemical properties [11]. Fermenting microorganisms are the main factors influencing the quality of yogurt [12]. Lactic bacteria are the dominant microbiota, responsible for the beneficial effects of yogurt [13, 14].

In order to extend the shelf life of yoghurt [15] and to give it a more pleasant taste [16], various stabilizers, preservatives and synthetic flavors are added to its composition, which often affect human health and inhibit the nutritional properties of yoghurt [17]. The use of berries (aronia, raspberry and strawberry) could be a healthy alternative to replacing synthetic products as preservatives. At the same time, the chemical composition of the fruits [18, 19, 20] has a direct impact on the quality of the yogurt-finished product [21, 22].

Current research has been made in search of a bactericidal substance and the lactic acid production for a potential bio-preservative. The proteins present in milk act as antimicrobial peptides precursors, improving the natural defense capacity by eliminating pathogenic microorganisms. The study demonstrates the possibility of using berries in yogurt as natural preservatives, as they can inhibit the growth of pathogenic bacteria by using biologically active substances as components for decomposition and oxidation reactions.

The aim of the research is to evaluate the physico-chemical and microbiological characteristics of goat's and cow's milk yogurt with berries. In order to achieve the goal, the following objectives were proposed:

1. Research on the physico-chemical indices of yogurt with selected cultures of *Lactobacillus lactis* and *Streptococcus thermophilus* during fermentation and during its storage.
2. Study of the scald berries addition influence on the quality of the fermentation process and the samples storage time investigated by microbiological aspects.

Materials and methods

Materials

Preparation of fruits pulp

The fruit puree was obtained according to the following manufacture stages: sorting by removing non-conforming fruits and inedible parts, washing by removing all impurities, drying, cutting, heating the pulp of hard fruits, and passing through a sieve to remove inedible parts, mixing until a homogeneous mass, heating at 95-98°C for 5 minutes, immediately pouring the fruit puree into sterile containers, cooling the packaged product, storing.

Preparation of fruit yogurt

To prepare fermented yogurt the goat and cow milk sample was received from the local farm. Before fermentation, the goat's milk was pasteurized at 85°C for 10 minutes and cow's milk was pasteurized at 95°C for 15 minutes after which it was cooled to the inoculation temperature 42 °C. For the yogurt manufacture the Lyofast YAB 205 starter culture was used for inoculation. Inoculation was done by direct inoculation of the culture in the required

amount of milk calculated depending on the milk volume. The contents were mixed for 5 minutes with sterile blender for better dispersion of the culture in the medium. In the inoculated milk mixture, the fruit puree was added, then transferred to the fermentation chamber for 6 hours. The end of the coagulation process was determined by the pH value and coagulum firmness. When the fermentation process was completed, all samples were taken to the refrigerator for storage at a temperature of $4 \pm 2^{\circ}\text{C}$ until the next control measurement.

The yogurt assortment obtained is presented in table 1:

Table 1

Notify the probe	
Sample code	Sample description
P1	50% goat's milk + 50% cow's milk, control sample
P2	45% goat's milk + 45% cow's milk + 10% aronia.
P3	45% goat's milk + 45% cow's milk + 10% raspberries.
P4	45% goat's milk + 45% cow's milk + 10% strawberry.
Sample code	Sample description
P1	goat's milk and cow's milk (50%:50%), control sample
P2	goat's milk and cow's milk (45%:45%) + 10% aronia.
P3	goat's milk and cow's milk (45%:45%) + 10% raspberries.
P4	goat's milk and cow's milk (45%:45%) + 10% strawberry.

Method

Physico-chemical methods

Titrateable acidity determination consists in the neutralization of acidic substances in milk with 0.1 n NaOH (KOH) solution and phenolphthalein as indicator [23]. The calculation formula is:

$$\text{Acidity } (^{\circ}\text{T}) = 10 \cdot V \quad (1)$$

where: V- is the volume of 0.1 N NaOH used in the titration.

Active acidity determination consists in determining the milk pH value using glass electrodes [23].

Water activity. To determine the activity of the water was used LabSwift, it is a portable equipment of high precision, designed by Novasin to measure the activity of the product. Novasin combines modern technology, speed and measurement accuracy. With an SD card for data storage [24].

Total dry matter content. Standard method of oven drying at $102 \pm 2^{\circ}\text{C}$ until a constant mass of the dry residue is obtained [25].

Viscosity was determined using the "Brookfield DV - III" rheometer, with indicator no. 04, 250 rotations / min, data were read after 30 seconds of rotations [26].

Ash content was determined by the direct heating method (standard method), [27]. The ash content was calculated according to the formula.

$$\% \text{ Ash} = \frac{Z-X}{Y-X} \times 100 \quad (2)$$

where: X = weight of the empty crucible;

Y = crucible weight + sample;

Z = crucible weight + ash.

Determination of the total protein content. The total protein contents of the were measured using the Kjeldahl method [28].

Microbiological methods.

Growth rate of lactic acid bacteria The methodology is based on the work of Lambert and others [29, 30]. The most common way to assess microbial growth in solution is the measurement of the optical density at 600 nm, or short OD₆₀₀. The method is described according [31 - 34].

To monitor the development of bacterial cells in the fermentation medium, a colorimetric determination is made on a Heidolf spectrophotometer ($\lambda = 600$ nm) after prior dilution with distilled water. For this purpose, 1 ml of homogeneous fermentation medium is diluted with 9 ml of distilled water, shaken and the extinction is read on a spectrophotometer in a 1 cm cuvette from the control represented by distilled water. The optical density is calculated according to the following formula:

$$DO = A_{600} \times 10, \quad (3)$$

where: A₆₀₀ – extinction cited at 600 nm;

10 – sample dilution.

It is noted that during the fermentation process other dilutions may be used, depending on the growth capacity, in order to be able to perform the measurements [32].

Monitoring of growth. The growth of lactobacilli was studied twice by measuring optical density (OD) at $\lambda = 600$ nm and pH value. The method is described according [35] and the formula:

$$\mu = \frac{\ln X - \ln X_0}{\Delta t}, \quad (4)$$

where: X – optical density in the end of the exponential growth phase,

X₀ – optical density in the beginning of the exponential growth phase,

Δt – the time interval between observations

Determination of lactic acid by titration. The amount of lactic acid was calculated depending on the amount of NaOH used to determine the acidity, taking into account that 1 ml of 0.1 N NaOH corresponds to 0.009008g lactic acid [36].

Determination of the total number of microorganisms. The method is described according [37].

Determination of the number of yeasts and molds. AOAC Official Method 2014.05 Enumeration of Yeast and Mold in Food. 2015 AOAC INTERNATIONAL [38].

Determination of lactic acid bacteria using deManRogosa Sharpe (MRS) agar. The lactic acid bacteria (LAB) in the yogurt were determined using deMan Rogosa Sharpe (MRS) Agar as described by Oxoid Manual [32] and the formula:

$$C_{fu/ml} = \text{average count} \times \text{dilution factor (DF)}, \quad (5)$$

Statistical analysis. The analysis of the variance of the results was performed by applying the Student test and the version of the Microsoft Office Excel 2010 program. All tests were performed in triplicate. Experimental results are expressed as mean \pm SD.

Results and discussions

The technology of making yogurt, used in research, is based on the addition of the selected culture, consisting of two lactic acid bacteria: *Streptococcus thermophilus* and *Lactobacillus bulgaricus* in a ratio of 1: 1 [39]. The inoculum was used in the form of a mixed culture, which has biotechnological properties corresponding to obtaining a quality yogurt. By using pure culture, a double effect was obtained - technological and hygienic. The technological effect consists in the fact that by the optimal concentration of specific microorganisms in milk the desired acidity and curd for yogurt was obtained. The hygienic effect was manifested by the creation of a favourable microflora dominance over resistant milk contaminants and in the yogurt manufacturing process contaminants.

The evolution of milk fermentation to obtain fruit yogurt

Milk fermentation is one of the most important phases of the yogurt manufacturing process that depends on creating the right conditions (temperature, time) for the development the specific microflora and plays an essential role in the transformation of milk into yogurt [40]. *Lactobacillus bulgaricus* has a strong tolerance to oxygen, so the lack of oxygen or the presence of oxygen in small quantities leads to its slow growth. *Streptococcus thermophilus*, being an active lactic acid producer, quickly performs the fermentation process at the optimum growth temperature (40 - 42°C) [41].

During fermentation, the fruit yogurt samples pH was determined at certain time periods (initially, 2, 4, 6 hours), in order to follow the evolution of the fermentation process. The addition influence of aronia, raspberry and strawberry fruits on the yoghurt fermentation process was evaluated, indicating different pH values depending on the type of fruit added.

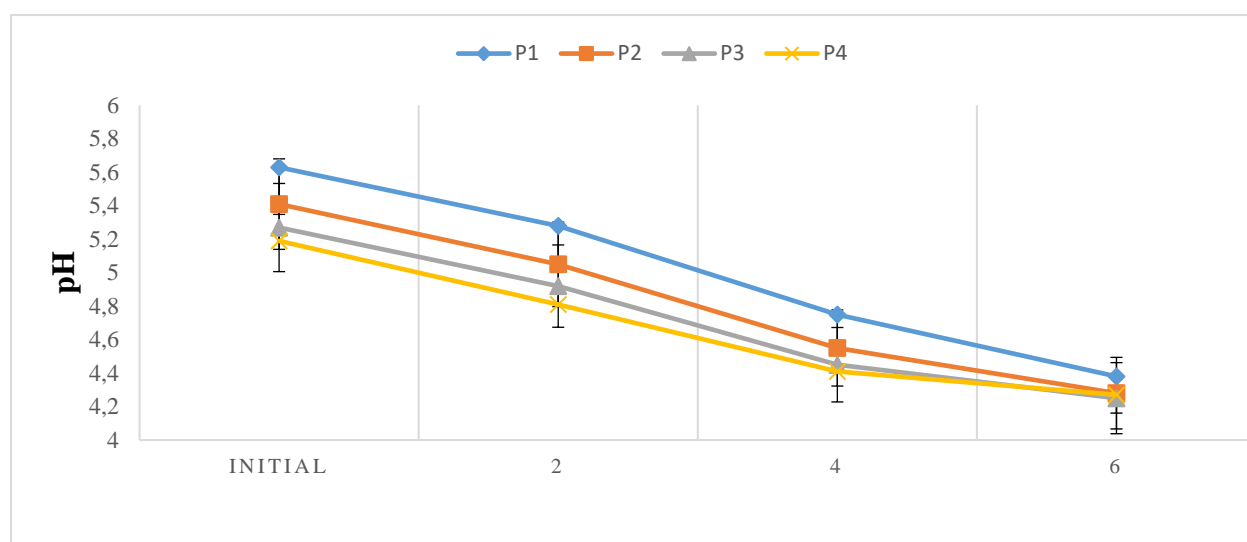


Figure 1. Fermentation time of yogurt samples, h.

From the data presented in figure 1, a specific dynamics of the microorganisms development according to the growth curve is observed. At the stopping time of the fermentation process, the pH value indicates results that the process is finished, the number of lactic microorganisms is at the peak of development, because they consume lactose as an

energy source, and as a result the pH value decreases. The results obtained for the yogurt samples during fermentation varied in each sample, P2 ($5.31 \pm 0.002 - 4.28 \pm 0.003$), P3 ($5.27 \pm 0.003 - 4.25 \pm 0.001$), and P4 ($5.19 \pm 0.002 - 4.27 \pm 0.003$) relative to P1 ($5.63 \pm 0.003 - 4.38 \pm 0.002$).

Due to its complex chemical composition [42], goat's or cow's milk [43] used in the yogurt manufacture is an excellent environment for the development of many microorganisms, lactic acid bacteria having favorable conditions. Goat's milk compared to cow's milk, in addition to a rich nutritional value, has better antimicrobial properties to pathogenic microorganisms. The antimicrobial properties of goat's milk are exerted by the lactoperoxidase system, which acts as a magnet for iron ions, thus depriving food pathogenic bacteria [44].

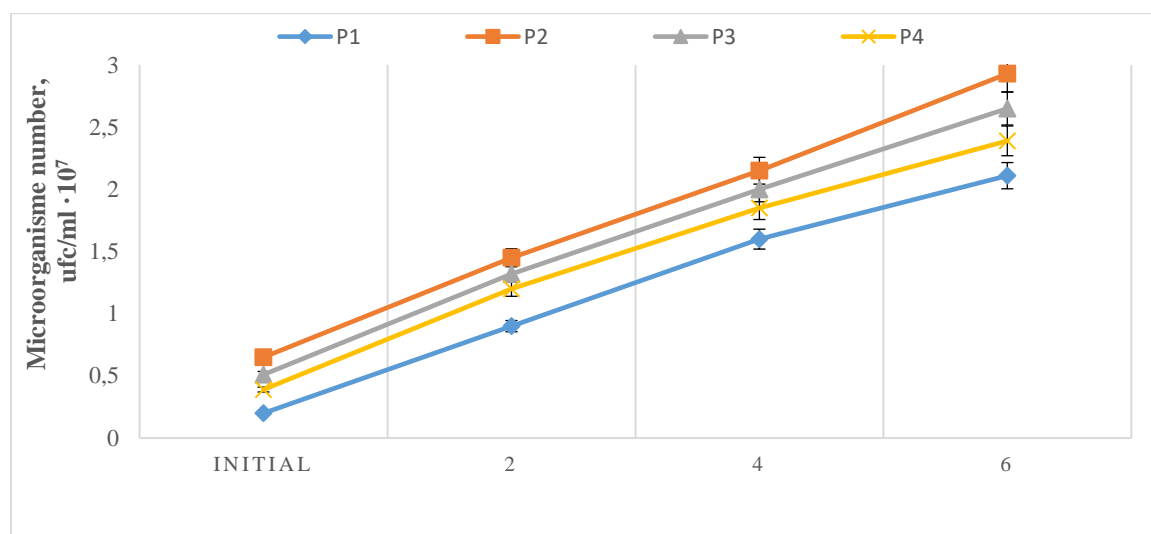


Figure 2. The growth curve of lactic acid bacteria in yogurt.

During fermentation the number of microorganisms increased exponentially and reached a maximum number at 6 hours (figure 2). The results obtained for P2 constitute $0.65 \cdot 10^7 - 2.93 \cdot 10^7$ in relation to the control sample P1- $0.20 \cdot 10^7 - 2.11 \cdot 10^7$, P3 has values of $0.51 \cdot 10^7 - 2.65 \cdot 10^7$, and P4 values of $0.39 \cdot 10^7 - 2.99 \cdot 10^7$. These results can be explained by the fact that the production of hydrogen peroxide by *Lactobacillus bulgaricus* partially damaged *Streptococcus thermophilus* cells and by the symbiotic relationship of *Lactobacillus bulgaricus* and *Streptococcus thermophilus* stimulates the increase in the number of lactic acid bacteria [45].

Accumulation of lactic acid bacteria in fruit yogurt

The yield of lactic acid production is the main indicator of the starter cultures activity, which is dependent on the biotechnological properties, but also on the physico-chemical and biological conditions [46]. The lactic acid accumulation reduces the ionization of the acidic functions of casein. The caseins average isoelectric point leads to the neutralization of electric charges, the sequestering power of α_s and β caseins against minerals decreases and the solubilisation of calcium and micellar phosphate takes place [47].

The difference in the lactic acid bacteria growth rate in the researched samples is probably due to the fact that the addition of berries constitutes an improvement of the bacterial growth medium. It was found that, in the control sample, the growth rate of lactic acid bacteria during the fermentation period for 6 h was P1 - 0.83μ and for P2 - 0.95μ , P3 - 0.93μ , respectively P4 - 0.90μ .

Table 2

Accumulation of lactic acid bacteria in fruit yogurt				
Fermentation time / Evaluated parameters	P1	P2	P3	P4
<i>Initial (0h)</i>				
Lactic acid quantity, $g.dm^{-3}$	2.53±0.02	3.36±0.02	2.79±0.03	2.49±0.02
A_{opt}, λ_{600nm}	0.084±0.007	0.058±0.005	0.047±0.006	0.092±0.005
<i>2h</i>				
Lactic acid quantity, $g.dm^{-3}$	14.13±0.03	16.90±0.02	15.12±0.03	14.60±0.01
A_{opt}, λ_{600nm}	0.161±0.007	0.215±0.005	0.175±0.003	0.136±0.006
Growth monitoring, μ	0.21	0.35	0.29	0.30
<i>4h</i>				
Lactic acid quantity, $g.dm^{-3}$	35.15±0.02	37.56±0.01	36.85±0.02	35.86±0.03
A_{opt}, λ_{600nm}	0.450±0.035	0.821±0.031	0.758±0.030	0.652±0.032
Growth monitoring, μ	0.51	0.78	0.76	0.72
<i>6h</i>				
Lactic acid quantity, $g.dm^{-3}$	68.18±0.02	81.56±0.03	80.94±0.02	79.64±0.02
A_{opt}, λ_{600nm}	0.961±0.025	1.526±0.028	1.428±0.030	1.400±0.026
Growth monitoring, μ	0.83	0.95	0.93	0.90

This share that lactic acid bacteria growth is due to both: the relevant berries chemical composition and the pH reduction of the fermentation medium [48, 49].

The Pearson correlation [50] between the pH and the lactic acid bacteria growth in the fermentation process in the classic yogurt samples and with the berries addition was calculated.

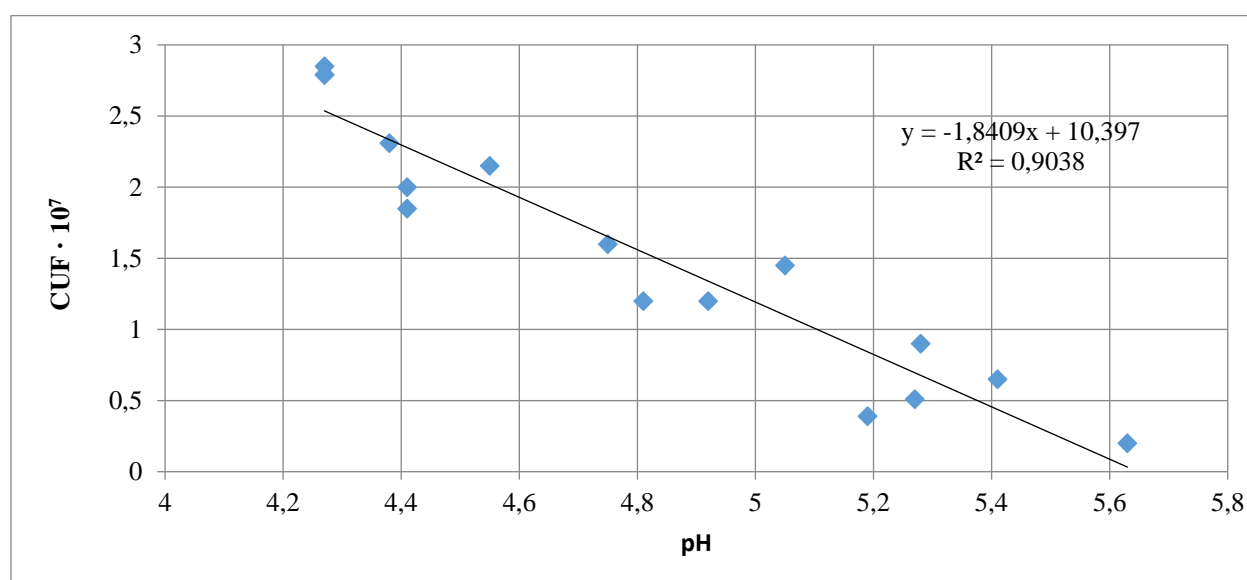
A high correlation was found - close relationship between variables, inversely proportional, because the values were obtained negative.

The results are presented in Table 3 and Figure 3.

Table 3

Pearson correlation between fruit yogurt fermentation parameters

Fermentation time, h	P1		P2		P3		P4	
	MC·10 ⁷	pH	MC·10 ⁷	pH	MC·10 ⁷	pH	MC·10 ⁷	pH
0 (initial)	0.2	5.63	0.65	5.41	0.51	5.27	0.39	5.19
2	0.9	5.28	1.45	5.05	1.2	4.92	1.2	4.81
4	1.6	4.75	2.15	4.55	2	4.41	1.85	4.41
6	2.31	4.38	2.85	4.27	2.79	4.27	2.79	4.27
Pearson coefficient Pc = f(pH and MC)	-0.99672		-0.99436		-0.9782		-0.96873	
General Pearson coefficient for all fruit yogurt samples -0.95066								

*Microbial counts (x10⁷ CFU/ml)**Figure 3.** The interdependence between pH and the lactic acid bacteria number in fruit yogurt.**Analysis of the fruit yogurt physico-chemical indices.**

In this research were studied the fruit yogurt physico-chemical indices. Measuring the yogurt titratable acidity (°T) is a valuable determining practice that must correlate with the additions introduced [51]. The added scald fruits had a great impact on the acidity values. Higher values were obtained for P3 - 98 ± 0.082 °T for P4 - 91 ± 0.079 °T and lower acidity for P2 - 85 ± 0.078 °T, as fruits contain more acid than milk, compared to P1 - 75 ± 0.080 °T (control sample). After fermentation, the maximum pH value was detected in P2 - 4.28 ± 0.002 , this pH may be caused by the buffering action of higher proteins and minerals present in yogurt. The lower value was obtained for sample P4 - 4.27 ± 0.003 and P3 - 4.25 ± 0.002 , possibly determined by the metabolic activity that persists during refrigeration [52], responsible for this decrease in yogurt pH values. The pH of sample P1 is 4.30 ± 0.003 which fits perfectly into the usual pH range of classic yogurt after fermentation (4.0-4.4).

The amount of water available to microorganisms is characterized by a_w . The water activity (a_w) measurement forms the product basis and provides information on the microorganisms growing possibility or on the product. As the water activity value is between 0.8 - 1, then we have a perishable product with a risk of rapid microorganisms development. The water activity differs in each sample, respectively showing the following values: P2 (0.875 ± 0.025), P3 (0.873 ± 0.028) and P4 (0.872 ± 0.023) compared to P1 (0.869 ± 0.021). The results obtained are due to the potential acting as a solvent and participating in chemical / biochemical reactions and the microorganisms growth [53].

Table 4

Physico-chemical indices of fruit yogurt

Indices	Yogurt Samples			
	P1	P2	P3	P4
Titrate acidity, °T	75±0,080	85±0,078	98±0,082	91±0,079
pH	4.30±0,003	4.28±0,002	4.25±0,002	4.27±0,03
A_w	0.869±0,021	0.875±0,025	0.873±0,028	0.872±0,023
Total dry matter, %	17.57±0,22	18.45±0,31	18.28±0,26	18.11±0,28
Viscosity, mPa·s	1250±0,027	2500±0,023	1906±0,022	1829±0,026
Ash content, %	0.65±0,12	0.89±0,10	0.79±0,12	0.69±0,10
Protein content, %	3.98±0.052	3.96±0.05	3.94±0.04	3.93±0,04

Total dry matter plays a significant role in developing the desired yogurt consistency. There were differences in the total solids content of the yogurt samples. The highest value was recorded in the case of sample P2 ($18.45 \pm 0.31\%$). This result indicated that dry matter increased compared to classic yogurt ($17.57 \pm 0.22\%$) with the addition of scald aronia fruit, and casein was in the isoelectric state in which the activity of water particles decreased, not affecting the hydrolysis effectiveness [54]. For the sample P3 and P4 were obtained $18.28 \pm 0.26\%$ and $18.11 \pm 0.28\%$ respectively.

Different technological factors influence the rheological properties of yogurt, such as: heat treatment of milk, incubation temperature, the type of culture used and the cooling process. The structure of yogurt gel is a proteins network formed during acid gelation [55]. The gel formation during the yogurt manufacture occurred due to the unstable casein complex that coagulated easily [56]. The viscosity of all fruit yogurt samples showed satisfactory values. Sample P2 recorded the highest values 2500 ± 0.023 mPa·s, because it has a firmer and well-formed curd than the other samples, due to the higher total dry matter content and the increase of the consistency index, process explained by the ratio of casein fractions to the ratio of casein: serum protein in raw materials. This confirms that the aronia addition contributes more to the whey retention in the gel structure and to the stable gel formation over time as a result of its arrangement in the protein network [57]. As a result of these findings, sample P3 indicates values of 1906 ± 0.022 mPa·s, sample P4 values of 1829 ± 0.026 mPa·s compared to values of sample P1 - 1250 ± 0.027 mPa·s.

Mineral salts have a high nutritional value and have an important influence in the technological processes where the milk coagulation phases take place. The addition of scald aronia, raspberry and strawberry has led to an increase in the yoghurt ash content [58]. The ash content changed in each sample, maximum values were obtained for P2 - $0.89 \pm 0.10\%$ and lower values for P3 - $0.79 \pm 0.12\%$, P4 - $0.69 \pm 0, 10\%$ in relation to P1 - $0.65 \pm 0.12\%$.

Protein [59] plays a key role in the yogurt nutritional and technological value. The values obtained for the protein content in yogurt samples were slightly influenced by the addition of scald fruit (Table 3).

Microbiological indices analysis of fruit yogurt

Yogurt production raises a large number of questions for microbiological safety technologies: how to prevent contamination with microorganisms, what to do with microorganisms that cannot be eliminated by various processing operations, how to preserve taste, texture and ensure durability of acceptable validity. In most "problematic" cases these are yeasts, fungi, heterofermentative lactobacilli [60].

Yeast [61] and mold [62] are agents of yogurt microbial spoilage. They may be present in yoghurt due to contamination during manufacturing, including added prepared fruit, from packaging materials. Overall, yogurt should contain 10^7 cfu / ml of viable bacteria [63].

Table 5

Microbiological indices of fruit yogurt

	P1	P2	P3	P4
MC, ufc/ml·10 ⁷	2,11± 0.17	2,93± 0.30	2,65± 0.25	2,39± 0.28
Yeast, ufc/1 g, max	Absent	Absent	Absent	Absent
Mold, ufc/1 g, max	Absent	Absent	Absent	Absent

Previous research [64 - 67], indicates that aronia, raspberry and strawberry have bactericidal and bacteriostatic effects on pathogenic and conditionally pathogenic microorganisms such as: *Salmonella*, *L. monocytogenes*, *E. coli*, *Klebsiella*, *Bacillus sp.* From the data presented in table 4 it results that the berries form a synergism in the control of the microbiological risk and the stability of the yogurt in storage.

The results of research [68] showed that the combined use of lactic acid bacteria with the berries addition had a synergistic effect, as expected, on the risk posed by *Bacillus bacteria* in food. Aronia was the most effective natural preservative, from the tested fruits, to prevent the damage of yogurt from cow's and goat's milk by *Bacillus*.

The effect of storage on the fruit yogurt physico-chemical indices

Titrateable acidity

Titrateable acidity describes the freshness of the yogurt, especially during storage. Milk acidification leads to the destruction of the internal structure of casein mycelium due to the solubilization of k-casein. During storage, due to the upward fermentation process, the titrateable acidity of fruit yogurt increases (figure 4). During the yogurt samples storage, the following data were recorded (minimum and maximum): 75 ± 0.080 - 82 ± 0.085 °T for P1, 85 ± 0.078 - 92 ± 0.080 °T for P2, 98 ± 0.082 - 105 ± 0.083 °T P3 and 91 ± 0.079 - 100 ± 0.081 °T P4. These results indicate that yogurt is a favorable environment for the lactic acid bacteria development [69]. The aronia, strawberry and raspberry fruits introduced in yogurt have a high acidity, thus leading to an increase in titrateable acidity compared to the control sample but maintaining it in the range of permissible values according to [70].

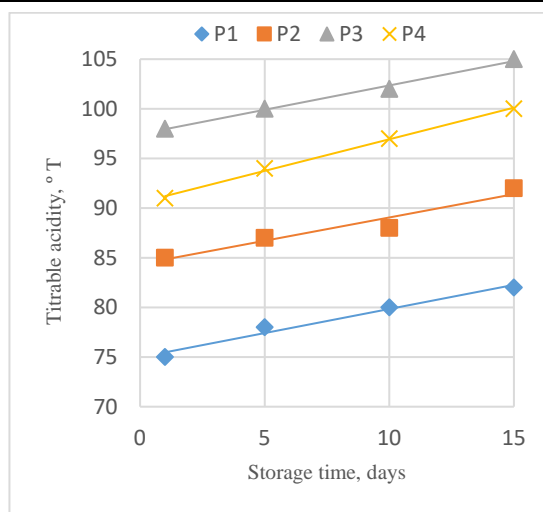


Figure 4. The evolution of the fruit yogurt titratable acidity on stored.

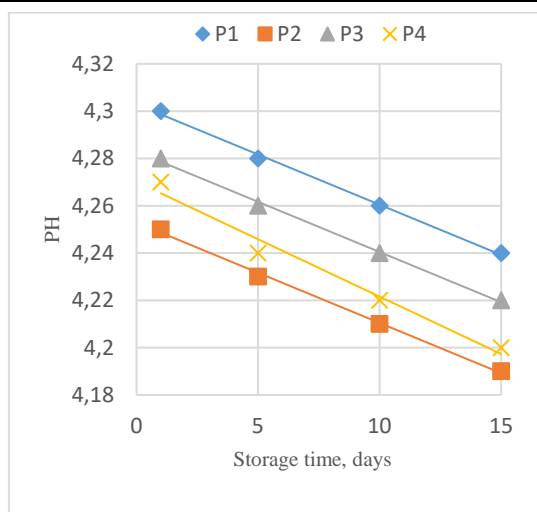


Figure 5. The evolution of the fruit yogurt pH on stored.

pH

The role of pH monitoring in the yogurt manufacture is crucial. PH measurement is considered a sensitive tool to detect changes in the yogurt active acidity. Some technological stages (heat treatment, fermentation, cooling) have a major influence in the finished product pH values during storage. Refrigeration temperature is responsible for lowering the fruit yogurt samples pH during storage. Analyzing the results presented in Figure 5, we observe differences in the pH values of fruit yogurt and the classic one after the first storage day. Initial pH values in yogurt samples vary, 4.28 ± 0.002 for P2, 4.27 ± 0.003 for P4, 4.25 ± 0.002 for P3 front of 4.30 ± 0.03 at P1. The change in pH during storage showed slightly decreasing values within 1 day 4.28 ± 0.002 and on day 15 4.22 ± 0.004 in P2, at sample P3 in 1 day the pH indicates results of 4.25 ± 0.002 and on the 15th day 4.19 ± 0.003 , at sample P4 in 1 day the pH indicates values of 4.27 ± 0.003 and at 15 days 4.20 ± 0.004 compared to sample P1 with values on 1 day 4.30 ± 0.002 and on the 15th day 4.24 ± 0.003 . Similar results, decreased pH values and increased titratable acidity values for yogurt samples during storage were also obtained by [71, 72, 73].

Lactic acid

In the mixed culture, between the lactic bacteria, cooperation relations are established that positively influence the growth of the other [74]. The production of lactic acid by *Lactobacillus bulgaricus* is stimulated at low concentrations of formic acid produced by *Streptococcus thermophilus* in the absence of oxygen and CO₂ released by fermentation [75]. *Streptococci* grow faster and are responsible for acidity while *lactobacilli* add flavour mainly due to the formation of acetic aldehyde. Through their activity, *lactobacilli* that have peptidase activity produce nitrogen compounds, assimilable for *streptococci*, which explains the synergistic relationship between *streptococci* and *lactobacilli* in the yogurt manufacture [76].

Optical density (λ , nm) is one of the important physico-chemical methods for evaluating the microorganism's growth and development. In the goat's milk nutrient medium [77] all strains are characterized by higher acidification rate - 4.4-7.7 hours, compared to cow's milk medium [78] - 4.6-9.3 hours.

Table 6

Indicators of fruit yogurt lactic fermentation					
Samp les nr.	Time, days	Titrate acidity , °T	pH	Lactic acid, g	Optical density, 600 nm
P 1	1	75±0.080	4.30±0.002	0.02167±0.025	1.146±0.058
	5	78±0.083	4.28±0.003	0.02908±0.026	1.232±0.055
	10	80±0.081	4.26±0.002	0.03569±0.023	1.331±0.052
	15	82±0.085	4.24±0.003	0.04980±0.027	1.466±0.053
P2	1	85±0.078	4.28±0.002	0.09782±0.027	2.531±0.054
	5	87±0.081	4.26±0.004	0.10719±0.025	2.613±0.055
	10	88±0.083	4.24±0.003	0.11563±0.031	2.873±0.053
	15	92±0.080	4.22±0.004	0.12250±0.028	2.922±0.056
P3	1	98±0.082	4.25±0.003	0.08855±0.028	2.241±0.056
	5	100±0.084	4.23±0.002	0.10599±0.025	2.519±0.059
	10	102±0.081	4.23±0.003	0.10989±0.028	2.765±0.057
	15	105±0.083	4.21±0.003	0.11512±0.026	2.868±0.051
P4	1	91±0.079	4.27±0.003	0.06215±0.028	2.162±0.058
	5	94±0.082	4.24±0.004	0.07656±0.029	2.391±0.053
	10	97±0.083	4.22±0.002	0.09818±0.025	2.692±0.055
	15	100±0.081	4.20±0.004	0.10008±0.026	2.754±0.055

According to the data recorded in Table 6, it is observed that the amount of lactic acid increased during the fruit yogurt storage period. The initial values of lactic acid vary in each sample. In the case of sample P2 the value obtained is 0.09782 ± 0.027 , for sample P3 is 0.08855 ± 0.028 , for sample P4 - 0.06215 ± 0.028 , compared to sample P1 0.02167 ± 0.025 . The change in lactic acid during the storage period showed slightly decreasing values within first day of 0.09782 ± 0.027 and on the 15th day of 0.12250 ± 0.028 in P2, for sample P3 in 1 day lactic acid indicates results of 0.08855 ± 0.028 and on the 15th day of 0.11512 ± 0.026 , for sample P4 in 1 day lactic acid indicates values of 0.06215 ± 0.028 and at 15 days of 0.10008 ± 0.026 compared to P1 with values at 1 day of 0.02167 ± 0.025 and on the 15th day of 0.04980 ± 0.027 . As the number of microorganisms increased, yogurt optical density increased in all samples. For sample P2 the results indicate values increasing at 1 day of 2.531 ± 0.054 nm and to the 15th day of 2.922 ± 0.056 nm, for P3 - 1 day of 2.241 ± 0.056 nm to the 15th of 2.868 ± 0.051 nm, for P4 - 1 day of 2.162 ± 0.058 nm to a 15th day of 2.754 ± 0.055 nm, compared to P1 - 1 day 1.146 ± 0.058 nm to the 15th day of 1.466 ± 0.053 nm. The rise in titratable acidity and the decline in pH was due to the activity of lactic acid bacteria to produce energy [79] through the fermentation process and by breaking the substrate into simpler components. At the same time, the intensive growth of bacteria did not lead to excessive lactic acid accumulation, favorably influenced the physico-chemical parameters of yogurt [80].

The effect of storage on the fruit yogurt microbiological quality

In the manufacture of yogurt, it is very important to facilitate the survival of the initial bacteria [81]. The viability of beneficial bacteria depends on the availability of nutrients, the

presence of growth promoters and / or inhibitors, sugar concentration, oxygen, incubation temperature, fermentation time and storage temperature [82].

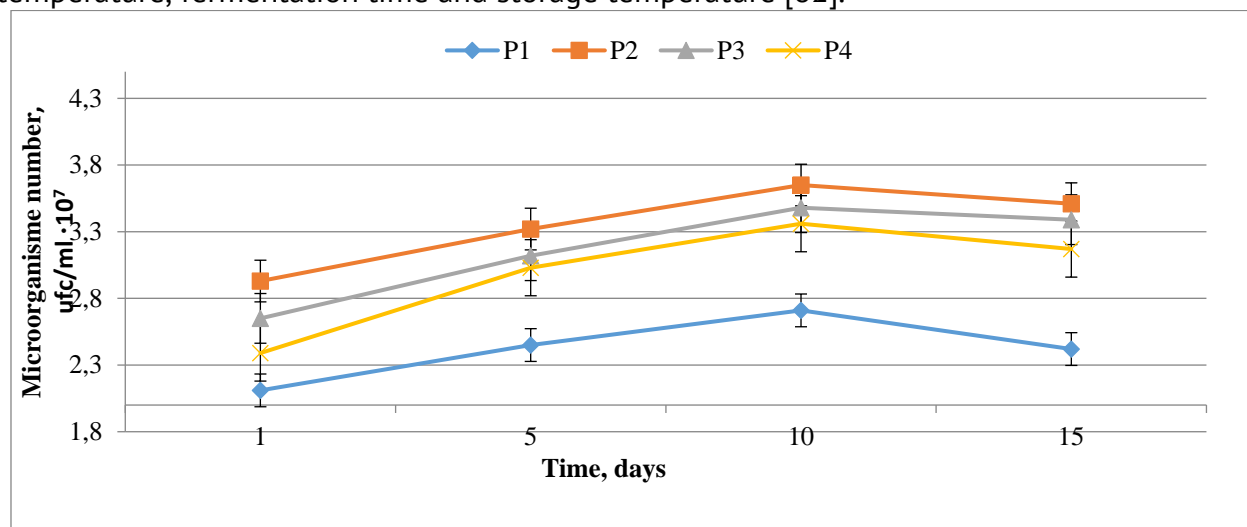


Figure 6. Yogurt lactic bacteria variation in storage.

In a standard environment with fructose or sucrose there is a microorganism's growth inhibition in the mixed culture. Moreover, such an inhibition could be partly due to the osmotic pressure and chemical composition of fruits containing fruit-oligo-saccharide (FOZ) [83].

The results obtained for the variation of fruit yogurt lactic bacteria are satisfactory during the storage period of 1 - 15 days at a temperature of 4 ° C and fall within the values stipulated in the normative documents [84]. During storage the lactic acid bacteria number increased, the values being between $2.93 \cdot 10^7 \pm 0.30$ and $3.51 \cdot 10^7 \pm 0.29$ for sample P2, between $2.65 \cdot 10^7 \pm 0.30$ and $3.39 \cdot 10^7 \pm 0.29$ for sample P3, between $2.39 \cdot 10^7 \pm 0.30$ and $3.17 \cdot 10^7 \pm 0.29$ for sample P4 compared to sample P1 $2.11 \cdot 10^7 \pm 0.30$ and $2.42 \cdot 10^7 \pm 0.29$. Such results suggested that berries have a strong effect by modulating the survival capacity of lactic acid bacteria, when simple sugars such as fructose and glucose were consumed almost entirely during fermentation [85], aronia having the greatest barrier role, in which the loss of lactic acid bacteria was the least reduced.

Conclusion

Based on the experimental study, it was shown that berries have a relevant composition in biologically active substances, have antimicrobial properties and form a synergism with starter culture in goat's and cow's milk yogurt with scald berries. The incorporation of aronia is highlighted by the best results of physico-chemical and microbiological indices in the initial phase and during storage period, compared to classic yogurt. The average Pearson correlation ($P_c = f(\text{pH and MC})$) for the yogurt samples tested was -0.95066.

Acknowledgments: This work was supported by Moldova State project 20.80009.5107.09 Improvement of food quality and safety by biotechnology and food engineering.

References

1. Rezac S., Kok C.R., Heermann M., Hutkins R. Fermented foods as a dietary source of live organisms. In: *Frontiers in Microbiology*, 2018, 9, pp. 1785.

2. Xiang H., Sun-Waterhouse D., Waterhouse G.I., Cui C., Ruan Z. Fermentation-enabled wellness foods: A fresh perspective. In: Food Science Human Wellness, 2019, 8, pp. 203 – 243.
3. Jesch E.D., Carr T.P. Food ingredients that inhibit cholesterol absorption. In: Preventive Nutrition and Food Science, 2017, 22, pp. 67.
4. Phelan M., Kerins D. The potential role of milk-derived peptides in cardiovascular disease. In: Food and Function, 2011, 2, pp. 153 – 167.
5. Garcia-Burgos M., Moreno-Fernandez J., Alferez M.J., Diaz-Castro J., Lopez-Aliaga I. New perspectives in fermented dairy products and their health relevance. In: Journal of Functional Foods, 2020, 72, pp. 104059.
6. Qian B., Xing M., Cui L., Deng Y., Xu Y., Huang M., Zhang S. Antioxidant, antihypertensive, and immunomodulatory activities of peptide fractions from fermented skim milk with *Lactobacillus delbrueckii* subsp. *bulgaricus* LB340. In: Journal of Dairy Research, 2011, 78, pp. 72.
7. Melini F., Melini V., Luziatelli F., Ficca A.G., Ruzzi M. Health-promoting components in fermented foods: An up-to-date systematic review. In: Journal of Nutrients, 2019, 11, pp. 1189.
8. Sanlier N., Gokcen B.B., Sezgin A.C. Health benefits of fermented foods. In: Critical Reviews in Food Science and Nutrition, 2019, 59, pp. 506 – 527.
9. Shiby V.K., Mishra H.N. Fermented milk and milk products as functional foods—A review. In: Critical Reviews in Food Science and Nutrition, 2013, 53, pp. 482 – 496.
10. Hill D., Sugrue I., Arendt E., Hill C., Stanton C., Ross R.P. Recent advances in microbial fermentation for dairy and health. In: F1000Research, 2017, pp. 6.
11. Pappalardo G., Lusk J. The role of beliefs in purchasing process of functional foods. In: Food Quality and Preference, 2016, 53, pp. 151–158.
12. Tamang J.P., Shin D.H., Jung S.J., Chae S.W. Functional properties of microorganisms in fermented foods. In: Frontiers in Microbiology, 2016, 7, pp. 578.
13. Tamang J.P., Cotter P.D., Endo A., Han N.S., Kort R., Liu S.Q., Mayo B., Westerik N., Hutkins R. Fermented foods in a global age: East meets West. In: Comprehensive Reviews in Food Science and Food Safety, 2020, 19, pp. 184 – 217.
14. Penas E., Martinez-Villaluenga C., Frias J. Sauerkraut. Production, composition, and health benefits. In: Fermented Foods in Health and Disease Prevention, In: Academic Press: Cambridge, MA, USA, 2017, pp. 557 – 576.
15. Abdalla O.M., Abdel Nabi Ahmed S.Z. Chemical Composition of Mish "A Traditional Fermented Dairy Product" from Different Plants during Storage. In: Pakistan Journal of Nutrition, 2010, 9, pp. 209 - 212.
16. Routray W., Mishra H., N. Scientific and Technical Aspects of Yogurt Aroma and taste: A Review, 2011, In: Comprehensive Reviews in Food Science and Food Safety, 10, pp. 208 - 220.
17. Nile S.,H., Park S.,W. Edible berries: bioactive components and their effect on human health. In: Journal of Nutrition, 2014, 30, pp. 134 – 144.
18. Kulling, S.,E., Rawel, H.,M. Chokeberry (*Aronia melanocarpa*)-A review on the characteristic components and potential health effects. In: Planta Medica, 2008, 74, pp. 1625 – 1634.
19. Giampieri F., Forbes-Hernandez T.Y., Gasparrini M., Alvarez-Suarez J.M., Afrin S., Bompadre S., Quiles J.L., Mezzetti B., Battino M. Strawberry as a health promoter: In: Food an Function, 2015, 6, pp. 1386 – 1398.
20. Caruso M.C., Galgano F., Tolve R., Pecora M., Tedesco I., Favati F., Condelli N. Nutraceutical properties of wild berry fruits from Southern Italy. In: Journal of Berry Research, 2016, 6, pp. 321 - 332.
21. Valcheva-Kuzmanova, S.V.; Belcheva, A. Current knowledge of *Aronia melanocarpa* as a medicinal plant. In: Journal of Folia Medica, 2005, 48, pp. 11–17.
22. Wang S.Y., Lin H.-S. Antioxidant activity in fruits and leaves of blackberry, raspberry and strawberry varies with cultivar and developmental stage. In: Journal of Agricultural and Food Chemistry, 2000, 48, pp. 140 – 146.
23. ISO/TS 11869| IDF/RM 150:2012 – Fermented milks – Determination of titratable acidity – Potentiometric method
24. Powitz R.W. (2007), Water activity: a New Food Tool. *Sanitarin's file*
25. Determination of the total solids content (Reference method). SM EN ISO 5534:2004/AC:2017
26. Brookfield DV3T *Viscometer Operating Instructions Manual*, No. M13–2100–A0415
27. Baraem P., Ismail *Food Analysis Laboratory Manual*. Determination of ash content. Editor: Springer International Publishing, 2017.
28. Association of Official Analytical Chemists. Official Methods of Analysis, Washington, DC, USA. In: 18 th edition, 2006.
29. Graph Pad Software Inc. Graph Pad Prism 4.00 for Windows. San Diego, California, 2006.

30. Lambert RJW, Pearson J. Susceptibility testing: accurate and reproducible minimum inhibitory concentration (MIC) and noninhibitory concentration (NIC) values. In: Journal of Applied Microbiology. 2000, 88, pp. 784 - 790.
31. Keiran S., et al. General calibration of microbial growth in microplate, 2016, Readers Scientific Reports, 6, nr. 38828
32. Sandulachi E., Bulgaru V. *Microbiologia industrială. Îndrumar metodic*. [Industrial microbiology. Methodical guidance]. Editura Tehnica-UTM, Chişinău. 2019, 68p.
33. Alan D. Welman, Ian S. Maddox, 2003, Exopolysaccharides from lactic acid bacteria: perspectives and challenges, In: TRENDS in Biotechnology, 21, pp. 269 – 274.
34. American Public Health Association, Standard Methods for the Examination of Dairy Products, 1978, 14th Ed., Washington D.C.
35. Kask S., Adamberg K., Orłowski A., Vogensen F.K., Møller P.L., Ardö Y., Paalme T. In: Food Research International, 2003, 36, pp. 1037 – 1046.
36. Guzun V. Tehnologia laptelui şi a produselor lactate. Lucrări de laborator şi practice. [Milk and dairy technology. Laboratory and practical work]. Editura CIVITAS, Chişinău, 2010.
37. SM EN ISO 4833-2:2014/AC:2017 Microbiology of the food chain. Horizontal method for the enumeration of microorganisms.
38. AOAC Official Method 2014.05 Enumeration of Yeast and Mold in Food. 2015 AOAC INTERNATIONAL.
39. Hassan, A., Amjad, I. Nutritional evaluation of yoghurt prepared by different starter cultures and their physiochemical analysis during storage. In: African Journal of Biotechnology, 2010, 9, pp.2913-2917.
40. Vieco-Saiz N., Belguesmia Y., Raspoet R., Auclair E., Gancel F., Kempf I., Drider D. Benefits and inputs from lactic acid bacteria and their bacteriocins as alternatives to antibiotic growth promoters during food-animal production. In: Frontiers in Microbiology, 2019, 10, pp. 57.
41. Mastanjevic K., Kovacevic D., Frece J., Markov K., Pleadin J. The effect of autochthonous starter culture, sugars, and temperature on the fermentation of Slavonian Kulen. In: Food Technology and Biotechnology, 2017, 55, pp. 67 – 76.
42. Mehta B.M. Chemical composition of milk and milk products. In: Handbook of Food Chemistry, 2015, pp. 511 – 553.
43. Kücükçetin, A., M. Demir, A. Asci, E. M. Comak. Graininess and roughness of stirred yogurt made with goat's, cow's or a mixture of goat's and cow's milk. Short communication. In: Journal of Small Ruminant Research, 2011, 96, pp. 173– 177.
44. Essione E. Lactic acid bacteria contribution to gut microbiota complexity: Lights and shadows. In: Frontiers in Cellular and Infection Microbiology, 2012, 2, pp. 86.
45. Vukotic G., Strahinic I., Begovic J., Lukic J., Kojic M., Fira D. Survey on proteolytic activity and diversity of proteinase genes in mesophilic lactobacilli. In: Journal of Microbiology, 2016, 85, pp. 33–41.
46. Bintsis T. Lactic acid bacteria as starter cultures: An update in their metabolism and genetics. In: AIMS Microbiology, 2018, 4, pp. 665.
47. Juturu V., Wu, J.C. Microbial production of lactic acid: The latest development. In: Critical Reviews in Biotechnology, 2016, 36, pp. 967–977.
48. Sandulachi E. *Окислительно-восстановительные свойства клубники и малины*, LAMBERT. [Redox properties of strawberries and raspberries], Academic Publishing, SIA Omni Scriptum Publishing, Latvia, 2018, p.109.
49. Ghendov-Moşanu A. *Compuşi biologici activi de origine horticolă pentru alimente funcţionale*. [Biologically active compounds of horticultural origin for functional foods] Editura Tehnica– UTM, Chişinău, 2018.
50. Immink, K. Schouhamer, Weber, J. Minimum Pearson distance detection for multilevel channels with gain and / or offset mismatch. In: IEEE Transactions on Information Theory, 2010, 60(10), pp. 5966 – 5974.
51. Bennama R., et al. Effect of fermentation conditions (culture media and incubation temperature) on exopolysaccharide production by *Streptococcus thermophilus* BN1. In: International Conference on Biology, Environment and Chemistry IPCBEE, 2011, 24, pp. 433 - 437.
52. Degeest B., Mozzi F., De Vuyst L. Effect of medium composition and temperature and pH changes on exopolysaccharide yields and stability during *Streptococcus thermophilus* LY03 fermentations. In: International Journal of Food Microbiology, 2002, 79, pp. 161 – 174.
53. Sanduachi E. *Activitatea apei în produsele alimentare: Monografie*. [Water activity in food products: Monograph.] Editura Tehnica-UTM, Chişinău, 2020.

54. Amatayakul T., F. Sherkat N. P. Shah. Syneresis in Set Yogurt as Affected by EPS Starter Cultures and Levels of Solids. In: International Journal of Dairy Technology, 2006, 59, pp. 216 - 221.
55. Sahana N., Yasarb K., Hayaloglu A.A. Physical, chemical and flavour quality of non-fat yogurt as affected by ab-glucan hydrocolloidal composite during storage. In: Food Hydrocolloids, 2008, 22, pp. 1291 – 1297
56. Amal, A., Matter, E., Mahmoud, A. M., Nahla, S., Zidan S. Fruit Flavored Yoghurt: Chemical, Functional and Rheological Properties. In: International Journal of Environmental & Agriculture Research, 2016, 2(5), pp. 57 - 66.
57. Chrubasik C., Li G., Chrubasik S. The clinical effectiveness of chokeberry: A systematic review. In: Phytotherapy Research, 2010, 24, pp. 1107 – 1114.
58. Boghra V.R., Mathur O.N. Physico-chemical status of major milk constituents and mineral at various stages of shrikhand preparation, In: Journal of Food Science Technology, 2000, 37, pp. 111 - 115.
59. Cui J., Dalgleish D., Singh H. Effect of homogenization and heat treatment on the behavior of protein and fat globules during gastric digestion of milk. In: Journal of Dairy Science, 2017, 100, pp. 36 – 47.
60. Papagianni M. Metabolic engineering of lactic acid bacteria for the production of industrially important compounds. In: Computational and Structural Biotechnology Journal, 2012, 3, pp. 8.
61. Lourens-Hattingh A., Viljoen B.C. Growth and survival of a probiotic yeast in dairy products. IN: Food Research International, 2001, 34(9), pp.791-796.
62. Li S., Marquardt R. R., Abramanson D. Immunochemical detection of molds: a review. In: Journal of Food Protection, 2000, 63, pp. 281–291.
63. Hasan M.N., Sultan M.Z., Mar-E-Um M. Significance of fermented food in nutrition and food science. In: Journal of Science Research, 2014, 6, pp. 373–386.
64. Sandulachi E., Cojocari D., Balan G., Popescu L., Ghendov-Moşanu A., Sturza R. Antimicrobial Effects of Berries on *Listeria monocytogenes*. In: Journal of Food and Nutrition Sciences, 2020, 11, pp. 873 - 886.
65. Sturza R., Sandulachi E., Cojocari D., Balan G., Popescu L., Ghendov-Moşanu A., Antimicrobial properties of berry powders in cream cheese, In: Journal of Engineering Science, 2019, 3, pp. 125 - 136.
66. Bulgaru V., Sandulachi E. *Prevenirea alterării produselor lactate acide cu bacterii din genul Bacillus (teze)*. Conferința Științifico-Practice Națională „INOVAȚIA: FACTOR AL DEZVOLTĂRII SOCIAL-ECONOMICE”, Facultatea de Economie, Inginerie și Științe Aplicate a Universității de Stat „Bogdan Petriceicu Hasdeu” din Cahul. 2020.
67. Cojocari D., Sandulachi E., Ghendov Moşanu A., Sturza, R. *Proprietățile antimicrobiene ale fructelor de pădure - metoda standard kirby-bauer disc (teze/rezumat)*. Conferința Științifico-Practice Națională „INOVAȚIA: FACTOR AL DEZVOLTĂRII SOCIAL-ECONOMICE”, Facultatea de Economie, Inginerie și Științe Aplicate a Universității de Stat „Bogdan Petriceicu Hasdeu” din Cahul, 2020.
68. Sandulachi E., Bulgaru V., Ghendov-Mosanu A., Sturza R., Controlling the Risk of Bacillus in Food Using Berries, In: Food and Nutrition Sciences, 2021, 12, pp. 557 - 577.
69. Pollard J., Kirk S.F.L., Cade J.E. Factors affecting food choice in relation to fruit and vegetable intake: A review. In: Nutrition Research Reviews, 2002, 15, pp. 373 – 387.
70. Biswas S., Chowdhury A.R. Development of ready to serve beverage with the inclusion of herbal components. In: International Journal of Latest Trends in Engineering and Technology, 2019, 8, pp.147–154.
71. Ochimian I., Grajowski J., Smolik M. Comparison of some morphological features, quality and chemical content of four cultivars of chokeberry fruits (*Aronia melanocarpa*). In: Notulae Botanicae Horti Agrobotanici Cluj-Napoca, 2012, 40(1), pp. 253–260.
72. Chee C.P., Gallaher J.J., Djordjevic D., Faraji H., McClements D.J., Decker E.A., Hollender R., Peterson D.G., Roberts R.F., Coupland J.N. Chemical and sensory analysis of strawberry-flavoured yogurt supplemented with an algae oil emulsion. In: Journal of Dairy Research, 2005, 72(3), pp. 311 - 316.
73. Karovicova J., Kohajdova Z. Lactic acid fermented vegetable juices. In: Horticultural Science, 2003, 30, pp. 152 – 158.
74. Mokoena M.P. Lactic acid bacteria and their bacteriocins: Classification, biosynthesis, and applications against uropathogens: A mini-review. In: Journal of Chemistry. Molecules, 2017, 22, pp. 1255.
75. Barrangou R., Alterman E., Hutkins R., Cano R., Klaenhammer. Functional and comparative genomic analyses of an operon involved in fructooligosaccharide utilization by *Lactobacillus acidophilus*. In: Proceedings of the National Academy of Sciences, 2003, 100, pp. 8957- 8962.
76. De Vrese M., Schrezenmeir J. Probiotics Prebiotics and Synbiotics. In: Advances in Biochemical Engineering/Biotechnology, 2008, 111(1), pp. 66.

77. Sandulachi E., Bulgaru V. Factor affecting quality of goat's milk yoghurt, In: *Advances in Social Sciences Research journal*, 2019, 6(2), pp. 205 – 221.
78. Fruscalso V. *Influence of the diet allowance, parity and lactation stadium on the physical-chemical and microbiological properties of the bovine milk and the occurrence of unstable not acid milk*. Master's Dissertation, 2007.
79. Chammas G. I., Saliba R., Corrieu G., Béal, C. Characterisation of lactic acid bacteria isolated from fermented milk "laban". In: *International Journal of Food Microbiology*, 2006, 10, pp. 52 – 61.
80. Shah N. P. Probiotic bacteria: Selective enumeration and survival in dairy foods. In: *Journal of Dairy Science*, 2000, 83, pp. 894 – 907.
81. Aleksandrak-Piekarczyk T., Mayo B., Fernandez M., Kowalczyk M., Alvarez-Martin P., Bardowski J. Updates in the Metabolism of Lactic Acid Bacteria. In: *Biotechnology of Lactic Acid Bacteria: Novel Applications*, 2015, 3, pp. 33.
82. Endo A., Dicks L.M.T. Physiology of the LAB In: *Lactic Acid Bacteria: Biodiversity and Taxonomy*, 2014, pp. 13 – 30.
83. Neves A.R., Pool W.A., Kok J., Kuipers O.P., Santos H. Overview on Sugar Metabolism and Its Control in *Lactococcus lactis* - the Input from in Vivo NMR. In: *FEMS Microbiology Review*, 2005, 29, pp. 531 – 554.
84. GD No. 158 of 07-03-2019, Regarding the approval of the Quality Requirements for Milk and Dairy Products. Official Gazette No. 111 - 118 art. 218, Annex 4, [in Romanian].
85. Barat A., Ozcan T. Growth of probiotic bacteria and characteristics of fermented milk containing fruit matrices. In: *International Journal of Dairy Technology*, 2018, 71, pp. 120 – 129.

[https://doi.org/10.52326/jes.utm.2021.28\(3\).14](https://doi.org/10.52326/jes.utm.2021.28(3).14)
CZU 638.165.8:581.331.2(478)



PALYNOLOGICAL, PHYSICO-CHEMICAL AND BIOLOGICALLY ACTIVE SUBSTANCES PROFILE IN SOME TYPES OF HONEY IN THE REPUBLIC OF MOLDOVA

Aurica Chirsanova*, ORCID ID: 0000-0002-1172-9900,

Tatiana Capcanari, ORCID ID: 0000-0002-0056-5939,

Alina Boistean, ORCID ID: 0000-0002-5374-5853

Technical University of Moldova, 168 Stefan cel Mare Blvd., MD-2004, Chişinău, Republic of Moldova

*Corresponding author: Aurica Chirsanova, aurica.chirsanova@toap.utm.md

Received: 07. 10. 2021

Accepted: 08. 28. 2021

Abstract. Three types of monofloral honey (rapeseed honey, buckwheat and lavender) from the Republic of Moldova were analyzed. The results of the palynological analysis showed that the samples had a dominant type of pollen (at least 45%). In the case of lavender honey, the pollen of the plant *Lavandula angustifolia* is present in an average value of 74.83 ± 0.3 ; in rapeseed honey - *Brassica napus* and for buckwheat honey - *Fagopyrum esculentum* in average values as follows: 56.07 ± 0.3 and $68.08 \pm 0.2\%$ respectively. The study of the content of biologically active substances showed that buckwheat honey is the richest in polyphenols (9.00 ± 0.11 mg gallic acid / kg) and carotenoids (4.24 ± 0.57 mg β carotE / kg), and maximum content of flavonoids is in rapeseed honey (4.52 ± 0.28 mg catechin / kg). Thus, the obtained results confirm that the honey from the Republic of Moldova falls within the limits recommended by the international regulation assuming adequate working conditions, handling, collection and storage of honey by beekeepers from the Republic of Moldova.

Keywords: honey, palynological analysis, physico-chemical properties, biologically active substances.

Introduction

The importance of beekeeping

For many years, honey was the only sweetener available, being an important food for Homo Sapiens since its inception [1], but the relationship between bees and human began in the Stone Age. During the evolution of mankind, bee honey was a valuable food product. Very often it was a commercial currency and had a high price. Some taxes could be paid with bee honey [2]. There has always been a strong connection between humans and bees. This relationship is largely based on the fact that 80% of the world's plants are pollinated by bees [3]. Beekeeping is becoming a key occupation for generating additional income for rural people, especially in developing countries [4]. It does not take a lot of capital to practice

beekeeping. This form of activity has a low maintenance and generates good income in a short period of time. [5, 6].

Beekeeping has the unique ability to contribute to the achievement of 15 of the 17 goals mentioned by the United Nations Sustainable Development Goals and among the most important goals are: eradication, poverty and hunger, contributing to maintaining health and a healthy lifestyle, achieving sustainable production and consumption systems, developing entrepreneurship, gender equality and others [7].

Characteristic of the beekeeping sector in the Republic of Moldova

Agriculture is one of the vectors of image of the Republic of Moldova and is a strategic sector of national importance, whose operation takes place under the social, climatic and economic impact, but also other specific factors, which determine the uniqueness of this sphere [8, 9].

In the context of its aspirations to become a member of the European Union, reforms in the agri-food sector must comply with EU regulations, which will allow it to adapt to the demands of international markets, especially in the field of food safety, security and authenticity. In this context, the report entitled "Evaluation of the National Food Control System of the Republic of Moldova [10] presented by the FAO [11] shows that in the agri-food sector, it is necessary to strengthen relations between producers, processors, exporters, representatives of academia and institutes. research to ensure the sustainability and authentication of food.

Among the agricultural crops that provide bees with nectar and pollen are sunflower, rapeseed and buckwheat, which are grown on large areas, so bees participate in their pollination by influencing the quality and quantity of seeds obtained.

The surfaces of the fruit plantations from the agricultural enterprises and the peasant households represent 44,323 ha, and for their pollination approximately 132,969 bee families are necessary.

In the Republic of Moldova during the years 2008 - 2017 was reported a slight increase in the number of bee families, their number ranging from 98.3 thousand in 2008 to 148.1 thousand pieces, in 2017, 1.51 times higher. Currently, over 5,250 apiaries have passports.

Honey on the market of the Republic of Moldova

The cost of producing one kilogram of honey in the Republic of Moldova depends largely on the amount of honey obtained, which is closely related to climatic conditions and is in the range of 1.65 - 1.80 US dollars in the case of a "normal" year.

According to a study conducted by the Organization for Investment Attraction and Export Promotion of Moldova in 2012, the annual costs of operating a hive are around US \$ 58. The honey-commodity productivity of bee families is around 24 kg / season, being closely dependent on the annual climatic conditions [12].

Compared to neighboring countries, the volume of exports to the European Union of the Republic of Moldova is relatively small.

At the same time, the quality of local honey is high (especially the glucose / fructose ratio), although its price is not highly competitive compared to the main competitors - Ukraine, China and Argentina. Thus, for the Republic of Moldova the opportunity to access the market is the sale of quality honey, including organic [13].

Honey export from Republic of Moldova

Maximum 15% of the total volume of honey produced in the Republic of Moldova is consumed locally. The main distribution channel consists of friends, neighbors and relatives of beekeepers.

The price of honey sold to individuals is twice as high as the wholesale price offered by large intermediaries. However, low wholesale prices as well as high production costs stop investment in the honey production sector.

The remaining about 85% of production volume is currently exported. For our country, the main market is that of the European Union, which assimilates over 90% of exported honey, and in 2015 the ratio was 98%. The main destinations of local honey are Italy, Germany, France, Slovakia, as well as some smaller, but still considerable markets such as Romania, Poland, Denmark, etc. (Table 1) [14].

Tabel 1

Export of honey from the Republic of Moldova in tons and thousands of US dollars [9]

Destination	2016		2017		2018		2019	
	Quantity, tons	Value, thousands of US dollars	Quantity, tons	Value, thousands of US dollars	Quantity, tons	Value, thousands of US dollars	Quantity, tons	Value, thousands of US dollars
Total	3 160,3	8 844,7	5 010,5	14 049,9	94 123,5	11 740,8	3 888,9	11 584,5
Including EU countries:								
Italy	632,5	1 887,0	867,7	2 680,4	784,2	2 523,5	923,8	3 055,6
Germany	535,9	1 370,1	445,3	1 176,4	424,8	1 090,5	264,7	705,0
France	336,0	1 106,8	756,0	2 205,5	546,0	1 601,7	525,0	1 651,0
Slovakia	251,1	700,5	468,9	1 439,7	471,8	1360,2	660,1	1 794,9
Romania	822,5	2 304,9	1 490,9	3 928,1	619,9	1 671,3	645,9	1 893,5
Poland	46,9	122,2	181,9	487,1	442,7	1 391,7	129,0	541,0
Danemark	60,3	140,4	-	-	-	-	-	-
Austria	121,2	288,5	80,0	153,1	-	-	21,0	55,5
Belgium	102,3	226,3	-	-	-	-	21,0	53,2
Other countries of the world:								
Macedonia	126,0	319,5	168,0	417,1	252,0	604,6	63,0	151,3

The Republic of Moldova exported a record amount of honey worth \$ 14.0 million in 2017. Exports increased from 245 tons in 2006 to 5010 tons in 2017. Honey is the only animal product that is exported to the EU, as it meets import requirements from EU third countries for products of animal origin. To achieve this, it is necessary to demonstrate that the country has a "residue monitoring mechanism" established for the analysis of honey for residues of antibiotics, sulphonamides, pesticides and heavy metals, as defined in the veterinary standard on measures for the supervision and control of certain substances and their residues in live

animals and their products, as well as of residues of veterinary medicinal products in products of animal origin, approved by Government Decision no. 298/2011 (harmonized with the provisions of Council Directive 96/23 / EC of 29 April 1996 on measures to monitor certain substances and their residues in live animals and animal products (EU OJ of 23 May 1996, L 125 , p. 10).

Adulteration and physico-chemical characteristics of honey

Adulteration of honey is generally a major concern of consumers but also of honest producers. Honey adulteration has been a challenge for analysis for decades. Adulteration has been used to increase economic benefits by adding honey or sugars at reduced prices during production or processing. In addition, these food adulterants are often unique, so they avoid being detected by routine tests [15]. In previous studies, various methods have been used to test the authenticity of honey, such as near-infrared spectroscopy, anion exchange chromatography coupled with pulsed amperometric detection [16], nuclear magnetic resonance [17, 18] high performance liquid chromatography [19, 20] Fourier transform infrared spectroscopy [21] and the ^{13}C / ^{12}C isotope ratio analysis method [22, 23].

The composition of bee honey represents is a natural, very complex mixture containing various chemical compounds. These compounds give bees honey important biological properties, such as the ability to promote wound healing [24], antimicrobial and anti-inflammatory capacity [25]. Antioxidant capacity is associated with its content of antioxidant compounds, such as polyphenols [26].

Its antimicrobial properties are associated, in particular, with the osmotic properties of bee honey, as well as with the presence of hydrogen peroxide and other minor compounds without peroxide, such as polyphenols and a special protein known as defensin-1 [27, 28].

The purpose of this study was to demonstrate the authenticity of honey by palynological analysis and to highlight the physico-chemical composition and biologically active compounds of some types of honey in the Republic of Moldova.

2. Materials and methods

This study was conducted using honey declared by beekeepers to be buckwheat, rapeseed and lavender purchased from local producers in Chisinau. The research was conducted between November 2020 and January 2021 in the laboratories of the Department of Food and Nutrition of the Faculty of Food Technology of the Technical University of Moldova. During the research, the honey samples were kept in laboratory conditions, packed in sealed glass jars at a temperature of 21 ± 2 ° C.

Palynological analysis

It was performed by microscopic analysis according to the method of Lutier and Vaissière (1993) [29,30].

Humidity

Mass fraction of water was determined using Honey humidity refractometer ATAGO 4422 PAL-22S, 12.0 to 30.0 %, acc. $\pm 0.2\%$.

Determination of pH

The pH of the samples was measured potentiometrically at 20 ° C. The pH meter was used (HANNA HI9124, Germany). The research solutions were prepared by dissolving 1 g of bee honey in 10 ml of distilled water.

Determination of Acidity

Free acidity was determined by titrimetric method. It is based on the titration of the honey sample diluted with water, with 0.1 n NaOH in the presence of phenolphthalein as indicator.

Diastase index

The basis of this method is the determination of amylase activity. The diastase index is defined as the number of milliliters of starch solution (1%) which has been converted to dextrin for one hour at temperature 45 ° C at the optimum pH of amylase containing 1 g of sample.

Hydroxymethylfurfural content

The Fiehe reaction is based on the fact that the hydroxymethylfurfural forms with the resorcinol, in hydrochloric acid medium, a complex colored in red, whose color intensity is proportional to the quantity of the respective compound. When the Fiehe reaction is positive, the honey is considered suspicious and the deconfirmation test is further performed by determining the hydroxymethylfurfural content.

Determination of total sugar content

The honey bees were dissolved in distilled water to obtain a 25% (w / v) solution. The total sugar content of the honey samples was determined using the refractometric method (portable refractometer ATAGO PAL-22S, Japan). The sucrose content was expressed in g / ml of honey.

Reducing sugar

To determine the reducing sugar (by the Elser method) it was taken into account that glucose and fructose, in the free state, have the ability to reduce copper sulfate in an alkaline and hot environment, which it transforms into copper oxide. The amount of copper oxide that is formed under specific working conditions is proportional to the concentration of the two reducing sugars in the solution to be researched.

Sucrose content

For the determination of sucrose (by Elser method) the direct reducing sugar was determined before and after inversion (acid hydrolysis), and from the difference sucrose is calculated.

Determination of flavonoids

The total flavonoid content was determined using the colorimetric method [31]. Sample of 1 ml bee honey was mixed with 4 ml of distilled water. 0.3 ml of NaNO₂ (5%, w / v) was added. After 5 min, 0.3 mL of AlCl₃ (10% w / v) was added. This was followed by the addition of 2 mL of NaOH (1N) 6. The volume of the mixture was adjusted to 10 ml by the addition of 2.4 ml of distilled water. The composition was stirred (VORTEX V-1 plus, BioSan) to ensure a homogeneous mixture. The absorbance was read at 510 nm. Results were expressed as mg equivalent of catechin (CEQ) per kg of honey.

Determination of total polyphenol contents

Total polyphenol contents were determined using the Folin-Ciocalteu colorimetric method [40]. The honey sample solution (0.1 mL) was mixed with Folin-Ciocalteu reagent (0.5 mL) and Na₂CO₃ (0.4 mL of 7.5%), and the absorbance was measured at wavelength 765 nm after 10 min at temperature 37°C. Total polyphenol contents were expressed as mg GAE gallic acid equivalents /100 g honey.

Determination of total carotenoid content

The total carotenoid content was determined spectrophotometrically a previously published method [32]. The absorbance was determined at wavelength 450 nm. The results were expressed as mg of β -carotene equivalents (β carotE) per kg of honey (mg β carotE / kg of honey).

Statistical Analyses

All analyzes were performed in triplicate, and the results were expressed as mean values with standard deviations (SD).

The significant differences represented by letters were obtained by a one-way analysis of variance (ANOVA) followed by Tukey's honestly significant difference (HSD) post hoc test ($p < 0.05$). Correlations were established using Pearson's correlation coefficient (r) in bivariate linear correlations ($p < 0.01$). These treatments were carried out using Microsoft office Excel 2007 and SPSS v. 18.0 program.

3. Results

Palynological analysis of honey

One of the fundamental criteria for the quality of honey that influences its commercial value is the declaration of botanical and geographical origin.


The results of the analysis of the pollen profile of honey allow us to determine the floral origin of honey and to confirm the identity of the honey source indicated by beekeepers. The pollen grains identified and their frequency in the three types of honey analyzed are shown in Table 2.

The results of the quantitative pollen analysis showed that the samples always had a dominant pollen type (at least 45%) and can be classified as monofloral thus confirming the name declared to the consumer as follows: buckwheat honey, rapeseed honey and lavender honey.


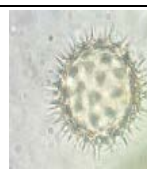
Monofloral status usually means the presence of pollen of the same type in the amount of more than 45% of the total pollen content in the sample.

We notice that in the analyzed samples the content of a single type of pollen is much higher than: the minimum figure in the case of lavender honey is present the pollen of the plant *Lavandula angustifolia* in average value of 74.83 ± 0.3 ; for rapeseed honey - *Brassica napus* pollen and for buckwheat honey the dominant pollen *Fagopyrum esculentum* is present in average values as follows: 56.07 ± 0.3 and $68.08 \pm 0.2\%$.

Table 2

Palynological characteristic						
The type of honey declared	Pollen type					Examples of images of dominant pollen
	Sunflower (<i>Helianthus annuus</i>)	Acacia (<i>Robinia pseudo acacia</i>)	Rapeseed (<i>Brassica napus</i>)	Buckwheat (<i>Fagopyrume sculentum</i>)	Lavender (<i>Lavandula angustifolia</i>)	
Buckwheat (n=5)						
Presence	3 S, 2 IM	2 IM, 3 S		5 PM	5 M	
%	53.5, 46.7	13.3, 86.7		100	100	
average± SD	22.4±0.1	8.47±0.3		68.08±0.2	1.05±0.1	

Continuation Table 2

Rapeseed (n=5)					
Presence	3 IM, 2 M	2 IM, 3 M	5 PM		
%	53.5, 46.7	13.3, 86.7	100		
average± SD	24,31±0,3	19,62±0,2	56,07±0,3		
Lavender (n=5)					
Presence	2 IM, 3 M	2 M	1 M	5 PM	
%	13.3, 86.7	100	100	100	
average± SD	13,01±0,1	10,11±0,1	2,05±0,2	74,83±0,3	

Note: predominant pollen (>45%) - P; secondary pollen, (16–45%)-S; important minor pollen, (3–15%)-IM; minor pollen, (1–3%)-M.

n = sample size

It should be noted that the pollen *Helianthus annuus* and *Robinia pseudoacacia* is present in all three types of honey analyzed, either as secondary pollen, as important minor pollen or as minor pollen. At the same time, the variations of the nectar content, together with other factors such as climatic and geographical conditions, soil type, practices applied by beekeepers and others, contribute to the existence of different types of honey and imprint their botanical origin [33 - 35].

Physico-chemical characteristics of the samples

Table 3 presents the physico-chemical parameters of the types of honey from the Republic of Moldova under study. Depending on the borane origin of honey, significant differences were observed in some of the physico-chemical parameters ($p < 0.05$).

The moisture content of *Apis mellifera* honey is well defined by international quality standards [36]. A high moisture content in honey can affect both its quality and its biological activity and organoleptic properties [37]. According to the results obtained, all honey samples examined were within acceptable limits. It is known that the moisture content of honey also depends on the ecological and geographical conditions, the maintenance of the apiary and the storage of the finished product [38, 39]. Thus, the results obtained suggest adequate working conditions, processing, collection and storage of honey by beekeepers from the Republic of Moldova.

Table 3

Physico-chemical parameters				
	Rapeseed (n=5)	Buckwheat (n=5)	Lavender (n=5)	Mean
Humidity %	22,0±0,01	15,60±0,02	17,00±0,01	18,2± 0,03
Ash, %	0,9±0,03	1,1±0,06	0,17±0,02	0,72±0,04
pH	3,32±0,10	3,48±0,11	3,68±0,04	3,49±0,08
Total acidity, cm ³	9,98±0,03	22,09±0,01	7,11±0,01	13,06±0,17
Hydroxymethylfurfural (mg/kg of honey)	70,81 ± 0,06	13,78 ± 0,04	27,16 ± 0,03	37,26±0,04
Diastase index (cm ³ /g)	22,13 ± 0,01	19,12 ± 0,03	14,11 ± 0,02	28,45±0,02

Continuation Table 3

Water insoluble matter:			
Cereal flour	Lack	Lack	Lack
Gelatin	Lack	Lack	Lack
Starch	Lack	Lack	Lack

It is known that honey is acidic nature. The values of pH obtained in the honey samples varied between 3.32 and 3.68 and fall within the previously reported values [40, 41].

Hydroxymethylfurfural (HMF) is used as an indicator of honey freshness [42]. In fresh honey, HMF may be absent or in small amounts, while high levels of HMF (> 80 mg / kg) indicate that honey may have been stored and handled in inappropriate conditions, such as abuse of high temperatures [43]. In the three types of honey analyzed, the HMF content was 13.78 ± 0.04 mg / kg for buckwheat honey, 27.16 ± 0.03 mg / kg for lavender honey and 70.81 ± 0.06 mg / kg for rapeseed honey. According to the presented results, all samples from the three types of monofloral honey analyzed were within the recommended limits and were in accordance with international regulations for this type of honey.

The diastatic index ranges from 14.11 ± 0.02 for lavender honey to 22.13 ± 0.01 for rapeseed honey. At the same time for buckwheat, this index is 19.12 ± 0.03 . The mean for the samples under study was 28.45 ± 0.02 . It should be noted that water-insoluble substances (cereal flour, gelatin or starch) were not detected. The presence of impurities in the end product of beekeeping can be introduced during preparation, process of centrifugation or process of packaging. An improper honey filtering process can be a source of insoluble substances in the finished product. Therefore, during this process, honey passes through several sieves [42]. No water-insoluble substances were detected in the analyzed honey. At the same time, the water-insoluble ingredients (at temperature $+80^{\circ}\text{C}$), present in honey, constitute the residue left after filtering the honey solution. High-quality honey should not contain more than 0.1g/100g of insoluble ingredients, except for pressed honey (norm: not more than 0.5g/100g) [44].

Total Sugar Content

None of the samples examined exceeded the maximum sugar content set for the total sugar content (Table 4) by the European Community Directive [44].

Means obtained are compared by using One-way ANOVA. In column, values with different superscripts letters indicate significant differences ($p < 0.05$)

Table 4

Total Sugar Content				
	Rapeseed (n=5)	Buck wheat (n=5)	Lavender (n=5)	Mean
Total sugar content mean \pm SD% (g/mL)	69,82 \pm 1,04 ^a	66,61 \pm 0,42 ^b	61,09 \pm 0,40 ^a	65,84 \pm 0,62
Reducing sugar mean \pm SD (%)	61,12 \pm 0,61 ^a	62,14 \pm 0,51 ^b	67,07 \pm 0,47 ^a	62,44 \pm 0,53
Sucrose mean \pm SD (%)	2,32 \pm 0,61	1,92 \pm 0,76	2,52 \pm 0,21	2,25 \pm 0,53

From the above we can see that the total sugar content is the highest in the samples of rapeseed honey and is 69.82 ± 1.04 g / ml, followed by buckwheat honey with a content of 66.61 ± 0.42 g / ml and then lavender honey with 61.09 ± 0.40 g / ml. Thus, the average total sugar content in the 15 samples analyzed was 65.84 ± 0.62 g / ml.

Bioactive compounds

Polyphenols, flavonoids and carotenoids were present in all samples subjected to the study (table 5).

Table 5

Content of bioactive substances				
	Rapeseed (n=5)	Buckwheat (n=5)	Lavender (n=5)	Mean
Polyphenols				
mean \pm SD (mg gallic acid/kg)	6,20 \pm 0,17 ^a	9,00 \pm 0,11 ^a	5,20 \pm 0,08 ^b	6,8 \pm 0,12
Flavonoids				
mean \pm SD (mg catechin/kg)	4,52 \pm 0,28 ^a	2,09 \pm 0,14 ^b	0,81 \pm 0,19 ^c	2,47 \pm 0,21
Carotenoids				
mean \pm SD (mg β carotE/kg)	2,60 \pm 0,23 ^a	4,24 \pm 0,57 ^b	0,70 \pm 0,31 ^c	2,51 \pm 0,37

Means obtained are compared by using One-way ANOVA. In column, values with different superscripts letters indicate significant differences ($p < 0.05$)

The average polyphenol content was 6.8 ± 0.12 (mg gallic acid / kg), and for buckwheat honey the amount of 9.00 ± 0.11 (mg gallic acid / kg) was identified. The average content of flavonoids was 2.47 ± 0.21 (mg catechin / kg), and for rapeseed honey it was the highest content - 4.52 ± 0.28 (mg catechin / kg). Phenolic acid (non-flavonoids) and flavonoids are responsible for inhibiting oxidation and destroying free radicals. Their identification and classification are based on their chemical structures, which consist of one or more hydroxyl groups which are fused to a closed ring structure and that way produce an aromatic ring containing 6 carbon atoms with hydrogen atoms [45]. The color tone of honey is influenced by both physical and chemical indicators and the botanical origin of honey, which contributes to the diversity of its assortment. Such compounds as polyphenols, carotenes and minerals also affect color of honey [46, 47]. Flavonoids are considered substances with a major effect on chromatic parameters [48, 49]. While collecting nectar, bees transfer these biologically active compounds from plants to honey [50].

Conclusions

This study showed following the palynological analysis that the three types of honey: rapeseed honey, buckwheat and lavender can be classified as monofloral thus confirming the name declared to the consumer. At the same time, the identification of the botanical origin of honey could be a useful tool for differentiating the product, in order to guarantee a better qualitative characterization and its traceability in itself.

It was demonstrated that the physico-chemical properties of the samples under study were within the recommended limits and were in accordance with international regulations for these parameters. The content of biologically active substances: polyphenols, flavonoids

and carotenoids in the studied samples is of great importance, therefore, these types of product can be used as a natural food ingredient, as well as a rich source of antioxidants in the diet of the population.

Acknowledgments: The results of the research presented were carried out within the project «Développement durable de l'apiculture: enjeux économiques, écologiques, de développement rural et de santé publique», which took place during the years 2019-2021. The project was funded by the "Agence Universitaire de la Francophonie en Europe Centrale et Orientale".

References

1. Suvro S. "Honey- The natural sweetener become a promising alternative therapeutic: a review." In: *South Indian Journal of Biological Sciences*, 2015, 1, pp. 103 - 114.
2. Crane E. A Short History of Knowledge about Honey Bees (Apis) up to 1800. In: *Bee World*, 2004, 85 (1), pp. 6 - 11.
Disponibil: <https://doi.org/10.1080/0005772X.2004.11099604>.
3. Baker T.F. *Bees and Beekeeping*, Bloomsbury Publishing, 2021, pp. 94.
4. Hinton J., Schouten C., Austin A., Lloyd D. An Overview of Rural Development and Small-Scale Beekeeping in Fiji. In: *Bee World*, 2020, 97 (2), pp. 39 - 44.
Disponibil: <https://doi.org/10.1080/0005772X.2019.1698104>.
5. Altunel T., Olmez B. Beekeeping as a Rural Development Alternative in Turkish Northwest. In: *Appl. Ecol. Environ. Res.* 2019, 17 (3), pp. 6017 - 6029. Disponibil: https://doi.org/10.15666/aeer/1703_60176029.
6. Pocol Cristina Bianca, Sedik Peter, Brumă Ioan Sebastian, Amuza Antonio, Chirsanova Aurica. Organic beekeeping practices in Romania: Status and perspectives towards a sustainable development. In: *Agriculture (Switzerland)*. 2021, nr. 4(11), pp. 1 - 18. ISSN 2077-0472.10.3390/agriculture11040281
Disponibil: <https://doi.org/10.3390/agriculture11040281>
7. Patel V., Pauli N., Biggs E., Barbour L., Boruff B. Why Bees Are Critical for Achieving Sustainable Development. In: *Ambio*, 2021, 50 (1), pp. 49 - 59.
Disponibil: <https://doi.org/10.1007/s13280-020-01333-9>.
8. Asociația Exportatorilor de Produse Apicole din Moldova (AEPAM)
Disponibil: <https://honeymoldova.md/about-hea/>
9. Eremia N., Modvala S., Naraevscaia I. Dinamica efectivului familiilor de albine și a suprafețelor pomilor fructiferi în Republica Moldova, Universitatea Agrară de Stat din Moldova, CZU 638.124(478)
Disponibil: <http://particip.gov.md/proiectview.php?l=ro&idd=4687#?l=ro&idc=507>
10. Chirsanova Aurica, Reșitca Vladislav. Factori de bază ce influențează politicile alimentare și nutriționale la nivel internațional. *Meredian ingineresc*. Univestitatea Tehnică a Moldovei. Nr. 3, 2013, ISSN 1683-853X. p.86-92.
Disponibil: https://ibn.idsi.md/ro/vizualizare_articol/27531
11. Chirsanova Aurica, Calcatiniuc Dumitru. The impact of food waste and ways to minimize IT. In: *Journal of Social Sciences*. 2021, nr. 4(1), pp. 128 - 139. ISSN 2587-3490.10.52326/jss.utm.2021.4(1).15
Disponibil: [https://doi.org/10.52326/jss.utm.2021.4\(1\).15](https://doi.org/10.52326/jss.utm.2021.4(1).15)
12. Eremia N., Scripcic E., Modvala S., Chiriac A. Influence of temperature on nectar collection and storage in the hive during honey harvest. University of Agricultural Sciences and Veterinary Medicine Iasi. 2017, pp. 40 - 44.
13. Hotărîrea guvernului Republicii Moldova, Cu privire la aprobarea Programului național de dezvoltare a apiculturii în Republica Moldova pentru anii 2021 - 2025 și a Planului de acțiuni privind implementarea acestuia pentru anii 2021-2022.
Disponibil: <https://gov.md/sites/default/files/document/attachments/subiect-14.pdf>
14. Chirsanova A., Capcanari T., Gîncu E. Jerusalem Artichoke (*Helianthus Tuberosus*) flour impact on bread quality. *Journal of Engineering Science*. Vol. XXVIII, no. 1, 2021, pp. 131 - 143. ISSN 2587-3474. Disponibil: [https://doi.org/10.52326/jes.utm.2021.28\(1\).14](https://doi.org/10.52326/jes.utm.2021.28(1).14)
15. Sobrino-Gregorio L., Vilanova S., Jaime Prohens, J., Escriche, I. Detection of honey adulteration by conventional and real-time PCR, *Food Control*, Volume 95, 2019, Pages 57-62, ISSN 0956-7135, <https://doi.org/10.1016/j.foodcont.2018.07.037>.

16. Wang J., Xue X., Du X. Identification of Acacia Honey Adulteration with Rape Honey Using Liquid Chromatography–Electrochemical Detection and Chemometrics. In: *Food Anal. Methods*, 2014, 7, pp. 2003–2012. Disponibil: <https://doi.org/10.1007/s12161-014-9833-7>
17. Song X., She D., Xin, M., Chen L., Li Y., Vander Heyden Y., Rogers K.M., Chen L. Detection of adulteration in Chinese monofloral honey using ¹H nuclear magnetic resonance and chemometrics, In: *Journal of Food Composition and Analysis*, 2020, 86, 103390, ISSN 0889-1575. Disponibil: <https://doi.org/10.1016/j.jfca.2019.103390>.
18. Fan, K., Zhang, M. Recent developments in the food quality detected by non-invasive nuclear magnetic resonance technology, *Critical Reviews in Food Science and Nutrition*, 2019, 59(14), pp.2202-2213. Disponibil: [10.1080/10408398.2018.1441124](https://doi.org/10.1080/10408398.2018.1441124)
19. Ghramh, H.A., Khan, K.A., Zubair, A., Ansari, M.J. Quality evaluation of Saudi honey harvested from the Asir province by using high-performance liquid chromatography (HPLC). In: *Saudi Journal of Biological Sciences*, 27(8), 2020, pp.2097-2105. Disponibil: <https://doi.org/10.1016/j.sjbs.2020.04.009>.
20. Zhu Z., Zhang Y., Wang J., Li X., Wang W., Huang Z. Sugaring-out assisted liquid-liquid extraction coupled with high performance liquid chromatography-electrochemical detection for the determination of 17 phenolic compounds in honey, In: *Journal of Chromatography A*, 2019, 1601, pp. 104 - 114. Disponibil: <https://doi.org/10.1016/j.chroma.2019.06.023>.
21. Cengiz M.F., Durak M.Z. Rapid detection of sucrose adulteration in honey using Fourier transform infrared spectroscopy, In: *Spectroscopy Letters*, 2019, 52(5), pp. 267 - 273. Disponibil: [10.1080/00387010.2019.1615957](https://doi.org/10.1080/00387010.2019.1615957)
22. Tosun M. Detection of adulteration in honey samples added various sugar syrups with ¹³C/¹²C isotope ratio analysis method, *Food Chemistry*, 2013, 138(2–3), pp. 1629 - 1632. Disponibil: <https://doi.org/10.1016/j.foodchem.2012.11.068>.
23. Geană E.-L., Ciucure C.T., Costinel D., Ionete R.E. Evaluation of honey in terms of quality and authenticity based on the general physicochemical pattern, major sugar composition and $\delta^{13}\text{C}$ signature, *Food Control*, 2020, 109, 106919. Disponibil: <https://doi.org/10.1016/j.foodcont.2019.106919>.
24. Alvarez-Suarez J.M., Giampieri F., Battino M. Honey as a source of dietary antioxidants: Structures, bioavailability and evidence of protective effects against human chronic diseases. In: *Curr. Med. Chem.*, 2013, 20, pp. 621 – 638.
25. Cooper, R. Honey for wound care in the 21st century. In: *J. Wound Care*, 2016, 25, pp. 544 – 552.
26. Cianciosi D., Forbes-Hernández T.Y., Ansary J., Gil E., Amici A., Bompadre S., Simal-Gandara J., Giampieri F., Battino M. Phenolic compounds from Mediterranean foods as nutraceutical tools for the prevention of cancer: The effect of honey polyphenols on colorectal cancer stem-like cells from spheroids, In: *Food Chemistry*, 325, 2020, 126881. Disponibil: <https://doi.org/10.1016/j.foodchem.2020.126881>.
27. Santos-Buelga C., González-Paramás A.M. Chemical Composition of Honey. In *Bee Products—Chemical and Biological Properties*. In: *Springer International Publishing: Cham*, Switzerland, 2017, pp. 43 – 82.
28. Vrabie, V., Yazlovitska, L., Ciochină, V., Rotaru, S. Comparative content of free aminoacids in pollen and honey. In: *Buletin Științific. Revista de Etnografie, Științele Naturii și Muzeologie (Serie Nouă)*, 2019, 30(43), pp. 71 - 78.
29. Chirsanova A., Covaliov E., Capcanari T., Suhodol N., Deseatnicova O., Boistean A., Resitca V., Sturza R. Consumer behavior related to salt intake in the Republic of Moldova. *Journal of Social Sciences*. Vol. III, no. 4, 2020, pp. 101 – 110. DOI: 10.5281/zenodo.4296387 CZU 366:613.2:664.41(478). Disponibil: https://jss.utm.md/wp-content/uploads/sites/21/2021/01/JSS-4-2020-pp_101-110.pdf
30. Palynological analysis of honey, value and quality characteristics Disponibil: <http://honey-land.ru/nauka-o-pchelakh/palinologicheskiiy-analiz-otsenki-botanicheskogo-proiskhozhdeniya-meda.php>
31. Zhishen J., Mengcheng T., Jianming W. The determination of flavonoid contents in mulberry and their scavenging effects on superoxide radicals. In: *Food Chem.*, 1999, 64, pp. 555 – 559.
32. Ferreira I.C.F.R., Aires E., Barreira J.C.M., Estevinho L.M. Antioxidant activity of Portuguese honey samples: Different contributions of the entire honey and phenolic extract. In: *Food Chem.*, 2009, 114, pp. 1438 – 1443.
33. Noviyanto A., Abdulla, W.H. Honey botanical origin classification using hyperspectral imaging and machine learning. In: *Journal of Food Engineering*, 265, 2020, 109684.

- Disponibil: <https://doi.org/10.1016/j.jfoodeng.2019.109684>.
34. Puścion-Jakubik, A., Borawska, M.H., Socha, K. Modern Methods for Assessing the Quality of Bee Honey and Botanical Origin Identification. In: *Foods*, 2020, 9, pp.1028.
Disponibil: <https://doi.org/10.3390/foods9081028>
 35. Machado A.M., Miguel M.G., Vilas-Boas M., Figueiredo A.C. Honey Volatiles as a Fingerprint for Botanical Origin—A Review on their Occurrence on Monofloral Honeys. In: *Molecules*, 2020, 25, pp.374. Disponibil: <https://doi.org/10.3390/molecules25020374>
 36. Boistean Alina, Chirsanova Aurica, Capcanari Tatiana, Siminiuc, Rodica. Evaluation of the color as a characterization parameter of honey from Tunisia, Romania and Moldova. In: *Biotehnologii moderne - soluții pentru provocările lumii contemporane*. 20-21 mai 2021, Chișinău. Chișinău, Republica Moldova: Tipografia "Artpoligraf", 2021, p. 43. ISBN 978-9975-3498-7-1
Disponibil: https://imb.md/sites/default/files/2021-06/Simpozion%20IMB2021%20Publica%C8%9Bii_compressed.pdf.
 37. Chen C. Relationship between Water Activity and Moisture Content in Floral Honey. In: *Foods*, 2019, 8, pp. 30. Disponibil: <https://doi.org/10.3390/foods8010030>
 38. Omczyk M., Tarapatsky M., Dżugan M. The influence of geographical origin on honey composition studied by Polish and Slovak honeys. In: *Czech J. Food Sci.*, 2019, 37, pp. 232 - 238.
 39. Maione R., Barbosa R., Barbosa R.M. Predicting the botanical and geographical origin of honey with multivariate data analysis and machine learning techniques: A review. In: *Computers and Electronics in Agriculture*, 2019, 157, pp.436-446. <https://doi.org/10.1016/j.compag.2019.01.020>.
 40. Matzen, R.D., Leth-Espensen, J.Z., Jansson, T., Nielsen, D.S., Lund, M.N., Matzen, S. "The Antibacterial Effect In Vitro of Honey Derived from Various Danish Flora", *Dermatology Research and Practice*, vol. 2018, Article ID 7021713, 10 pages, 2018.
Disponibil: <https://doi.org/10.1155/2018/7021713>
 41. Boussaid A., Chouaibi M., Rezig L., Hellal R., Donsi F., Ferrari G., Hamdi S. Physicochemical and bioactive properties of six honey samples from various floral origins from Tunisia, In: *Arabian Journal of Chemistry*, 11(2), 2018, pp. 265 - 274.
Disponibil: <https://doi.org/10.1016/j.arabjc.2014.08.011>.
 42. Shapla U.M., Solayman M., Alam N. 5-Hydroxymethylfurfural (HMF) levels in honey and other food products: effects on bees and human health. In: *Chemistry Central Journal*, 2018,12(35). Disponibil: <https://doi.org/10.1186/s13065-018-0408-3>
 43. Pasiakos I.N., Kiriakou I.K., Kaitatzis A., Koutelidakis A.E., Proestos C. Effect of late harvest and floral origin on honey antibacterial properties and quality parameters, *Food Chemistry*, 2018, 242, pp. 513 - 518.
Disponibil: <https://doi.org/10.1016/j.foodchem.2017.09.083>.
 44. Council Directive of the European Union. Council directive 2001/110/ec of 20 december 2001 relating to honey. Off. J. Eur. Communities 2002, pp. 47 - 52.
Disponibil: <https://eur-lex.europa.eu/legal-content/EN/ALL/?uri=CELEX:32001L0110>
 45. She S., Chen L., Song H., Lin G., Li Y., Zhou J., Liu C. Discrimination of geographical origins of Chinese acacia honey using complex ¹³C/¹²C, oligosaccharides and polyphenols. In: *Food Chemistry*, 2019, 272, pp. 580 - 585. Disponibil: <https://doi.org/10.1016/j.foodchem.2018.07.227>
 46. Szabó R.T., Mézes M., Szalai T., Zajác E., Kovács-Weber M. Colour identification of honey and methodical development of its instrumental measuring. In: *Columella J. Agric. Environ. Sci.*, 2016, 3, pp. 29 - 36.
 47. Vela L., De Lorenzo C., Pérez R.A. Antioxidant capacity of Spanish honeys and its correlation with polyphenol content and other physicochemical properties. In: *J. Sci. Food Agric.* 2007, 87, pp. 1069 - 1075.
 48. Combarros-Fuertes P., Valencia-Barrera R.M., Estevinho L.M., Dias L.G., Castro J.M., Tornadijo M.E., Fresno, J.M. Spanish honeys with quality brand: A multivariate approach to physicochemical parameters, microbiological quality, and floral origin. In: *J. Apic. Res.*, 2019, 58, pp. 92 - 103.
 49. Ciappini M.C., Gatti M.B., Di Vito M.V. El color como indicador del contenido de flavonoides en miel. In: *Rev. Cienc. Tecnol.* 2013, 19, pp. 53 - 63.
 50. De Silva P.M., Gauche C., Gonzaga L.V., Costa A.C.O. Honey: Chemical composition, stability and authenticity. In: *Food Chem.*, 2016, 196, pp. 309 - 323.

[https://doi.org/10.52326/jes.utm.2021.28\(3\).15](https://doi.org/10.52326/jes.utm.2021.28(3).15)

CZU 663.252.61:579



DEVELOPMENT OF THE REAL-TIME PCR METHODOLOGY FOR TESTING MYCOTOXIGENIC MICROORGANISMS IN GRAPE MARC

Rodica Sturza¹, ORCID ID: 0000-0002-2412-5874,
Valentin Mitin², ORCID ID: 0000-0001-9328-9672,
Irina Mitina², ORCID ID: 0000-0002-1550-6739,
Dan Zgardan^{1*}, ORCID: 0000-0002-1296-0864,
Antoanela Patras³, ORCID ID: 0000-0002-4054-4884,
Emilia Behta^{1,4}, ORCID ID: 0000-0001-8519-9714

¹Technical University of Moldova, 168 Stefan cel Mare Blvd., Chisinau, RM

²Institute of Genetics, Physiology and Plant Protection, 20 Pădurilor st., Chisinau, RM

³"Ion Ionescu de la Brad" Iasi University of Life Sciences, 3 Mihail Sadoveanu Alea, Iași, Romania

⁴"Nicolae Testemitanu" State University of Medicine and Pharmacy, 165 Stefan cel Mare Bd., Chisinau, RM

*Corresponding author: Dan Zgardan, dan.zgardan@enl.utm.md

Received: 07. 23. 2021

Accepted: 08. 28. 2021

Abstract. Agro-industrial waste management is an important problem of modern society as agriculture and food industry are important sources of waste. Wine production generates a considerable amount of winemaking waste (grape marc). Grape marc can be a source of natural dyes, antioxidants and could have various applications, if it is confirmed that it does not contain technogenic contaminants or unwanted microorganisms, for example, producers of mycotoxins. The paper developed the Real-Time Polymerase Chain Reaction (Real-Time PCR) methodology for testing the presence of potentially mycotoxigenic fungal species capable of producing ochratoxin A (OTA), which could be applied before grape marc processing. Based on the non-ribosomal peptide sequence of OTA, involved in ochratoxin biosynthesis, the primers have been developed for the detection of microorganisms potentially capable of producing ochratoxin A.

Keywords: Mycotoxin, OTA, Real-Time PCR, grape marc, *Aspergillus*, *Penicillium*.

Introduction

Grape marc is a by-product of the vinification process, which constitutes approximately 20-30% of the mass of processed grapes [1]. The rich content of bioactive substances in the composition of grape marc, derived from grape skin, remaining pulp, seeds and stems is an opportunity for its use in the pharmaceutical industry, cosmetics and, especially, in the food industry [2, 3, 4]. The rich content of dietary fiber, up to 85% and polyphenols, up to 70% [5, 6], increased antioxidant activity [7] are important arguments in favor of capitalizing on this byproduct [8, 9]. The recovery of by-products of vinification is also an important issue for the management of agro-industrial waste [10, 11].

Grape marc is usually stored, used as fertilizer or for animal nutrition [12]. The storage and spread of grape mark in the environment can cause damage to the environment, lead to water pollution and, finally, create inconvenience to nearby towns, because due to low pH and the presence of tannins, biodegradation of this byproduct occurs very slowly [13]. The use of grape marc for animal feed is not reasonable, because it is poor in nutrients and the tannins are difficult to digest [14, 15].

At the same time, the recovery of bioactive components from grape marc requires its rigorous control, because, especially in years with precipitation during the ripening period of grapes they can be contaminated with mycotoxins [16]. Mycotoxigenic molds, capable of colonizing grapes, especially affect the skin of the berries, so there are risks that after the vinification process, they remain in the marc. Thus, there are risks of contamination of grape marc, derived products and grape marc extracts with mycotoxins, especially when marc is not processed immediately after the vinification process [17].

In order to ensure the innocuousness of the products obtained from grape marc, it is necessary to check the presence of mycotoxinogenic microorganisms before processing the pomace. Previous research has shown that the Real-Time PCR methodology can be successfully applied for the analysis and quantification of mycotoxigenic fungi in maize [18], as well as for the detection of *Brettanomyces/Dekkera* in wines [19]. The purpose of this research was to develop a rapid method real-time PCR to verify the presence of microorganisms capable of producing mycotoxins in grape marc.

Materials And Methods

Grape marc samples were collected from different geographical zones. Table 1 shows the details of the samples used in this study.

Table 1

Grape marc samples used in this study*			
Sample name	Sample type	Variety of grape/wheat	Sample origin
A2	Grape marc	Feteasca Neagra	Speia, Anenii-Noi
A3	Grape marc	Cabernet-Sauvignon	Popeasca, Stefan-Voda
A4	Grape marc	Cabernet-Sauvignon	Cojusna, Straseni
A6	Grape marc	Cabernet-Sauvignon	Pleseni, Cantemir
A8	Grape marc	Merlot	Salcuta, Causeni
A9	Grape marc	Cabernet-Sauvignon	Abaclia, Basarabeasca
A10	Grape marc	Cabernet-Sauvignon	Tigheci, Leova
A11	Grape marc	Pinot Noir	Taraclia
B12	Wheat grain	Wheat with visual signs of fungal infection	Chisinau, IGPPP*

*Institute of Genetics, Physiology and Plant Protection

Isolation of the DNA

Total deoxyribonucleic acid (DNA) was extracted from wine using SDS-based DNA extraction methods [20] with some modifications. The procedure was carried at the room temperature. Briefly, 0.5 g of grape marc was homogenized to fine powder with 0.5 g of aluminium oxide and resuspended in 4 mL of the Extraction buffer (Tris-HCl 0.2 M pH 8.0, NaCl 0.25 M, Na₂EDTA 0.025 M, SDS 5% w/v) and heated at 65°C for 1 hour. After 10 minute centrifugation at 10000 min⁻¹ the supernatant was transferred to a fresh tube, mixed with an

equal volume of isopropanol and incubated at -20 °C for 30 minutes. The samples were centrifuged, the pellet washed with 70% ethanol, air dried and dissolved in 100 µL of water; 2 µL of the resulting DNA solution was used per polymerase chain reaction (PCR). The qualitative and quantitative verification of the isolated DNA was made by spectrophotometric analyses.

Polymerase Chain Reaction Amplifications

The Real-Time PCR allows precise quantification of specific nucleic acids in a complex solution by fluorescent detection of labeled PCR products. In a Real Time PCR, a positive reaction is detected by accumulation of a fluorescent signal. For the experiments, we used SYBR Green I nonspecific dye as the fluorescent agent. The quantification cycle (C_q) represents the number of cycles required for the fluorescent signal to cross the threshold (i.e., to pass the background level). C_q levels are inversely proportional to the amount of target nucleic acid in the sample. The lower the C_q level the higher is the concentration of target nucleic acid in the sample. We used 40 cycles of amplification [21].

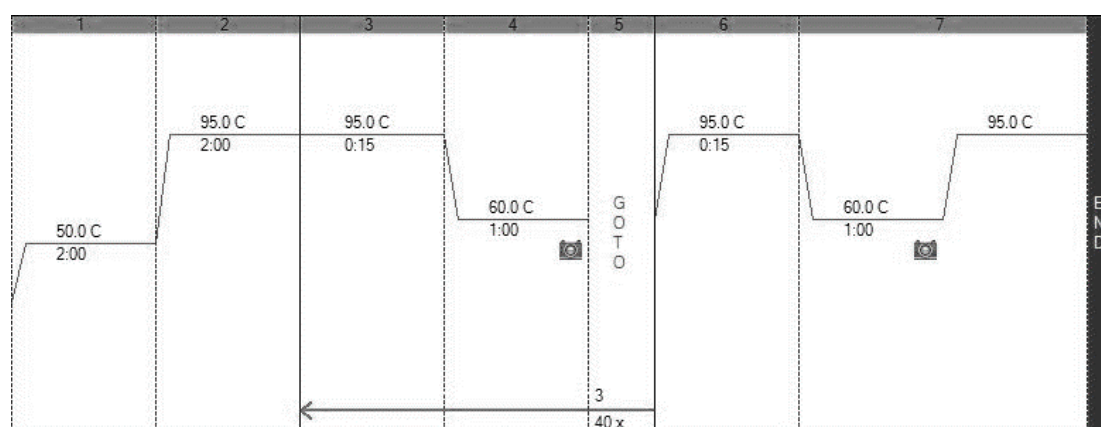


Figure 1. Temperature cycling conditions

In our research Real-Time PCR has been done at Real-Time PCR Detection Systems CFX96 Touch™ BIORAD. PCR conditions were as recommended by SybrGreen producer (Applied Biosystems) - initial incubation at 50 °C for 2 minutes, initial denaturation at 95 °C for 2 minutes, and alternation at 95 °C for 15 seconds and 60 °C for 1 minute for 40 cycles. For melting curve construction, samples were heated at 95 °C for 15 seconds, then incubated at 60°C for 1 minute (1.6 °C/s ramp rate), then heated at 95°C for 15 seconds (0.15°C/s ramp rate). Cycling conditions are shown in Figure 1. The detection was done at SYBR channel.

Results and discussion

During this work, two pairs of primers based on *Vitis vinifera* 26S ribosomal RNA gene sequence were developed. Using these primers in PCR reaction can confirm that the extracted DNA is of PCR quality and is free of PCR inhibitors. Besides, these primers allow normalizing the amount of the input DNA in PCR reaction for estimation of the amount of pathogen DNA relative to plant DNA in different samples.

Though for primer design *Vitis vinifera* 26S ribosomal RNA gene sequence was used, they can recognize a vast number of eukaryotic organisms according to the BLAST analysis. Table 2 shows names, sequences and characteristics of the primers used for detection of eukaryotic DNA in the sample.

The gene bank accession used as a template was DQ667962.1 *Vitis vinifera* 26S ribosomal RNA gene, partial sequence.

Table 2

Primers used for detection of eukaryotic DNA in the sample

Primer name	Orientation	Sequence (5'→3')	Length	T _m	GC%	Self complement	Self 3' complement	Product length
P183	Forward primer	CGGGTAAACGGCGGGAGTAA	20	62.22	60.00	3	1	131
P184	Reverse primer	TGGCTGTGGTTTCGCTGGAT	20	62.41	55.00	2	2	
P185	Forward primer	CCGGAAACGGCGAAAGTGAA	20	61.50	55.00	4	0	150
P186	Reverse primer	GCCAAACTCCCCACCTGACA	20	62.35	60.00	3	3	

Primers for detection of the potential producers of OTA were designed based on the sequence of OTA non-ribosomal peptide synthetase gene. This is a gene involved in OTA biosynthesis. These primers can recognize the following pathogens containing OTA non-ribosomal peptide synthetase gene in their genome, and thus potentially capable of producing OTA: *Aspergillus nidulans*, *Aspergillus tubingensis*, *Aspergillus tamarii*, *Aspergillus niger*, *Aspergillus ochraceus*, *Aspergillus carbonarius*, *Penicillium viridicatum*, *Penicillium carneum*, *Penicillium aurantiogriseum*, *Penicillium melanoconidium*, *Penicillium nordicum*, *Penicillium verrucosum*. Table 3 shows primer names, sequences and characteristics.

Table 3

Primers used for detection of potential OTA producers

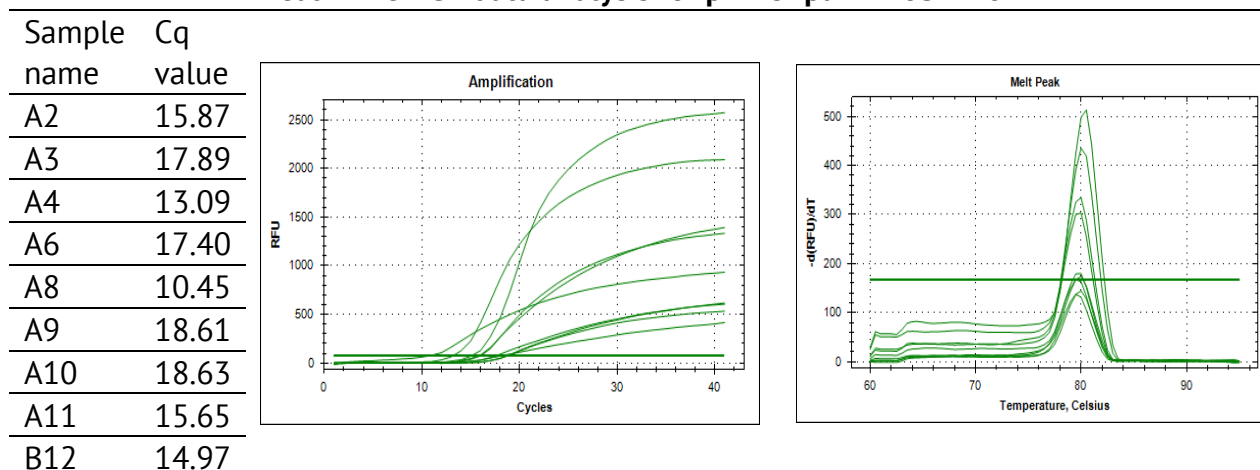
Primer name	orientation	Sequence (5'→3')	Length	T _m	GC%	Self complement	Self 3' complement	Product length
P71	Forward primer	GGCTTCGTGTTGTCCCTTCT	20	60.25	55.00	2	0	97
P72	Reverse primer	GTCCATTCTCGACGTGTTCCA	21	60.34	52.38	4	1	
P73	Forward primer	CATGGTCGTTTGGACGATGTGA	22	61.18	50.00	5	1	155
P74	Reverse primer	CAGCTCGGCTCGATCAACAG	20	61.14	60.00	4	2	
P75	Forward primer	GCCGCAAGGTCAGTGAATGT	20	61.24	55.00	5	1	119
P76	Reverse primer	TGTGGGACTCCACTCAAAGTAAGA	24	61.18	45.83	5	1	
P77	Forward primer	CCGCAAGGTCAGTGAATGTACTC	23	61.47	52.17	5	2	144
P78	Reverse primer	TCGACGTGTTCCATTTCATACCA	24	60.80	41.67	4	0	

The gene bank accession used as a template was GenBank: JN097804.1 *Aspergillus ochraceus* strain CBS 589.68 OTA non-ribosomal peptide synthetase gene, partial cds.

Next, the grape marc DNA samples were analyzed by real-time PCR using the designed primers. In this study, we analyzed 8 grape marc samples of different grape varieties from different zones (Table 1, Materials and Methods). As a positive control for the primers, we used wheat with visible signs of fungal infection, previously shown to contain OTA non-ribosomal peptide synthetase gene. First, the amplificability of DNA from grape marc was tested, using primer pairs p. 183 - 184 and p. 185 - 186. Table 4 shows the results of real-time PCR analysis with primer pair p. 183 - 184.

Table 4

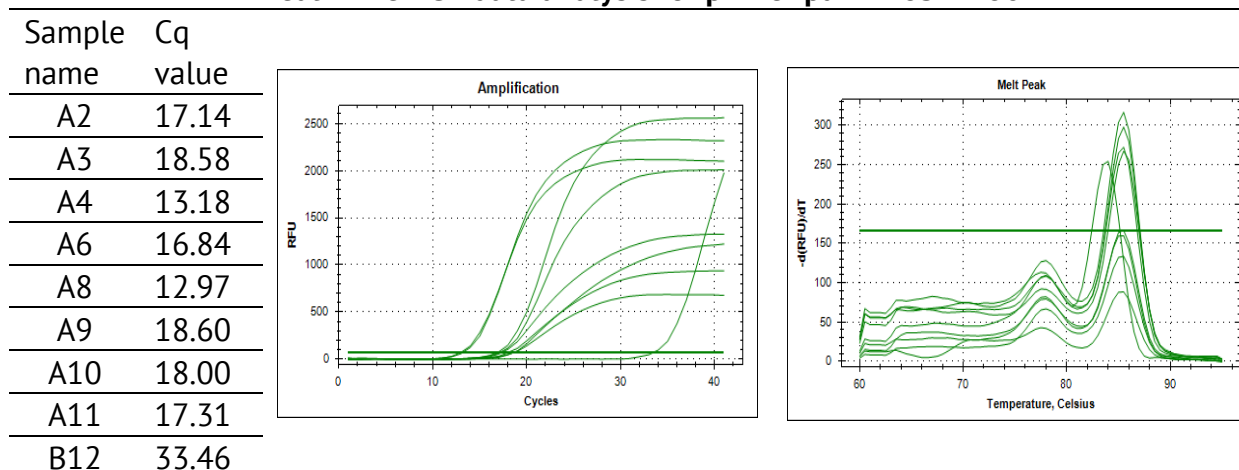
Real-Time PCR data analysis for primer pair P183-P184



These data show that every sample had the DNA template that could be amplified by this primer pair. The Cq values vary from 10.45 in A8 sample to 18.63 in A10 sample. The melting curve shows a single well pronounced peak with similar melt temperature for all samples. This indicates that the amplified fragment is uniform. Table 5 shows the results of real-time PCR analysis with primer pair p. 185 - 186. In this case, the template DNA could as well be amplified by this primer pair. The Cq values vary from 12.97 in A8 sample to 33.46 in B12 sample, table 5. High Cq value for the wheat DNA sample means that the threshold fluorescence level is reached later in this sample. This can be explained by either low DNA content or lower primer affinity to this template.

Table 5

Real-Time PCR data analysis for primer pair P185-P186

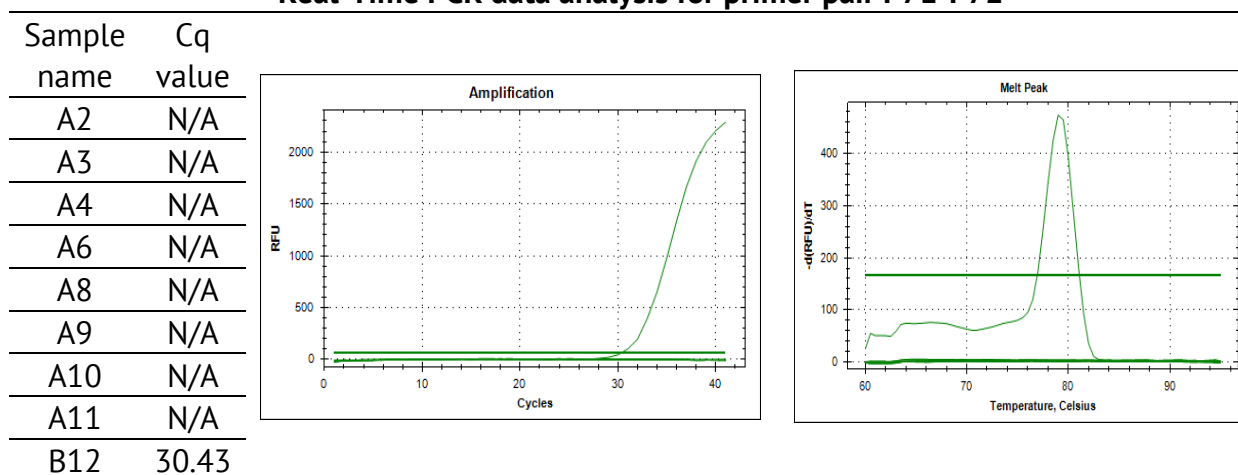


Since the other primer pair p185-186, did not produce such a low Cq value for B12 sample, and since the primers were designed using *Vitis vinifera* gene as a template, one can assume that the higher Cq value is caused by lower affinity of the primer pair p. 185 - 186 to the wheat DNA. Another evidence favoring this explanation is a slightly different melting temperature for the melting peak of B12 (wheat) sample. Anyways, both primer pairs showed amplification in all analyzed samples, confirming that the analyzed DNA is of PCR quality.

Next, we analyzed the same samples using primers to *ochratoxin A non-ribosomal peptide synthetase gene* to detect potential OTA producer in the grape marc. Table 6 shows the results of Real-Time PCR analysis with primer pair p71-p72.

Table 6

Real-Time PCR data analysis for primer pair P71-P72



As one can see from the Table 6, no signal was obtained for either grape marc sample. The only positive signal obtained in this experiment was for B12 (wheat) control, with the Cq value 30.43. The melt curve shows a single well pronounced peak indicating that a single fragment is amplified in the PCR reaction.

Similar results were obtained for the other 3 primer pairs (p. 73 - 74, p. 75 - 76 and p. 77 - 78). Table 7 shows the Cq values obtained by different primer pairs designed to *OTA non-ribosomal peptide synthetase gene*.

Table 7

The Cq values for different primer pairs designed to *OTA non-ribosomal peptide synthetase gene*

Sample name	Cq value for primer pairs			
	P71-72	P73-74	P75-76	P77-78
A2	N/A	N/A	N/A	N/A
A3	N/A	N/A	N/A	N/A
A4	N/A	N/A	N/A	N/A
A6	N/A	N/A	N/A	N/A
A8	N/A	N/A	N/A	N/A
A9	N/A	N/A	N/A	N/A
A10	N/A	N/A	N/A	N/A
A11	N/A	N/A	N/A	N/A
B12	30.43	30.53	31.09	30.70

As one can see, no grape marc sample was positive for the OTA non-ribosomal peptide synthetase gene, involved in OTA synthesis, though every primer pair recognized this gene in the positive control wheat sample. Thus, though the grape marc DNA was of a sufficient quality for PCR reaction, no DNA belonging to potential OTA producers from genera *Aspergillus* and *Penicillium* was detected. This can speak in favor of grape marc biological safety for further use.

Conclusions

1. Based on the sequence of *OTA non-ribosomal peptide synthetase*, involved in ochratoxin biosynthesis, four pairs of primers for detection of the microorganisms potentially capable of producing OTA were developed.
2. For internal control of DNA quality, two pairs of primers capable of recognizing eukaryotic DNA, using the sequence of *Vitis vinifera 26S ribosomal RNA gene* as a template were developed.
3. SDS-based method of DNA extraction was adapted for purifying the DNA from grape marc.
4. No microorganisms potentially capable of producing OTA were detected in the analyzed grape marc samples, which makes them suitable for further use.
5. The proposed Real-Time PCR method for verifying the presence of mycotoxigenic microorganisms in grape marc would avoid further contamination of grape marc, derived products and grape marc extracts, obtained from this by-product of vinification.

Acknowledgments: The authors would like to thank the Project 2SOFT/1.2/83 “INTELLIGENT VALORISATION OF AGRO-FOOD INDUSTRIAL WASTES (INTELWASTES)”, funded by the European Union, within the program Cross border cooperation Romania - Republic of Moldova 2014-2020.

References

1. Dwyer K., Hosseinian F., Rod M.R. The market potential of grape waste alternatives. In: *Journal of Food Research*, 2014, 3, 91.
2. Spinei A., Sturza R., Moşanu A., Zagnat M., Bordeniuc Gh. The use of anthocyanin extract obtained from wine products in the prevention of experimental dental caries. In: *Romanian Journal of Dentistry*, 2017, 20 (3), pp. 161 - 175.
3. Antonic B., Jancikova S., Dordevic D., Tremlova B. Grape Pomace Valorization: A Systematic Review and Meta-Analysis. In: *Foods*, 2020, 9, p. 1627.
4. García-Lomillo J., González-Sanjósé M.L. Applications of wine pomace in the food industry: Approaches and functions. In: *Comprehensive Reviews in Food Science and Food Safety*, 2017, 16, pp. 3 - 22.
5. Quiles A., Campbell G. M., Struck S. et al. Fiber from fruit pomace: A review of applications in cereal-based products. In: *Food Reviews International*, 2018, 34 (2), pp. 162 - 181.
6. Sousa E.C., Uchoa-Thomaz A., Carioca J., Morais S., Lima A., Martins C., Alexandrino C., Ferreira P., Rodrigues A., Rodrigues S., et al. Chemical composition and bioactive compounds of grape pomace (*Vitis vinifera* L.), *Benitaka* variety, grown in the semiarid region of Northeast Brazil. In: *Food Science and Technology*, 2014, 34, pp. 135 - 142.
7. Cristea E., Sturza R., Jauregi P., Niculaua M., Ghendov-Moşanu A., Patras A. Influence of pH and ionic strength on the color parameters and antioxidant properties of an ethanolic red grape marc extract. In: *Journal of Food Biochemistry*, 2019, e12788.
8. Adámez J.D., Samino E.G., Sánchez E.V., González G.D. *In vitro* estimation of the antibacterial activity and antioxidant capacity of aqueous extracts from grape-seeds (*Vitis vinifera* L.). In: *Food Control*, 2012, 24, pp. 136 - 141.
9. Peixoto C.M., Dias M.I., Alves M.J., Calhelha R.C., Barros L., Pinho S.P., Ferreira I.C. Grape pomace as a source of phenolic compounds and diverse bioactive properties. In: *Food Chemistry*, 2018, 253, pp. 132 - 138.

10. Sadh P.K., Duhan S., Duhan J.S. Agro-industrial wastes and their utilization using solid state fermentation: a review. In: *Bioresources and Bioprocessing*, 2018, 5 (1).
11. Musteață Gr., Balanuță A., Reșitca V. Filimon R.V., Băetu M., Patraș A. Capitalization of secondary wine products – an opportunity for the wine sector of Republic of Moldova and Romania. In: *Journal of Social Sciences*, 2021, 4(2), pp. 117 - 127.
12. Andelkovic M., Radovanovic B., Milenkovic-Andelkovic A., Radovanovic V., Zarubica A., Stojkovic N., Nikolic V. The determination of bioactive ingredients of grape pomace (*Vranac variety*) for potential use in food and pharmaceutical industries. In: *Advanced Technologies*, 2015, 4, pp. 32 - 36.
13. Bustamante M.A., Moral R., Paredes C., Pérez-Espinosa A., Moreno-Caselles J., Pérez-Murcia M.D. Agrochemical characterisation of the solid by-products and residues from the winery and distillery industry. In: *Waste Management*, 2008, 28, pp. 372 - 380.
14. Nistor E., Dobrei A., Bampidis V., Ciolac V. Grape pomace in sheep and dairy cows feeding. In: *The Journal of Horticultural Science and Biotechnology*, 2014, 18, pp. 146 - 150.
15. Abarghuei M., Rouzbehan Y., Alipour D. The influence of the grape pomace on the ruminal parameters of sheep. In: *Livestock Science*, 2010, 132 (1-3), pp. 73 - 79.
16. Sturza R., Iazacovici O. Quantification of ochratoxin A in Moldavian wines. In: *Scientific Study & Research. Chemistry & Chemical Engineering, Biotechnology, Food Industry*, 2017, 18 (3), pp. 339 - 334.
17. Sturza R., Găină B., Ionete E., Costinel D. *Authenticity and harmlessness of uvological products*. "MS Logo" Publishing House, Chisinau, 2017, 264 p. (In Romanian).
18. Mitina I., Mitin V., Tumanova L., Zgardan D., Sturza R. Detection and quantification of mycotoxigenic fungi in maize by real-time PCR. In: *Journal of Engineering Science*, 2020, 27(3), pp. 225-231.
19. Mitina I., Zgardan D., Sturza R., Scutaru Iu. The methodological aspects of using real-time polymerase chain reaction (RT-PCR) in *Brettanomyces/Dekkera* detection. In: *Journal of Engineering Science*, 2019, 26 (2), pp. 117 - 125.
20. ISO 21571:2005 Foodstuffs - Methods of analysis for the detection of genetically modified organisms and derived products - Nucleic acid extraction. A.2 Preparation of PCR-quality DNA using polyvinyl-pyrrolidone (PVP)-based DNA extraction methods. Available: <https://www.iso.org/standard/34616.html>
21. Boistean A., Chirsanova A., Zgardan D., Mitina I., Gaina B. Methodological aspects of real-time PCR usage in acetobacter detection. In: *Journal of Engineering Science*, 2020, 3, pp. 232 - 238.